AD-A246 239

OCUMENTATION PAGE

Form Approved
OMB No. 0704-0188

2. REPORT DATE	3. REPORT TYPE AND DATES COVERED
1992 January	Reprints/Technical

1

4. TITLE AND SUBTITLE

AFRRI Reports, Fourth Quarter 1991

5. FUNDING NUMBERS

PE: NWED QAXM

6. AUTHOR(S)

7. PERFORMING ORGANIZATION NAME(S) AND ADDRESS(ES)

Armed Forces Radiobiology Research Institute
Bethesda, MD 20889-5145

8. PERFORMING ORGANIZATION REPORT NUMBER

SR91-42 - SR91-53

9. SPONSORING/MONITORING AGENCY NAME(S) AND ADDRESS(ES)

Defense Nuclear Agency
6801 Telegraph Road
Alexandria, VA 22310-3398

10. SPONSORING/MONITORING AGENCY REPORT NUMBER

11. SUPPLEMENTARY NOTES

12a. DISTRIBUTION/AVAILABILITY STATEMENT

Approved for public release; distribution unlimited.

12b. DISTRIBUTION CODE

13. ABSTRACT *(Maximum 200 words)*

This volume contains AFRRI Scientific Reports SR91-42 through SR91-53 for Oct-Dec 1991.

92-04078

SUBJECT TERMS

15. NUMBER OF PAGES
96

16. PRICE CODE

17. SECURITY CLASSIFICATION OF REPORT	18. SECURITY CLASSIFICATION OF THIS PAGE	19. SECURITY CLASSIFICATION OF ABSTRACT	20. LIMITATION OF ABSTRACT
UNCLASSIFIED	UNCLASSIFIED	UNCLASSIFIED	UL

92 2 18 050

SECURITY CLASSIFICATION OF THIS PAGE

CLASSIFIED BY:

DECLASSIFY ON:

CONTENTS

ANTIMICROBIAL AGENTS AND CHEMOTHERAPY, Aug. 1991, p. 1685–1687
0066-4804/91/081685-03$02.00/0

Vol. 35, No. 8

Ofloxacin and Penicillin G Combination Therapy in Prevention of Bacterial Translocation and Animal Mortality after Irradiation

ITZHAK BROOK* AND G. DAVID LEDNEY

Wound Infection Management Program, Experimental Hematology Department, Armed Forces Radiobiology Research Institute, Bethesda, Maryland 20889-5145

Received 30 January 1991/Accepted 14 May 1991

The efficacies of 40 mg of ofloxacin per kg/day given orally and 250 mg of penicillin per kg/day given intramuscularly, alone or in combination, were evaluated in the prevention of mortality of C3H/HeN female mice given 8.2 Gy of ^{60}Co radiation. Mortalities were 51 of 60 mice (85%) in the control group, 46 of 60 mice (77%) among those treated with penicillin, 32 of 60 mice (53%) among those treated with ofloxacin ($P < 0.05$), and 5 of 60 mice (8%) among those treated with ofloxacin and penicillin ($P < 0.001$). The organisms recovered from the livers of control mice were members of the family *Enterobacteriaceae* and *Streptococcus* spp. A reduction in the number of the *Enterobacteriaceae* was noted only in ofloxacin-treated mice, and a reduction in the number of *Streptococcus* spp. was noted only in the penicillin-treated mice. Reductions in the numbers of both groups of organisms were noted only in the animals treated with both agents. This study shows the advantage of the combination of ofloxacin and penicillin in the prevention of bacterial translocation and animal mortality after irradiation.

Ionizing radiation enhances susceptibility to systemic bacterial infections caused by endogenous and exogenous organisms (4, 6). One source of endogenous infections is the bacterial gastrointestinal tract flora (4). Following irradiation, members of that flora translocate to the liver and spleen and can be associated with fatal septicemia (4, 5). The most important bacterial species isolated from septic animals are members of the family *Enterobacteriaceae* and *Streptococcus* spp. (4, 5). Prevention of bacterial translocation in irradiated animals and control of the subsequent sepsis by these organisms enhance survival in models of experimental infection (3).

In previous studies, we found the quinolone antibiotics to be efficacious in controlling systemic infections following irradiation (2, 3). The efficacies of these agents are believed to be due to their selective ability to eradicate members of the family *Enterobacteriaceae* while preserving the anaerobic gut flora. However, animal mortality was not completely prevented in those studies, and quinolone-resistant *Streptococcus* spp. were isolated in the organs of animals that succumbed to infection.

This study was designed to evaluate the efficacy of supplementing the antimicrobial therapy of irradiated mice with a quinolone with penicillin, which is effective against *Streptococcus* spp. We found that combined antibiotic therapy with ofloxacin and penicillin prevented bacterial translocation to the liver and resulted in 90% survival of mice given lethal doses of radiation.

Female C3H/HeN mice (age, approximately 12 weeks) were obtained from the National Cancer Institute Animal Breeding Facility (Frederick, Md.). Animals were maintained as described previously (3). The mice were provided commercial rodent chow and acidified water (pH 2.2) that was changed to tap water 48 h before irradiation. All experimental procedures were done in compliance with National Institutes of Health and Armed Forces Radiobiology Research Institute guidelines regarding animal use and care.

Mice were placed in Plexiglas restrainers and given a whole-body dose of 8.2 Gy of radiation at 0.4 Gy/min from a ^{60}Co source. The dose rate was determined at the midline, as described previously (3). The tissue-air ratio in this experiment was 0.98.

The lethal dose for 50% of C3H/HeN female mice 30 days after exposure was 7.9 Gy. The dose of 8.2 Gy is a lethal dose, and it was used because survival (80 to 90% in 30 days) from radiation-induced hematopoietic damage is possible if antibacterial treatments are successful.

The antibiotics used were ofloxacin (Ortho Pharmaceutical Corp., Raritan, N.J.) and procaine penicillin G (Wyeth Laboratories, Philadelphia, Pa.). Both antibacterial agents were given once every 24 h. Ofloxacin was given by oral gavage in a dose of 40 mg/kg/day in a volume of 0.1 ml of distilled water. Procaine penicillin was administered by intramuscular (i.m.) injection to alternate thighs in a dose of 250 mg/kg/day in a volume of 0.1 ml of saline. All control animals received 0.1 ml of sterile distilled water by oral gavage and 0.1 ml of normal saline i.m.

Concentrations of the antibiotics in serum were determined in each of six irradiated mice 1 and 23.5 h after the administration of the antimicrobial agents on day 5 of therapy. *Bacillus subtilis* ATCC 6633 was used as a test organism in a Mueller-Hinton agar (pH 7.4).

Mice were observed for mortality and symptoms of disease for 30 days. Five mice were selected at random from each group on days 4, 6, 8, 10, and 12 following irradiation. When fewer than five mice in a group survived, all mice were studied that day. Mice were euthanized by cervical dislocation. Specimens of livers were processed for the presence of bacteria. No other organs were examined and no blood samples were obtained, because studies showed that positive liver cultures correlate best with sepsis (4). The livers were aseptically removed and homogenized immediately. The liver specimens were swabbed onto blood and MacConkey agars, and the organisms were identified by conventional

* Corresponding author.

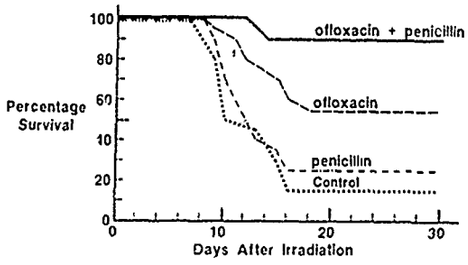

FIG. 1. Survival of 80 C3H/HeN mice irradiated with 8.2 Gy of ^{60}Co and treated orally with ofloxacin and i.m. with procaine penicillin G. Twenty mice were included in each group. The data represent results of one experiment; an identical experiment showed similar data (see text).

methods (9). The susceptibilities of the isolates were determined by the Kirby-Bauer method.

Antimicrobial therapy was initiated 72 h after irradiation, and antimicrobial agents were administered for 10 days. A total of 200 mice were included in each of the three replicate experiments comprising both survival (80 mice) and bacterial translocation (120 mice) studies. However, microbial analysis of the liver was done only twice. Each experiment consisted of three antibiotic therapy groups and the water-saline-treated control group. Each group consisted of 50 mice: 20 were observed for mortality and 30 were used for cultures of liver on each of 5 designated days. The first group of mice received ofloxacin, the second group received penicillin, the third group received a combination of ofloxacin and penicillin, and the fourth group received distilled water orally and saline i.m.

Statistical analyses were done by the Cox-Mantel test (8).

Mortalities in the groups that received ofloxacin or ofloxacin and penicillin were significantly ($P < 0.05$) less than those in the saline- or penicillin-treated groups (Fig. 1). The mortalities in all experiments were similar, and the data were therefore pooled. Of the 60 water-saline-treated mice, 51 (85%) died, 46 of the 60 (77%) penicillin-treated mice died, 32 of 60 (53%) ofloxacin-treated mice ($P < 0.05$) died, and 5 of 60 (8%) mice treated with ofloxacin and penicillin ($P < 0.001$) died.

Most of the organisms were isolated on days 8, 10, and 12 after irradiation (Table 1). Analysis of the data obtained on those days showed recoveries of members of the family *Enterobacteriaceae* in 11 of 13 (85%) of the livers of control mice and *Streptococcus* spp. in 6 of 13 (46%) of the livers of control mice. No other types of isolates were recovered. No significant reduction in the rate of isolation was noted in the recovery of the *Enterobacteriaceae* in penicillin-treated mice (7 of 12 mice). However, the number of livers that harbored *Streptococcus* spp. was reduced to 1 of 12 (8%; $P < 0.05$). The recovery rate of the *Enterobacteriaceae* was reduced in the ofloxacin-treated mice (1 of 14 mice; $P < 0.05$); however, the rate of isolation of *Streptococcus* spp. was not altered (8 of 14; 57%). Therapy with ofloxacin and penicillin reduced the rate of recovery of both the *Enterobacteriaceae* (1 of 15 mice) and *Streptococcus* spp. (0 of 15 mice).

In the second experiment, the *Enterobacteriaceae* were isolated in 12 of 14 (86%) of the livers of control mice, and *Streptococcus* spp. were recovered in 7 of 14 (50%) of the livers of control mice. As in the first experiment, no reduction was noted in the isolation rate of the *Enterobacteriaceae*

TABLE 1. Recovery of bacteria from livers of C3H/HeN mice given 8.2 Gy of ^{60}Co and treated with ofloxacin and penicillin

Organism and treatment	No. of animals with bacteria/no. of animals studied on the following day after inoculation[a]:				
	4	6	8	10	12
Enterobacteriaceae family					
Control	0/5	1/5	3/5	5/5	3/3
Penicillin	0/5	1/5	2/5	3/5	2/2
Ofloxacin	0/5	0/5	0/5	0/5	1/4
Ofloxacin and penicillin	0/5	0/5	0/5	0/5	1/5
Streptococcus spp.					
Control	0/5	1/5	2/5	3/5	1/3
Penicillin	0/5	0/5	0/5	1/5	0/2
Ofloxacin	0/5	0/5	3/5	2/5	3/4
Ofloxacin and penicillin	0/5	0/5	0/5	0/5	0/5

[a] The data represent results of one experiment; one replicate showed similar data (see text).

in penicillin-treated mice (6 of 11 mice; 55%), but the number of livers harboring *Streptococcus* spp. was reduced to 1 of 11 (9%; $P < 0.05$). The recovery rate of the *Enterobacteriaceae* was reduced in ofloxacin-treated mice (1 of 13 mice; $P < 0.05$); however, the rate of recovery of *Streptococcus* spp. was unchanged (7 of 13; 54%). A significant reduction was noted in the recovery of both the *Enterobacteriaceae* (0 of 15 mice) and *Streptococcus* spp. (2 of 15 mice; 13%) in mice treated with ofloxacin and penicillin ($P < 0.05$). All the *Enterobacteriaceae* were susceptible to ofloxacin and resistant to penicillin. All *Streptococcus* spp. were susceptible to penicillin and resistant to ofloxacin.

The mean concentrations of ofloxacin in serum were 2.4 ± 0.3 μg/ml at 1 h and 0.4 ± 0.2 μg/ml at 23.5 h. The mean concentrations of penicillin G were 38.5 ± 4.6 μg/ml at 1 h and 6.2 ± 2.5 μg/ml at 23.5 h.

This is the first study demonstrating that, although the quinolone ofloxacin can reduce mortality following exposure to radiation, the addition of penicillin can further reduce mortality. Although ofloxacin decreased the translocation of the *Enterobacteriaceae*, *Streptococcus* spp. continued to disseminate to the liver, and mortality was not prevented in almost half of the animals. While penicillin was ineffective in controlling mortality by itself, its addition to ofloxacin was successful in controlling the spread of *Streptococcus* spp. and reduced mortality even further.

Several quinolones have been used empirically in immunocompromised patients to decrease the colonization of the gastrointestinal tract and the systemic spread of the *Enterobacteriaceae* (10). The efficacies of these agents are due to their activities against the *Enterobacteriaceae* and their lack of activity against anaerobic bacteria (1). Furthermore, since the quinolones are also absorbed from the gastrointestinal tract, they can eradicate any susceptible pathogens that have spread systemically. Although prophylactic quinolone therapy reduced the occurrence of bacteremia caused by the *Enterobacteriaceae* in immunocompromised patients, it did not prevent infection with *Streptococcus* spp. or reduce the subsequent mortality from infection (7).

The findings of this study suggest that the addition of penicillin therapy directed at the organisms that are not inhibited by quinolone therapy may prevent their translocation and the subsequent development of infection with these quinolone-resistant organisms. These findings support the

preliminary observations in neutropenic patients, in whom the addition of penicillin to a quinolone prevented treatment failures with the quinolone caused by streptococci (7). Another possible explanation for the synergistic effect of adding penicillin to ofloxacin is that penicillin acts synergistically against the *Enterobacteriaceae*, which are the major pathogens. Further studies of patients to explore the usefulness of this approach in controlling bacterial infection in the immunocompromised host are indicated.

We acknowledge the secretarial assistance of Carolyn Wooden.

This study was supported by the Armed Forces Radiobiology Research Institute, Defense Nuclear Agency, under work unit 4440-00129.

REFERENCES

1. **Bauernfeind, A., and C. Petermiller.** 1983. *In vitro* activity of ciprofloxacin, norfloxacin and nalidixic acid. Eur. J. Clin. Microbiol. Infect. Dis. **2**:111–115.
2. **Brook, I., T. B. Elliott, and G. D. Ledney.** 1990. Quinolone therapy of *Klebsiella pneumoniae* sepsis following irradiation: comparison of pefloxacin, ciprofloxacin and ofloxacin. Radiat. Res. **122**:215–217.
3. **Brook, I., and G. D. Ledney.** 1990. Oral ofloxacin therapy of *Pseudomonas aeruginosa* sepsis after irradiation. Antimicrob. Agents Chemother. **34**:1387–1389.
4. **Brook, I., T. J. MacVittie, and R. I. Walker.** 1984. Recovery of aerobic and anaerobic bacteria from irradiated mice. Infect. Immun. **46**:270–271.
5. **Brook, I., R. I. Walker, and T. J. MacVittie.** 1988. Effect of antimicrobial therapy on the gut flora and bacterial infection in irradiated mice. Int. J. Radiat. Biol. **53**:709–716.
6. **Kaplan, H. W., R. S. Speck, and F. Jawetz.** 1965. Impairment of antimicrobial defenses following total body irradiation of mice. J. Lab. Clin. Med. **40**:682–691.
7. **Kelsey, S. M., M. E. Wood, E. Shaw, and A. C. Newland.** 1989. Intravenous ciprofloxacin as empiric treatment of febrile neutropenic patients. Am. J. Med. **87**:274s–277s.
8. **Lee, T. E.** 1980. Statistical methods for survival data analysis, p. 127–129. Lifetime Learning Publication, Belmont, Calif.
9. **Lennette, E. H., A. Balows, W. Hausler, and J. H. Shadomy (ed.).** 1985. Manual of clinical microbiology, 4th ed. American Society for Microbiology, Washington, D.C.
10. **Pecquet, S., A. Andermont, and C. Tancrede.** 1986. Selective antimicrobial modulation of the intestinal tract by norfloxacin in human volunteers and in gnotobiotic mice associated with a human fecal flora. Antimicrob. Agents Chemother. **29**:1047–1052.

Oral Aminoglycoside and Ofloxacin Therapy in the Prevention of Gram-Negative Sepsis after Irradiation

Itzhak Brook and G. David Ledney

Wound Infection Management Program, Experimental Hematology Department, Armed Forces Radiobiology Research Institute, Bethesda, Maryland

To investigate whether oral gentamicin or ofloxacin therapy protects against gram-negative sepsis after irradiation, B6D2F1 mice were exposed to 7.5 Gy of radiation from ^{60}Co, infected with 10^7 *Pseudomonas aeruginosa* or *Klebsiella pneumoniae* orally 3 days after irradiation, and treated with oral (15 mg/kg/day) or intramuscular (im; 7.5 mg/kg/day) gentamicin or oral (40 mg/kg/day) ofloxacin. For *P. aeruginosa*, gentamicin therapy was started orally 10 and 24 h and im 24 h after inoculation. For *K. pneumoniae*, gentamicin was started orally 24, 48, and 72 h and im 24 h after inoculation; ofloxacin was started 24 h after inoculation. Mice that received oral gentamicin early (10 h for *P. aeruginosa*, 24 h for *K. pneumoniae*), im gentamicin, or oral ofloxacin showed significantly ($P < .05$) reduced colonization, translocation, and mortality compared with mice that received oral gentamicin late. These data support the use of selective antimicrobial therapy to reduce colonization, translocation, and mortality from gram-negative bacteria in irradiated animals.

Exposure to ionizing radiation enhances the recipient's susceptibility to systemic infections due to endogenous and exogenous organisms [1, 2]. *Pseudomonas aeruginosa* and *Klebsiella pneumoniae*, two of the most frequent causes of gram-negative bacterial sepsis [3, 4], are especially prevalent in immunocompromised patients.

We have developed a model of acquired *P. aeruginosa* and *K. pneumoniae* [5, 6] infection in irradiated mice that may represent the mode of acquisition of external pathogens into an irradiated host. We observed that the number of endogenous aerobic and anaerobic bacteria in the gastrointestinal tract declined 24 h after irradiation and the decline was maximal at 7 days [7]. This decrease in endogenous bacterial flora may make the host more susceptible to the acquisition of external pathogens such as *P. aeruginosa* and *K. pneumoniae*.

Selective decontamination of the gastrointestinal tract has been advocated as a treatment to reduce the frequency of infections due to endogenous or exogenous gram-negative bacteria in neutropenic patients [8]. This is achieved by oral ingestion of nonabsorbable antimicrobials that are mostly effective against gram-negative enteric organisms and spare the normal anaerobic gastrointestinal flora. Agents that were used for such treatment were polymyxin, bacitracin, and occasionally aminoglycosides [9]. However, in recent years a new class of antimicrobials, the quinolones, have increasingly been used in an attempt to reduce infections in neutropenic individuals [10–12]. Unlike nonabsorbable antimicrobials, the quinolones are absorbed, and they can eradicate organisms that might have spread systemically and reduce the number of enteric bacteria in the gut's lumen.

We investigated whether aminoglycoside activity achieved only within the gut's lumen can protect against gram-negative infections in irradiated animals as successfully as systemically administered therapy.

Materials and Methods

Animals. Female B6D2F1 mice 12 weeks old were obtained from Jackson Laboratories (Bar Harbor, ME). All animals were kept in quarantine for ~2 weeks before being transferred to a room with a 12-h (6 A.M.–6 P.M.) light-dark cycle. Representative samples were examined to ensure the absence of specific bacteria and common murine diseases. Animals were maintained in a facility accredited by the American Association for Accreditation of Laboratory Animal Care in Microlsolator cages on hardwood-chip bedding and were provided commercial rodent chow and acidified water (pH 2.2) that was changed to tap water 48 h before irradiation. This was done to facilitate colonization of the gastrointestinal tract with the gram-negative bacteria [5].

^{60}Co irradiation. Mice were placed in Plexiglas restrainers and given a whole-body dose of 7.5 Gy at 0.4 Gy/min from bilaterally positioned ^{60}Co sources. Before the experiment, the dose rate at the midline of an acrylic mouse phantom was measured using a 0.5-cm^3 tissue-equivalent ionization chamber (Exradin, Chicago). The dose rate at the same location with the phantom removed was then measured using a 50-cm^3 ionization chamber (Armed Forces Radiobiology Research Institute

Received 1 April 1991, revised 31 May 1991.

Research was conducted according to the principles of the Institute of Laboratory Animal Resources, National Research Council.

Views presented are those of the authors, no endorsement by the Defense Nuclear Agency was given or should be inferred.

Reprints or correspondence: Dr. Itzhak Brook, Armed Forces Radiobiology Research Institute, Bethesda, MD 20889-5145.

The Journal of Infectious Diseases 1991;164:917–21

0022-1899/91/6405-0013

[AFRRI]). The ratio of these two dose rates, the tissue-air ratio, was then used to determine the animal doses for routine experimental procedures.

All ionization chambers used had calibration factors traceable to the National Institute of Standards and Technology. The dosimetry measurements were made following the American Association of Physicists in Medicine Task Group 21 protocol [13]. The dose within the exposure field varied by 3% as determined by thermoluminescent dosimetry with acrylic mouse phantoms. The LD_{50} was 9.65 ± 0.36 Gy 30 days after exposure. The dose of 7.0 Gy was, therefore, a sublethal dose and was chosen after previous studies showed that feeding the mice *P. aeruginosa* [5] and *K. pneumoniae* [6] produced mortality of 80%–90% in 30 days.

Bacteria. Two bacterial strains were used in this study. One was a clinical isolate of *P. aeruginosa* strain PA220 that was isolated from a blood sample taken at the National Naval Medical Center (Bethesda, MD). The organism is serotype 1, exotoxin A– and protease-positive, sensitive to serum-mediated killing, and relatively virulent for normal mice. The other strain was a clinical isolate of *K. pneumoniae* with a capsule type 5 (AFRRI no. 7). The organisms were harvested in the logarithmic phase of growth in brain-heart infusion media. A concentration of 10^8 organisms/ml of saline was prepared, and 0.1 ml was fed to each animal by gavage using a 20-gauge animal feeding tube fitted to a 1.0-ml syringe.

Antimicrobials. Gentamicin (Schering Laboratories, Kenilworth, NJ) and ofloxacin (Ortho Pharmaceutical, Raritan, NJ) were obtained from the manufacturer. Standard powder formulations with known potencies were used for in vitro and in vivo studies. Ofloxacin was given orally once every 24 h in a dose of 40 mg/kg/day, administered in a volume of 0.1 ml by oral gavage with a 20-gauge feeding tube fitted to a 1.0-ml syringe. Control animals received 0.1 ml of sterile distilled water by oral gavage. Gentamicin was given orally or intramuscularly (im). The im dose was 7.5 mg/kg/day given as one dose, and the oral dose was 15 mg/kg/day given every 12 h.

Antimicrobial serum concentration. Serum concentrations of the antimicrobials were determined in six mice 1 and 23.5 h after oral administration of ofloxacin on day 5 of therapy and 1 and 11.5 h after administration of oral or im gentamicin. *Bacillus subtilis* ATCC 6633 was used as a test organism, and Mueller-Hinton agar (pH 7.4) was used as a test agar. The method could not detect antimicrobial concentrations <0.2 μg/ml.

In vitro susceptibility. MICs and MBCs were determined in Mueller-Hinton broth that was inoculated with 1.5×10^5 organisms/ml from an overnight culture. MICs and MBCs of ofloxacin for *P. aeruginosa* and *K. pneumoniae* were 0.12 and 0.24 μg/ml, of gentamicin for *P. aeruginosa* were 0.25 and 0.5 μg/ml, and of gentamicin for *K. pneumoniae* were 0.125 and 0.25 μg/ml.

Microbiologic methods. Mice challenged with bacteria were treated with gentamicin, ofloxacin, or water by different routes starting at different times for a total of 10 therapy groups (see below). Five animals were selected at random from each group on days 4, 6, 8, and 10 after irradiation. Animals were killed by cervical dislocation. Specimens of livers and ileum were processed for the presence of bacteria. No other organs were processed and no blood samples were obtained, because previous studies showed that liver cultures correlated best with sepsis [2]. The livers were aseptically removed and homogenized immediately. The ileum was opened, and ileal content samples were obtained using a swab. The liver and ileum specimens were swabbed onto blood and MacConkey agars, and the organisms were identified using conventional methods [14].

Experimental design. Each mouse was fed 10^7 organisms 72 h after irradiation, because previous work showed that mice are susceptible to gram-negative bacterial sepsis after feeding with gram-negative bacteria 48–72 h after irradiation [10, 11]. Antimicrobial therapy was started at different intervals after bacterial feeding to examine the effect of delay on the prevention of systemic spread of organisms.

In groups of mice fed *P. aeruginosa*, gentamicin therapy was given as follows: orally starting 10 h after inoculation, orally starting 24 h after inoculation, and im starting 24 h after inoculation. Control mice were given distilled water orally 24 h after inoculation. No ofloxacin therapy was given to mice fed *P. aeruginosa*. Each of the four therapies tested was given to 20 mice, for a total of 80 mice in each run of the experiment. The experiment was run three times, for a total of 240 mice used in *P. aeruginosa* studies.

In groups of mice fed *K. pneumoniae*, ofloxacin therapy was given 24 h after inoculation. Gentamicin therapy was given as follows: orally starting 24 h after inoculation, im starting 24 h after inoculation, orally starting 48 h after inoculation, and orally starting 72 h after inoculation. Control mice were given distilled water orally starting 24 h after inoculation. Each of the six therapies tested was given to 20 mice, for a total of 120 mice used in each run of the experiment. The experiment was run three times, for a total of 360 mice used in *K. pneumoniae* studies.

All therapies were given daily as long as there were living animals in a group, for a total of 15 days.

Microbial analyses of liver and ileal contents were similar to the mortality studies: 80 mice fed *P. aeruginosa* were given four therapies using gentamicin and water, and 120 mice fed *K. pneumoniae* were given six therapies using ofloxacin, gentamicin, and water (see above). Five mice were picked at random from each of the 10 therapy groups on days 4, 6, 8, and 10 after irradiation to process liver and ileum for microbial analysis. This experiment was run twice, for a total of 160 mice given *P. aeruginosa* and 240 mice given *K. pneumoniae*.

Statistical methods. Statistical analyses were done using the Cox-Mantel test [15].

Results

Mortality studies. In all three runs of the experiment using *P. aeruginosa*, mortality in the groups given oral gentamicin starting 10 h after inoculation or im gentamicin starting 24 h after inoculation was significantly ($P < .05$) less than for mice given oral gentamicin starting 24 h after inoculation or mice given only water (control).

Mortality in the first run of the experiment (figure 1) was 8

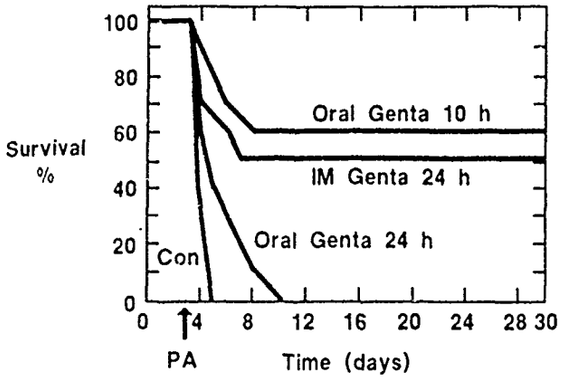

Figure 1. Survival of B6D2F1 mice irradiated with 7.5 Gy of ^{60}Co, inoculated with 10^7 *Pseudomonas aeruginosa* (PA), and given oral gentamicin (Genta) starting 10 h after inoculation, intramuscular (IM) or oral gentamicin starting 24 h after inoculation, or water (Con). Twenty mice were included in each group. Data represent one experiment, two replicates of each showed similar data.

(40%) in mice given oral gentamicin starting 10 h after inoculation, 10 (50%) in mice given im gentamicin starting at 24 h, all 20 mice given oral gentamicin starting at 24 h, and all 20 mice given only water.

Mortality in the second run was 9 (45%) in mice given oral gentamicin starting at 10 h, 9 (45%) in mice given im gentamicin starting at 24 h, 19 (95%) in mice given oral gentamicin starting at 24 h, and all 20 mice given only water.

Mortality in the third run was 6 (30%) in mice given oral gentamicin starting at 10 h, 7 (35%) in mice given im gentamicin starting at 24 h, 18 (90%) in mice given oral gentamicin starting at 24 h, and all 20 mice given only water.

For the experiment using *K. pneumoniae*, mortality in all three runs in mice given ofloxacin, oral gentamicin, or im gentamicin starting 24 h after inoculation was significantly ($P < .05$) less than that of the water-treated (control) mice or those given gentamicin orally starting 48 h and 72 h after inoculation.

In the first run (figure 2) mortality was 0 in mice given ofloxacin, 2 (10%) in mice given im gentamicin starting 24 h after inoculation, 4 (20%) in mice given oral gentamicin starting at 24 h, 12 (60%) in mice given oral gentamicin starting at 48 h, and 16 (80%) in mice given oral gentamicin starting at 72 h. No mice given only water survived.

Mortality in the second run was 2 (10%) in mice given ofloxacin, 3 (15%) in mice given oral gentamicin starting at 24 h, 3 (15%) in mice given im gentamicin starting at 24 h, 15 (75%) in mice given oral gentamicin starting at 48 h, 15 (75%) in mice given oral gentamicin starting at 72 h, and all 20 mice given only water.

In the third run, mortality was 0 in mice given ofloxacin, 1 (5%) in mice given im gentamicin starting at 24 h, 3 (15%) in mice given oral gentamicin starting at 24 h, 16 (80%) in mice given oral gentamicin starting at 48 h, all 20 mice given gentamicin after 72 h, and all 20 mice given only water.

Microbial analyses: liver and ileum. *P. aeruginosa* was isolated from all control mice and most (5/7) mice given oral gentamicin starting 24 h after inoculation. The bacterium was less often isolated from mice given oral gentamicin starting at 10 h and from mice given im gentamicin starting at 24 h (table 1).

K. pneumoniae was isolated more often in the control mice and in mice given oral gentamicin starting at 48 and 72 h after inoculation than in mice given ofloxacin, oral gentamicin starting at 24 h, or im gentamicin starting at 24 h ($P <$ 05; table 2).

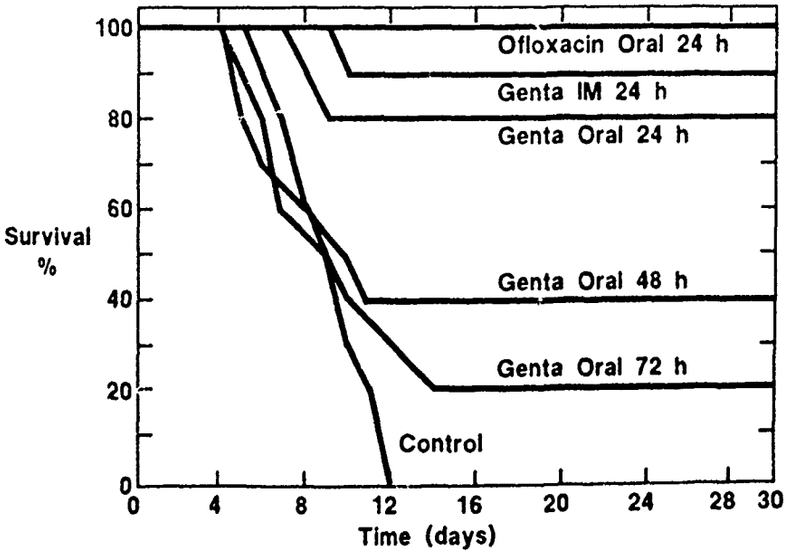

Figure 2. Survival of B6D2F1 mice irradiated with 7.5 Gy of ^{60}Co, inoculated with 10^7 *Klebsiella pneumoniae*, and given oral ofloxacin starting 24 h after inoculation; oral gentamicin (Genta) starting 24 h, 48 h, and 72 h after inoculation; intramuscular (IM) gentamicin starting 24 h after inoculation; or water (control). Twenty mice were included in each group. Data represent one experiment; two replicates of each showed similar data.

Table 1. Recovery of *Pseudomonas aeruginosa* from B6D2F1 mice exposed to 7.5 Gy of ^{60}Co, fed with 10^7 *P. aeruginosa*, and treated with gentamicin.

Organ, experiment, treatment group	Days after inoculation				
	4	6	8	10	Total
Liver					
1. Water (control)	5/5	0/0	0/0	0/0	5/5
Gentamicin oral, 10 h	1/5	1/5	0/5	0/2	2/17*
Gentamicin oral, 24 h	4/5	1/2	0/0	0/0	5/7
Gentamicin im, 24 h	2/5	1/5	0/5	0/1	3/16*
2. Water (control)	4/4	0/0	0/0	0/0	4/4
Gentamicin oral, 10 h	1/5	0/5	0/4	0/0	1/14*
Gentamicin oral, 24 h	4/5	1/1	0/0	0/0	5/6
Gentamicin im, 24 h	2/5	1/5	0/5	0/2	3/17*
Ileal contents					
1. Water (control)	5/5	0/0	0/0	0/0	5/5
Gentamicin oral, 10 h	3/5	2/5	1/5	0/2	6/17*
Gentamicin oral, 24 h	3/5	1/2	0/0	0/0	4/7
Gentamicin im, 24 h	4/5	2/5	0/5	1/1	7/16*
2. Water (control)	4/4	0/0	0/0	0/0	4/4
Gentamicin oral, 10 h	2/5	2/5	0/4	0/0	4/14*
Gentamicin oral, 24 h	2/5	1/1	0/0	0/0	3/6
Gentamicin im, 24 h	3/5	2/5	1/5	0/2	6/17*

NOTE. im = intramuscular. Data are no. of animals with bacteria/number studied.
* $P < .05$ compared with control.

Serum antibiotic concentration. The mean concentrations of ofloxacin were 2.6 ± 0.4 μg/ml at 1 h after administration and 0.4 ± 0.2 μg/ml at 23.5 h after administration. Mice given im gentamicin showed mean concentrations of 5.5 ± 1.8 μg/ml at 1 h and 1.4 ± 0.3 μg/ml at 11.5 h after administration. Mice given oral gentamicin showed no detectable serum concentrations.

Discussion

This study demonstrates that oral gentamicin administered early prevents gastrointestinal colonization, bacterial translocation, and mortality due to *P. aeruginosa* and *K. pneumoniae* in irradiated mice. Because oral gentamicin was not absorbed through the gastrointestinal tract, the gentamicin prevented bacterial sepsis because it inhibited the colonization of the gastrointestinal tract by the inoculated bacteria. However, when colonization had already occurred and translocation had taken place, administering gentamicin orally was ineffective. In contrast, im administration of gentamicin successfully reduced both systemic spread of the bacteria and gastrointestinal colonization. Orally administered ofloxacin also achieved these results.

The quinolone ofloxacin was effective for treating *P. aeruginosa* infection because it might have locally inhibited the organism's growth in the gut lumen but preserved the anaerobic gut flora [10–12]. Also, ofloxacin's systemic antibacterial activity prevented the infection within the body. Orally administered gentamicin also effectively reduced the growth of *P. aeruginosa* and *K. pneumoniae* in the gastrointestinal tract without suppressing the growth of the indigenous anaerobic flora.

The higher virulence of *P. aeruginosa* compared with that of *K. pneumoniae* in our animal model facilitated the progression of fatal bacteremia in inoculated mice; therefore, we administered gentamicin 10 h after bacterial inoculation. Oral gentamicin was ineffective when administered 24 h after *P. aeruginosa* were fed to the mice but was effective when administered 24 h after *K. pneumoniae* were fed.

The ability of *P. aeruginosa* and *K. pneumoniae* to cause systemic infection in irradiated mice may be due to the following factors: the bacterial void created in the gut after the decline in the number of other organisms [7], the increased permeability of the mucosal cells damaged by irradiation, and the decrease in the local and systemic immune defenses.

The results of this study support the use of early selective decontamination to prevent colonization of the gastrointestinal tract in irradiated hosts. Judicious use of early selective

Table 2. Recovery of *Klebsiella pneumoniae* from B6D2F1 mice exposed to 7.5 Gy of ^{60}Co, fed with 10^7 *K. pneumoniae*, and treated with gentamicin or ofloxacin.

Organ, experiment, treatment group	Days after inoculation				
	4	6	8	10	Total
Liver					
1. Water (control)	3/5	3/5	2/3	0/0	8/13
Gentamicin oral, 24 h	1/5	0/5	1/5	0/3	2/18*
Gentamicin oral, 48 h	3/5	3/5	1/3	0/0	7/13
Gentamicin oral, 72 h	4/5	3/5	1/1	0/0	8/11
Gentamicin im, 24 h	0/5	0/5	0/5	0/4	0/19*
Ofloxacin oral	0/5	0/5	0/5	0/5	0/20*
2. Water (control)	3/5	4/5	2/3	0/0	9/13
Gentamicin oral, 24 h	2/5	1/5	0/5	0/3	3/18*
Gentamicin oral, 48 h	3/5	3/5	2/3	0/0	8/13
Gentamicin oral, 72 h	2/5	2/5	1/1	0/0	5/11
Gentamicin im, 24 h	0/5	1/5	0/5	0/4	1/19*
Ofloxacin oral	1/5	0/5	0/5	0/5	1/20*
Ileal contents					
1. Water (control)	4/5	3/5	2/4	0/0	9/14
Gentamicin oral, 24 h	0/5	0/5	0/5	0/2	0/17*
Gentamicin oral, 48 h	2/5	3/5	2/2	0/0	7/12
Gentamicin oral, 72 h	2/5	3/5	0/0	0/0	5/10
Gentamicin im, 24 h	1/5	2/5	0/5	0/3	3/18*
Ofloxacin oral	0/5	0/5	1/5	0/4	1/19*
2. Water (control)	2/5	3/5	3/4	0/0	8/14
Gentamicin oral, 24 h	0/5	1/5	0/5	0/2	1/17*
Gentamicin oral, 48 h	2/5	3/5	1/2	0/0	6/12
Gentamicin oral, 72 h	3/5	3/5	0/0	0/0	6/10
Gentamicin im, 24 h	2/5	2/5	0/5	0/3	4/18*
Ofloxacin oral	0/5	0/5	0/5	0/4	0/19*

NOTE. im = intramuscular. Data are no. of animals with bacteria/number studied.
* $P < .05$ compared with control.

decontamination may prevent fatal bacteremia with gram-negative organisms.

Selective decontamination of the gut with orally administered quinolones prevents sepsis in immunocompromised hosts and manages septic episodes in neutropenic patients [10–12]. The availability of an oral route of administration, the long half-life of ofloxacin, which allows daily administration [16], the ability to selectively inhibit potential pathogens in the gut, and the ability to treat systemic infection make the quinolones promising agents for oral therapy for orally acquired *P. aeruginosa* and other gram-negative infections in irradiated hosts.

Acknowledgment

We thank Carolyn Wooden for secretarial assistance.

References

1 Kaplan HW, Speck RS, Jawetz F Impairment of antimicrobial defenses following total body irradiation of mice J Lab Clin Med 1965;40:682–91.
2 Brook I, MacVittie TJ, Walker RI. Recovery of aerobic and anaerobic bacteria from irradiated mice Infect Immun 1984;46:270–1.
3 Maki DG Nosocomial bacteremia. An epidemiologic overview. Am J Med 1981;70:719–32.
4. Weinstein MP, Reller LB, Murphy JR, Lichtenstein KA. The significance of positive blood cultures: a comprehensive analysis of 500 episodes of bacteremia and fungemia in adults. I. Laboratory and epidemiologic observations. Rev Infect Dis 1983;5:35–53.
5 Walker RI, Brook I, Costerton JW, MacVittie TJ, Myhal ML. Possible association of mucous blanket integrity with post-irradiation colonization resistance Radiat Res 1985;104:346–57
6 Brook I, Elliott TB, Ledney GD. Quinolone therapy of *Klebsiella pneumoniae* sepsis following irradiation: comparison of pefloxacin, ciprofloxacin and ofloxacin. Radiat Res 1990;122:215–7.
7 Brook I, Walker RI, MacVittie TJ. Effect of antimicrobial therapy on the gut flora and bacterial infection in irradiated mice Int J Radiat Biol 1988;53 709–16.
8. Hathorn JW, Rubin M, Pizzo PA. Empiric antibiotic therapy in the febrile neutropenic cancer patent clinical efficacy and impact of monotherapy. Antimicrob Agents Chemother 1987;31 971–7
9 Mulder NH, Nieweg HW, Sleyfer DT Infection prevention in granulocytopenic patients by selective decontamination of the digestive tract In van der Waaij D, Verhoef J, eds New criteria for antimicrobial therapy maintenance of digestive tract colonization resistance Amsterdam: Excerpta Medica, 1979 113–6
10. Pecquet S, Andermont A, Tancrede C Selective antimicrobial modulation of the intestinal tract by norfloxacin in human volunteers and in gnotobiotic mice associated with a human fecal flora Antimicrob Agents Chemother 1986;29:1047–52.
11. Rozenberg-Arska M, Dekker AW, Verhoef J Ciprofloxacin for selective decontamination of the alimentary tract in patients with acute leukemia during remission induction treatment. the effect in fecal flora. J Infect Dis 1985;142:104–7.
12 Liang RH, Young RWH, Chan TK, et al Ofloxacin versus co-trimoxazole for prevention of infection in neutropenic patients following cytotoxic chemotherapy. Antimicrob Agents Chemother 1990;34:215–8.
13. Task Group 21, Radiation Therapy Committee, American Association of Physicists in Medicine. Protocol for the determination of the absorbed dose from high-energy photon and electron beams Med Phys 1983;10.1–30.
14. Lennette EH, Balows A, Hausler W, Shadomy JH, eds Manual of clinical microbiology. 4th ed. Washington, DC: American Society for Microbiology, 1985.
15. Lee TE. Statistical methods for survival data analysis Belmont, CA: Lifetime Learning Publication, 1980:127–9.
16. Monk JP, Campoli-Richards DM. Ofloxacin: a review of its antibacterial activity, pharmacokinetic properties and therapeutic use Drugs 1987;33:346–91.

Relation between postprandial gastric emptying and cutaneous electrogastrogram in primates

S. BRULEY DES VARANNES, M. MIZRAHI, AND A. DUBOIS
Laboratory of Gastrointestinal and Liver Studies, Digestive Diseases Division, Department of Medicine, Uniformed Services University of the Health Sciences, Bethesda 20814-4799; and Department of Physiology, Armed Forces Radiobiology Research Institute, Bethesda, Maryland 20814-5145

BRULEY DES VARANNES, S., M. MIZRAHI, AND A. DUBOIS. *Relation between postprandial gastric emptying and cutaneous electrogastrogram in primates.* Am. J. Physiol. 261 (Gastrointest. Liver Physiol. 24): G248–G255, 1991.—The relation between the cutaneous electrogastrogram (EGG) and gastric emptying was investigated in six rhesus monkeys. Gastric emptying was measured using scintigraphy after administration of two 80-ml mixed solid liquid meals (1.5 and 5.0 kcal/kg) tagged with ^{99m}Tc-sulfur colloid and ^{111}In-diethylenetriamine pentaacetic acid. Six epigastric bipolar recordings of the EGG were concurrently obtained, digitized, and band-pass filtered. Portions of the signal with motion artifacts were automatically detected and excluded using two microwave motion sensors. During the early postprandial period, gastric emptying was greater after the 1.5-kcal/kg meal than after the 5-kcal/kg meal, and EGG amplitude increased significantly compared with fasting only after the 1.5-kcal/kg meal. Both emptying and EGG amplitude subsequently decreased after the 1.5-kcal/kg meal, whereas these two parameters increased after the 5-kcal/kg meal. As a result, EGG amplitude was significantly correlated with gastric emptying of solids in all six animals. In contrast, EGG frequency was not significantly different between the two meals and was not correlated with emptying. These results indicate that both the EGG and gastric emptying are modified differently by meals with different caloric contents and that the EGG may represent a useful, although indirect, index of gastric emptying.

emptying of solids; emptying of liquids; caloric meals; gastric motility

---

ANTRAL MECHANICAL ACTIVITY is known to increase markedly after mixed meals, and this increase is directly correlated with gastric emptying of radiolabeled solids (2, 12). In addition, emptying of liquids is believed to be determined by the pressure gradient between stomach and duodenum as well as by coordinated motor events involving stomach, pylorus, and duodenum (4, 8, 20). Because various normal and abnormal patterns of gastric contractility may be responsible for different rates of emptying, it is important to further develop clinically applicable methods to measure gastric motility.

Intraluminal manometry permits the evaluation of fasting and postprandial distal antral motility (2), but this technique is invasive and difficult to use in unanesthetized animals. In addition, because the stomach is a cavity that may be filled with variable and possibly large volumes of fluids, solids, and air, the Pascal principle predicts that intraluminal manometry does not provide reliable recording of the contractile activity of the proximal stomach (35). The electrical activity recorded from the stomach is thought to reflect neuromuscular events that control gastric motility. In healthy primates, several types of electrical and mechanical activities can be recorded: the proximal stomach exhibits small electrical fluctuations at 1/min and concurrent tonic contractions, but propagated phasic contractions have not been detected (18). The mid- and distal stomach generate electrical potentials at ~3/min that are called slow waves or electrical control activity (ECA). In addition, fast electrical potentials called spikes or electrical response activity (ERA) may be superimposed onto the ECA. The ERA, but not the ECA, is accompanied by detectable phasic contractions that propagate in an aboral direction (29). However, serosal recording of gastric electrical activity requires surgical implantation of electrodes, which is feasible in animals but is rarely possible in humans. The use of suction electrodes and magnetic force maintaining intraluminal electrodes in contact with the gastric mucosa has been proposed (1), but these techniques are invasive and may modify gastric motility.

Cutaneous electrogastrography (EGG) has been shown to reflect accurately both the electrical and mechanical activity of the stomach (26) and therefore represents an attractive alternative to serosal or mucosal gastric electromyography. However, the exact nature of this type of recording remains controversial, and its precise quantitation has been difficult. Finally, the exact relation between the EGG and gastric emptying is unknown.

We therefore obtained multidirectional recordings of the cutaneous EGG and simultaneously measured gastric emptying of solids and liquids using scintigraphy. We determined *1*) whether meals with different emptying rates induce different gastric electrical activities that could be detected using the cutaneous EGG and *2*) whether the EGG is correlated with gastric emptying of solids and/or liquids. We observed that gastric emptying and the amplitude of the cutaneous EGG follow a similar time course after two meals with different caloric contents and that these parameters were significantly correlated in most animals.

MATERIALS AND METHODS

Animals. Six male 3- to 5-yr-old purpose-bred domestic rhesus monkeys, *Macaca mulatta* (wt 3-5 kg), were transferred to our facility. Upon arrival, they were housed in individual stainless steel cages in conventional holding rooms of an American Association for Accreditation of Laboratory of Animal Care (AAALAC)-accredited animal facility, where they were quarantined for 45 days. Monkeys were provided with tap water ad libitum, commercial primate chow, and fruits. After they had three negative tuberculosis tests performed 2 wk apart, two 4-h habituation sessions were held. During those sessions, as well as during subsequent studies, animals were seated in a primate restraining chair placed inside a ventilated, lighted, and sound-absorbing booth that had the rear side cut to position a gamma camera close to the monkey. Studies were performed between 8:00 A.M. and 12:00 P.M. after an 18-h fast and at intervals of at least 4 days.

Cutaneous electrogastrogram. Six adhesive cutaneous electrodes (Ag-AgCl, Red Dot, 3M, St Paul, MN) were placed on the epigastric area that had been previously shaved and cleaned with alcohol. A drop of electrode paste (EKGsol, Beck-Lee, Phoenix Scientific, Rochester, NY) was poured onto the electrodes that were positioned 2.5 cm apart in a hexagonal configuration. A seventh electrode was placed in the center of the hexagon and used as the reference (Fig. 1). The electrodes were held in place using a large adhesive tape wrapped around the abdomen. In addition, a grounding electrode was placed on the left leg. The electrodes were attached to a head selector box interfaced to a multichannel EGG recorder amplifier (Synectics Bos, Anaheim, CA), providing bipolar recordings between each of the six peripheral electrodes and the central one (channels I–VI). In addition, the movements of the monkey were detected using two microwave motion sensors (model D7, Microwave Sensors, Ann Arbor, MI), rewired as previously described (24) and placed on either side of the monkey inside the booth (Fig. 2).

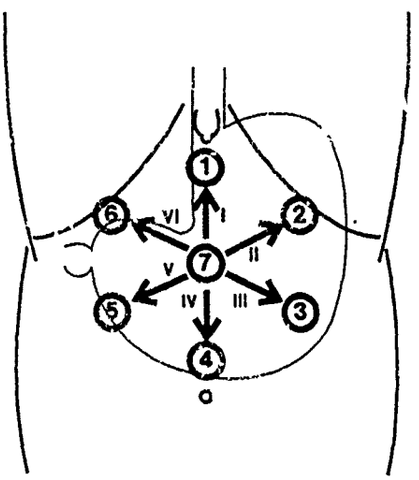

FIG. 1. Positions of cutaneous electrodes used to record electrogastrogram from epigastric area. Central electrode was used as a reference to obtain 6 bipolar recordings.

The two motion signals and the six EGG channels were low-pass filtered at 30 Hz but not high-pass filtered (DC-30 Hz), amplified, displayed on paper, and taped using a multichannel analog recorder (model PR2230, Ampex, Redwood City, CA) for subsequent digitization and computer analysis. Before and after each session, a 1-mV sinusoidal signal (frequency 3 cycles/min) produced by a sine-wave generator (model 5100, Wavetek, San Diego, CA) was recorded for subsequent calibration of the six EGG channels.

Experimental procedure. A 10-Fr double-lumen nasogastric Ventrol Levine tube (National Catheter, Mallinckrodt, Argyle, NY) was introduced into the stomach. Proper positioning was verified by aspirating 3 ml of the gastric contents; if <3 ml of fluid were obtained, a water recovery test was performed with 5 ml, and the position of the tube was adjusted accordingly. The seated monkey was then placed in the booth described above. The chair could be rotated on its vertical axis, permitting the positioning of the monkey with either its front or its back facing a gamma camera. Two video cameras allowed continuous observation of the monkey on a video monitor without opening the booth. After a 1-h basal recording of the EGG was obtained, the door of the booth was opened and one of two 80-ml mixed solid-liquid meals at 20°C was administered intragastrically in 2 min through the nasogastric tube. The tube was then removed and the door was closed.

Test meals. The meals were either 1) a low-caloric meal (LCM) (1.5 kcal/kg), prepared by adding 40 ml of tap water to 40 ml of radiolabeled chicken liver ground to 1- to 2-mm-diam particles and suspended in tap water (5) (caloric composition: proteins 64%, 3.6 kcal; lipids 27%, 1.5 kcal; carbohydrates 9%, 0.5 kcal); or 2) a high-caloric meal (HCM) (5 kcal/kg) made of two bouillon cubes (Wyler) diluted in 40 ml of water added to the 40 ml isotopic meal (caloric composition: proteins 31%, 5.9 kcal; lipids 25%, 4.8 kcal; carbohydrates 44%, 8.5 kcal).

Measurement of gastric emptying. The solid phase of the meal was tagged according to the method of Wirth et al. (34) and was composed of 1.2 g chicken liver and 0.5 mCi of ^{99m}Tc-sulfur colloid bound to 0.5 g for analytic-grade cation exchange resin with a diameter from 0.3 to 0.85 mm (Chelex-100, Bio-Rad Laboratories, Richmond, CA). The average labeling efficiency was 98.5%, and the in vitro stability was >99%, with an average loss of 0.7% of the total activity in simulated gastric fluid. Animal studies have also demonstrated the in vivo stability of the binding, with an average of 0.045% of the administered ^{99m}Tc appearing in the blood at 1 h and 0.41% appearing in the 24-h urine collection (34). Initial validation studies using ^{111}In-sulfur colloid-tagged chicken liver concurrently with the ^{99m}Tc-sulfur colloid-tagged resin showed identical emptying curves of the two markers. The liquid phase (40 ml of water) was tagged with 0.1 mCi of ^{111}In-diethylenetriamine pentaacetic acid (5).

Images were acquired using a gamma camera (Pho/Gamma HP, Nuclear-Chicago, Searle, Chicago, IL) and a medium energy collimator with a 20% window around the 140-keV peak for the ^{99m}Tc activity and a 20% window around the 247-keV peak for the ^{111}In activity.

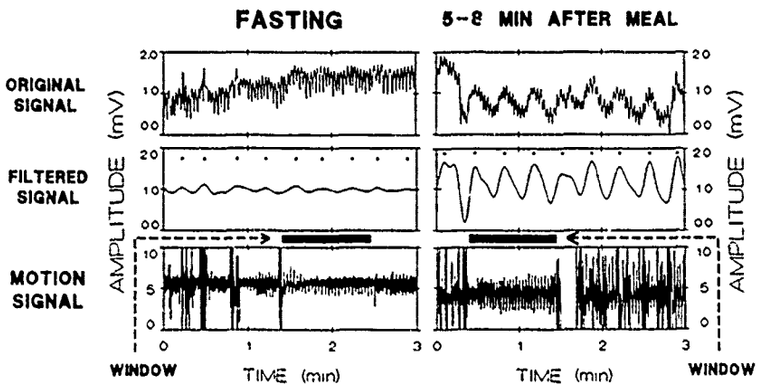

FIG. 2. Example of recordings obtained during present experiments. *Top*: EGG recorded before (*left*) and 5 min after (*right*) a mixed liquid-solid meal. *Middle*: same signals after digital filtering (0.02–0.11 Hz); +, peak of each wave as detected using software. *Bottom*: concurrent recording of movements (including respiration) of animal. Thick black lines define windows during which no motion artifacts are present. Note that motion artifacts occasionally appear to increase the amplitude of the EGG or to modify the shape of the wave.

One-minute anterior and posterior images were obtained at 2, 5, 10, 13, 16, and 20 min after the administration of the meal and at 10-min intervals during the subsequent 160 min. Data were stored on-line on a computer (Medical Data System A^3, Ann Arbor, MI) for subsequent analysis.

Gastric emptying was analyzed using a previously described method (5). Briefly, gastric and intestinal outlines were defined as the regions of interest in sequential scans, and the activity of each isotope was determined within these areas. Corrections were made for ^{99m}Tc decay and for Compton scatter from ^{111}In into the ^{99m}Tc window. The geometric mean over anterior and posterior activities was calculated, and the percentage of each phase of the meal remaining in the stomach was expressed as the ratio of the stomach activity divided by the sum of the gastric and intestinal activities (Fig. 3, *A* and *B*). Gastric emptying of solids and liquids was then expressed in three different manners.

First, curve fitting of the entire emptying of liquids and solids was performed using the Weibull function (32), also described as the power exponential model (6), and using the equation

$$x_t = 2^{-(t/t_{1/2})^{\beta}}$$

where x_t is the amount of marker present in the stomach at *time* t, $t_{1/2}$ is the half-emptying time, and β reflects the shape of the curve. We then calculated the fractional emptying rate (FER) using the equation

$$\text{FER} = t_{1/2}/\ln (0.5)$$

Second, because we were interested in evaluating the relation between the EGG and gastric emptying in a minute-by-minute fashion, we calculated the FER for each 3- to 10-min time interval using the following linear function

$$\text{FER} = [(x_{t_i} - x_{t_{i+1}})/x_{t_i} \times 100]/(t_{i+1} - t_i)$$

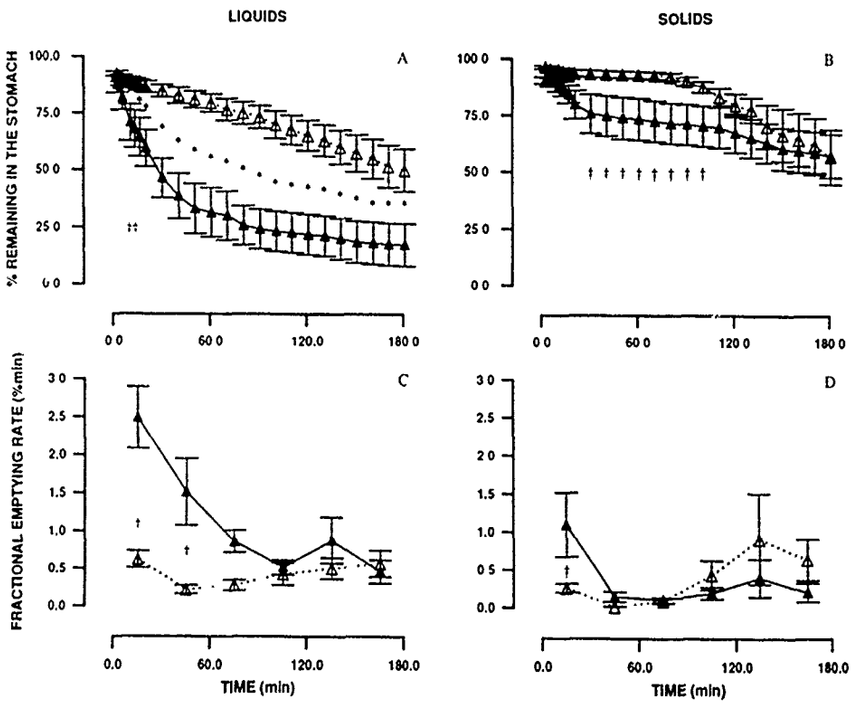

FIG. 3. Percentage of marker remaining in stomach (*A* and *B*) and fractional emptying rate (*C* and *D*) for liquids and solids in 6 rhesus monkeys after administration of LCM (1.5-kcal/kg meal; ▲) and HCM (5.0-kcal/kg meal; △). Values are means ± SE. LCM compared with HCM: * $P < 0.01$; † $P < 0.05$.

where x_{t_i} and $x_{t_{i+1}}$ are the percentages remaining in the stomach at *times* t_i and t_{i+1}, respectively. Because this linear function was used only for short (3–10 min) intervals, these values of "linear" FERs are very similar to those that would be calculated using the equation

$$\text{FER} = [\ln(x_{t_{i+1}}/x_{t_i}) \times 100]/(t_{i+1} - t_i)$$

In addition, when the complete curve is considered, a series of straight lines satisfactorily approximate an exponential curve (discrete calculation method). The average FER was then calculated for each 30-min-period (Fig. 3, *C* and *D*).

Analysis of EGG. The taped signals were digitized at 2 Hz with a 1-Hz low-pass analog filter (model 3342, Krohn-Hite, Avon, MA) for the six EGG channels and at 20 Hz with a 10-Hz low-pass analog filter for the sum of the two motion signals. Each digitized EGG channel was then band-pass filtered with an optimal finite impulse response filter (0.02–0.11 Hz, i.e., 1.20–6.60 cycles/min), designed using the Remez exchange algorithm (22) and converted to millivolts using the previously recorded calibration signals. EGG peaks were detected in the filtered signal using a Compaq 386/20 computer (Houston, TX), with the Xenix operating system (Santa Cruz Operations, Santa Cruz, CA) and locally developed software (Fig. 2) (9). The software locates peaks by detecting increasing and decreasing trends in a signal. The points at which these trends change are the peak begin point, end point, and crest. A trend is defined as a user-specified minimum number of consecutive local changes. A local change is considered to occur when a point is less than the local minimum or greater than the local maximum plus a user-specified minimum increase.

The sum of the two motion signals was used to select the periods of the EGG signals that lasted at least 1 min, did not contain motion artifacts, and could be reliably analyzed (Fig. 2). After the detection of the end of a motion artifact, the next period started 5 s later so as to discard any residual abnormality in the EGG signal because of this last motion. An interval of 5 s was chosen after carefully examining initial recordings and demonstrating to our satisfaction that all tracings had returned to baseline within that time interval. Automatic analysis of the peaks detected in each artifact-free period was performed in each of the six EGG channels, providing the mean instantaneous frequency (reciprocal of the distance between two peaks) and the amplitude of each peak. The weighted mean of each of these parameters was then calculated for each 10- and 30-min interval (Figs. 4–6). All recordings were visually inspected to verify that no artifact remained in any selected period. Because the absolute value of EGG amplitude is influenced by exogenous factors such as electrode-skin resistance, tissue conductivity, and electrode distance to the stomach (7, 10), basal values (Table 1) were subtracted from postprandial values to obtain the change (Δ) in frequency and amplitude for each time interval (Figs. 4–6).

Statistical analysis. Results were expressed as means ± SE. An analysis of variance with repeated measures (33) was used to determine the effects due to meal, time, or channel on the time courses of emptying and EGG parameters. This statistical method takes into account the fact that measurements are repeated in the same animals over time by establishing a distinction between a factor that classifies the subjects into groups (grouping factor) and a factor for which each subject is measured at all levels (within-subject factor). Computer implementation of this statistical method was performed using locally developed programs. For the EGG, analysis of variance was performed first on the average of the six channels determined in each animal (1 value/animal, 6 values/meal) and second on all six channels considered simultaneously in each monkey (6 values/animal, 36 values/meal). This latter approach permitted subsequent testing of the effect of meal and time for each channel individually. A priori analysis (i.e., a test that is planned before collection of data) was conducted to examine the statistical significance of the effect of the meal at *time* t_i (simple effect of meals at each time). The significance of the difference of an EGG parameter after a meal compared with fasting was assessed using Dunnett's method for a posteriori multiple comparisons of individual mean values with a control (33).

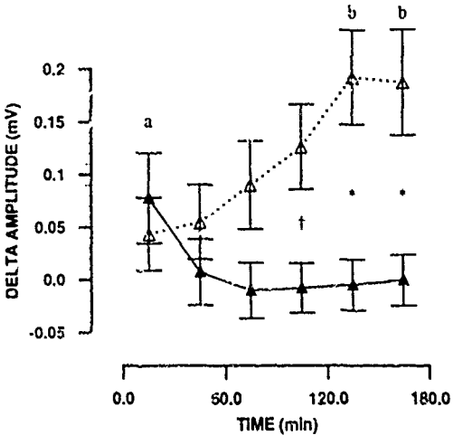

FIG. 4. Mean EGG Δamplitude in 6 rhesus monkeys after administration of LCM (1.5-kcal/kg meal; ▲) and HCM (5.0-kcal/kg meal; △). Fasting values were subtracted from postprandial values and these calculated Δamplitudes are represented as means ± SE. $^a P < 0.05$ for LCM compared with fasting, $^b P < 0.05$ for HCM compared with fasting. LCM compared with HCM: * $P < 0.01$; † $P < 0.05$.

In each monkey, a joint multivariate normal distribution of the variables was assumed to calculate an unbiased minimum variance estimate of the multiple correlation coefficient between FER and all six EGG channels taken concurrently (33). This coefficient is an estimate of the maximum correlation that can be attained between one variable (i.e., FER for each interval) and a linear combination of other variables (i.e., EGG amplitude in channels I–VI for the corresponding intervals). No weighting factors were applied among channels.

RESULTS

Effect of meals on gastric emptying. Emptying of liquids tended to be exponential after LCM and was approxi-

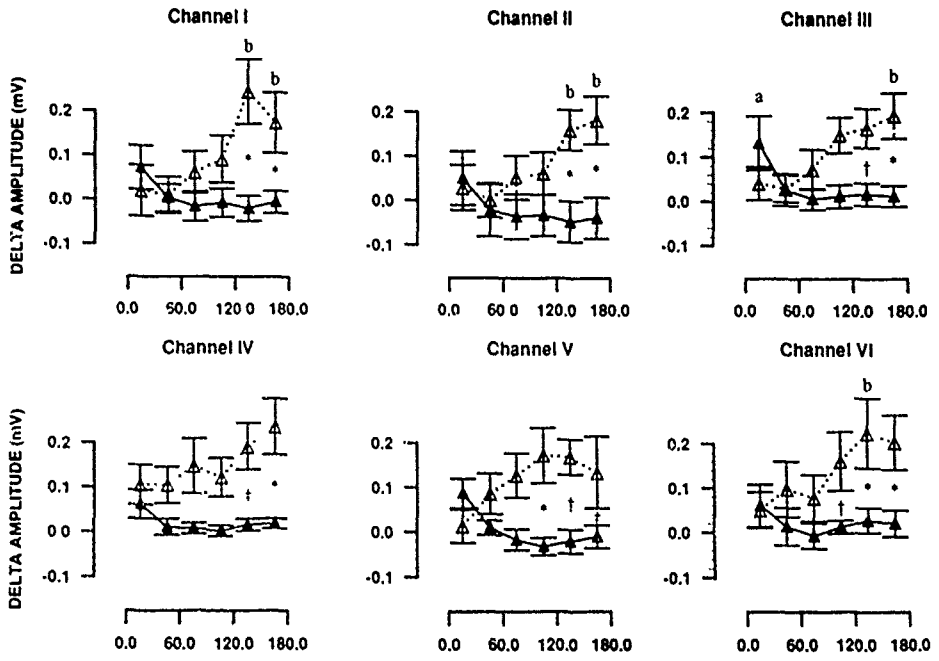

FIG. 5. Mean EGG Δamplitude in channels I–VI as recorded in 6 rhesus monkeys after administration of a 1.5- (▲) and a 5.0-kcal/kg meal (△). Fasting values were subtracted from postprandial values, and these calculated Δamplitudes were averaged in each monkey. Mean EGG Δamplitude values were then calculated for group of 6 monkeys and are represented as means ± SE. $^{a}P < 0.05$ for LCM compared with fasting; $^{b}P < 0.05$ for HCM compared with fasting. LCM compared with HCM: $^{*}P < 0.01$; $^{\dagger}P < 0.05$.

mately linear after HCM. The mean percentage of liquids remaining in the stomach after HCM was significantly higher compared with LCM from 16 to 180 min ($P < 0.05$; Fig. 3*A*). FER, when calculated for the entire curve using the power exponential model, was significantly less after HCM than after LCM (0.36 ± 0.08 vs. 2.99 ± 1.18%/min; $P < 0.05$). In addition, the coefficient β (representing the shape of the curve, especially during initial emptying) tended to be greater after HCM than after LCM, but the difference was not statistically significant (1.35 ± 0.22 vs. 0.84 ± 0.09; NS). Finally, the time course of emptying after the two meals was different: FER was significantly less after HCM than after LCM only from 0 to 60 min ($P < 0.05$; Fig. 3*C*), whereas it was similar after the two meals from 90 to 180 min.

Gastric emptying of solids was nonlinear after both meals. The percentage of solid markers remaining in the stomach was significantly greater after HCM than after LCM from 30 to 100 min (Fig. 3*B*). However, parameters for emptying were not significantly different between the two meals when FER calculated for the entire emptying curve (0.42 ± 0.22 vs. 0.26 ± 0.09; NS) and coefficient β (1.69 ± 0.74 vs. 2.73 ± 0.86; NS) were used. In contrast, FER was significantly ($P < 0.05$) greater after LCM than after HCM from 0 to 30 min (Fig. 3*D*), and FER decreased with time after LCM and increased with time after HCM.

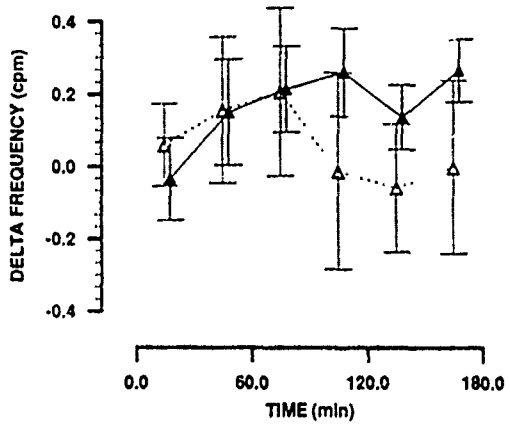

FIG. 6. Mean EGG Δfrequency in 6 rhesus monkeys after administration of a 1.5- (▲) and a 5.0-kcal/kg meal (△). Fasting values were subtracted from postprandial values, and these calculated Δfrequencies were averaged in each monkey. Mean EGG Δfrequencies were then calculated for group of 6 monkeys and are represented as means ± SE.

Fasting cutaneous EGG. As shown in Table 1, values for EGG parameters during fasting did not vary significantly among channels, although EGG amplitude was greatest in channel II and smallest in channel IV.

Effects of LCM on cutaneous EGG. Both average Δamplitude (i.e., the average of the means of the 6 channels in each animal) and Δamplitude in channel III increased significantly ($P < 0.05$) during the first 30 min after LCM compared with fasting and returned toward 0 from 30 to 180 min (Figs. 4 and 5, denoted by a). There was no statistically significant variation of either average or channel Δfrequency after LCM (Fig. 6).

TABLE 1. *Fasting EGG parameters*

Channel	Frequency, cpm	Amplitude, μV
I	3.79±0.14	143±33
II	3.80±0.18	156±37
III	3.79±0.15	124±20
IV	3.83±0.13	83±28
V	4.09±0.19	139±33
VI	4.13±0.24	131±29
Avg	3.90±0.08	131±29

Values are means ± SE of values obtained in 6 monkeys on 6 cutaneous bipolar derivations (channels I–VI; see Fig. 1 for disposition). Averages were obtained by calculating means of 6 channels in each animal and then average (± SE) of these means.

Effects of HCM on cutaneous EGG. Average and channel I and II Δamplitude increased significantly ($P < 0.05$) compared with fasting from 120 to 180 min after HCM (Figs. 4 and 5, denoted by b). In addition, a significant increase compared with that after fasting was observed in channel III from 150 to 180 min and in channel VI from 120 to 150 min (Fig. 5, denoted by b). There was no statistically significant variation of either average or individual channel Δfrequency after HCM (Fig. 6).

Difference between EGGs after two meals. Average and channel V and VI Δamplitude was significantly greater after HCM than after LCM from 90 to 180 min (Figs. 4 and 5). In addition, a significant difference was observed between the two meals from 120 to 180 min in channels I–IV (Fig. 5). Neither average nor channel Δfrequency was significantly different between the two meals (Fig. 6).

Correlations between FER and EGG parameters. EGG Δamplitude was significantly correlated with FER in all six monkeys for solids and in three of six monkeys for liquids (Table 2). EGG Δfrequency was significantly correlated with FER in two of the six monkeys for both solids and liquids.

DISCUSSION

Increasing the caloric contents of a meal has been shown to slow gastric emptying of both solids and liquids (13, 19). However, the exact role of gastric motility in the regulation of gastric emptying after mixed meals with various caloric loads remains unclear. After solid meals containing a fixed amount of calories, the average antral motility index was found to be directly correlated with emptying of solids and inversely correlated with the duration of the lag phase for emptying of solids (2). In addition, the rate of coordinated antral contractions was inversely correlated with the half time for emptying of solids (excluding the lag phase) (12). To further study the relation between emptying and gastric motility, we determined concurrently the time courses of emptying and EGG amplitude.

The EGG is believed to represent gastric motility, because experiments in which serosal or mucosal electrodes were used concurrently with cutaneous electrodes demonstrated the gastric origin of the 3/min component of the EGG (10, 16, 26, 27). Furthermore, both EGG amplitude and gastric motor activity increase at the time of appearance of ERA, which reflects mechanical activity (7, 10, 14, 26, 27). These observations were recently confirmed clinically by showing that the 3/min activity disappeared after gastrectomy but not after colectomy (21).

TABLE 2. *Correlation coefficients between fractional emptying rate and EGG amplitude*

	Monkey No.					
	1	*2*	*3*	*4*	*5*	*6*
Solids	0.48*	0.73*	0.48*	0.47*	0.51*	0.68*
Liquids	0.21	<0.10	<0.10	0.56*	0.73*	0.49*
df	31	25	26	32	26	32

Note that degrees of freedom (df) vary among animals because some intervals have no artifact-free windows for EGG in some monkeys. * $P < 0.01$.

The major technical difficulty that precluded extensive utilization of the cutaneous EGG in animals and in humans is its sensitivity to motion artifacts. Because this problem is most prominent with monopolar recordings, we obtained bipolar recordings as suggested by Van der Schee et al. (31). In addition, we used high-quality digital filtering to eliminate low- and high-frequency noise (10). Even so, we found that motion artifacts occasionally altered the EGG, and we excluded from analysis the periods during which the animal was not still. Another difficulty encountered by previous investigators was to determine the best number and the relative position of the cutaneous electrodes. In some studies, recordings were obtained from the epigastric sites that were producing the highest signal amplitude during a basal period (7). The disadvantages of this procedure are that it may enlarge interstudy variability and that the "basal" site may not remain important and relevant during the entire session. Therefore we placed seven electrodes in a hexagonal (also called "rosette") configuration (11, 17). This approach permitted a multidirectional mapping of the entire gastric area and allowed better interstudy reproducibility. Furthermore, the sensitivity to interindividual anatomic variations was reduced because the positioning of the electrodes was not based on the quality of the signal recorded during fasting.

In the past, the EGG has been analyzed using the fast Fourier transform technique, thus providing graphic illustration of the predominant frequencies by gray scale or pseudo-three-dimensional running spectrum (28, 30). However, these techniques seldom provided quantitative information regarding the amplitude of the EGG (7). In the present studies, we therefore used a different approach and developed a peak detection program to determine the amplitude and frequency of the EGG during 4-h studies. Using this time-domain method, we found that mean fasting amplitudes (Table 1) tended to be greater for the channels that corresponded approximately to the longitudinal axis of the corpus (channels I and II) and of the antrum (channels V and VI), although the difference was not statistically significant. After the meals, EGG amplitude varied significantly only in certain channels and only at specific times during the postprandial period (Fig. 5). These observations confirm that the EGG reflects vectorial projections of gastric activity onto different axes (17), similar to the way the ECG reflects projections of the electrical activity of the heart.

To our knowledge, minute-by-minute correlation between EGG amplitude and gastric emptying has not been previously investigated. By determining the FER for short intervals, we demonstrated that both gastric emptying and the EGG followed a time course that depended on the type of meal. As illustrated by the solid and dotted lines in Figs. 3, *C* and *D*, 4, and 5, peak values for both FER and EGG amplitude were reached during the immediate postprandial period after the 1.5-kcal/kg meal (LCM) and between 90 and 180 min after the 5-kcal/kg

meal (HCM). Previous studies using either power spectrum or qualitative analysis of recordings obtained in humans have also demonstrated significant increases in EGG amplitude during the early emptying period of barium or milk meals (7, 10, 15). Similar to our observation, one of these studies showed that the increase in EGG amplitude was followed by a return to fasting levels in about 30 min (10). Other studies in humans showed increases in EGG amplitude during the first 35 min (7) or 55 min after a 239-kcal meal (i.e., 3.4 kcal/kg) (31). In addition, the different postprandial responses of the EGG amplitude that we observed after different meals are analogous to the variations of the gastric motor activity described after different nutrient meals (8). Thus the early increase of EGG amplitude after LCM and the late increase of amplitude after HCM probably reflect increased gastric mechanical contractions that in turn may be responsible for the concurrent stimulation of gastric emptying.

Our demonstration of significant correlations between FER and EGG amplitude in a majority of animals agrees with the observation of postprandial increases in mechanical responses measured using intraluminal antral manometry (2) or implanted force transducers (8). Similarly, our finding that the frequency of the EGG was not significantly modified postprandially confirms observations in humans immediately after a barium or a nutritive meal using fast Fourier transform and visual analysis (14, 15). However, others observed a short-lasting postcibal decrease in frequency when using running spectrum analysis of EGGs obtained in humans (7, 31). This discrepancy could be due to differences in methodology or to the fact that we analyzed our results in 30-min intervals, which may average out an early and short-lasting change in frequency. The observation that amplitude was increased and frequency tended to be decreased 90 min after HCM (Figs. 4–6) may be related to the progressive occurrence of stronger antral contractions, because a similar association was seen in dogs both during fasting (25, 27, 30) and after solid nutrient meals (8, 27).

In summary, the present study documents the significant differences in the cutaneous EGG after two mixed solid-liquid caloric meals that empty at different rates, which indicate that the amplitude of postprandial EGG depends on the nutrient content of the meal. In addition, our observations that the amplitude of the EGG is significantly correlated with emptying indicates that further investigations are warranted to explore the possibility of using this noninvasive method for the study of gastric emptying.

The authors gratefully acknowledge the technical assistance of P. Curran, N. Fleming, M. Flynn, J. Stewart, and J. Warrenfeltz.

S. Bruley des Varannes was supported by a grant from SmithKline Beecham and by the Centre Hospitalier Regional et Universitaire de Nantes, France.

The opinions and assertions contained herein are the private ones of the authors and are not to be construed as official or reflecting the views of the Department of Defense, the Uniformed Services University of Health Sciences, or the Defense Nuclear Agency.

The experiments reported herein were conducted according to the principles set forth in the "Guide for the Care and Use of Laboratory Animals," Institute of Laboratory Animal Resources, National Research Council, HHS/NIH Publ. No. 85-23.

Address for correspondence: A. Dubois, Dept. of Medicine, Uniformed Services University of the Health Sciences, F. E. Hebert School of Medicine, 4301 Jones Bridge Rd., Bethesda, MD 20814-4799.

Received 16 February 1990; accepted in final form 14 March 1991.

REFERENCES

1. ABELL, T. L., AND J. R. MALAGELADA. Glucagon-evoked gastric dysrhythmias in humans shown by an improved electrogastrographic technique. *Gastroenterology* 88: 1932–1940, 1985
2. CAMILLERI, M., J.-R. MALAGELADA, M. L. BROWN, G. BECKER, AND A. R. ZINSMEISTER. Relation between antral motility and gastric emptying of solids and liquids in humans. *Am. J Physiol.* 249 (*Gastrointest Liver Physiol.* 12): G580-G585, 1985.
3. CHEN, J., J. VANDEWALLE, W. SANSEN, E. VAN CUTSEM, G. VANTRAPPEN, AND J. JANSSENS. Observations of phase shift from cutaneous electrogastrography. *Proc. IEEE Eng Med. Biol. Soc. 10th Int. Conf.* 10: 992–993, 1988.
4. DOOLEY, C. P., AND J. E. VALENZUELA. Antropyloroduodenal activity during gastric emptying of liquid meals in humans. *Am J Physiol.* 255 (*Gastrointest. Liver Physiol.* 18): G93-G98, 1988.
5. DUBOIS, A., J. P. JACOBUS, M. P. GRISSOM, R. R. ENG, AND J. J. CONKLIN. Altered gastric emptying and prevention of radiation-induced vomiting in dogs. *Gastroenterology* 86. 444–448, 1984.
6. ELASHOFF, J. D., T. J. REEDY, AND J. H. MEYER. Analysis of gastric emptying data. *Gastroenterology* 83: 1306–1312, 1982.
7. GELDOF, H., E. J. VAN DER SCHEE, M. VAN BLANKENSTEIN, AND J. L. GRASHUIS. Electrogastrographic study of gastric myoelectrical activity in patients with unexplained nausea and vomiting. *Gut* 27. 799–808, 1986
8. GILL, R. C., M. A. PILOT, P. A. THOMAS, AND D. L. WINGATE. Effect of feeding on motor activity of canine stomach. *Dig. Dis Sci* 34: 865–872, 1989.
9. GUETTA, O., J. HAMILTON, J. J. CONKLIN, AND A. DUBOIS. Interfacing the stomach with a computer, an automated analysis of gastric electrical activity. *Proc DECUS Soc Dallas, TX* p. 73–77, 1986.
10. HAMILTON, J. W., B. E. BELLAHSENE, M. REICHELDERFER, J. G. WEBSTER, AND P. BASS. Human electrogastrograms. Comparison of surface and mucosal recordings. *Dig. Dis. Sci.* 31. 33–39, 1986.
11. HÖLZL, R. Surface gastrograms as measures of gastric motility. In. *Psychophysiology of the Gastrointestinal Tract—Experimental and Clinical Applications*, edited by R. Holzl and W. E. Whitehead. New York: Plenum, 1983, p. 69–121.
12. HOUGHTON, L. A., N. W. READ, R. HEDDLE, M. HOROWITZ, P. J. COLLINS, B. CHATTERTON, AND J. DENT. Relationship of the motor activity of the antrum, pylorus, and duodenum to gastric emptying of a solid-liquid mixed meal. *Gastroenterology* 94: 1285–1291, 1988.
13. HUNT, J. N. Regulation of gastric emptying by neurohumoral factors and by gastric and duodenal receptors. In. *Esophageal and Gastric Emptying*, edited by A. Dubois and D. O. Castell. Boca Raton: CRC, 1984, p. 65–71.
14. KOCH, K. L., AND R. M. STERN. The relationship between the cutaneously recorded electrogastrogram and antral contractions in man. In. *Electrogastrography. Methodologies, Validation and Applications*, edited by R. M. Stern and K. L. Koch. New York. Praeger, 1985, p. 116–131.
15. KOCH, K. L., W. R. STEWART, AND R. M. STERN. Effect of barium meals on gastric electromechanical activity in man. A fluoroscopic-electrogastrographic study. *Dig. Dis. Sci.* 32. 1217–1222, 1987.
16. LAPORTE, J. L., L. O'CONNELL, A. DURAKOVIC, R. SJOGREN, J. J. CONKLIN, AND A. DUBOIS. Cross correlation analysis of gastric motility following exposure to ionizing radiation in primates (Abstract). *Dig. Dis Sci.* 29: 565, 1984.
17. MARTIN, A., AND J.-L. THILLIER. L'électrogastroentéro-graphie. *Presse Med.* 79: 1235–1237, 1971.
18. MEYER, J. H. Motility of the stomach and gastroduodenal junction. In: *Physiology of the Gastrointestinal Tract* (2nd ed.), edited by L. R. Johnson. New York: Raven, 1987, p. 613–629.

19. MOORE, J. G., P. E. CHRISTIAN, J. A. BROWN, C. BROPHY, F. DATZ, A. TAYLOR, AND N. ALAZRAKI. Influence of meal weight and caloric contents on gastric emptying of meals in man. *Dig. Dis. Sci.* 29: 513-519, 1984
20. PARASKEVOPOULOS, J. A., L. A. HOUGHTON, I. EYRE-BROOK, A. G. JOHNSON, AND N. W. READ. Effect of composition of gastric contents on resistance to emptying of liquids from stomach in humans. *Dig. Dis. Sci.* 33: 914-918, 1988.
21. PEZZOLLA, F., G. RIEZZO, M. A. MASELLI, AND I. GIORGO. Electrical activity recorded from abdominal surface after gastrectomy or colectomy in humans. *Gastroenterology* 97: 313-320, 1989.
22. RABINER, L. R., AND B. GOULD. *Theory and Application of Digital Processing.* Englewood Cliffs, NJ: Prentice-Hall, 1975, p. 136-140.
23. READ, N. W., AND L. A. HOUGHTON. Physiology of gastric emptying and pathophysiology of gastroparesis. *Gastroenterol. Clin. N. Am.* 18: 359-373, 1989.
24. SHIRES, J., N. FIALA, AND A. DUBOIS. Automatic motion detection in rhesus monkeys. *Proc. IEEE Eng Med. Biol. Soc. 10th Int. Conf.* 10: 1862-1863, 1988.
25. SMOUT, A. J. P. M., AND E. J. VAN DER SCHEE. Gastric pacemaker rhythm in conscious dogs. *Am. J Physiol.* 237 (*Endocrinol. Metab. Gastrointest Physiol* 6): E279-E282, 1979.
26. SMOUT, A. J. P. M., E. J. VAN DER SCHEE, AND J. L. GRASHUIS. What is measured in electrogastrography? *Dig. Dis. Sci.* 25: 179-187, 1980
27. SMOUT, A. J. P. M., E. J. VAN DER SCHEE, AND J. L. GRASHUIS. Postprandial and interdigestive gastric electrical activity in the dog recorded by means of cutaneous electrodes. In: *Gastrointestinal Motility*, edited by J. Christensen. New York: Raven, 1980, p. 187-194.
28. STERN, R. M., K. L. KOCH, H. W. LEIBOWITZ, AND I. M. LINDBLAD. Spectral analysis of tachygastria recorded during motion sickness. *Gastroenterology* 92: 92-97, 1987.
29. SZURSZEWSKI, J. H. Electrical basis for gastrointestinal motility. In: *Physiology of the Gastrointestinal Tract* (2nd ed.), edited by L. R. Johnson. New York: Raven, 1987, p. 383-422.
30. VAN DER SCHEE, E. J., AND J. L. GRASHUIS. Contraction-related, low-frequency components in canine electrogastrographic signals *Am. J. Physiol.* 245 (*Gastrointest. Liver Physiol.* 8): G470-G475, 1983.
31. VAN DER SCHEE, E. J., A. J. P. M. SMOUT AND J. L. GRASHUIS. Application of running spectrum analysis to electrogastrographic signals recorded from dog and man. In: *Motility of the Digestive Tract*, edited by M. Wienbeck. New York: Raven, 1982, p. 241-250.
32. WEIBULL, W. A statistical distribution function of wide applicability. *J. Appl. Mech.* 49: 293-297, 1951.
33. WINER, B. J. *Statistical Principles in Experimental Design* (2nd ed.). New York: McGraw-Hill, 1971.
34. WIRTH, N., D. SWANSON, B. SHAPIRO, M. NAKAJO, J. L. COFFEY, F. ECKHAUSER, AND C. OWYANG. A conveniently prepared Tc-99m resin for semisolid gastric emptying studies. *J. Nucl. Med.* 24: 511-514, 1983.
35. YOU, C. H., AND W. Y. CHEY. Study of electromechanical activity of the stomach in humans and in dogs with particular attention to tachygastria. *Gastroenterology* 86: 1460-1468, 1984.

INT. J. RADIAT. BIOL., 1991, VOL. 60, NO. 4, 613-626

Analysis by pulsed-field gel electrophoresis of DNA double-strand breakage and repair in *Deinococcus radiodurans* and a radiosensitive mutant

J. K. GRIMSLEY†, C. I. MASTERS‡, E. P. CLARK†
and K. W. MINTON‡§

†Department of Radiation Biochemistry, Armed Forces Radiobiology Research Institute, Bethesda, MD 20814-5145, USA
‡Department of Pathology, Uniformed Services University of the Health Sciences, Bethesda, MD 20814-4799, USA

(Received 3 July 1990; revision received 4 January 1991; accepted 18 March 1991)

Double-strand break (dsb) induction and rejoining after ionizing radiation was analysed in *Deinococcus radiodurans* and a radiosensitive mutant by pulsed-field gel electrophoresis. Following 2 kGy, migration of genomic DNA (not restriction cleaved) from the plug into the gel was extensive, but was not observed after 90 min postirradiation recovery. By this time *D. radiodurans* chromosomes were intact, as demonstrated by restoration of the *Not* I restriction cleavage pattern of 11 bands, which we found to be the characteristic pattern in unirradiated cells. Following the higher exposure of 4 kGy, dsb rejoining took approximately 180 min, twice as long as required following the 2 kGy exposure. Restoration of dsb in the radiosensitive mutant strain 112, which appears to be defective in recombination, was markedly retarded at both 2 and 4 kGy. The *Not* I restriction fragments of wild-type *D. radiodurans* and the radiosensitive mutant were identical, totaling 3·58 Mbp, equivalent to $2{\cdot}36 \times 10^9$ daltons per chromosome

1. Introduction

Members of the genus *Deinococcus* are extremely resistant to ionizing radiation (Moseley 1983, Murray 1986). *D. radiodurans* (formerly *Micrococcus radiodurans*, Brooks and Murray 1981) the most-studied species of this group, can tolerate several hundred double-strand breaks (dsb) per chromosome without any loss of viability or mutagenesis (Moseley 1983). Highly efficient dsb rejoining in this organism has been demonstrated by DNA viscosity measurements (Dean *et al.* 1966) and neutral sucrose velocity sedimentation (Kitayama and Matsuyama 1968 and 1971).

Recently, pulsed field gel electrophoresis (PFGE) has been employed to detect dsb in high molecular weight DNA (Contopoulou *et al.* 1987, Blocher *et al.* 1989, Ager *et al.* 1990, Stamato and Denko 1990). The various PFGE configurations have in common frequent alternations in the direction of the electric field. This permits resolution of larger DNA molecules than conventional gel electrophoresis, because the time required for the DNA to re-orient before it can migrate in the direction of the second electric field is a sensitive index of size for large DNA molecules (Lai *et al.* 1989). Resolution of the intact yeast chromosomes by PFGE permitted

§To whom correspondence should be addressed.

Contopoulou and co-workers (1987) to observe ionizing radiation-induced dsb in whole yeast chromosomes and their repair with postirradiation incubation. Other studies used various PFGE configurations to assay dsb in mammalian cell DNA. As mammalian chromosomes are much larger than yeast chromosomes, the breakage of individual chromosomes could not be studied. Instead, the total amount of DNA migrating from the agarose plug into the gel was measured (Blöcher *et al.* 1989, Stamato and Denko 1990) and the molecular weight distribution of the released DNA fragments approximated by electrophoretic mobility (Ager *et al.* 1990). These parameters could be correlated with the expected number of dsb in genomic DNA.

We now report the application of PFGE to the analysis of dsb and their repair in the DNA of the radioresistant bacterium *D. radiodurans*. To our knowledge this is the first example of the use of PFGE to detect dsb and their repair in bacteria. Because the chromosome of *D. radiodurans* is small, we have resolved it into 11 individual restriction-cleavage fragments. Following cellular irradiation, the extent of migration of unrestricted DNA from the agarose plug into the gel correlates with the appearance (or disappearance) of the individual restriction-cleavage fragments characteristic of the chromosome. Restoration of the restriction-cleavage fragments following irradiation provides additional evidence of proper chromosomal restoration. We have also examined repair of a radiosensitive mutant of *D. radiodurans* that is deficient in recombination, and find that dsb rejoining is retarded.

2. Materials and methods

2.1. *Culture conditions*

D. radiodurans strain R1 (wild-type) and its mutagenized derivative, strain 112, were grown at 32°C in TGY broth with aeration, or on TGY plates solidified with 1·5% agar (Tirgari and Moseley 1980).

2.2. *Ionizing radiation*

Aliquots of overnight cultures were dispensed into 75 cm^2 tissue culture flasks. The flasks were maintained on ice for 30 min prior to irradiation and during ^{60}Co irradiation. Irradiation was at 210 Gy/min. For example, 4 kGy (4×10^5 rad) required a 19 min exposure. For PFGE, irradiated cells were either harvested immediately or maintained at 32°C with aeration for various periods of time. For survival measurements, cells were diluted and plated on TGY agar immediately following irradiation. The plates were incubated at 32°C for 3 days prior to counting colonies.

2.3. *Ultraviolet irradiation*

Bacterial cultures were pelleted and resuspended in 67 mM phosphate buffer, pH 7·0 to a final OD_{600} of 0·4. Thin layers of bacterial suspension were irradiated with a germicidal lamp (254 nm) at room temperature, at a rate of 2·0 J/m^2 per second. Samples were taken at intervals, diluted and plated. The plates were incubated at 32°C for 3 days prior to counting colonies.

2.4. *Mitomycin C exposure*

Bacterial cultures were grown to an OD_{600} of 0·5 and resuspended in 1/6 volume of fresh TGY broth. Mitomycin C was added to a final concentration of

2 μg/ml and the suspension maintained at room temperature. Samples were taken at intervals, diluted and plated on TGY agar. Colonies were counted 3 days later.

2.5. *Transformation*

Preparation of genomic DNA from a spontaneous *rif*^{R} *D. radiodurans* mutant was previously described (Tirgari and Moseley 1980, Smith *et al.* 1988). Transformation was by the method of Tirgari and Moseley (1980). Briefly, 300 μl of recipients (approximately $1{\cdot}5 \times 10^8$ cells) in fresh TGY were rendered competent by the addition of $CaCl_2$, 30 mM final concentration. The suspension was held on ice for 10 min, and 10 μl aliquots of varying concentrations of transforming DNA were added and mixed gently for 90 min at 32°C. Five millilitres of TGY was added and the suspension incubated overnight to permit phenotypic expression. Dilutions were plated onto TGY agar without rifampicin and TGY agar containing 25 μg/ml rifampicin. Colonies were counted after 3 days of incubation at 32°C.

2.6. *Pulsed-field gel electrophoresis*

D. radiodurans cultures were pelleted by centrifugation for 10 min, resuspended in butanol-saturated phosphate buffer, pelleted and washed once in a butanol-free solution of 1 M NaCl, 10 mM Tris, pH 7·6, and then resuspended again in this solution at 2×10^9 cells/ml. The exposure to butanol-saturated buffer described above terminates rejoining in irradiated cells and renders *Deinococcus* cells sensitive to lysozyme degradation (Driedger and Grayston 1970). Subsequent steps for preparation of intact chromosomal DNA, suitable for PFGE, were described elsewhere (Smith and Cantor 1987). Briefly, the *D. radiodurans* cell suspension was mixed with an equal volume of 2% low melting point agarose and allowed to solidify in a mould that formed plugs of approx. 2 × 2 × 20 mm. Cell lysis, DNA purification, and restriction enzyme digestion were carried out by transferring the agarose plugs into a series of solutions. Because the DNA is immobilized in the agarose plug, shearing of large DNA molecules is minimized. Treatment of the plugs included an overnight incubation at 37°C with a lysis solution containing 0·2% sodium dodecyl sulphate and 1 mg/ml lysozyme; a 2-day incubation at 50°C in 1% sarcosyl and 1 mg/ml proteinase K; and a 6–10 h incubation at 37°C with 30 units of *Not* I restriction enzyme in a total volume of 100 μl. This yields a *Not* I limit digest, as longer incubation or additional *Not* I enzyme did not produce increased cleavage of chromosomal DNA measured by PFGE (not shown). An LE agarose gel was cast (1%, Beckman Low Endo-osmosis; LE) measuring 10 cm long × 7·6 cm wide × 0·64 cm thick, and containing nine wells. The 2 × 2 × 20 mm DNA-containing plug was sliced perpendicular to its long axis to yield plugs of approx. 2 × 2 × 4 mm. These slices were placed in the bottom of the wells of the LE agarose gel such that the long axis of the plug was parallel to the width of the gel, and sealed in place by the addition of a small amount of LE agarose. Each well contained $1{\cdot}3 \times 10^8$ cells, equal to approximately 2 μg of DNA.

PFGE was performed with a transverse alternating field electrophoresis (TAFE) unit. The TAFE apparatus, yeast chromosomal standards and neutral running buffer (10 mM Tris, 0·5 mM EDTA, and 4·4 mM acetic acid, pH 8·0) were from Beckman Instruments, Palo Alto, CA. The TAFE apparatus is a modification of that developed by Gardiner and co-workers (1986). Briefly, the gel is positioned vertically within the chamber, with electrodes placed on either side so that each lane is subjected to the same electric field. Two electrode pairs (20 cm between positive

and negative electrodes of each pair) produce two alternating fields with an angle between fields of 115°. The alternating fields cause the DNA to zigzag through the thickness of the gel, resulting in straight lanes. Electrophoresis of *Deinococcus* DNA was at 150 mA constant current (approx. 240 V), with field alternation every 25 s for 20 h at 12°C. Gels were stained in running buffer containing 0·1 μg/ml ethidium bromide and viewed on a transilluminator (Fotodyne, New Berlin, WI). Using these conditions the largest *Not* I restriction fragment of the *D. radiodurans* R1 chromosome migrated 1·9 cm, while the smallest migrated 5·3 cm.

2.7. *Densitometry*

Gels were photographed with type 55 Polaroid film. All gels were photographed several times using different exposures. Negatives used for densitometry were lightly exposed. Those positives shown as figures (Figures 5, 6 and 10) are overexposed to render the low molecular weight restriction fragments and other faint areas within the lane clearly visible by eye. Negatives were densitometrically scanned (Hoefer model GS300 transmittance and reflectance scanning densitometer) using transmittance mode, and data collected and plotted using a Shimadzu C-R1B Chromatopac. Areas under the peaks were determined by cutting out and weighing the appropriate regions of the plot. To avoid possible artifacts due to lane-to-lane variability in the amount of DNA loaded in the plug, the amount of DNA in the lane and the amount in the plug (as plotted in Figure 9) are expressed as a fraction of the amount of DNA in the well plus the lane, rather than as an absolute value.

3. Results

3.1. *Ionizing radiation sensitivity of* D. radiodurans *strain* 112

D. radiodurans strain R1 is the type strain of the genus *Deinococcus* (Murray 1986). Strain 112 is a strain R1-derivative obtained by chemical mutagenesis and characterized by Evans (1985) as non-transformable and sensitive to ultraviolet radiation and mitomycin C (MMC). This strain had been desiccated and stored since 1984 at room temperature in the laboratory of B. E. B. Moseley at the University of Edinburgh. For this study, strain 112 was revived and its phenotype verified (Figures 1-3). These results are essentially identical to those obtained by Evans (1985), confirming the non-transformability and sensitivity to ultraviolet radiation

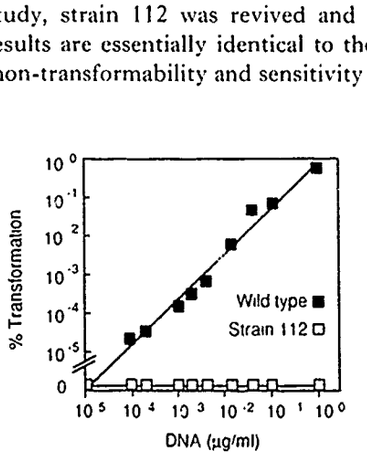

Figure 1. Transformation of *D. radiodurans* to rifampicin resistance by homologous genomic DNA.

and MMC. The apparent deficiency in recombination in strain 112 (as suggested by non-transformability) prompted us to assess the sensitivity of this strain to ionizing radiation (Figure 4). Compared to wild-type, strain 112 is markedly sensitive to ionizing radiation, possibly related to reduced ability to perform recombination. In an attempt to elucidate the basis of the ionizing radiation sensitivity of strain 112, this strain and wild-type *D. radiodurans* were compared with regard to double-strand break rejoining capacity, as described below.

3.2. *Size of* D. radiodurans *R1 chromosome*

The *Not* I restriction enzyme recognizes the 8 base palindrome 5'..GC/GGCCGC..3' (Roberts 1984). Consequently, it cleaves genomic DNA much less frequently than other type II restriction endonucleases that recognize shorter palindromes. *Not* I resolves the *Escherichia coli* genome into 22 separate restriction fragments (Smith *et al.* 1987). We found that this enzyme digested the *D. radiodurans* R1 chromosome into 11 separate restriction fragments. These fragments could be widely separated by using both prolonged electrophoresis times and switching intervals, allowing determination of the sizes of the 11 fragments: 498, 418, 388, 365, 320, 307, 303, 277, 253, 230, and 216 kbp, totalling 3·58 Mbp or $2{\cdot}36 \times 10^9$ daltons per chromosome.

For practical purposes, in the strand break studies we employed a short electrophoresis time (20 h) and switching interval (25 s), that permitted resolution of the restriction fragments; however, under these conditions restriction fragments 2 and 3 were often poorly separated (Figure 5). *Not* I-cleaved genomic DNA from wild-type R1, and the R1-derivative, strain 112, were identical (Figure 5 and unpublished results).

3.3. *Ionizing radiation-induced release of DNA from agarose plugs without restriction cleavage*

Wild-type and strain 112 were exposed to 2 kGy and either harvested immediately or maintained at 32°C for recovery periods up to 6 h prior to harvesting. Restriction cleavage was omitted from preparation of the agarose plugs for PFGE. Results are shown in Figure 6 (lower panels), Figure 7, and Figure 9 (upper panels). The lower panels of Figure 6 are gel photographs that show release of DNA from agarose plugs made from wild-type and strain 112 cultures. Figure 7 shows densitometric scans performed on negatives of these gels that were briefly exposed

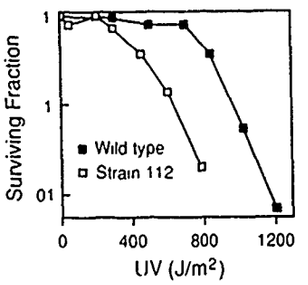

Figure 2. Survival of *D. radiodurans* following exposure to UV.

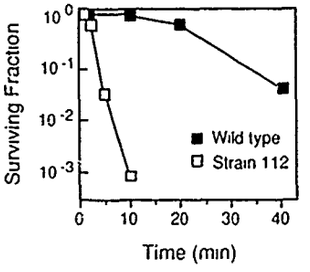

Figure 3. Survival of *D. radiodurans* following exposure to 2 μg/ml mitomycin C.

(as compared to the higher exposures shown in Figures 5, 6 and 10) as described in §2. The upper panels of Figure 9 show the fractions of DNA retained in the wells and migrating into the lane determined from scans in Figure 7.

Irradiation of *D. radiodurans* strains R1 and 112 resulted in a substantial amount of cellular DNA migrating from the plug into the gel (Figure 6, lower panels, zero min lanes; Figure 7, zero min), corresponding to approximately 80% of total cellular DNA (Figure 9, upper left). With postirradiation recovery, less DNA migrated into the gel. For wild-type, densitometry showed that the amount of DNA in the lane was reduced to background levels by 60-90 min following irradiation (Figure 7). In Strain 112, postirradiation incubation resulted in a much slower disappearance of DNA from the lanes, with substantial amounts of DNA remaining in the lane in the 180 min and, to a lesser extent, the 6 h postirradiation recovery samples (Figure 6, lower right; Figure 7; Figure 9, upper left). The decrease of DNA migrating into the lane as a result of postirradiation incubation is consistent with cellular repair of dsb (Blocher *et al.* 1989), and the slow time-course in strain 112 suggests a defect in dsb repair.

3.4. *Ionizing radiation-induced release of DNA from agarose plugs treated with* Not *I restriction enzyme*

As above, wild-type and strain 112 cells were exposed to 2 kGy and harvested at various times thereafter. In addition to the usual preparation of the agarose plugs, the plugs were also incubated with *Not* I under limit digest conditions (see §2).

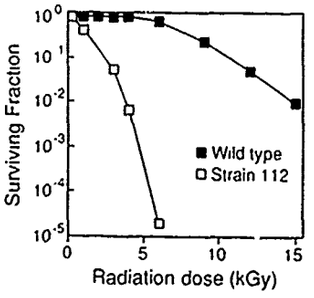

Figure 4. Survival of *D. radiodurans* following ionizing radiation exposure.

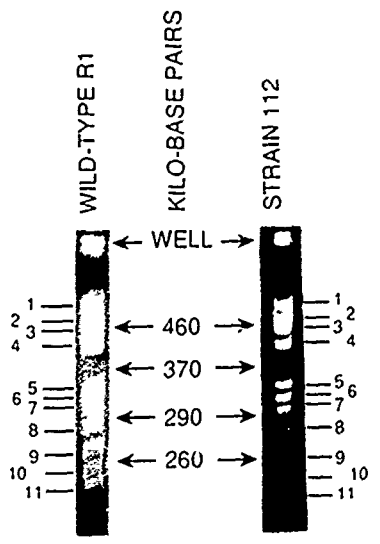

Figure 5. PFGE of *Not* I-cleaved genomic DNA of *D. radiodurans* strain R1 (wild-type), and the radiosensitive R1-derivative, strain 112. The size markers represent approximate location of yeast chromosomal standards.

Results are shown in Figure 6 (upper panels), Figure 8, and Figure 9 (lower panels). Like plugs that were not treated with restriction enzyme, a 2 kGy exposure of wild-type and strain 112 with no postirradiation incubation resulted in the release of approximately 80% of the DNA into the lane (Figure 9, lower left). Visually (Figure 6, upper panels, zero min lanes) this is not as obvious as in the case of no restriction digestion (Figure 6, lower panels, zero min), due to different photographic exposures. However, the release of a large fraction of DNA into the lanes is apparent via densitometry (Figure 8, zero min). The distribution of DNA fragments in the *Not* I-cleaved samples at zero min for both wild-type and strain 112 was shifted to the lower molecular weight region as compared to samples that were not restriction cleaved (compare Figures 7 and 8, zero min), possibly due to *Not* I cleavage of the larger DNA fragments remaining after irradiation.

In plugs of wild-type samples that were treated with *Not* I there was a substantial reduction in the amount of DNA in the lane as a result of 30 or 60 min postirradiation recovery (Figure 8; Figure 9, lower left). Strain 112 DNA plugs treated with *Not* I showed a slower reduction of DNA migrating into the lane as a function of postirradiation recovery through 60 min (Figure 9, lower left). Plugs made from wild-type cells following 90 min, 180 min, or 6 h postirradiation incubation release more DNA into the lane than plugs made from strain 112, due to the migration of restriction fragments from wild-type DNA plugs into the gel (Figure 6, upper panels; Figure 8; Figure 9, lower panels). The faint banding pattern detected in the strain 112 *Not* I-cleaved zero min point and subsequent times (Figure 6, upper right) may be due to small amounts of DNA that have not sustained dsb following irradiation. At lower exposures (e.g. 1 kGy) such bands were usually detectable at zero min (not shown). At 2 kGy, damage was sufficient to render these restriction fragments at zero min undetectable (e.g. Figure 6, upper left) or barely detectable (e.g. Figure 6, upper right). As expected, at higher

exposures residual restriction fragments were never detected at zero min (e.g. Figure 10).

After a 4 kGy exposure, *Not* I-cleaved DNA from wild-type cells showed extensive migration of DNA into the gel (Figure 10, left). Restriction cleavage with *Not* I did not yield the typical restriction digest pattern until 180 min, twice as long as that required for 2 kGy. Following 4 kGy, the radiosensitive strain 112 showed no evidence of dsb rejoining at 6 h, and after overnight incubation only a faint suggestion of some restriction fragments (Figure 10, right).

4. Discussion

4.1. *Size of* D. radiodurans *R1 chromosome*

We found that *Not* I digested the *D. radiodurans* R1 chromosome into 11 separate restriction fragments, totaling 3·58 Mbp or $2{\cdot}36 \times 10^9$ daltons per chromosome. The complexity of the *D. radiodurans* genome was measured by Hansen (1978) by DNA renaturation kinetics, yielding a complexity of $2{\cdot}0 \pm 0{\cdot}3 \times 10^9$ daltons. Our electrophoretic measurement is slightly larger than the upper limit of Hansen's complexity measurement. We have recently found that *D. radiodurans* strains SARK and R1 contain a specific repetitive DNA sequence present in about

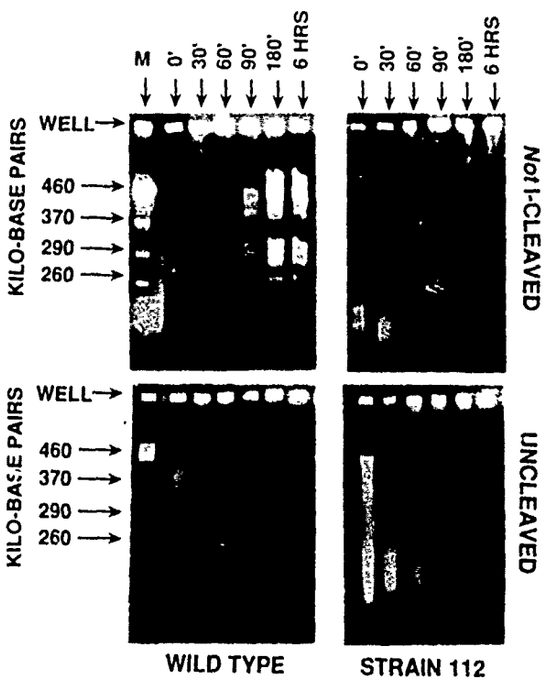

Figure 6. PFGE of genomic DNA of *D. radiodurans* following ^{60}Co irradiation of 2 kGy. Time refers to the postirradiation recovery period. The size markers are yeast chromosomal standards. Upper left: strain R1 (wild-type) DNA cleaved with *Not* I prior to PFGE; upper right: strain 112 DNA cleaved with *Not* I prior to PFGE; lower left: strain R1 (wild-type) DNA with no restriction cleavage; lower right: strain 112 DNA with no restriction cleavage.

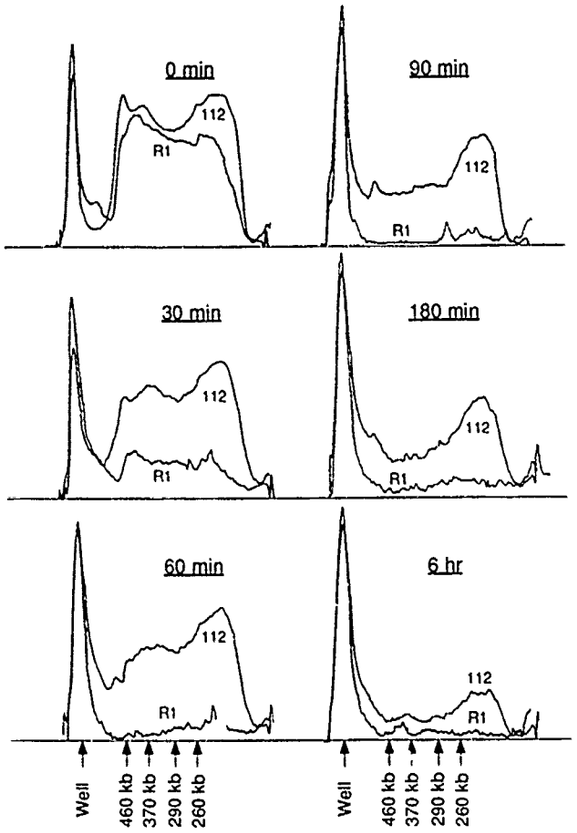

Figure 7. Densitometric trace of negatives of PFGE results shown in lower panels of Figure 6 (no restriction cleavage of DNA). Times refer to duration of postirradiation recovery prior to harvesting of cells. Location of well and yeast chromosomal markers indicated at bottom. R1: *D. radiodurans* strain R1 (wild-type); 112: R1-derivative strain 112.

50 copies per chromosome (Lennon and Minton 1990, and unpublished results). Reduction of chromosomal complexity by the presence of repeated DNA is expected (Gillis *et al.* 1970), and may have contributed to the slightly smaller size that Hansen determined by renaturation kinetics.

4.2. *Upper limit of DNA that may be released from the plug*

A significant percentage of DNA was not released from plugs made from cells irradiated at 2 kGy or 4 kGy, including plugs made from cells with no postirradiation recovery, either with or without *Not* I cleavage prior to PFGE (zero min lanes of Figures 6 and 10). Given the high degree of damage following irradiation, migration of all DNA from the plug into the gel might be expected. This 'non-elutable' fraction was about 20% of total DNA (Figure 9, right). Similar observations have been made by others using PFGE, and various mechanisms proposed,

including radiation-induced crosslinking of DNA to itself or other molecules (Ager *et al.* 1990), and 'trapping' of some DNA fragments in the agarose plug, such that they are not susceptible to migration (Stamato and Denko 1990). We observed much greater amounts of residual DNA in the plug using the unmodified Smith and Cantor (1987) protocol for preparation of bacterial DNA in agarose plugs. *D. radiodurans* is resistant to lysozyme (Driedger and Grayston 1970). Driedger and Grayston found that washing cells with butanol-saturated buffer prior to lysozyme exposure renders *D. radiodurans* sensitive to this enzyme, possibly due to the removal of lipoproteins. By modifying the Smith and Cantor protocol to include this procedure prior to embedding cells in agarose, the 'non-elutable' fraction was minimized. Even with this modification some degree of incomplete protoplastation might persist, contributing to residual DNA in the plug.

4.3. *Restoration of restriction digest fragments lags behind diminution of DNA in the lane*

In samples from wild-type cells exposed to 2 kGy (no restriction digestion) the fraction of DNA present in the lanes was substantially reduced by 30 and 60 min

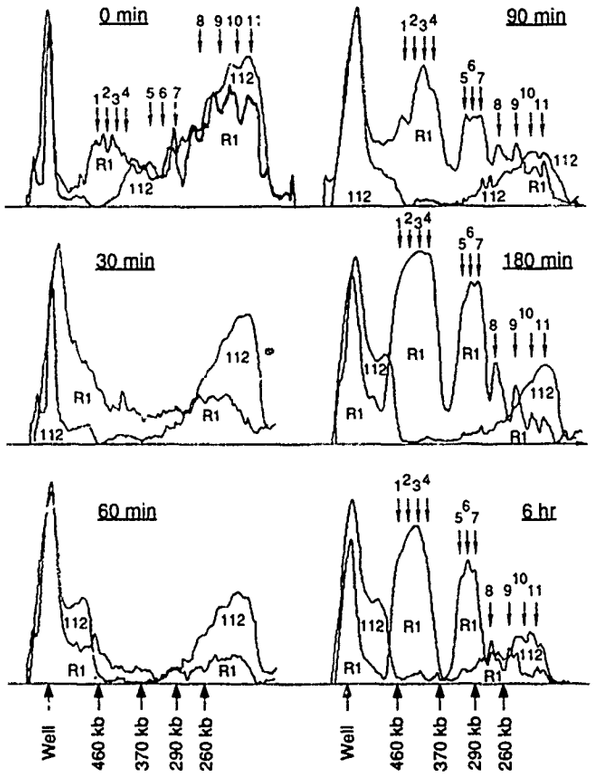

Figure 8. Densitometric trace of negatives of PFGE results shown in upper panels of Figure 6 (plugs treated with *Not* I prior to PFGE). Designations as for Figure 7. In addition the locations of the 11 *Not* I restriction fragments of the *D. radiodurans* R1 chromosome are indicated by vertical arrows; '1' refers to the largest restriction fragment, and '11' is the smallest restriction fragment.

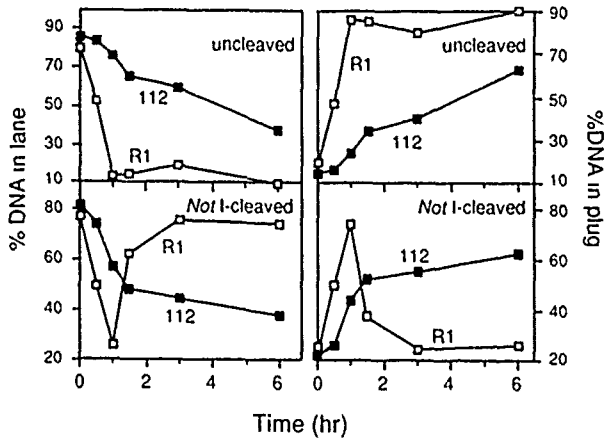

Figure 9. Percentage of total DNA remaining in the lane (left) and in the plug (right). Each are expressed as a fraction of total DNA in lane plus plug. Calculated from densitometric scans as described in § 2. DNA migrating above the upper electrophoretic compression zone was included in the measurement of the amount of DNA in the lane. Time refers to duration of postirradiation incubation prior to harvesting. Upper panels: correspond to Figure 7 (no restriction clevage); lower panels: correspond to Figure 8 (*Not* I-treated plugs); ■, strain 112; □, strain R1 (wild-type).

postirradiation recovery prior to harvesting of cells for PFGE (Figure 7; Figure 9, upper left), presumably due to repair. However, in corresponding wild-type samples that *were* treated with *Not* I, there was a similar reduction in the fraction of DNA migrating into the lanes at these early time points (30 and 60 min; Figure 8; Figure 9, lower left) and there was no evidence of restriction fragments in the gel

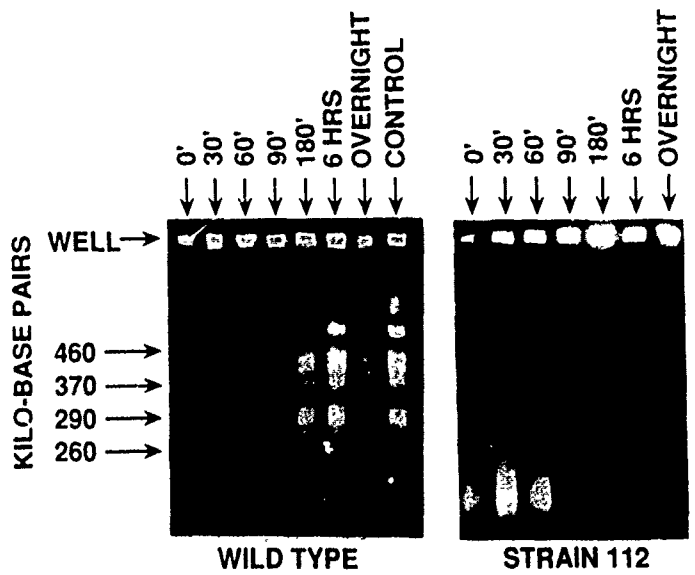

Figure 10. PFGE of *Not* I-cleaved genomic DNA of *D. radiodurans* following ^{60}Co irradiation of 4 kGy. Time refers to the postirradiation recovery period. Left: strain R1 (wild-type); right: strain 112.

(30 and 60 min; Figure 6, upper left; Figure 8). Thus, any ostensibly repaired DNA accumulating in cells as the result of the 30 or 60 min postirradiation recovery periods does not appear to be subject to restriction enzyme digestion and/or electrophoretic migration at these early times. Ager and co-workers (1990) found that following irradiation of CHO-K1 cells, replication forks showed reduced PFGE-induced migration out of the plug. One possible mechanism accounting for this observation is that DNA in a branched-replicating structure retards electrophoretic migration. If so, this mechanism may be applicable in the current case. If recovery from high levels of damage following 2 kGy proceeds via recombination, it would be anticipated that much, if not all, of the larger fragments will be associated with branched and looped structures during postirradiation recovery. Consequently, the increased fraction of DNA in the plug at early time points probably represents DNA undergoing recombinational repair rather than DNA that has completed repair. According to this view, only as cellular DNA is restored to normal conformation would restriction digestion yield discrete unbranched restriction fragments of characteristic electrophoretic mobility, as seen later at 90 min, 180 min and 6 h postirradiation of wild-type cells (Figure 6, upper left; Figure 8). As predicted by this model, the amount of DNA in the plug (visually in Figure 6, upper left; plotted in Figure 9, lower right) increases during the 0-60 min postirradiation incubation interval, and then, once the *Not* I-cleaved DNA becomes subject to electrophoretic migration, the amount of DNA in the plug decreases, as seen during the 90 min-6 h interval.

4.4. *All restriction fragments appear simultaneously*

The current results suggest that all restriction fragments appear simultaneously in wild-type samples at 90 min following 2 kGy (Figure 6, upper left; Figure 8) and 180 min following 4 kGy (Figure 10, left). This observation could be the result of processive repair. Recombinational complexes formed following irradiation of *D. radiodurans* may not be resolved at random times. Instead, recombinational complexes might be resolved on a chromosome-by-chromosome basis, with recombination proteins not released until a circular chromosome is restored. Thus, new restriction fragments following *Not* I digestion would appear in 1:1 stoichiometry. As more chromosomes are restored the fraction of DNA that migrates increases with time, with all restriction fragments in equimolar quantity (larger fragments being brighter due to the amount of ethidium bromide bound) as seen following 2 kGy over the 90-180 min postirradiation recovery interval (Figure 6, upper left; Figure 7; Figure 9, lower left).

An alternative explanation for the simultaneous appearance of all restriction fragments is that resolution of recombinational complexes might be subject to a rate-limiting event, such that the great majority of covalent rejoining occurs over a brief period. Thus, rapid resolution of pre-existing complexes would yield the impression that all restriction fragments are restored simultaneously. It is known that inhibition of protein or RNA synthesis following irradiation strongly inhibits dsb rejoining (Kitayama and Matsuyama 1968, 1971). One potential candidate for the rate-limiting event is the duration required to transcriptionally induce and synthesize proteins required for completion of repair. As no other studied organism approaches the *Deinococcus* spp. in their ability to mend very large numbers of dsb per chromosome, the nature of any rate-limiting step(s) in such repair remains highly speculative.

4.5. *Defect in strain 112*

Following exposure of radiosensitive strain 112 cells to 2 kGy or 4 kGy, treatment of plugs with *Not* I failed to regenerate the characteristic PFGE restriction digest pattern in samples from all postirradiation time points examined (Figure 6, upper right; Figure 8; Figure 10, right). However, the fraction of DNA retained in the well increased, and DNA in the lane decreased, as a result of postirradiation incubation. In the case of 2 kGy this is visually apparent as increased fluorescence in the wells at latter postirradiation recovery times (Figure 6, upper right) and confirmed by densitometry (Figure 8, 180 min and 6 h; Figure 9, lower right). At later times there are also substantial amounts of DNA of indeterminate size above the upper electrophoretic compression zone (60 min through 6 h in Figures 6 and 8). Following 4 kGy, increased DNA in the plug as the result of postirradiation recovery is visually apparent (Figure 10, right). As suggested for wild-type at the early times of 30 and 60 min, in strain 112 the increased amount of DNA in the wells (and upper compression zone) resulting from postirradiation incubation may not represent repaired DNA. Instead it may consist of DNA fragments associated in unresolved recombinational complexes and/or misrepaired DNA. Unlike wild-type cells, strain 112 may not be able to resolve recombinational complexes readily, contributing to the progressive accumulation of DNA in plugs during the postirradiation incubation time course that was studied.

The observation of Evans (1985) that strain 112 was non-transformable (Figure 1) prompted us to assess the ionizing radiation resistance of this strain, which was substantially reduced (Figure 4). As transformation requires successful completion of recombination of exogenous homologous DNA with the host chromosome, it has been used in naturally transformable organisms as a measurement of recombinational proficiency (Moseley 1983). Experiments here described indicate that the radiosensitivity of strain 112 can be attributed, in sum or in part, to diminished dsb repair. In turn, we suggest that diminished dsb repair in strain 112 is due to a defect in a specific recombinational function that is also required for transformation.

Acknowledgements

We thank Bevan E. B. Moseley for strain 112. C.I.M. and K.W.M. are supported by USPHS Grant GM39933.

References

Ager, D. D., Dewey, W. C., Gardiner, K., Harvey, W., Johnson, R. T. and Waldren, C. A., 1990, Measurement of radiation-induced DNA double-strand breaks by pulsed-field gel electrophoresis. *Radiation Research*, **122**, 181–187.

Blöcher, D. Einspenner, M. and Zajackowski, J., 1989, CHEF electrophoresis, a sensitive technique for the determination of DNA double-strand breaks. *International Journal of Radiation Biology*, **56**, 437–448.

Brooks, B. W. and Murray, R. G. E., 1981, Nomenclature for '*Micrococcus radiodurans*' and other radiation-resistant cocci: *Deinococcaceae* fam. nov. and *Deinococcus* gen. nov., including five species. *International Journal of Systematic Bacteriology*, **31**, 353–360.

Contopoulou, C. R., Cook, V. E. and Mortimer, R. K., 1987, Analysis of DNA double strand breakage and repair using orthogonal field alternation gel electrophoresis. *Yeast*, **3**, 71–76.

Dean, C. J., Feldschreiber, P. and Left, J. T., 1966, Repair of x-ray damage to the deoxyribonucleic acid in *Micrococcus radiodurans*. *Nature*, **209**, 49–52.

DRIEDGER, A. A. and GRAYSTON, M. J., 1970, Rapid lysis of cell walls of *Micrococcus radiodurans* with lysozyme: effects of butanol pre-treatment on DNA. *Canadian Journal of Microbiology*, **16**, 889-893.

EVANS, D. M., 1985, Repair of DNA damage in *Deinococcus radiodurans*. Ph.D. thesis, University of Edinburgh.

GARDINER, K., LAAS, W. and PATTERSON, D., 1986, Fractionation of large mammalian DNA restriction fragments using vertical pulsed-field gradient gel electrophoresis. *Somatic Cell and Molecular Genetics*, **12**, 185-195.

GILLIS, M., DE LEY, J. and DE CLEENE, M., 1970, The determination of molecular weight of bacterial genome DNA from renaturation rates. *European Journal of Biochemistry*, **12**, 143-153.

HANSEN, M. T., 1978, Multiplicity of genome equivalents in the radiation-resistant bacterium *Micrococcus radiodurans*. *Journal of Bacteriology*, **134**, 71-75.

KITAYAMA, S. and MATSUYAMA, A., 1968, Possibility of the repair of double strand scissions in *Micrococcus radiodurans* DNA caused by gamma-rays. *Biochemical and Biophysical Research Communications*, **33**, 418-422.

KITAYAMA, S. and MATSUYAMA, A., 1971, Double-strand scissions in DNA of gamma-irradiated *Micrococcus radiodurans* and their repair during postirradiation incubation. *Agricultural and Biological Chemistry*, **35**, 644-652.

LAI, E., BIRREN, B. W., CLARK, S. M., SIMON, M. I. and HOOD, L., 1989, Pulsed field gel electrophoresis. *Biotechniques*, **7**, 34-42.

LENNON, E. and MINTON, K. W., 1990, Gene fusions with *lacZ* by duplication insertion in the radioresistant bacterium *Deinococcus radiodurans*. *Journal of Bacteriology*, **172**, 2955-2961.

MOSELEY, B. E. B., 1983, Photobiology and radiobiology of *Micrococcus (Deinococcus) radiodurans*. *Photochemical and Photobiological Reviews*, **7**, 223-275.

MURRAY, R. G. E., 1986, The biology and ecology of the *Deinococcaceae*. *Perspectives in Microbial Ecology*, edited by F. Megusar and M. Gantar (Proc. IV. Int. Symp. Microbial Ecology), pp. 153-158.

ROBERTS, R. J., 1984, Restriction and modification enzymes and their recognition sequences. *Nucleic Acids Research*, **12**, r167-r204.

SMITH, C. L. and CANTOR, C. R., 1987, Purification, specific fragmentation and separation of large DNA molecules. *Methods in Enzymology*, **155**, 449-467.

SMITH, C. L., ECONOME, J. G., SCHUTT, A., KLCO, S. and CANTOR, C. R., 1987, A physical map of the *Escherichia coli* K12 genome. *Science*, **236**, 1448-1453.

SMITH, M. D., LENNON, E., MCNEIL, L. B. and MINTON, K. W., 1988, Duplication insertion of drug resistance determinants in the radioresistant bacterium *Deinococcus radiodurans*. *Journal of Bacteriology*, **170**, 2126-2135.

STAMATO, T. D. and DENKO, N., 1990, Assymetric field inversion gel electrophoresis: a new method for detecting DNA double-strand breaks in mammalian cells. *Radiation Research*, **121**, 196-205.

TIRGARI, S. and MOSELEY, B. E. B., 1980, Transformation in *Micrococcus radiodurans*: measurement of various parameters and evidence for multiple, independently segregating genomes per cell. *Journal of General Microbiology*, **119**, 287-297.

INT. J. RADIAT. BIOL., 1991, VOL. 59, NO. 5, 1217–1226

Radioprotective properties of DNA methylation-disrupting agents

J. F. KALINICH†, G. N. CATRAVAS and S. L. SNYDER‡

Radiation Biochemistry Department, Armed Forces Radiobiology Research Institute, Bldg. 42, NNMC-NCR, Bethesda, MD 20889-5145, USA

(Received 1 August 1990; revision received 22 November; accepted 28 November 1990)

5-Azacytidine and sodium butyrate, two DNA methylation-disrupting agents, were tested for radioprotective properties on V79A03 cells. Both compounds can activate genes not previously expressed (e.g. metallothionein). 5-Azacytidine treatment (3 μM, 24 h) caused a 50% decrease in the 5-methylcytosine content of V79A03 DNA whereas sodium butyrate treatment (1 mM, 24 h) resulted in a 700% increase in 5-methylcytosine content. Additionally, 5-azacytidine treatment resulted in the increased survival of V79A03 cells, with treatment 24 h prior to exposure to gamma radiation providing a dose reduction factor of 1·8. Sodium butyrate treatment did not result in a significant increase in survival. These results indicate that the hypomethylation of genomic DNA prior to exposure to gamma radiation correlates with an increase in survival of V79A03 cells, possibly due to the activation of the enzymes involved in repair.

1. Introduction

The methylation of cytosine residues in DNA has been shown to be involved in several cellular processes including gene expression, carcinogenesis, and DNA repair. The hypomethylation of DNA can result in the activation of normally quiescent genes (Compere and Palmiter 1981), whereas methylated genes tend not to be expressed (Sutter and Doerfler 1980). Tumour cell DNA is also undermethylated, when compared to normal cells, with the extent of hypomethylation dependent upon the tumour type (Gama-Sosa *et al.* 1983). DNA methylation has also been postulated to play a role in DNA repair. The occurrence of 5-methylcytosine in DNA may allow the cell to discriminate between strands in mis-match repair (Hare and Taylor 1985, Jones *et al.* 1987, Wiebauer and Jiricny 1989). Damage to 5-methylcytosine residues, resulting in deamination to thymine, could be corrected by the appropriate repair enzymes by using the undamaged DNA strand, containing 5-methylcytosine as a marker, as a template for repair. Therefore, by disrupting the normal methylation pattern of the cell, the ability to survive damage resulting from radiation exposure might also be affected. To examine this possibility the radioprotective properties of two DNA methylation-disrupting agents, 5-azacytidine and sodium butyrate, were tested.

First synthesized as a cancer chemotherapeutic agent (Piskala and Sorm 1964), 5-azacytidine differs from cytidine by the presence of a nitrogen atom in the 5-position of the pyrimidine ring. 5-Azacytidine has the ability to induce the

†To whom correspondence should be addressed.
‡Present address: Office of Naval Research, Code 121D, 800 N. Quincy St., Arlington, VA 22217-5000, USA.

expression of inactive genes in eukaryotic cells by inhibiting DNA methylation. 5-Azacytidine can be converted to 5-azadeoxycytosine triphosphate using the normal nucleotide-synthesizing pathways in the cell (Lee *et al.* 1974, Liacouras and Anderson 1979), after which it can be incorporated into DNA (Li *et al.* 1970). Treatment with 5-azacytidine inhibits the methylation of newly synthesized DNA (Jones and Taylor 1980), Wilson *et al.* 1983). It was originally thought that the decrease in methylation was because 5-azacytidine has a nitrogen at the 5-position and is thus unable to accept a methyl group. However, the degree of substitution of 5-azacytidine for cytosine was not sufficient to account for all the observed inhibition of methylation. It was later found that 5-azacytidine inhibits DNA methyltransferases, if the 5-azacytidine is incorporated into the DNA (Tanaka *et al.* 1980), although 5-azacytidine alone does not inhibit the methyltransferase activity. The methyltransferase may form a covalent bond with the incorporated 5-azacytidine, resulting in the irreversible covalent bonding of the enzyme to DNA (Santi *et al.* 1983).

Sodium butyrate, the sodium salt of the four-carbon fatty acid, has been reported to increase DNA methylation (de Haan *et al.* 1986) by some as yet undiscovered mechanism, as well as activating some genes (Leder *et al.* 1975, Rubinstein *et al.* 1979, Plesko *et al.* 1983), including metallothionein (Birren and Herschman 1986).

These two methylation-disrupting agents were tested on a Chinese hamster lung fibroblast line (V79A03) in order to determine if 5-azacytidine or sodium butyrate treatment prior to exposure to ^{60}Co gamma radiation could result in increased cell survival.

2. Materials and methods

2.1. *Cell culture conditions*

Alpha minimal essential medium, foetal calf serum, penicillin, streptomycin, gentamicin and L-glutamine were purchased from Gibco Labs (Grand Island, NY, USA). *N*-2-Hydroxyethylpiperizine-*N'*-2-ethane-sulphonic acid (HEPES) was obtained from Sigma Chemical (St. Louis, MO, USA).

Chinese hamster lung (V79) clone A03 was maintained in monolayer (at 37°C in 5% Co_2 in air) in alpha minimal essential medium supplemented with 10% fetal calf serum, 100 units/ml penicillin, 100 μg/ml streptomycin, 20 μl/ml gentamicin, 2 mM L-glutamine and buffered with 25 mM HEPES.

2.2. *Cell survival curves*

Cells, plated in tissue culture flasks, were treated with 5-azacytidine (final concentration 3 μM) or sodium butyrate (final concentration 1 mM) at various times before and after irradiation. Cells were allowed to attach to the tissue culture flask for 4 h before the addition of the 5-azacytidine or sodium butyrate. 5-Azacytidine (Sigma) was prepared as a 100 μM solution in tissue culture medium and stored at −20°C for not longer than 1 week. Sodium butyrate (Sigma) was prepared as a 100 mM solution in tissue culture medium and was stored at −20°C for periods of up to 1 month. Irradiations were performed bilaterally in the AFRRI ^{60}Co radiation facility at room temperature with a dose rate of 1 Gy/min. Dosimetry was performed as per the AAPM Task Group 21 protocol for the determination of the absorbed dose from high-energy photon and electron beams (Radiation Therapy

Committee 1983). Total doses ranged from 0 to 10 Gy. Control flasks (Unirradiated) and flasks receiving 0·5 and 1 Gy of radiation were seeded with 100 cells per flask. Flasks receiving 3 Gy were seeded with 150 cells per flask. Flasks receiving 5 and 7 Gy were seeded with 300 and 500 cells per flask, respectively, whereas flasks receiving 10 Gy were seeded with 1000 cells per flask. Prior to radiation exposure, the drug-containing medium was removed from the cells and replaced with fresh medium without the drugs. After irradiation the medium was replaced with fresh medium. After 5 days colonies were stained (Giemsa), counted, and cell survival determined.

2.3. *DNA isolation and 5-methylcytosine determination*

V79A03 DNA was isolated and purified following the method of Blin and Stafford (1976). The purified DNA was hydrolyzed to deoxyribonucleotides using the enzymatic method of Christman (1982). Nucleotides were separated by high-performance liquid chromatography (HPLC) using a Beckman Model 344 gradient liquid chromatograph equipped with an Altex Ultrasphere 5 μm-particle octadecylsilane column (4·6 mm i.d. × 25 cm). Samples were eluted with 0·1 M sodium phosphate buffer (pH 5·5) over 45 min at ambient temperature with a flow-rate of 1 ml/min (Christman 1982). Detection was at 254 nm with a detector sensitivity of 0·05 AUFS. Data were analysed with an IBM System-9000 computer interfaced with the HPLC system. Deoxyribonucleotide standards were purchased from Sigma.

3. Results

As both 5-azacytidine and sodium butyrate induce the expression of genes (Jones and Taylor 1980, Plesko *et al.* 1983), some of which may be involved in the repair of cell damage, their effect on cell survival following exposure to ionizing radiation was investigated.

Before the possible radioprotective properties of 5-azacytidine and sodium butyrate could be investigated, the toxicity of these drugs on V79A03 cells had to be ascertained. After plating the cells, medium containing 5-azacytidine or sodium butyrate was added. Twenty-four hours later the medium was aspirated and fresh medium added. The cells were grown for 5 days, after which time they were stained with Giemsa and the colonies counted. Figure 1 shows the percentage survival of V79A03 cells after 24 h in concentrations of 5-azacytidine ranging from 1 nM to 1 mM. Concentrations of 5-azacytidine greater than 10 μM were toxic to the cells. As a result 3 μM was the 5-azacytidine concentration selected for subsequent studies. The percentage survival of V79A03 cells in sodium butyrate concentrations ranging from 1 nM to 100 mM is shown in Figure 2. Sodium butyrate concentrations greater than 10 mM were toxic to V79A03 cells. A sodium butyrate concentration of 1 mM was selected for subsequent experiments.

Table 1 shows the effect of 5-azacytidine or sodium butyrate treatment on the 5-methylcytosine content of V79A03 DNA. Treatment with 3 μM 5-azacytidine for 24 h resulted in the hypomethylation of DNA as seen by the decrease in the percentage of 5-methylcytosine from 4·69 to 2.77%. In contrast, sodium butyrate treatment hypermethylates V79A03 DNA, with 37% of the cytosine residues in DNA being methylated by treatment of V79A03 cells with 1 mM sodium butyrate for 24 h.

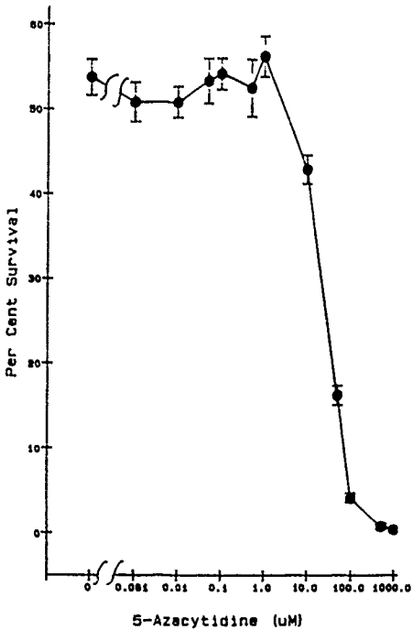

Figure 1. Toxicity of 5-azacytidine on V79A03 cells. V79A03 cells were treated with various concentrations of 5-azacytidine for 24 h. After that time the medium was changed and the cells were grown for 5 days. The colonies were stained with Giemsa and counted. Results are the mean of 24 determinations. Error bars indicate standard deviation.

Figure 3 shows the survival fractions of V79A03 cells treated with 3 μM 5-azacytidine at 24, 12, 6, 3 and 1 h pre-irradiation and immediately post-irradiation (30 min). There are differences observed between the survival of 5-azacytidine treated V79A03 cells and control cells in all instances.

The survival fractions of V79A03 cells treated with 1 mM sodium butyrate 24, 12, 6, 3 and 1 h pre-irradiation and immediately post-irradiation (30 min) are shown in Figure 4. There are only minor differences between the survival of treated and control V79A03 cells at all experimental times.

The differences in the radiosensitivities of 5-azacytidine and sodium butyrate treated V79A03 cells were determined and compared to control cells using the mean inactivation dose. The mean inactivation dose ($\bar{D}$) is equal to the area under the survival curve (Kellerer *et al.* 1976, Fertil *et al.* 1984, Debieu *et al.* 1985). $\bar{D}$ can be calculated from the parameters α and β, which in turn are determined by regression analysis of the natural logarithm of the survival fraction (SF) (Fertil *et al.* 1984, Taylor 1986). The advantage of using $\bar{D}$ is that it is representative of the entire cell population rather than just a fraction of it. In addition, comparisons of different survival curves can easily be accomplished because each curve is represented by a single value.

Table 2 shows the mean inactivation dose for control, 5-azacytidine and sodium butyrate treated V79A03 cells and also contains the dose reduction factors (DRF)

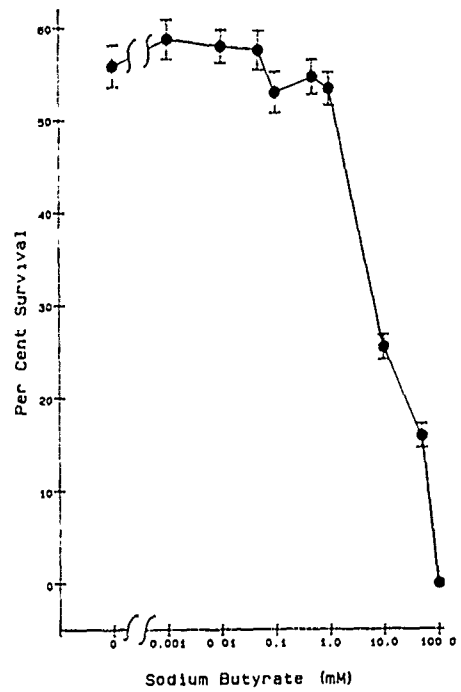

Figure 2. Toxicity of sodium butyrate on V79A03 cells. V79A03 cells were treated with various concentrations of sodium butyrate for 24 h. After that time the medium was charged and the cells were grown for 5 days. The colonies were stained wth Giemsa and counted. Results are the mean of 24 determinations. Error bars indicate standard deviation.

for the various treatment times. The DRF was calculated using the following equation: DRF = $\bar{D}$ (treated)/$\bar{D}$ (control).

5-Azacytidine treated cells exhibited an increase in the DRF at all treatment times, with the 24 h pre-irradiation treatment time showing the highest DRF value (1·8). Sodium butyrate treatment, except for the 3 h pre-irradiation treatment, did not result in any significant increase in the DRF.

Table 1. 5-methylcytosine levels in V79A03 cells following treatment with 5-azacytidine or sodium butyrate.

Treatment	5-methylcytosine (%)	Error (SD)
Control	4·69	0·56
5-Azacytidine (3 μM per 24 h)	2·77	0·04
Sodium butyrate (1 mM per 24 h)	37·23	2·14

Results are the mean of three determinations. Errors are given as standard deviation (SD). Percentage of 5-methylcytosine (5-M-C) was computed using the following equation: %5-M-C = [amt 5-M-C/(amt 5-M-C + amt cytosine)] × 100. The probability, using Student's *t*-test, that the values of the treated samples are not significantly different from the control value is $<0{\cdot}001$ in both cases.

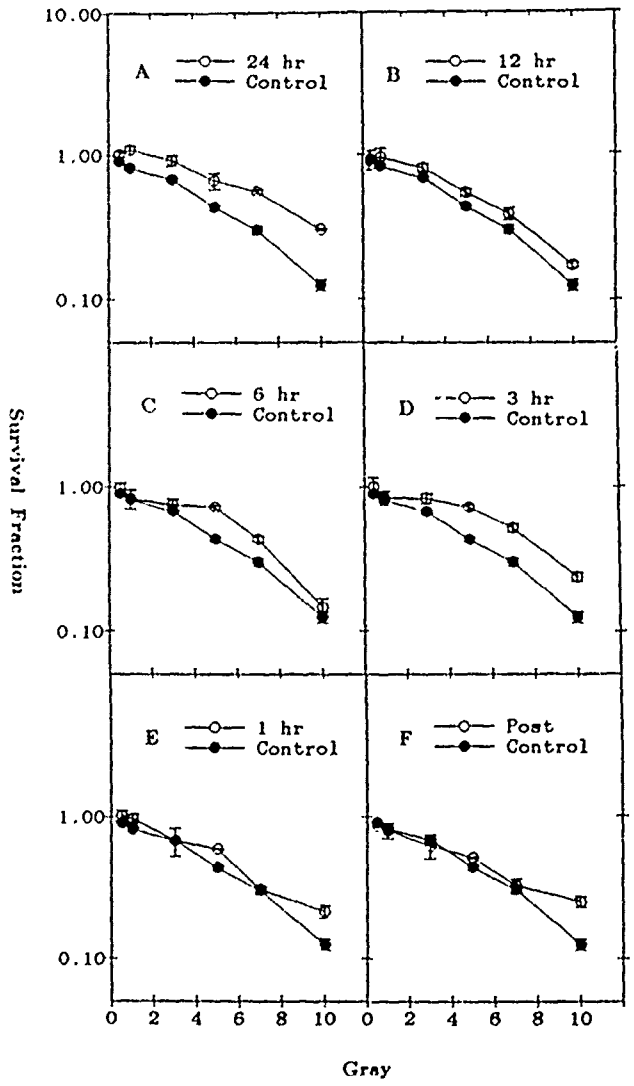

Figure 3. Survival of 5-azacytidine-treated V79A03 cells following ^{60}Co gamma irradiation. Curves show survival fraction versus radiation dose of V79A03 cells treated with 3 μM 5-azacytidine at (A) 24, (B) 12, (C) 6, (D) 3, and (E) 1 h pre-irradiation and (F) post-irradiation. Results are the mean of six determinations. Error bars indicate standard deviation.

4. Discussion

The methylation of DNA plays a major role in several cellular processes, including packaging of DNA (Ball *et al.* 1983), strand selection for DNA repair (Hare and Taylor 1985, Jones *et al.* 1987, Wiebauer and Jiricny 1989). and gene expression (Compere and Palmiter 1981). A previous study has shown that exposure to gamma radiation results in a decrease in the 5-methylcytosine content of mammalian cell DNA (Kalinich *et al.* 1989). Whether this radiation-induced

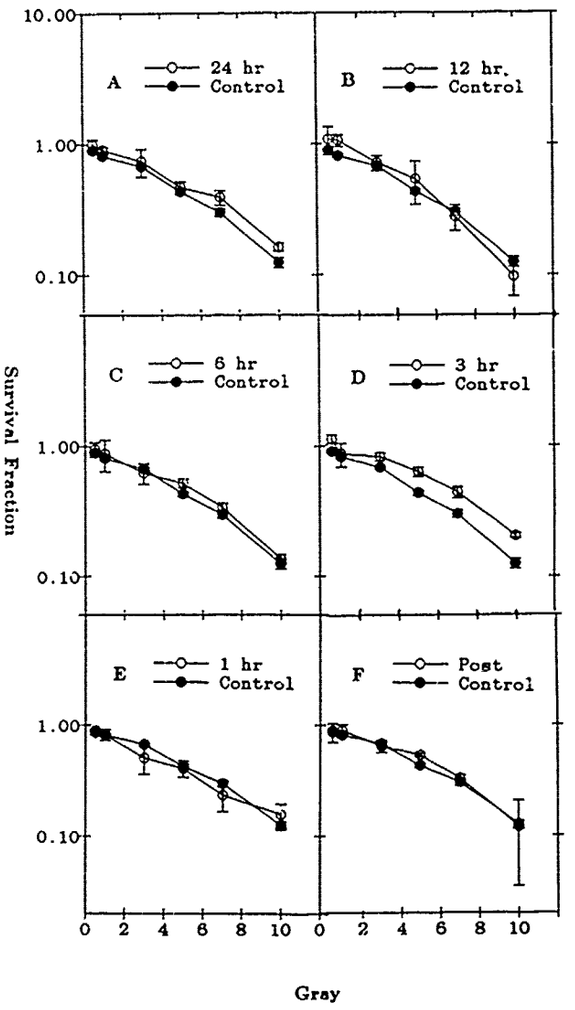

Figure 4. Survival of sodium butyrate-treated V79A03 cells following ^{60}Co gamma irradiation. Curves show survival fraction versus radiation dose of V79A03 cells treated with 1 mM sodium butyrate at (A) 24, (B) 12, (C) 6 (D) 3 and (E) 1 h pre-irradiation and (F) post-irradiation. Results are the mean of six determinations. Error bars indicate standard deviation.

hypomethylation represents a damage end-point or a repair response to radiation exposure is not yet known. If hypomethylation is the initial step in the repair response to radiation exposure, it should be possible to afford radioprotection to cells by disrupting the normal DNA methylation pattern. In order to determine if a disruption of the normal cellular DNA methylation pattern prior to exposure to gamma irradiation would affect survival, two DNA methylation-disrupting agents, 5-azacytidine and sodium butyrate, were utilized.

Table 2. Mean inactivation dose ($\bar{D}$) and dose reduction factors (DRF) for 5-azacytidine and sodium butyrate treated V79A03 cells.

Time of treatment before irradiation (h)	5-Azacytidine		Sodium butyrate	
	$\bar{D}$	DRF	$\bar{D}$	DRF
24	879·5	1·77	566·4	1·13
12	524·7	1·06	539·0	1·08
6	626·7	1·26	532·6	1·07
3	703·9	1·42	644·6	1·29
1	606·9	1·22	501·0	1·00
Post-irradiation (30 min)	667·2	1·34	526·5	1·05

DRF calculated using a control $\bar{D}$ value of 496·72.

The treatment of V79A03 cells, a Chinese hamster lung fibroblast line, with 3 μM 5-azacytidine for 24 h resulted in a decrease of the 5-methylcytosine content of almost 60% of the control value, whereas treatment with 1 mM sodium butyrate for 24 h increased 5-methylcytosine levels to almost 800% of control. This high degree of methylation suggests that cytosines not in the usually methylated 5′-CpG-3′ sequence are being methylated. Both compounds have the ability to activate quiescent genes. In fact, metallothionein expression can be induced by both 5-azacytidine and sodium butyrate (Compere and Palmiter 1981, Birren and Herschman 1986). 5-Azacytidine induced gene activation is the result of decreased DNA methylation, which is due to the inhibition of the DNA methyltransferase (Tanaka *et al.* 1980, Santi *et al.* 1983). The mechanism of sodium butyrate induced gene activation is, however, unknown at this time.

5-Azacytidine treatment of V79A03 cells 24, 12, 6, 3 and 1 h pre-irradiation or immediately post-irradiation gave various degrees of radioprotection. Treatment 24 h prior to irradiation gave the highest DRF of 1·8. Treatment times closer to radiation exposure also resulted in increased survival, but not to the extent seen with the 24 h pre-irradiation treatment. The survival of 5-azacytidine treated V79A03 cells did not exhibit a time-dependent response with respect to treatment times. Indeed, treatment of the cells with 3 μM 5-azacytidine after exposure to gamma radiation (within 30 min) resulted in increased survival, thus suggesting that the observed radioprotection is the result of the activation of genes, possibly those involved in repair processes. Interestingly, Jeggo and Holiday (1986) have shown that treatment with 5-azacytidine can activate a DNA repair gene in X-ray sensitive CHO cells. In addition it has recently been shown that 5-azacytidine can induce O^6-alkyguanine–DNA alkyltranferase activity in mouse Ha821 cells (Mitani *et al.* 1989). This enzyme is responsible for removing O^6-alkylguanines from DNA. It is therefore tempting to postulate that other repair enzymes may also be under methylation control and could also be induced by 5-azacytidine treatment.

Treatment of V79A03 cells with 1 mM sodium butyrate, a DNA hypermethylating agent, at 24, 12, 6, 3 and 1 h prior to irradiation or immediately after exposure did not result in a significant increase in survival. An exception is the 3 h pre-irradiation treatment time which resulted in a DRF of 1·3. The reason for this is unclear at this time. It is clear that whereas 5-azacytidine may activate quiescent

repair genes, these genes appear not to be similarly activated by sodium butyrate treatment.

If genes were activated prior to radiation exposure, including those involved in repair processes, it might be possible to afford radioprotection to cells. It has been shown here that hypomethylating cellular DNA via treatment with 5-azacytidine is correlated with an increased survival following exposure to gamma radiation. However, DNA hypermethylation with sodium butyrate resulted in little or no protection. Whereas the mechanism of protection exhibited by 5-azacytidine is not known, one possibility is that the genes involved in repair processes may be activated on treatment with 5-azacytidine. If this occured, the enzymes needed to repair the damage inflicted by radiation would already be present, and the cell might better tolerate the radiation insult. Another possibility is that an azacytidine induced cell cycle block contributes to the observed radioprotection. This has not as yet been ruled out. Nevertheless, the possibility that the activation of gene expression enhances survival following radiation exposure remains an interesting concept.

Acknowledgements

This work was supported by the Armed Forces Radiobiology Research Institute, Defense Nuclear Agency, under work unit 04230. Views presented in this paper are those of the authors; no endorsement by the Defense Nuclear Agency has been given or should be inferred.

References

American Association of Physicists in Medicine, Task Group 21, Radiation Therapy Committee 1983, A protocol for the determination of absorbed dose from high-energy photon and electron beams. *Medical Physics*, **10**, 741–771.

Ball, D. J., Gros[illegible] D. S. and Garrard, W. T., 1983, 5-Methylcytosine is localized in nucleosomes that contain histone H1. *Proceedings of the National Academy of Sciences, USA* **80**, 5490–5494.

Birren, B. W. and Herschman, H. R., 1986, Regulation of the rat metallothionein-I gene by sodium butyrate. *Nucleic Acids Research*, **14**, 853–867.

Blin, N. and Stafford, D. W., 1976, A general method for isolation of high molecular weight DNA from eukaryotes. *Nucleic Acids Research*, **3**, 2303–2308.

Christman, J. K., 1982, Separation of major and minor deoxyribonucleoside monophosphates by reverse-phase high-performance liquid chromatography: a simple method applicable to quantitation of methylated nucleotides in DNA. *Analytical Biochemistry*, **119**, 38–48.

Compere, S J. and Palmiter, R. D., 1981, DNA methylation controls the inducibility of the mouse metallothionein-I gene in lymphoid cells. *Cell*, **25**, 233–240.

Debieu, D., Deschavanne, P J., Midander, J., Larrson, A. and Malaise, E. P., 1985, Survival curves of glutathionine synthetase deficient human fibroblasts: correlation between radiosensitivity of hypoxia and glutathionine synthetase activity. *International Journal of Radiation Biology*, **48**, 525–543.

Fertil, B., Dertinger, H., Courdi, A. and Malaise, E. P., 1984, Mean inactivation dose: a useful concept for intercomparison of human cell survival curves. *Radiation Research*, **99**, 73–84.

Gama-Sosa, M. A., Slagel, V. A., Trewyn, R. W., Oxenhandler, R., Kuo, K., Gehrke, W., and Ehrlich, M., 1983, The 5-methylcytosine content of DNA from human tumors. *Nucleic Acids Research*, **11**, 6883–6894.

de Haan, J. B., Gevers, W. and Parker, M. I., 1986, Effects of sodium butyrate on the synthesis and methylation of DNA in normal cells and their transformed counterparts. *Cancer Research*, **46**, 713–716.

HARE, J. T. and TAYLOR, J. H., 1985, One role for DNA methylation in vertebrate cells is strand discrimination in mismatch repair. *Proceedings of the National Academy of Sciences, USA*, **82**, 7350–7354.

JEGGO, P. A. and HOLLIDAY, R., 1986, Azacytidine-induced reactivation of a DNA repair gene in Chinese hamster ovary cells. *Molecular and Cellular Biology*, **6**, 2944–2949.

JONES, P. A. and TAYLOR, S. M., 1980, Cellular Differentiation, cytidine analogs and DNA methylation. *Cell*, **20**, 85–93.

JONES, M., WAGNER, R. and RODMAN, M., 1987, Mismatch repair of deaminated 5-methylcytosine. *Journal of Molecular Biology*, **194**, 155–159.

KALINICH, J. F., CATRAVAS, G. N. and SNYDER, S. L., 1989, The effect of gamma radiation on DNA methylation. *Radiation Research*, **117**, 185–197.

KELLERER, A. M., HALL, E. J., ROSSI, H. H. and TECDLA, P., 1976, RBE as a function of neutron energy. II. Statistical analysis. *Radiation Research*, **65**, 172–186.

LEDER, A., ORKIN, S. AND LEDER, P., 1975, Butyric acid, a potent inducer of erythroid differentiation in cultured erythroleukemic cells. *Cell*, **5**, 319–322.

LEE, T., KARON, M. and MOMPARLER, R. L., 1974, Kinetic studies on phosphorylation of 5-azacytidine with purified uridine-cytidine kinase from calf thymus. *Cancer Research*, **34**, 2482–2488.

LI, L. H., OLIN, E. J., BUSKIRK, H. H. and RINEKE, L. M., 1970, Cytotoxicity and mode of action of 5-azacytidine on L1210 leukemia. *Cancer Research*, **30**, 2760–2769.

LIACOURAS, A. S. and ANDERSON, E. P., 1979, Uridine-cytidine kinase. IV. Kinetics of the competition between 5-azacytidine and the two natural substrates. *Molecular Pharmacology*, **15**, 331–340.

MITANI, H., YAGI, T., LEILER, C. Y. M and TAKEBE, H., 1989, 5-Azacytidine-induced recovery of O^6-alkylguanine-DNA alkyltransferase activity in mouse Ha821 cells. *Carcinogenesis*, **10**, 1879–1882.

PISKALA, A. and SORM, F., 1964, Nucleic acids components and their analogues. Synthesis of 1-glycosyl derivatives of 5-azauracil and 5-azacytosine. *Collection of Czechoslovak Chemical Communications*, **29**, 2060–2067.

PLESKO, M. M., HARGROVE, J. L., GRANNER, K. and CHALKLEY, R., 1983, Inhibition by sodium butyrate of enzyme induction by glucocorticoids and dibutyryl cyclic AMP. *Journal of Biological Chemistry*, **258**, 13738–13744.

RUBINSTEIN, P., SCALY, L., MARSHALL, S. and CHALKLEY, R., 1979, Cellular protein synthesis and inhibition of cell division are independent of butyrate-induced histone hyperacetylation. *Nature*, **280**, 692–693.

SANTI, D. V., GARRET, C. E. and BARR, P. J., 1983, On the mechanism of inhibition of DNA-cytosine methyltransferases by cytosine analogs. *Cell*, **33**, 9–10.

SUTTER, D. and DOERFLER, W., 1980, Methylation of integrated adenovirus type-12 DNA sequences in transformed cells in inversely correlated with viral gene expression. *Proceedings of the National Academy of Sciences, USA*, **77**, 253–256.

TANAKA, M., HIBASAMI, H., NAGAI, J. and IKEDA, T., 1980, Effects of 5-azacytidine on DNA methylation in Ehrlichs' ascites tumor cells. *Austrian Journal of Experimental Biology, Medicine, and Science*, **58**, 391–396.

TAYLOR, J., 1986, Calculating the mean inactivation dose *Radiation Research*, **108**, 112.

WIEBAUER, K. and JIRICNY, J., 1989, In vitro correction of G-T mispairs to G-C pairs in nuclear extracts from human cells. *Nature*, **339**, 234–236.

WILSON, V. L., MOMPARLER, R. L. and JONES, P. A., 1983, Inhibition of DNA methylation of L1210 leukemic cells by 5-aza-2'-deoxycytidine. A possible mechanism of chemotherapeutic action. *Cancer Research*, **43**, 3493–3496.

RADIATION RESEARCH 126, 218–222 (1991)

Role of Neurotensin in Radiation-Induced Hypothermia in Rats

SATHASIVA B. KANDASAMY, WALTER A. HUNT, AND ALAN H. HARRIS

Behavioral Sciences Department, Armed Forces Radiobiology Research Institute, Bethesda, Maryland 20814-5145

KANDASAMY, S. B., HUNT, W. A., AND HARRIS, A. H. Role of Neurotensin in Radiation-Induced Hypothermia in Rats. *Radiat. Res.* 126, 218–222 (1991).

The role of neurotensin in radiation-induced hypothermia was examined. Intracerebroventricular (ICV) administration of neurotensin produced dose-dependent hypothermia. Histamine appears to mediate neurotensin-induced hypothermia because the mast cell stabilizer disodium cromoglycate and antihistamines blocked the hypothermic effects of neurotensin. An ICV pretreatment with neurotensin antibody attenuated neurotensin-induced hypothermia, but did not attenuate radiation-induced hypothermia, suggesting that radiation-induced hypothermia was not mediated by neurotensin.

INTRODUCTION

Exposure to ionizing radiation causes changes in core body temperature. This effect depends partly upon the species of animal, with hyperthermia occurring in cats, rabbits (*1*), and humans (*2*), and a biphasic response (i.e., a fall in temperature followed by a rise) in monkeys (*3*). In rats, the direction of the temperature change is dose dependent with hyperthermia occurring when radiation doses are less than 15 Gy and hypothermia occurring when doses are greater than 20 Gy. In rats, the temperature response appears to be centrally mediated because irradiation of the head alone causes these effects, while irradiation of the trunk only does not (*4, 5*).

The chemical mediators identified thus far include prostaglandins (*5*) and histamine (*5*), while serotonin has been shown not to be involved (*4*). It is not known if histamine release is a primary response to irradiation or secondary to the release of other substances, such as neurotensin, liberated in the cascade of events following radiation injury.

Neurotensin, an endogenous tridecapeptide found in the central nervous system, particularly in hypothalamus, caudate nucleus, globus pallidus, putamen, nucleus accumbens and amygdala (*6–9*), and gastrointestinal tract (*10*), acts as a neurotransmitter or a neuromodulator (*11*). Specific neurotensin binding sites have been identified in the midbrain (*6, 12*), and interactions between neurotensin and dopamine have been shown (*13*). Central administration of neurotensin produces a variety of behavioral and physiological effects, including the stimulation of histamine release (*14*). One of the more potent effects of neurotensin is the induction of hypothermia after intracisternal or intraventricular administration (*15–17*). The purposes of this study were to investigate the role of neurotensin in radiation-induced hypothermia and to elucidate the mechanisms involved in neurotensin-induced hypothermia.

METHODS

Drugs. The drugs used were neurotensin (Sigma Chemical Co., St. Louis, MO), neurotensin antibody (Accurate Chemical and Scientific Corporation, Westbury, NY), disodium cromoglycate (Fisons Corporation, Bedford, MA), mepyramine maleate (Mallinckrodt Inc., St. Louis, MO), cimetidine (Smith Kline and French Laboratory, Philadelphia, PA), ketamine hydrochloride (Parke-Davis, Detroit, MI), xylazine (Hayer Lockhart, Shawnee, KS), and acepromazine (Ayerst Laboratories, NY). Neurotensin, neurotensin antibody, mepyramine, and disodium cromoglycate were dissolved in sterile, nonpyrogenic saline. Cimetidine was dissolved in 0.1 ml of 1 *N* HCl and diluted to the final volume with saline.

Animals. Male Sprague-Dawley Crl:CD(SD)BRD rats (Charles River Breeding Laboratories, Kingston, NY) weighing 200–300 g were used in these experiments. Rats were quarantined on arrival and screened for evidence of disease by serology and histopathology. The rats were housed individually in polycarbonate isolator cages (Lab Products, Maywood, NJ) on autoclaved hardwood contact bedding (Beta Chip, Northeastern Products Corp., Warrensburg, NY), and were provided commercial rodent chow (Wayne Rodent Blok, Continental Grain Co., Chicago, IL) and acidified water (pH 2.5 using HCl) *ad libitum*. Animal holding rooms were kept at 21 ± 1°C with 50 ± 10% relative humidity on a 12-h light/dark cycle with no twilight.

Radiation exposure. Rats were placed in clear plastic well-ventilated containers for approximately 5 min before irradiation or sham exposure. The animals were then exposed bilaterally to γ rays using a ^{60}Co source at a rate of 20 Gy/min to a total dose of 50 Gy. Prior to the experiment, the dose rate at the midline of an acrylic rat phantom was measured using a 0.5-cc tissue-equivalent ionization chamber manufactured by Exradin, Inc. The dose rate at the same location with the phantom removed was measured using a 50-cc ionization chamber fabricated at AFRRI. The ratio of these two dose rates, the tissue–air ratio, was used to determine the doses for animals receiving routine experimental exposures, in this experiment, the tissue–air ratio was 0.93. All ionization chambers have calibration factors traceable to the National Institute for Standards and Technology. Dosimetry measurements were performed following the AAPM Task Group 21 Protocol for the Determination of the Absorbed Dose from High-Energy Photon and Electron Beams (*18*).

0033-7587/91 $3.00

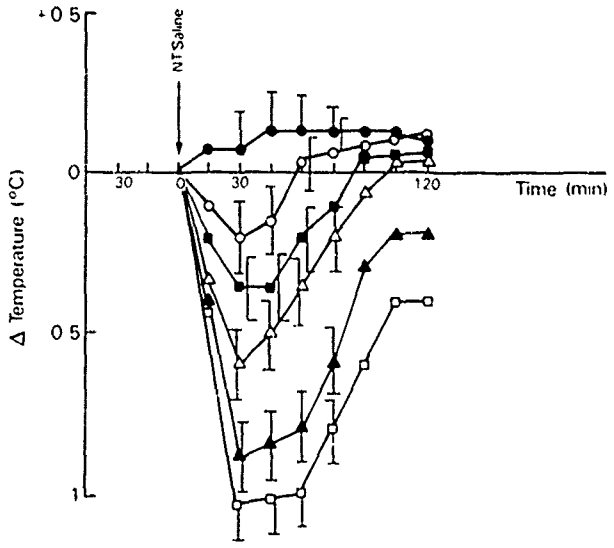

FIG. 1. Changes in rectal temperature of rats induced by intracerebroventricular (ICV) injection of neurotensin (NT): 1 μg (○), 3 μg (■), 5 μg (△), 10 μg (▲), 20 μg (□), and saline (●). Each point represents the mean ± SE of observations of five animals. Zero on the ordinate represents the temperature at the time of injection.

Central administration of drugs. Rats were anesthetized with 1 ml/kg of a mixture of ketamine (50 mg/kg), xylazine (5 mg/kg), and acepromazine (1 ml/kg) given intramuscularly, and were placed in a rat stereotaxic apparatus (David Kopf Instruments, No 320). A single cannula was inserted aseptically into the lateral ventricle according to coordinates derived from the atlas of Pelligrino *et al.* (*19*): 0.8 mm posterior to bregma, 2.5 mm lateral. The cannula was lowered until cerebrospinal fluid rose in the cannula. Dental acrylic was used to secure the cannula. Animals were allowed to recover for 1 week before they were used for experiments. After the end of an experiment, injection sites were verified histologically. Injections and irradiations were performed at the same time of day (0900) to avoid diurnal variations in temperature. The antagonists (neurotensin antibody, disodium cromoglycate, mepyramine, and cimetidine) were given 30 min before the radiation and neurotensin were administered.

Measurement of body temperature. All experiments were performed at a room temperature of 22 ± 1°C. The animals were placed in restraining cages 1 h before starting the experiments, and body temperature was measured every 15 min for 2 h with thermistor probes (YSI series 700, Yellow Springs Co., Inc., Yellow Springs, OH) inserted approximately 6 cm into the rectum and connected to a datalogger (Minitrend 205). After each experiment, all animals were killed immediately with an overdose of carbon dioxide by inhalation.

Statistics Statistical evaluations were performed using analysis of variance with a significance level of $P < 0.05$. Intergroup comparisons were made using Tukey's test (*20*).

RESULTS

An ICV administration of 1–20 μg of neurotensin induced hypothermia in a dose-dependent manner (Fig. 1). An ICV pretreatment with 0.25–1.0 mg of neurotensin antibody attenuated the hypothermia induced by ICV administration of 5 μg of neurotensin, but did not reduce the hypothermia produced by 50 Gy of ionizing radiation (Fig. 2). Figure 2 also shows that administration of neurotensin antibody alone had no effect on body temperature. An ICV administration of the mast cell stabilizer disodium cromoglycate did not change the body temperature of control animals but did block, in a dose-dependent manner, the hypothermia produced by the ICV injection of 5 μg neurotensin (Fig. 3). Mepyramine and cimetidine are specific H_1 and H_2 receptor antagonists, respectively (*21*). Mepyramine (100–300 ng, ICV) or cimetidine (100–300 ng, ICV) was administered before neurotensin to examine the role of histaminergic H_1 and H_2 receptors in neurotensin-induced hypothermia. Previous studies (*4, 5*) indicate that the same doses of mepyramine and cimetidine are specific H_1 and H_2 receptor antagonists, respectively, and did not change the body temperature in control animals. Both mepyramine and cimetidine, which are found to antagonize histamine-induced hypothermia (*4, 5*) attenuated neurotensin-induced hypothermia (Fig. 4).

DISCUSSION

Ionizing radiation induces either hyperthermia or hypothermia depending upon the dose; temperature changes appear to be centrally mediated (*4, 5*). Histamine has been implicated in the actions of ionizing radiation, including hypotension, reduced cerebral blood flow, and performance decrement (*22*). Furthermore, concentrations of histamine in circulating blood have been elevated in humans undergoing radiation therapy (*23*) as well as in dogs and monkeys (*24–26*) following radiation exposure. Histamine is present in a high concentration in the hypothalamus (*27, 28*), and is localized in nerve terminals (*29*), suggesting that it may act as a central neurotransmitter. Also, histamine is involved in many physiological functions, including thermoregulation, and could underlie radiation-induced hypothermia (*4, 5, 30*).

Histamine is stored in mast cells throughout the body (*31*), including the brain (*32, 33*), and neurotensin has been used to stimulate histamine release (*34–38*). When injected into the lateral cerebral ventricle, neurotensin induced a dose-dependent hypothermia in rats and mice (*15–17*), confirming previous results. Neurotensin is contained in the normal cerebrospinal fluid (*39, 40*), and may play a role in thermoregulation, because central administration of neurotensin decreases colonic temperature in rodents (*15–17*), but is ineffective following peripheral administration (*15*). In addition, Muraki *et al.* (*41*) reported a decrease in the level of neurotensin-like immunoreactivity in the cerebrospinal fluid of children with febrile aseptic meningitis,

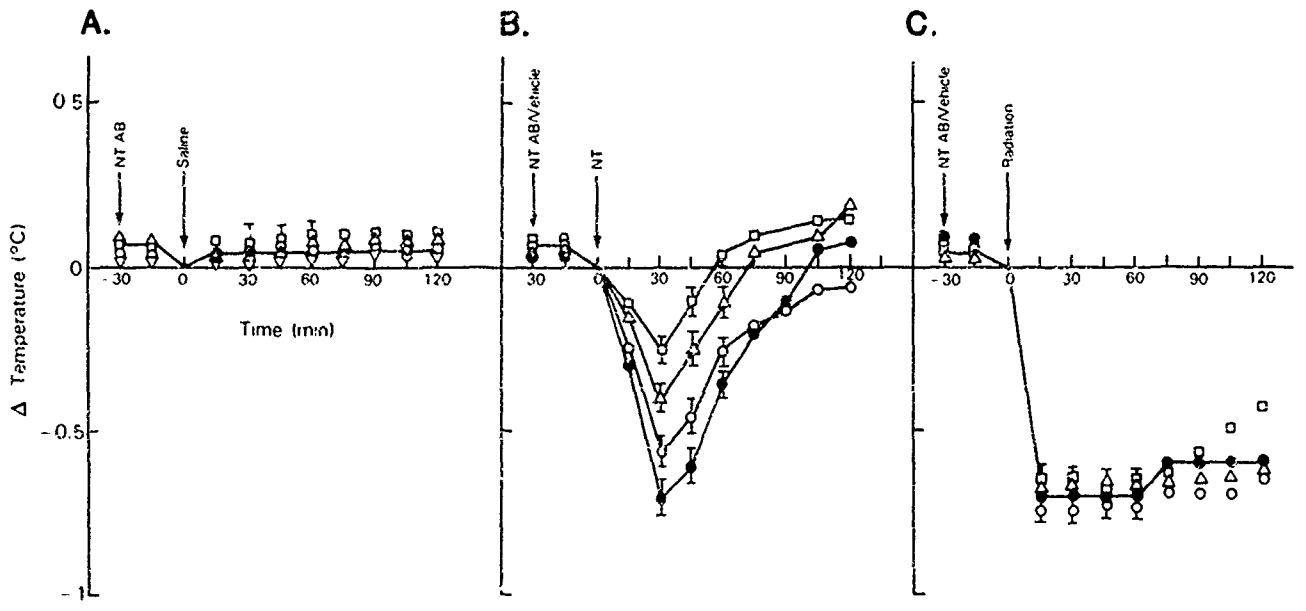

FIG. 2 Effect of neurotensin antibody (NT-AB), ICV, on NT-or radiation-induced hypothermia. (A) Nonirradiated controls given 25 μg (○), 50 μg (△), or 100 μg (□) NT-AB; (B) 5 μg of NT alone (●) or in the presence of 25 μg (○), 50 μg (△), or 100 μg (□) NT-AB; (C) 50 Gy irradiation alone (●) or in the presence of 25 μg (○), 50 μg (△), or 100 μg (□) NT-AB Each point represents the mean ± SE of observations of five animals. Zero on the ordinate represents the temperature at the time of second injection

suggesting an important role for neurotensin in thermoregulation.

Disodium cromoglycate is a potent inhibitor of the immunological release of chemical mediators secreted from mast cells (*21*). It has been reported that neurotensin stimulates the release of histamine *in vivo* (*37, 38, 42*), and pretreatment with disodium cromoglycate inhibits the neurotensin-induced release of histamine (*34, 36, 37, 43*). The attenuation of neurotensin-induced hypothermia by disodium cromoglycate and histamine H_1 and H_2 receptor antagonists in this study suggests that neurotensin-induced hypothermia was mediated by histamine.

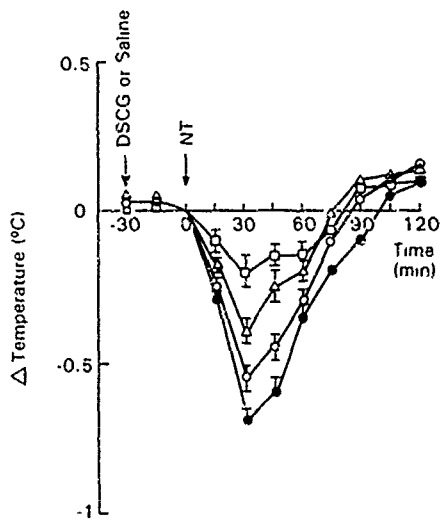

FIG. 3. Effect of disodium cromoglycate (DSCG), ICV, on NT-induced hypothermia. The 5 μg of NT alone (●) or in the presence of 100 ng (○), 300 ng (△), or 500 ng (□) DSCG. Each point represents the mean ± SE of observations of five animals. Zero on the ordinate represents the temperature at the time of second injection.

There are no specific antagonists available to antagonize neurotensin-induced hypothermia; therefore, specific antibodies to neurotensin were used to eliminate endogenous neurotensin, because they would bind and inactivate the neuropeptide (*43–45*). Researchers have reported that the centrally administered neurotensin antibody inhibits neurotensin-induced nociception and hypothermia (*44, 45*). In our experiments, pretreatment with neurotensin antibody attenuated neurotensin-induced hypothermia, but had no inhibitory effect on radiation-induced hypothermia, suggesting that neurotensin may not be involved in radiation-induced hypothermia. Although Cockerham *et al.* (*46*) found a nonsignificant increase in plasma neurotensin levels following exposure to ionizing radiation, because neurotensin is degraded rapidly, they think tissue levels might be significantly increased, causing the release of histamine from mast cells (*46*). In our study, pretreatment with neurotensin antibody, which attenuated neurotensin-induced hypothermia, did not reduce radiation-induced hypothermia.

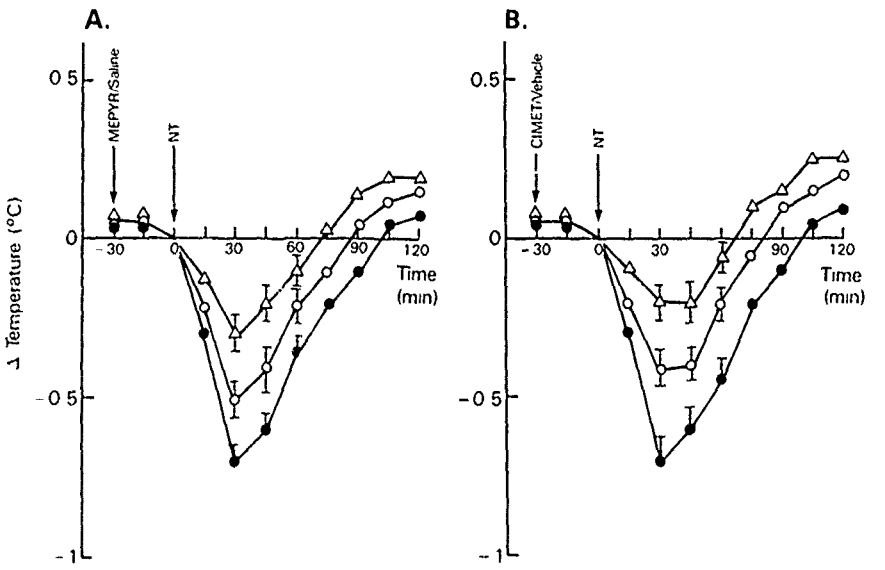

FIG. 4. Effect of mepyramine (MEPYR), ICV, or cimetidine (CIMET), ICV, on NT-induced hypothermia. (A) 5 μg of NT alone (●) or in the presence of 100 ng (○) or 300 ng (△) mepyramine (B) 5 μg of NT alone (●) or in the presence of 100 ng (○) or 300 ng (△) cimetidine. Each point represents the mean ± SE of observations of five animals. Zero on the ordinate represents the temperature at the time of second injection.

Although neurotensin-induced hypothermia is mediated by histamine, we could not determine if radiation-induced hypothermia is mediated by endogenous neurotensin.

RECEIVED: April 26, 1990; ACCEPTED: December 13, 1990

REFERENCES

1 T S VENINGA, Implications of bioamines in the X-ray-induced temperature response of cats and rabbits. *Radiat Res.* **48**, 358–367 (1971)

2 H. FANGER and C. C. LUSHBAUGH, Radiation death from cardiovascular shock following a criticality accident. *Arch. Pathol.* **84**, 446–460 (1967).

3 W. L. MCFARLAND and J. A. WILLIS, *Cerebral Temperature Changes in the Monkey (Macaca mulatta) after 2500 rads Ionizing Radiation.* Scientific Report SR 74-4, Armed Forces Radiobiology Research Institute. Bethesda, Maryland, 1974.

4 S. B. KANDASAMY, W. HUNT, and G. A. MICKLEY, Implication of prostaglandins and histamine H1 and H2 receptors in radiation-induced temperature responses of rats. *Radiat. Res.* **114**, 42–53 (1988).

5 S. B. KANDASAMY and W. A. HUNT, Involvement of prostaglandins and histamine in radiation-induced temperature responses in rats. *Radiat Res.* **121**, 84–90 (1990).

6 G. R. UHL and S. H. SNYDER, Regional and subcellular distribution of brain neurotensin. *Life Sci.* **19**, 1827–1832 (1976).

7. G. R. UHL, M. J. KUHAR, and S. H. SNYDER, Neurotensin: Immunohistochemical localization in rat central nervous system. *Proc. Natl. Acad. Sci USA* **74**, 4509–4063 (1977).

8. R. CARRAWAY and S. E. LEEMAN, Radioimmunoassay for neurotensin, a hypothalamic peptide. *J Biol. Chem* **251**, 7035–7044 (1976).

9 R. M. KOBAYASHI, M. BROWN, and W. VALE, Regional distribution of neurotensin and somatostatin in rat brain. *Brain Res.* **126**, 584–588 (1977).

10 R. E. CARRAWAY and S. E. LEEMAN, Characterization of radioimmunoassayable neurotensin in the rat: Its differential distribution in the central nervous system, small intestine and stomach. *J. Biol Chem* **251**, 7045–7052 (1976).

11 D R. BROWN and R. G. MILLER, Neurotensin. *Br Med. Bull.* **38**, 239–245 (1982).

12 G. R. UHL, R. R. GOODMAN, and S. H. SYNDER, Neurotensin-containing cell bodies, fibers, and nerve terminals in the brain stem of the rat. *Brain Res* **167**, 77–91 (1979).

13 D. R. HAUBRICH, G. E. MARTIN, B. PFLUEGER, and M. WILLIAMS, Neurotensin effects on brain dopaminergic systems. *Brain Res* **321**, 216–221 (1982).

14 S. A. ST PIERRE, R. KEROUAC, R. QUIRION, F. B. JOLICOEUR, and F. RIOUX, Neurotensin. *Pept Protein Rev.* **2**, 83–171 (1984).

15 G. BISSETTE, C. B. NEMEROFF, P. T. LOOSEN, A. J. PRANGE, and M. A. LIPTON, Hypothermia and cold intolerance induced by the intracisternal administration of hypothalamic peptide neurotensin. *Nature* **262**, 607–609 (1976).

16. C. B. NEMEROFF, G. BISSETTE, A. J. PRANGE, P. T. LOOSEN, and M. A. LIPTON, Neurotensin: Central nervous system effects of a hypothalamic peptide. *Brain Res.* **128**, 485–498 (1977).

17 G. A. MASON, C. B. NEMEROFF, D. LUTTINGER, O. L. HATLEY, and A. J. PRANGE, Neurotensin and bombesin: Differential effects on body temperature of mice after intracisternal administration. *Regul. Pep* **1**, 53–60 (1980).

18. Task Group 21, Radiation Therapy Committee AAPM, A protocol for the determination of absorbed dose from high energy photon and electron beams. *Med. Phys.* **10**, 741 (1983).

19. L. S. PELLIGRINO, A. S. PELLIGRINO, and A. J. CUSHMAN, *A Stereotaxic Atlas of the Rat Brain.* Plenum, New York, 1979.

20. G. V. GLASS and J. C. STANLEY, In *Statistical Methods in Education and Psychology.* Prentice-Hall, Englewood Cliffs, NJ, 1970.
21. A. GOTH. In *Medical Pharmacology,* 11th ed. C. V. Mosby, St. Louis, MO, 1984.
22 T. F. DOYLE, J. E. TURNS, and T. A. STRIKE, Effect of an antihistamine on early transient incapacitation on monkeys subjected to 4 rads of mixed gamma-neutron radiation. *Aerospace Med.* **42,** 400–403 (1971).
23 E. C. LASSER and K. W. STENSTROM, Elevation of circulating blood histamine in patients undergoing deep roentgen therapy. *Am. J. Roentgenol.* **72,** 985–988 (1954).
24. T. F. DOYLE and T. A. STRIKE, Radiation-released histamine in the rhesus monkey as modified by mast cell depletion and antihistamine. *Experientia* **33,** 1047–1048 (1977).
25 L. G. COCKERHAM, T. F. DOYLE, M. A. DONLON, and E. A. HELGESON, Canine post-radiation histamine levels and subsequent response to compound 48/80. *Aviat. Space Environ. Med.* **55,** 1041–1045 (1984).
26 L. G. COCKERHAM, T. F. DOYLE, M. A. DONLON, and C. J. GOSSETT-HAGERMAN, Antihistamines block radiation-induced intestinal blood flow in canines. *Fundam. Appl. Toxicol.* **5,** 597–604 (1985).
27 H. M. ADAMS and H. K. A. HYE, Concentration of histamine in different parts of the cat and its modification by drugs. *Br J. Pharmacol* **28,** 137–152 (1966).
28. J. F. LIPINSKI, H. SCHAUMBURG, and R. J. BALDESSARINI, Regional distribution of histamine in human brain. *Brain Res* **52,** 403–408 (1973).
29 S. H. SNYDER and K. M. TAYLOR, Histamine in the brain: A neurotransmitter. In *Perspectives in Neuropharmacology* (S. H. Synder, Ed.), pp. 43–73. Oxford Univ. Press, New York, 1972.
30 S. B. KANDASAMY and W. A. HUNT, Involvement of histamine H_1 and H_2 receptors in hypothermia induced by ionizing radiation in guinea pigs. *Life Sci* **42,** 555–563 (1988).
31 D D. METCALF, M. KALINER, and M. A. DONLON. In *CRC Critical Reviews in Immunology* (M. Z. Atassi, Ed.), pp. 23–74. CRC Press, Boca Raton, FL, 1981.
32 L. EDVINSSON, J. CERVOS-NAVARRP, L. LARRSON, C. H. OWMAN, and A. L. RONNBERG, Regional distribution of mast cells containing histamine, dopamine, or 5-hydroxytryptamine in the mammalian brain. *Neurology* **27,** 878–883 (1977).
33 P. M. GROSS, Cerebral histamine: Indications for neuronal and vascular regulation. *J Cereb. Blood Flow Metabol* **2,** 3023 (1982).
34 R. E. CARRAWAY, D. E. COCHRANE, J. B. LANSMAN, S. E. LEEMAN, B. M. PATERSON, and H. J. WELCH, Neurotensin stimulates exocytotic histamine secretion from rat mast cells and elevates plasma histamine levels. *J. Physiol.* **323,** 403–414 (1982).
35. D. E. COCHRANE, C. EMIGH, G. LEVINE, R. E CARRAWAY, and S. E. LEEMAN, Neurotensin alters cutaneous vascular permeability and stimulates histamine release from isolated skin. *Ann. N Y Acad Sci* **400,** 396–397 (1982).
36. D. E. COCHRANE, W. BOUCHER, and P. BIBB, Neurotensin stimulates histamine release in *in vitro* skin blisters: An effect inhibited by cromolyn or somatostatin. *Int. Arch. Allergy Appl Immunol* **80,** 225–230 (1986).
37. R. KEROUAC, S. ST PIERRE, and F. RIOUX, Participation of mast cell 5-hydroxytryptamine in the vasoconstrictor effect of neurotensin in the rat perfused hindquarter. *Life Sci.* **34,** 947–959 (1984).
38. F. RIOUX, R. KEROUAC, and S. ST PIERRE, Release of mast cell mediators, vasoconstriction and edema in the isolated, perfused head of the rat following intracarotid infusion of neurotensin. *Neuropeptides* **6,** 1–12 (1985).
39. P. J. MANBERG, C. B. NEMEROFF, L. L. IVERSEN, M. M ROSSER, J. S. KIZER, and A. J. PRANGER, Human brain distribution of neurotensin in normals, schizophrenics, and Huntington's choreics. *Ann N Y Acad Sci.* **400,** 354–367 (1982).
40. E. WIEDERLOV, L. H LINDSTROM, G. BESEV, P. J. MANBERG, C. B. NEMEROFF, G. R. BRESSE, J. S. KIZER, and A. J. PRANGE, Subnormal CSF levels of neurotensin in a subgroup of schizophrenics and normalization after neuroleptic treatment. *Ann N.Y Acad Sci* **400,** 418–419 (1982).
41. K. MURAKI, Y. NISHI, H. OKAHATA, M. ARAI, H. YAMADA, S PUJITA, Y. MIYACHI, K. UEDA, S. YAMAWAKI, and H. YAJIMA, Neurotensin-like immunoreactivity (NTLI) concentration in the cerebrospinal fluid of children and its alteration in a febrile aseptic meningitis. *Life Sci.* **40,** 1365–1370 (1987).
42. M. OISHI, J. ISHIKO, C. INAGAKE, and S. TAKAORI, Release of histamine and adrenaline *in vivo* following intravenous administration of neurotensin. *Life Sci.* **32,** 2231–2239 (1983)
43. A. DUPONT and Y. MERAND, Enzyme inactivation of neurotensin by hypothalamic and brain extracts of the rats. *Life Sci.* **22,** 1623–1630 (1978).
44. R. J. BODNAR, M. M. WALLACE, G NILAVER, and E. A. ZIMMERMAN, The effects of centrally administered antisera to neurotensin and related peptides upon nociception and related behaviors *Ann N Y Acad. Sci.* **400,** 244–258 (1982).
45 G. BISSETTE, D. LUTTINGER, G. A. MASON, D. E. HERNANDEZ, and P. T. LOOSEN, Neurotensin and thermoregulation. *Ann. N Y Acad Sci.* **400,** 268–282 (1982).
46. L. G. COCKERHAM, E. L. PAUTLER, R. E. CARRAWAY, D. E. COCHRANE, and J. D. HAMPTON, Effect of disodium cromoglycate (DSCG) and antihistamines on postirradiation cerebral blood flow and plasma levels of histamine and neurotensin *Fundam Appl Toxicol* **10,** 233–242 (1988).

Heat induces intracellular acidification in human A-431 cells: role of Na^+-H^+ exchange and metabolism

JULIANN G. KIANG, LESLIE C. McKINNEY, AND ELAINE K. GALLIN
Department of Physiology, Armed Forces Radiobiology Research Institute, Bethesda, Maryland 20814-5145

KIANG, JULIANN G., LESLIE C. McKINNEY, AND ELAINE K. GALLIN. *Heat induces intracellular acidification in human A-431 cells. role of Na^+-H^+ exchange and metabolism.* Am. J. Physiol. 259 (Cell Physiol. 28): C727–C737, 1990.—The resting intracellular pH (pH_i) of A-431 cells at 37°C in Na^+ Hanks' solution is 7.23 ± 0.02. In the presence of amiloride (100 μM) pH_i decreases to 7.08 ± 0.03. Hyperthermia induces a temperature- and time-dependent intracellular acidification of 0.2 pH units in either bicarbonate-free or bicarbonate-buffered solutions. After heat treatment (45°C, 10 min) pH_i returns to normal 1 h after incubation at 37°C. The activity of the Na^+-H^+ exchanger was examined in heated and unheated cells in the absence of bicarbonate. Unheated cells recover from an acid load in a $[Na^+]_o$-dependent and amiloride-sensitive manner. The apparent Michaelis constant for extracellular Na^+ is 38 ± 9 mM, and the apparent mean affinity constant for amiloride is 11 ± 3 μM. In heated cells the apparent affinity of the Na^+-H^+ exchanger for extracellular Na^+ is not changed, but the maximal recovery rate is ~40% slower than that of unheated cells. The rate of recovery from acid loading returns to normal 2 h after heat treatment. $[Na^+]_i$ and intrinsic buffering power in heated cells are the same as those in unheated cells. Decreases in both intracellular ATP and lactic acid are observed in heated cells. 2-Deoxy-D-glucose and sodium azide induce an intracellular acidification but prevent most of the acidification induced by heat. Heat treatment causes no further acidification in cells that are acidified by both amiloride and 2-deoxy-D-glucose together. These data are the first to suggest that thermally induced intracellular acidification is due to both an inhibition of Na^+-H^+ exchange and an inhibition of metabolic pathways.

intracellular pH; hyperthermia; epithelial cells; metabolic inhibitors; thermal injury; 2′,7′-bis(carboxyethyl)-5,6-carboxyfluorescein; adenosine 5′-triphosphate; intracellular sodium concentration; buffering power; proton efflux

---

HEAT STRESS induces several different cellular responses, including inhibition of cell growth (21), activation of heat-stress gene expression (43), and synthesis of heat-shock proteins (43). The mechanism(s) by which heat-shock responses are induced has not been elucidated, although a number of intracellular parameters change following heat treatment, including intracellular pH (pH_i). pH_i is known to modulate DNA replication and cell proliferation in some cell systems (19). In mutant fibroblasts that lack a functional Na^+-H^+ exchanger, growth factor-induced alkalinization in bicarbonate-free buffer is blocked and cell growth is inhibited, although cell growth is normal in these cells in bicarbonate-containing medium (35). Furthermore, in 3T3 and Vero cells, the expression of a yeast proton pump, which results in an increase in pH_i of 0.2 units, is sufficient to induce tumorgenicity and growth in suspension culture (34). Additionally, it has been reported that pH_i has important effects on second messenger levels. In avian heart fibroblasts (8) and rat hepatocytes (47), an intracellular acidification induces a decrease in cytosolic Ca^{2+} and intracellular adenosine 3′,5′-cyclic monophosphate (cAMP) levels, and intracellular alkalinization causes an increase in cytosolic Ca^{2+} and intracellular cAMP levels even in the presence of $NaHCO_3$ (5 mM). These findings demonstrate that pH_i can affect cell growth, intracellular cAMP levels, and Ca^{2+}. Therefore, changes in pH_i following thermal injury may also affect these parameters.

The relationship between temperature and pH_i has not been examined in human cells, but in cells from other species there is a variable relationship between temperature and pH_i (see review in Ref. 36). For example, in giant barnacle muscle fibers (23) and mouse soleus muscle (1), pH_i falls linearly as the temperature increases from 5 to 40°C. Similarly, pH_i decreases when mouse mastocytoma cells are exposed to 43°C for 1 h (48), when salivary gland cells of *Drosophila* are heat treated at 35°C for 20 min (9), and when yeast cells are heat treated at 40°C for 45 min (46). In contrast, the pH_i of rat ventricular cells is unaffected by temperatures from 25 to 35°C (11), and no pH_i changes are found in murine NG108–15 neuroblastoma cells exposed to 43.5°C for 1 h (7). In Chinese hamster ovary cells, no pH_i changes are found following heat treatment at 43.5°C for 55 min. However, an intracellular acidification is found in these cells in the absence of external Na^+. Interestingly, an intracellular alkalinization is noted when these cells are acid-adapted before heat treatment (6).

In those studies the mechanism(s) underlying the heat-induced pH_i changes was not delineated. It is possible that thermal injury may directly affect the ability of cells to regulate pH_i. That is, heat treatment may modify the different ion transporters that are involved in pH_i homeostasis, including Na^+-H^+ exchange and Na^+-dependent and Na^+-independent Cl^--HCO_3^- exchange (18, 19). Alternatively, heat-induced pH_i changes may result from heat-induced metabolic inhibition. Several metabolic inhibitors have been shown to produce an intracellular acidification (3, 10, 32), although the effect of thermal injury on metabolism has not been characterized.

This study examines the effects of thermal injury on

pH$_i$ of human epidermoid carcinoma A-431 cells and investigates the mechanisms underlying the pH$_i$ changes that occur following heat treatment. We studied an epidermal cell line because skin cells are especially vulnerable to heat shock following burn injuries. A-431 cells were selected for these studies for several reasons. They have been used as an epidermal cell model in studies on the effects of epidermal growth factor (12, 41, 42). In addition, a Na^+-dependent amiloride-sensitive Na^+-H^+ exchanger has been identified in these cells (28, 37, 38), and its role in regulating pH$_i$ has been partially characterized (37, 38). Finally, the effect of heat treatment on the metabolism of a tumor cell line is of interest to those who use hyperthermia as an adjuvant treatment in cancer therapy (21, 24), since the inhibitory effect of hyperthermia on the growth of tumor cells may be related to changes in pH$_i$.

METHODS

Cell culture. Human epidermoid carcinoma A-431 (American Type Culture Collection, Rockville, MD) were grown in 75-cm^2 tissue culture flasks (Costar, Cambridge, MA) in a 5% CO_2 incubator at 37°C. The tissue culture medium was Dulbecco's modified Eagle's medium supplemented with 0.03% glutamine, 4.5 g/l glucose, 25 mM *N*-2-hydroxyethylpiperazine-*N'*-2-ethanesulfonic acid (HEPES), 10% fetal bovine serum, 50 μg/ml penicillin, and 50 U/ml streptomycin (GIBCO Laboratories, Grand Island, NY). Cells were fed every 3–4 days. Cells from passages 28–35 were used for experiments.

Heat treatment was performed by adding Hanks' solution at 37, 42, 45, or 50°C to the cells and placing the cells in the same temperature water bath for 10 s or 5, 10, 20, or 30 min. Cell viability was determined in three different ways: trypan blue exclusion, ethidium bromide-acridine orange staining, and lactate dehydrogenase release (13). The plating efficiency of heat-treated cells was examined by trypsinizing cells after heat treatment, replating, and 24 h later counting the percentage of adherent cells.

pH$_i$ measurements. Confluent epithelial cells were trypsinized with 0.025% trypsin containing 0.2 mg/ml EDTA (Biofluid, Rockville, MD) for 10 min at 37°C. The cells were centrifuged and resuspended in Hanks' solution containing 5 mM glucose and 0.2% bovine serum albumin at 37°C for 1 h to allow them to recover from trypsinization (30). After this, the cells were centrifuged again, resuspended to 2×10^6 cells/ml in Hanks' solution supplemented with 5 mM glucose, 0.2% albumin, and 2 μM 2',7'-bis(carboxyethyl)carboxyfluorescein acetoxymethyl ester (BCECF/AM), and incubated for 30 min at 37°C. At the end of the incubation period cells were washed twice with Na^+ Hanks' solution. Aliquots of cells were centrifuged, resuspended to 10^6 cells/ml in Na^+ Hanks' solution without glucose and albumin, and transferred to a cuvette maintained at 37°C. The BCECF fluorescence was measured with an SLM 8000C spectrofluorometer as the ratio of emission at 530 nm for dual excitation at 497 and 437 nm (slit width 4 nm). BCECF leaks out of A-431 cells at a rate of 0.77 ± 0.26%/min (n = 3) and 2.18 ± 0.11%/min (n = 3) at 37 and 45°C, respectively. Cells exposed to 45°C for 10 min and then returned to 37°C have a leak rate of 0.54 ± 0.05%/min (n = 3) that is not significantly different from the rate observed in unheated cells. The extracellular dye carried over from washes is 6 ± 1% (n = 3). The fluorescence signal was calibrated using a method modified from Thomas et al. (44) and summarized as follows. Cells were suspended in K^+ Hanks' solution [containing (in mM) 145 KCl, 5 NaCl, 1.2 $MgCl_2$, 1.6 $CaCl_2$, and 10 HEPES, pH 7.35 at 24°C; 145 mM K^+ is near the normal [K^+]$_i$ for these cells: [K^+] = 137 ± 13 mM]. Nigericin (3 μM) and valinomycin (3 μM) were added to the cell suspension for 5 min. The solution was then titrated with KOH or HCl and the fluorescence signal recorded. Extracellular pH (pH$_o$) was recorded using a Corning model 125 pH meter. The calibration curves were fitted by a sigmoid line, and pH$_i$ values were calculated using the fitted parameter values. Calibration curves for cells maintained at 37°C and for cells heated at 45°C for 10 min, then either held at 45°C or returned to 37°C for measurements, were similar for all treatment groups (Fig. 1). In a related experiment, cells were heated in Hanks' solution buffered with 25 mM HCO_3^--5% CO_2, and pH$_i$ was measured in the presence of HCO_3^--CO_2.

To measure the initial alkalinization rate (recovery from acidification) of acid-loaded cells, cells were incubated for 10 s–15 min in Hanks' solution containing NH_4Cl (5–70 mM) with NaCl (75–140 mM) added to maintain isosmolarity. After NH_4Cl loading, cells were resuspended in NH_4Cl and Na^+-free Hanks' solution for 2 min to set pH$_i$ to different levels. Recovery from acidification was measured as soon as the cells were resuspended in Na^+-containing Hanks' solution. The initial rate of recovery was determined by measuring the

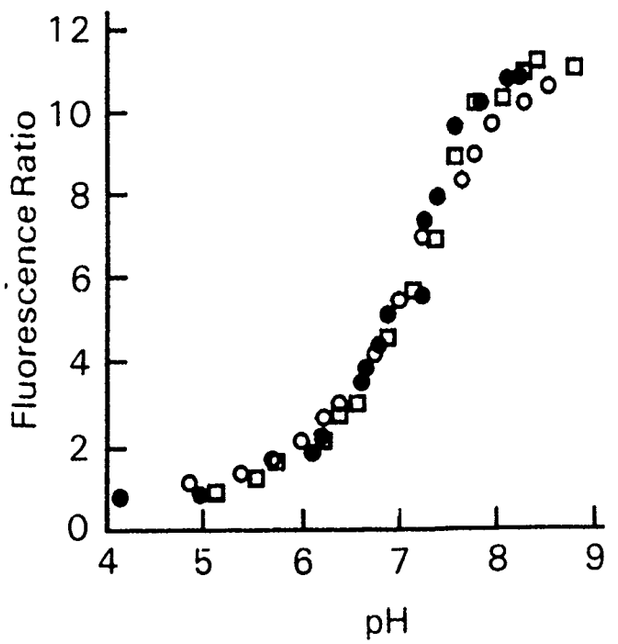

FIG. 1. Relationship of fluorescence ratio to pH. Cells were heated at 45°C for 10 min, then returned to 37°C (○) or held at 45°C (□) in K^+ Hanks' solution before taking the fluorescence measurement (n = 15). Non-heat-treated cells were held at 37°C (●).

slope of a fitted straight line to the initial 30 s of the fluorescence trace.

Measurement of H^+ extrusion. The rate of H^+ extrusion from suspended cells is derived from measurement of external pH according to the method of Grinstein et al. (17). Continuously shaken cell suspensions (4×10^6 cells) were maintained in lightly buffered (0.5 mM HEPES) Hanks' solution at 37 or 45°C for 10 min, and pH_o was then measured at 37°C every 2 min for 10 min using a Corning model 125 or 250 pH meter. The pH in the Hanks' solution was in the range of 7.1–7.3. H^+ extrusion was calculated by multiplying the change in pH_o between 0 and 10 min by the buffering power of the medium, which was determined by titration. Results are expressed in units of nmoles H^+ extruded per 10^6 cells per minute.

Measurement of intracellular buffering power. Cellular buffering power was measured according to methods of Boron (2) and Ng and Dudley (31). pH_i of cells (1×10^6 cells/ml) was set by exposing the cells to nigericin (2 mM) for 5 min in K^+ Hanks' solution having pH ranging from 6.5 to 7.8. After incubation, cells were centrifuged, washed, and resuspended in 145 mM K^+ Hanks' solution containing 1% nonesterified fatty acid-free bovine serum albumin, which scavenged nigericin from the cell membrane. Aliquots of NH_4Cl (1–8 mM) were then added, and alkalinization of the cells was measured. Buffering power was calculated from the equation

$$\text{Buffering power} = \Delta[NH_4^+]/\Delta pH_i$$
$$= [NH_3]_i \times 10^{(pK_a - pH_i)}/\Delta pH_i$$

where pH_i is the value following addition of NH_4Cl. The pK_a of NH_4^+ is 8.89 at 37°C and is assumed to be unchanged inside the cell. $[NH_3]_i$ is assumed to be equal to $[NH_3]_o$, which is calculated from the Henderson-Hasselbach equation.

Intracellular Na^+ measurements. Cells (2×10^7) were centrifuged through Versilube F50 silicone fluid (General Electric) using a Beckman microfuge. The aqueous phase and the oil phase were gently aspirated and discarded. The cell pellet was resuspended in 1 ml deionized distilled water for 1 h and sonicated for 5 min to completely lyse the cells. Lysates were centrifuged at 1,500 *g* for 10 min to remove particulate debris, and the supernatant was collected. The Na^+ content of the supernatant was determined by emission flame photometry (Instrumentation Laboratory model 09430-12). To determine cell water content, the tip of the polypropylene centrifuge tube containing the cell pellet was weighed before and after drying at 80°C for 72 h, with the difference representing the wet weight of the cell. Wet weight was found to be 33 $\mu l/10^6$ cells. Values for intracellular Na^+ and water content were corrected for extracellular fluid trapped in the cell pellet after centrifugation through the oil cushion using [^{3}H]sucrose (Du Pont-New England Nuclear, Boston, MA) as an extracellular marker (25).

ATP measurements. Cellular ATP was determined after extracting 1×10^6 cells/sample with ATP-releasing reagent (a detergent containing NaOH, product no. FL-SAR, Sigma Chemical, St. Louis, MO) for 15 min at 0°C. The extract was assayed for ATP contents by using the luciferase-luciferin assay (kit FL-ASC, Sigma) with a luminometer (Picolite model 6500).

Solutions. Hanks' solution contained (in mM) 148 NaCl, 4.6 KCl, 1.2 $MgCl_2$, 1.6 $CaCl_2$, and 10 HEPES (pH 7.26 at 37°C). The pH of Na^+ Hanks' solution heated to 45°C is 7.11. In Na^+-free Hanks' buffer, NaCl was substituted by equimolar concentrations of either choline chloride, *N*-methyl-(+)-glucamine chloride (NMG), or D-(+)-glucosamine chloride. In bicarbonate-buffered Na^+ Hanks' solution, HEPES was replaced by 25 mM $NaHCO_3$ and bubbled with 5% CO_2 (pH 7.26 at 37°C).

Statistical analysis. All data are expressed as means ± SE. Nonlinear least-squares fits to the data were carried out using the RS1 statistical package (BBN Software, Cambridge, MA). Analysis of variance (ANOVA), Studentized range test, Bonferroni's inequality, Student's *t* test, linear regression, and Mann-Whitney test were used for comparison of groups (40).

Chemicals. BCECF/AM, nigericin, and valinomycin were purchased from Molecular Probes (Eugene, OR). Other chemicals used in this study were sodium azide, 2-deoxy-D-glucose, trypan blue, ethidium bromide, acridine orange, amiloride, bovine serum albumin (fatty acid and globulin-free, product no. A-0281, Sigma), choline chloride, *N*-methyl-(+)-glucamine, and D-(+)-glucosamine chloride (Sigma).

RESULTS

Heat-induced intracellular acidification in bicarbonate-free Na^+ Hanks' solution. The resting pH_i of A-431 cells at 37°C in Hanks' solution (pH_o 7.26) is 7.23 ± 0.02 (n = 24). Cells subjected to temperatures >37°C for 10 min exhibit an intracellular acidification that is temperature dependent, and maximal acidification (−0.25 pH units) is observed at 50°C (Fig. 2). Further acidification is not observed >50°C (data not shown). The degree of acidification also depends on the duration of exposure to heat (Fig. 3). The pH_i of cells exposed to 45°C for 10 s–30 min decreases from 7.20 ± 0.05 to 6.99 ± 0.06. In this study heat treatment decreased the pH_o from 7.26 to 7.11, but

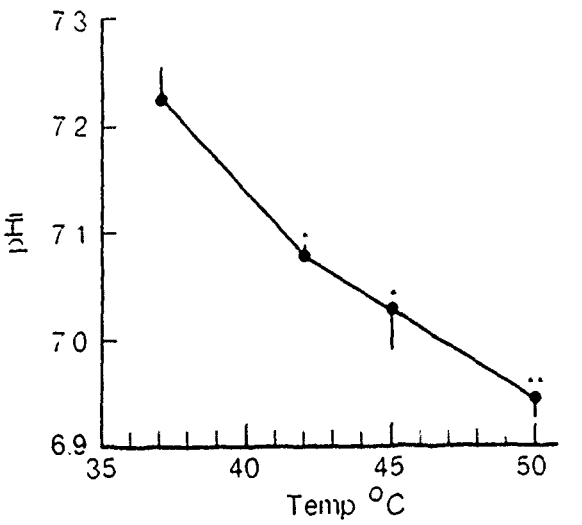

FIG. 2. Effect of temperature on intracellular pH (pH_i). Cells were exposed to 37, 42, 45, or 50°C for 10 min, then pH_i was measured (n = 3–22). * $P < 0.05$ vs. 37°C, ** $P < 0.05$ vs. 37 and 42°C, 1-way ANOVA and Bonferroni's inequality test.

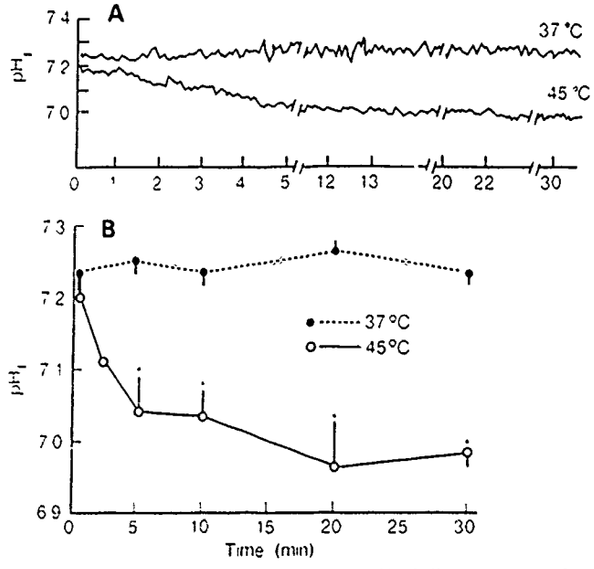

FIG. 3. Effect of duration of heating on pH$_i$. Cells were exposed to 45°C for different times (n = 3–17). *A*: fluorometer tracing of cells exposed to 45°C. *B* pH$_i$ decreases with duration of heat exposure. *P < 0.05 vs. control, 2-way ANOVA and Bonferroni's inequality test.

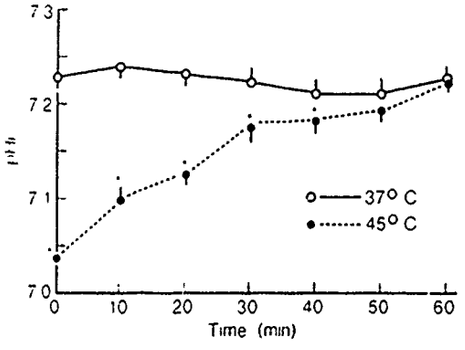

FIG. 4. Recovery after acidification induced by exposure to 45°C for 10 min (n = 4–6). *P < 0.05 vs. 37°C, 2-way ANOVA and Bonferroni's inequality test.

the degree of acidification is similar even when pH$_o$ is maintained at 7.26. Although heat treatment under these conditions does not induce acidification below pH$_i$ of ~6.95, this value did not represent an absolute limit. That is, cells that were preacidified to 6.9 ± 0.01 (n = 3) by a prepulse of NH_4Cl and maintained in Na^+-free Hanks' solution during heat treatment (45°C for 10 min) still show a decrease in pH$_i$ to 6.78 ± 0.04 (n = 4). Furthermore, cells exposed to K^+ Hanks' solution (145 mM KCl) have a lower than normal resting pH$_i$ of 7.0 ± 0.04 (n = 7) but still acidify in response to heat treatment to 6.8 ± 0.04 (n = 4).

Recovery from the acidification induced by heat treatment was examined in cells exposed to 45°C for 10 min, then incubated at 37°C for up to 1 h. Figure 4 demonstrates that the pH$_i$ in heat-treated cells returns to control (unheated) levels after 1 h. Amiloride prevents the recovery from heat-induced acidification. Cells that had been heat treated (45°C for 10 min), then incubated at 37°C for 1 h in the presence of amiloride (100 μM), have a pH$_i$ of 7.07 ± 0.02 (n = 4). This value is not statistically different from the pH$_i$ of cells immediately after heat treatment (7.03 ± 0.02, n = 16) but is significantly less than the pH$_i$ of heat-treated cells allowed to recover in the absence of amiloride (7.22 ± 0.01, n = 4).

To assess whether the heat-induced pH$_i$ changes are related to cell death, cell viability was measured using several different methods. The data in Table 1 demonstrate that the viability of heat-treated cells (45°C for 5 or 10 min) assessed by trypan blue exclusion and ethidium bromide-acridine orange staining is not different from that of unheated cells. Cells exposed to 45°C for 30 min exhibit a small (5–10%) decrease in viability, which is confirmed by lactate dehydrogenase measurements. Because it is possible that the cells are viable immediately after heat treatment, but become nonfunctional later, the plating efficiency of heated cells was examined 24 h after heat treatment. Cells heated at 45°C for 10 or 30 min were replated on culture dishes immediately after heat treatment, and 24 h later the percentage of adherent cells in heat-treated groups was compared with that of adherent cells in the control groups. Exposure to 45°C for 10 min has little effect on plating efficiency, but a 30-min exposure to heat decreases the plating efficiency by 10%. Based on these results and the data on heat-induced acidification, heat treatment at 45°C for 10 min was selected for subsequent experiments.

Heat-induced intracellular acidification in HCO_3^--CO_2-buffered Hanks' solution. Cassel et al. (5) and Ganz et al. (14) have reported that stimulus-induced pH$_i$ changes can be attenuated in the presence of bicarbonate. To determine whether heat-induced intracellular acidification occurs in the presence of bicarbonate, we measured the heat-induced pH$_i$ changes in cells suspended in Na^+ Hanks' solution buffered with 5% CO_2–25 mM HCO_3^- (pH$_o$ 7.26). As noted by Cassel et al. (5), the resting pH$_i$ of A-431 cells in the presence of bicarbonate (7.42 ± 0.03, n = 13) is higher than that in Na^+ Hanks' solution (7.23 ± 0.02, n = 24). Surprisingly, amiloride (100 μM) decreases the pH$_i$ of cells in bicarbonate Hanks' solution to 7.29 ± 0.04, supporting the view that the Na^+-H^+ exchanger contributes to the resting pH$_i$ even in the presence of bicarbonate. However, even in the presence of bicarbonate, pH$_i$ declines from 7.42 ± 0.03 (n = 13) to 7.22 ± 0.04 (n = 9) following heat treatment for 10 min at 45°C. This heat-induced intracellular acidification is

TABLE 1. *Cell viability following thermal injury*

	Viability, %			
	Trypan blue	EB/AO	LDH	Plating efficiency
Control	100	100	9.3±0.8	94±1
Heated				
5 Min	99±1	*	8.8±0.5	*
10 Min	97±2	97±0.4	11.2±1.6	90±1
30 Min	90±4†	95±1†	23.4±3.7†	84±2†

Values are means ± SE expressed as percentage of total cell population (n = 3–6 experiments). Cells were heated at 45°C for indicated periods of time, then returned to 37°C and assayed. EB/AO, ethidium bromide-acridine orange; lactate dehydrogenase (LDH) measurements represent percentage of total cellular LDH released into supernatant. * Not done. † P < 0.05 vs. control, determined by Student's t test.

not observed when cells are heat treated in the presence of amiloride (100 μM) (pH$_i$ = 7.29 ± 0.04 at 37°C, 7.25 ± 0.05 at 45°C; n = 7 for both groups). Thus heat-induced acidification occurs under physiological buffering conditions.

Because the steady-state pH$_i$ of A-431 cells in the absence or presence of bicarbonate is well above electrochemical equilibrium (~6.2 at 37°C assuming pH$_o$ 7.25 and membrane potential = −65 mV), energy-dependent processes must be involved in maintaining steady-state pH$_i$. Inhibition of any of these by heat treatment can result in intracellular acidification. The rest of our study is focused on determining the effect of heat treatment on the functioning of one transport system involved in regulating pH$_i$, Na^+-H^+ exchange, and metabolism, which supplies the energy necessary for maintaining ionic gradients. These experiments were conducted in bicarbonate-free Na^+ Hanks' solution to eliminate the effect of bicarbonate-dependent process on pH$_i$.

Characterization of Na^+-H^+ exchange. In cells in which Na^+-H^+ exchange contributes to resting pH$_i$, an inhibition of this exchange could lead to intracellular acidification. Na^+-H^+ exchanger activity was determined in resting cells by measuring the effect of amiloride on resting pH$_i$. Amiloride (100 μM) causes resting pH$_i$ to decrease from 7.23 ± 0.02 (n = 24) to 7.08 ± 0.01 (n = 5) (Fig. 5, *top tracing*). As will be discussed later, amiloride does not reduce the resting pH$_i$ of heated cells (Fig. 5, *bottom tracing*).

Recovery from an imposed acid load is also mediated by Na^+-H^+ exchange in these cells. Acid-loaded cells (prepulsed with 40 mM NH_4Cl Hanks' solution for 15 min) have a pH$_i$ of 6.69 ± 0.02 (n = 22) in Na^+-free (NMG) Hanks' solution, but their pH$_i$ returns to 7.2 within 4 min after being placed in Na^+ Hanks' solution (Fig. 6*A*, *inset*). Recovery is both $[Na^+]_o$ dependent and inhibited by amiloride. The initial rate of recovery is inhibited 96% in Na^+-free solution. Increasing $[Na^+]_o$ from 0 to 145 mM increases the rate of recovery, with an apparent Michaelis constant (K_m) for extracellular Na^+ of 38 ± 9 mM (Fig. 6*A*). Amiloride (100 μM) inhibits the initial rate of recovery from acidification in Na^+ Hanks' solution by 96%. Inhibition is concentration dependent with an apparent mean affinity constant ($K_{\frac{1}{2}}$) for amiloride of 11 ± 3 μM (Fig. 6*B*). Because the rate of recovery is inhibited by 96% in both Na^+-free and amiloride-containing solutions, Na^+-H^+ exchange appears to be the primary process responsible for recovery from an acid load in these cells in bicarbonate-free buffer. Thus, if heat treatment inhibits the activity of the Na^+-H^+ exchanger, then the rate of recovery from an acid load should be inhibited in heated cells.

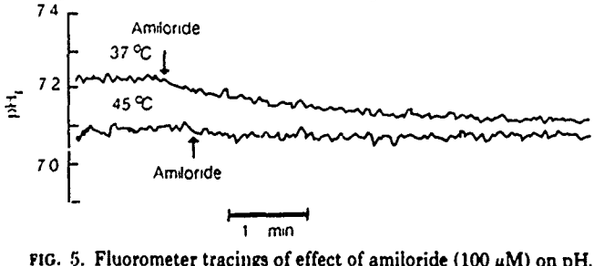

FIG. 5. Fluorometer tracings of effect of amiloride (100 μM) on pH$_i$ of control (37°C) and heat-treated (45°C) cells.

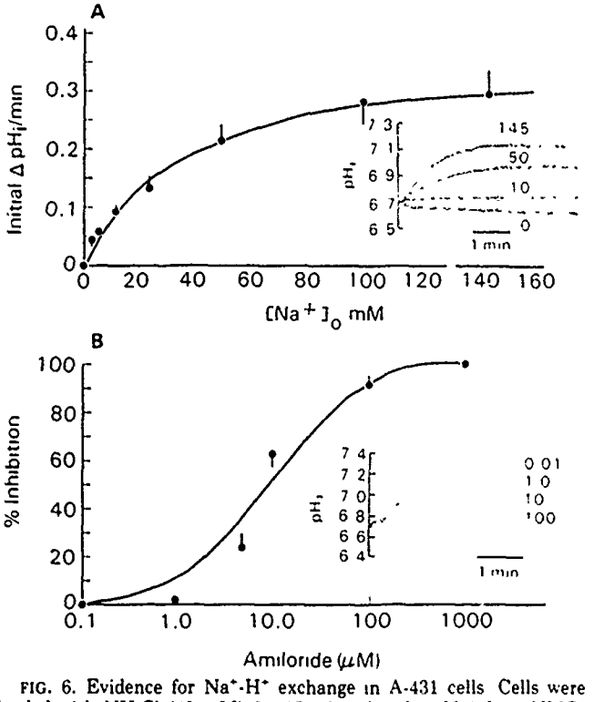

FIG. 6. Evidence for Na^+-H^+ exchange in A-431 cells. Cells were loaded with NH_4Cl (40 mM) for 15 min, placed in Na^+-free (NMG) medium for 2 min, then resuspended in buffer containing different concentrations of Na^+. *A*: rate of alkalinization following acid loading is dependent on $[Na^+]_o$ (n = 3–4). Na^+-sensitive portion of recovery was substracted from these values. Apparent K_m for Na^+ is 38 ± 9 mM. *Inset*: fluorometer tracings of time required for acid-loaded cells to alkalinize in the presence of several Na^+ concentrations. No recovery is observed in Na^+-free Hanks' solution. *B*: amiloride blocks recovery from acid loading (n = 3–4). Apparent $K_{\frac{1}{2}}$ for amiloride is 11 ± 3 μM. *Inset*: fluorometer tracings with different concentrations of amiloride (in μM).

Heat-induced inhibition of recovery from acidification. The effect of heat treatment (45°C for 10 min) on the rate of recovery from an acid load is shown in Fig. 7. After heat treatment, cells were returned to 37°C for either 2 min or 1 or 2 h, then acid loaded and allowed to recover. The fluorescence tracings from these experiments are shown in Fig. 7*A*. Cells allowed to recover for either 2 min or 1 h before acid loading show a reduced rate of recovery. In cells allowed to recover for 2 h before they are acid loaded, the rate of recovery from acid loading is not different from that of control cells.

In A-431 cells, as in other cell types, the initial rate of recovery from acidification is proportional to the magnitude of acidification (4, 39). Figure 7*B* shows that heat treatment changes the slope of the pH$_i$ vs. recovery rate curve. Cells that had been heat treated and allowed to recover for either 2 min or 1 or 2 h were acid loaded to different pH$_i$ values, and the initial rate of recovery was measured as a function of pH$_i$. (It should be noted that the cells allowed to recover from heat treatment for 2 min were acid loaded to pH$_i$ values of only 6.73 or greater because acid loading below that value required >5-min incubation periods.) The dependence of the rate of recovery on pH$_i$ for unheated and heat-treated cells allowed

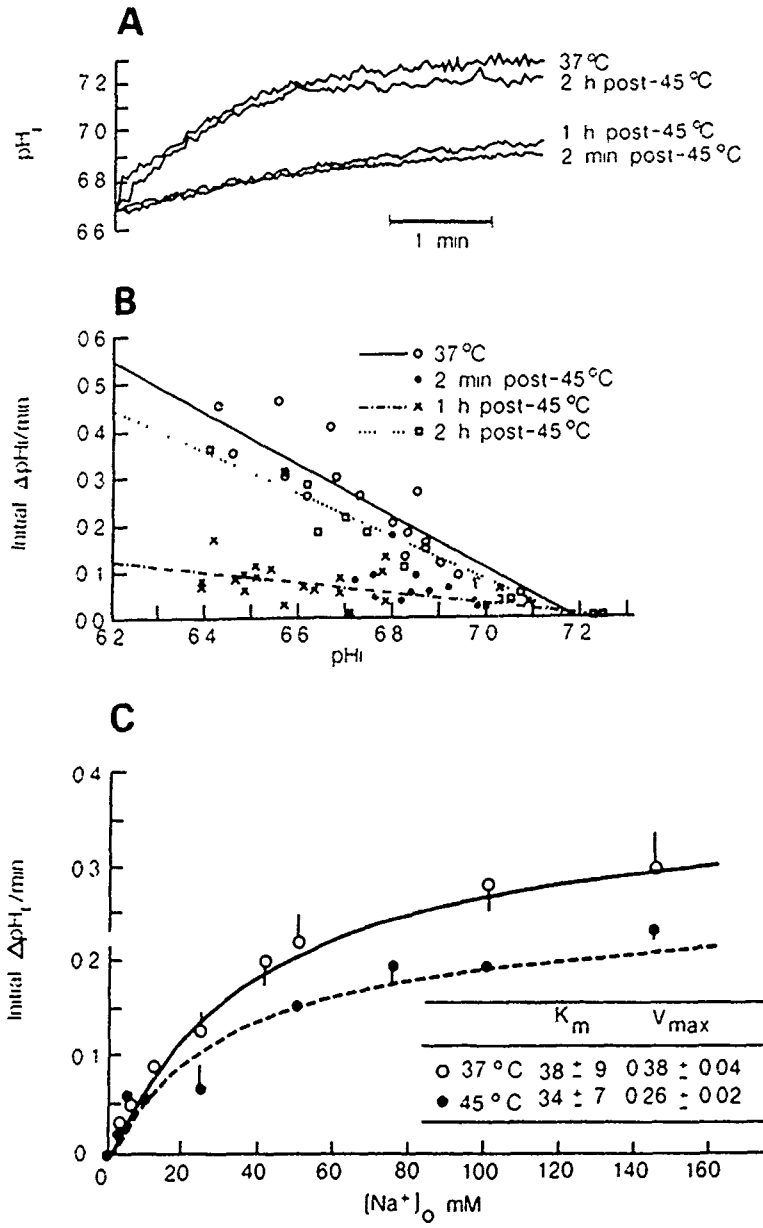

FIG. 7. Effect of heat treatment on rate of alkalinization of acid-loaded cells. Cells were heated at 45 °C for 10 min, acid-loaded by pulsing with NH_4Cl (5–70 mM) immediately or 1 or 2 h after heat treatment, then placed in Na^+-free (NMG) media for 2 min to set their pH_i, then resuspended in Na^+ Hanks' solution for measurements. *A*: fluorometer tracings of effect of acid loading the cells at different times after heat treatment. *B*: relationship of initial rate of alkalinization to the level of acidification following acid loading of unheated cells ($n = 18$) and cells loaded 2 min ($n = 15$), 1 h ($n = 20$), or 2 h ($n = 12$) after heat. Correlation coefficients of the linear regression lines are 0.92, 0.97, and 0.88 for unheated, 1 h postheat, and 2 h postheat, respectively. *C*: initial rates of alkalinization from an acid load with different $[Na^+]_o$ in heated cells 1-h postheat treatment. Inserted table represents the V_{max} and apparent K_m for external Na^+ in unheated and heat-treated cells 1 h after heating.

to recover for 2 h is the same. However, the rate of recovery for heat-treated cells either 2 min or 1 h after heat treatment is significantly reduced over a wide range of pH_i. The *x*-intercept of the line for the data obtained 1 h after thermal injury is not significantly different from the *x*-intercept of the line through the data obtained from unheated cells, indicating no shift in the "set point" of the curve. This is consistent with the observation that the resting pH_i of heat-treated cells is normal after 1 h.

Because the apparent inhibition of Na^+-H^+ activity could be due to a change in maximal initial alkalinization rate (V_{max}) of the exchanger, or to changes in the affinity of the exchanger for extracellular Na^+ or intracellular H^+, the apparent affinity for extracellular Na^+ was evaluated in cells that were heat treated at 45°C for 10 min, then returned to 37°C for 1 h. Figure 7*C* shows that the apparent K_m for extracellular Na^+ in heat-treated cells is not statistically different from that of unheated cells, whereas the apparent V_{max} is ~40% slower than that of unheated cells. The apparent affinity for H^+ was not calculated.

Although our data are consistent with the idea that Na^+-H^+ exchange has been inhibited, changes in either cellular buffering capacity or the Na^+ gradient could also produce these effects. Cellular buffering power in unheated and heat-treated cells 1 h after heating was measured (Fig. 8). As has been shown in many other cell types (2, 31, 36), buffering power values vary with pH_i. In A-431 cells, buffering power remains constant in the pH_i range 7.2–7.8 in both groups but is inversely proportional to pH_i below pH_i 7.2. However, heat treatment does not change the buffering power in these cells. Furthermore, the $[Na^+]_i$ in both groups is not statistically different (unheated: 27 ± 3 mmol/l cell water, $n = 7$; heat treated: 29 ± 9 mmol/l cell water, $n = 7$), indicating that heat induced intracellular acidification is not due to a decrease in the Na^+ gradient. These results are similar to the

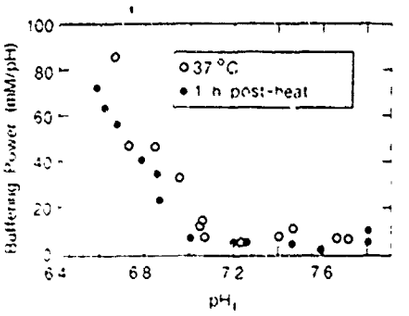

FIG. 8. Relationship of cellular buffering power to pH, in cells suspended in nominally bicarbonate-free buffer exposed to 37 or 45°C for 10 min (n = 18–22).

TABLE 2. *Removal of Na^+ reduces magnitude of heat-induced acidification*

	pH_i		
	37°C	45°C	Decrease
Na^+	7.23±0.02	7.03±0.03	0.20±0.02
Choline	6.93±0.03	6.83±0.03	0.10±0.03*
D-(+)-Glucosamine	7.08±0.02	6.95±0.02	0.13±0.02*
N-methyl (+)-glucamine	7.52±0.01	7.37±0.02	0.15±0.02*

Values are means ± SE (n = 3–24 experiments). Cells were heated in specified Hanks' solution at 45°C for 10 min. pH_i, intracellular pH. * $P < 0.05$ vs. Na^+ Hanks' solution, Student's t test.

observation that intracellular Na^+ does not change in mouse mastocytoma p815 cells exposed to 43°C for 1 h (48).

Magnitude of heat-induced acidification is reduced under conditions that inhibit the Na^+-H^+ exchanger. The relationship between heat-induced intracellular acidification and the activity of the Na^+-H^+ exchanger was determined by measuring the magnitude of heat-induced acidification in the presence of amiloride. If heat-induced acidification were due solely to an inhibition of Na^+-H^+ exchange, then amiloride-treated cells should not be acidified upon heating. The pH_i of amiloride-treated cells is 7.08 ± 0.03 (n = 4), while the pH_i of cells heated at 45°C for 10 min in amiloride-containing Na^+ Hanks' solution is 6.990 ± 0.006 (n = 5). The magnitude of the heat-induced pH_i change is only 50% of the heat-induced pH_i change in the absence of amiloride. Conversely, when amiloride (100 μM) is added to heat-treated cells (7.03 ± 0.02, n = 16) the pH_i is not reduced further (6.99 ± 0.04; n = 6; Fig. 5, *bottom tracing*).

Experiments were also conducted in Na^+-free Hanks' solution in which the activity of the Na^+-H^+ exchanger was inhibited by removing extracellular Na^+. Heat treatment produces additional intracellular acidification in the absence of extracellular Na^+, although the degree of acidification is reduced (Table 2). When either choline or D-(+)-glucosamine was used as a Na^+ substitute, the resting pH_i decreases, as it did in the presence of amiloride, presumably because the Na^+-H^+ exchanger is inhibited. The heat-induced acidification is still observed, but its magnitude is 50% of that in Na^+-containing Hanks' solution. When NMG is used as a Na^+ substitute, the resting pH_i becomes more alkaline (7.52 ± 0.01, n = 3), probably as a result of the entry of this weak base into the cell (39). Heat-induced acidification is also observed in this solution, although its magnitude is only 25% of that of the control. The data obtained with Na^+ substitutes together with the amiloride data indicate that an inhibition of Na^+-H^+ exchange accounts for ~50% of the heat-induced acidification.

Heat-induced inhibition of steady-state H^+ efflux. To further test the hypothesis that Na^+-H^+ exchange is inhibited by heat treatment, steady-state H^+ efflux, with an without amiloride or Na^+, was measured by monitoring the external pH of suspended cells in lightly buffered (0.5 mM HEPES) Na^+ Hanks' solution. This experiment also allows us to determine whether heat-induced intracellular acidification is the result of an increased uptake of external H^+. The results in Table 3 show that a suspension of control cells (Na^+ Hanks', 37°C) extrudes H^+ and that the rate of acid extrusion is reduced 80% in the presence of amiloride (100 μM) or in Na^+-free Hanks' solution, presumably due to inhibition of Na^+-H^+ exchange. In heated-treated cells, a decreased rate of acidification of the medium is observed, consistent with the hypothesis that Na^+-H^+ exchange is inhibited by heat treatment, and also consistent with the hypothesis that intracellular acidification is not a result of H^+ uptake. The rate of H^+ efflux recovers by ~50% at 1 h after heating and completely recovers at 2 h after heating. The time course of recovery is similar to that previously characterized for recovery of Na^+-H^+ exchange as shown in Fig. 7. Amiloride (100 μM) given immediately after heat treatment blocks the recovery of H^+ efflux (Table 3). Taken together, the measurements of pH_i and H^+ efflux indicate that heat-induced intracellular acidification is not the result of uptake of extracellular H^+, but rather a result of a reduced rate of acid extrusion, most probably via Na^+-H^+ exchange.

Heat-induced metabolic inhibition. It is known that metabolic inhibition can produce an intracellular acidification (3, 10, 32) and a reduction of intracellular ATP levels (20, 50). A previous study on A-431 cells (4) has demonstrated that reducing the cellular ATP content (to levels that were ~8% of control levels) inhibits Na^+-H^+ exchange by modulating an intracellular H^+-dependent regulatory mechanism. Therefore, to investigate further the mechanisms underlying the heat-induced acidification, experiments were performed to determine whether heat treatment inhibits ATP production in A-431 cells, resulting in an inhibition of Na^+-H^+ exchanger activity.

TABLE 3. *Heat treatment reduces steady-state H^+ efflux*

	H^+ Efflux, nmol·10^6 cells^{-1}·min^{-1}			
	37°C	Time after heat treatment		
		30 s	1 h	2 h
NMG	0.52±0.001	0.63±0.01	0.63±0.02	0.41±0.04
Na^+	2.27±0.13‡	0.26±0.01*	1.26±0.30†	1.92±0.40‡
Na^+ + amiloride	0.51±0.02§	0.25±0.12	0.49±0.03§	0.28±0.06§

Values are means ± SE (n = 3–5 experiments). Cells were exposed to 45°C for 10 min and then returned to 37°C to determine external pH in the medium lightly buffered with 0.5 mM HEPES. *N*-methyl-(+)-glucamine (NMG) replaced Na^+ in Na^+-free buffer. * $P < 0.05$ vs. Na^+ at 37°C and 1 and 2 h postheating. † $P < 0.05$ vs. Na^+ buffer at 37°C and 30 s postheating. ‡ $P < 0.05$ vs. NMG at 37°C and Na^+ buffer 30 s postheating. § $P < 0.05$ vs. Na^+ buffer.

Heat treatment (45°C for 10 min) reduces cellular ATP content, with longer exposures leading to further decreases in ATP levels (Fig. 9*A*). When heat-treated cells are returned to 37°C in Hanks' solution (containing no nutrients), ATP levels continue to fall, reaching a minimum 20 min after heating. The ATP content then returns slowly to control levels (that also decreased) 90 min after heat treatment (Fig. 9*B*). At 120 min the ATP content in both control and heat-treated cells is reduced by 46 ± 1 and 47 ± 2%, respectively. Nevertheless, as shown in Fig. 7*A*, and Table 3, the rate of recovery from acidification of cells and H^+ efflux 2 h after heat treatment is normal, and the resting pH_i of both unheated and heat-treated cells is similar to control cells at the beginning of the experiment. These findings indicate that Na^+-H^+ exchange in A-431 cells is unaffected by a reduction of >50% in intracellular ATP content.

The effect of heat on anaerobic glycolysis was studied by measuring lactic acid production. Lactic acid is reduced by 25 ± 5 and 42 ± 9% in cells exposed to 45°C for either 10 or 30 min, respectively (Fig. 10*A*). Thirty minutes after treatment (45°C, 10 min) the lactic acid content is still lower than controls but returns to normal levels 1 h after heat treatment (Fig. 10*B*).

Effect of metabolic inhibitors on heat-induced acidification. Because only 50% of the heat-induced acidification can be ascribed to inhibition of Na^+-H^+ exchange,

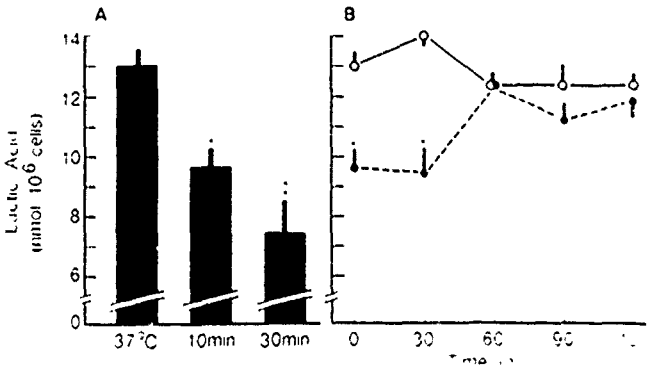

FIG. 10. Role of metabolism in heat-induced acidification. *A*: heat reduces lactic acid content. Cells were heated at 45°C for 10 or 30 min (n = 4–9). * $P < 0.05$ vs. 37°C, 1-way ANOVA and Bonferroni's inequality test, ** $P < 0.05$ vs. 37°C for 10 min and 45°C for 10 min. *B*: recovery of lactic acid content at various times after heating at 45°C for 10 min (n = 4–9). * $P < 0.05$ vs. 0 min postheat, 2-way ANOVA and Bonferroni's inequality test. ●, Heated cells, ○, unheated cells

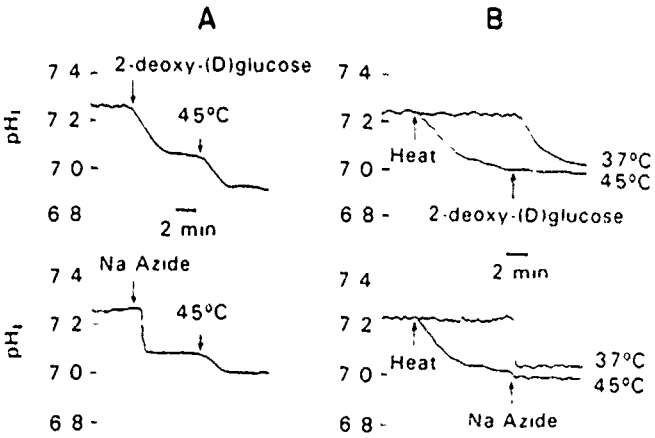

FIG. 11. Effects of 2-deoxy-D-glucose or sodium azide, given before or after heat treatment, on heat-induced intracellular acidification. *A*: fluorometer tracings of cells treated with heat after administration of 2-deoxy-D-glucose (10 mM) or sodium azide (10 mM). *B*: fluorometer tracings of cells exposed to 2-deoxy-D-glucose (10 mM) or sodium azide (10 mM) after heat treatment.

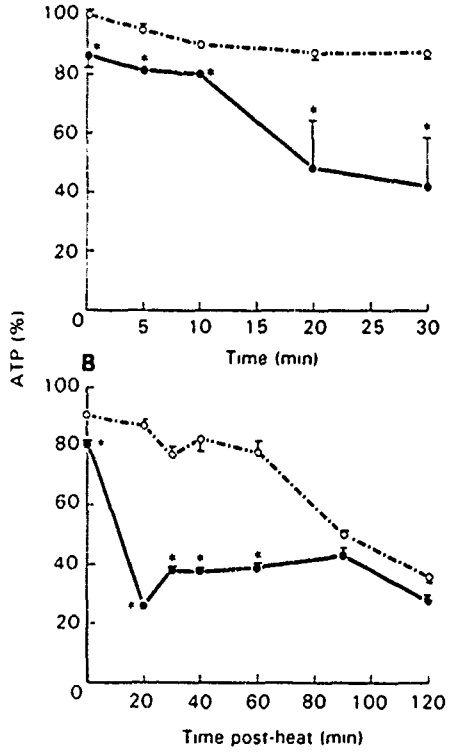

FIG. 9. Effects of heat treatment on ATP content. *A*: heat reduces cellular ATP content. Cells were heated at 45°C for 10 s or 5, 10, 20 or 30 min (n = 4). Data are expressed as percentage of control cell ATP content at the start of experiment (4.160 ± 0.003 nmol/10^6 cells). * $P <$ 0.05 vs. 37°C. *B*: recovery of cellular ATP content at various times after heating at 45°C for 10 min (n = 3–4). Values are expressed as percentage of control cell ATP content at the start of experiment. * P 0.05 vs. 37°C, 2-way ANOVA and Bonferroni's inequality test. ●, Heated cells; ○, unheated cells.

and because metabolic activity is reduced by heat treatment, we tested the hypothesis that the remaining inhibition could be due to metabolic inhibition. We examined the effects of 2-DG (10 mM), a glucose antagonist that inhibits glycolysis, and sodium azide (10 mM), an inhibitor of oxidative phosphorylation, on pH_i. Both agents induce an intracellular acidification that is maintained for 10 min. The maximal acidification induced by 2-DG (7.046 ± 0.020, n = 3) occurs within 5 min, while the maximal acidification induced by sodium azide (7.080 ± 0.037, n = 4) is immediate (Fig. 11*A*). Addition of either inhibitor to cells 5 min before heat treatment reduces the magnitude of intracellular acidification (controls: 0.200 ± 0.036 units; with 2-DG: 0.094 ± 0.029 unit; with sodium azide: 0.06 ± 0.044 unit, n = 3–24; $P < 0.05$). In contrast, when cells are heated before addition of 2-DG no further acidification is noted (Fig. 11*B*). Addition of sodium azide further acidifies heat-treated cells only slightly. The results support the view that the inhibition of glycolysis and oxidative phosphorylation contributes to heat-induced acidification.

In these studies the cellular ATP content of cells treated with 2-DG or sodium azide in Na^+ Hanks' solution for 5 min are 72 ± 2% (n = 6) and 37 ± 10% (n = 6) of controls, respectively (controls: 3.94 ± 0.074 nmol/10^6 cells, n = 6). To determine whether metabolic inhibition by 2-DG or sodium azide acidifies the cells by lowering ATP content, thereby inhibiting Na^+-H^+ exchange, cells were placed in either Na^+-free Hanks' solution for 5 min or Hanks' solution containing amiloride (1 mM) for 10 min to block the Na^+-H^+ exchanger. Then, 2-DG (10 mM) or sodium azide (10 mM) was applied to the cells for 5 min. Under these conditions, intracellular acidification is still observed even though Na^+-H^+ exchange is blocked (in Na^+-free Hanks' solution, 2-DG: 0.07 ± 0.03 units; sodium azide: 0.126 ± 0.07 units, n = 4; in amiloride Hanks' solution, 2-DG: 0.09 ± 0.05 units; sodium azide: 0.14 ± 0.03 units, n = 4).

The possibility that the heat-induced acidification is due to the inhibition of both Na^+-H^+ exchange and metabolism was tested by treating cells with both amiloride and 2-DG for 5 min, and then exposing these cells to 45°C for 10 min. Treatment with both amiloride (100 μM) and 2-DG (10 mM) induces a maximal acidification (7.05 ± 0.02, n = 4) within 5 min that is maintained during the next 10 min. Figure 12 shows that heat does not induce further acidification in cells treated with both amiloride and 2-DG (7.00 ± 0.02, n = 5; $P > 0.05$).

DISCUSSION

This study demonstrates that hyperthermia produces an intracellular acidification (~0.2 pH units) in human epidermoid carcinoma A-431 cells that is temperature and time dependent. Acidification is not related to cell death, because cells that are heated at 45°C for 10 min remain viable, have the same plating efficiency as unheated cells, and recover their pH_i to normal levels 1 h after heat treatment. Similar levels of heat-induced acidification have been noted in nonepithelial cells. For example, mouse mastocytoma cells acidify by 0.35 pH units following heat treatment for 30 min at 43°C (48), and mouse soleus muscle acidifies by 0.16 pH units when heated from 28 to 37°C (1). Likewise, *Drosophila* salivary gland cells acidify by 0.47 pH units when heated from 25 to 35°C (9), and yeast cells acidify by 0.65 pH units when heated from 23 to 40°C (46).

To investigate the mechanisms underlying the heat-induced acidification, we examined the properties of the Na^+-H^+ exchanger in control and thermally injured A-431 cells. Our findings in unheated A-431 cells in suspension are similar to those of Rothenberg et al. (37, 38), who previously characterized Na^+-H^+ exchange in adherent A-431 cells. In agreement with our results, they reported a resting pH_i of 7.3 ± 0.1 at 37°C (pH_o 7.2) that declines in the presence of amiloride, indicating that the Na^+-H^+ exchanger is necessary to maintain resting pH_i. A similar role for the Na^+-H^+ exchanger has been reported in principal and intercalated cells of rabbit cortical collecting tubule (45). Also in agreement with our results, Rothenberg et al. (37, 38) found that a significant fraction (at least 50%) of the recovery from acidification under nominally bicarbonate-free conditions is mediated by Na^+-H^+ exchange. The amiloride sensitivity of Na^+-H^+ exchange (11 ± 3 μM) in our studies is similar to the 4 μM found by Zhuang et al. (49).

The rate of recovery from acid loading, probably mediated by Na^+-H^+ exchange, is markedly inhibited in heat-treated cells over a wide range of pH_i values. In cells heat treated at 45°C for 10 min and returned to 37°C for 1 h, the V_{max} is ~40% slower than that of unheated cells. The apparent K_m for $[Na^+]_o$ is unchanged. Similar results have been reported in a preliminary study of EM T6 cells treated with heat at 45°C for 30 min (27). There are only a few reports of stimulus-induced inhibition of Na^+-H^+ exchange in other systems to be compared with our findings. Parathyroid hormone (PTH) inhibits Na^+-H^+ exchange in renal brush border vesicles (26) and in cultured kidney (OK) cells (22). Interestingly, in OK cells the PTH-induced inhibition results in a reduction of V_{max}, similar to our results with A-431 cells (Fig. 7*B*). Inhibition of Na^+-H^+ exchanger activity has also been induced in rat osteosarcoma cells by osmotic swelling (16). Other factors that can alter the activity of the Na^+-H^+ exchanger include growth factors and osmotic shrinkage, but these treatments result in stimulation of the Na^+-H^+ exchanger (17, 18).

Three observations support the view that the acidification produced by thermal injury is due in part to an inhibition of Na^+-H^+ exchange. First, the rate of recovery from acidification, which is mediated primarily by Na^+-H^+ exchange, is inhibited by heat treatment. This inhibition is not due to a reduction in the gradient of Na^+ or changes in buffering capacity. Second, acidification is reduced in Na^+-free solutions or in the presence of amiloride. Heat treatment of control cells leads to an acidification of ~0.2 pH units, whereas heat treatment of cells that are placed in Na^+-free or amiloride-containing solution produces an acidification of ~0.1 pH units, indicating that about half of the acidification induced by thermal injury is due to an inhibition of Na^+-H^+ exchange. Third, heat-treated cells demonstrate less steady-state H^+ efflux than do unheated cells, and recovery of the H^+ efflux occurs 2 h after heat treatment and is blocked by amiloride.

Previous studies on A-431 cells by Cassel et al. (4) have demonstrated that depletion of intracellular ATP (to <10% of control levels) inhibits Na^+-H^+ antiporter activity due to modulation of an intracellular H^+-dependent regulatory mechanism. In addition, in other cell

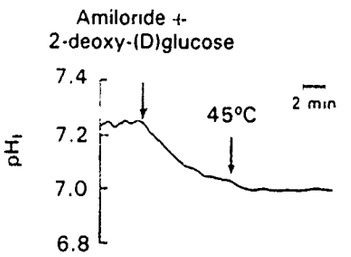

FIG. 12. Effects of 2-deoxy-D-glucose and amiloride, added before heat treatment, on heat-induced intracellular acidification. Fluorometer tracing of cells treated with 2-deoxy-D-glucose (10 mM) and amiloride (100 μM) together 5 min before heat treatment at 45°C for 10 min.

types, inhibition of glycolysis is associated with an intracellular acidification (3, 15). Therefore, we examined the possibility that the heat-induced acidification in A-431 cells was related to an inhibition of metabolism by measuring the levels of both ATP and lactic acid in unheated and heat-treated cells. Our data indicate that exposing cells to 45°C for 10 min inhibits glycolysis and reduces intracellular ATP by 23 ± 2 and 25 ± 5%, respectively. Under our experimental conditions (i.e., in the absence of nutrients), intracellular ATP contents of both heat-treated and control cells continue to decrease so that by 120 min after heat treatment the ATP content of both heated and unheated cells is 36% of the ATP content of unheated cells immediately before heat treatment. The pH_i for both groups of cells at this time is identical to the pH_i of the unheated cells at the start of the experiment. Furthermore, the rate of alkalinization after an acid load for both unheated and heat-treated cells 120 min after the start of the experiment (when their ATP content was reduced) is similar to unheated cells at the start of the experiment (Fig. 7*B*). These data indicate that the Na^+-H^+ exchanger functions normally even though the ATP content is reduced by 64%. Thus heat-induced inhibition of the Na^+-H^+ exchanger is not secondary to a heat-induced ATP reduction. The differences between our data and that of Cassel et al. (4) can be explained by the fact that ATP levels in our study are not depleted as fully as in their study.

To further investigate the role of metabolism in heat-induced acidification, we examined the effects of sodium azide and 2-DG on pH_i in unheated and heat-treated cells. (We also attempted to study the effects of 2,4-dinitrophenol, an inhibitor of oxidative phosphorylation, but its inherent flourescence interfered with the assay.) 2-DG substitutes for glucose but cannot be metabolized beyond the hexose monophosphate shunt. This reduces ATP production via anaerobic glycolysis and subsequently slows aerobic glycolysis and the electron transport chain due to the low level of pyruvate in cells (20, 50). In A-431 cells 2-DG (10 mM) produces an acidification but does not further acidify cells that have been heat treated, supporting the view that the acidification induced by 2-DG is mediated via pathway(s) in common with acidification induced by heat. However, another explanation of these results is possible. 2-DG might not be able to acidify cells further because other buffers (that are not heat sensitive) may maintain the pH_i when it is <6.9. This possibility is unlikely, since data on cells that have been acidified in high-K^+ Hanks' solution or by acid loading to set pH_i to ~6.9 indicates that acidification induced by heat treatment can occur below pH_i 6.9. Sodium azide, an inhibitor of oxidative phosphorylation (29), also produces an acidification but more rapidly than does 2-DG. As is shown in Fig. 11*B*, application of sodium azide to heat-treated cells results in a small additional acidification that is possibly due to sodium azide acting as a weak acid (pK_a = 4.7) (3, 36).

Several observations suggest that heat-induced acidification in bicarbonate-free medium is caused by at least two different mechanisms: an inhibition of Na^+-H^+ exchange and metabolic inhibition. First, heat-treated cells are not acidified further by the addition of metabolic inhibitors, but heat treatment after the addition of metabolic inhibitors still produced an acidification that is ~50% of that produced in the absence of metabolic inhibitors. Second, the possibility that the changes in pH_i produced by 2-DG and sodium azide are due to an effect on Na^+-H^+ exchange are negated by the observation that cells become acidified in Na^+-free or amiloride-containing buffer (to inhibit Na^+-H^+ exchange) after the addition of metabolic inhibitors. Finally, heat treatment fails to induce acidification in cells treated with both amiloride and 2-DG.

To determine the physiological relevance of these changes, we also investigated the effects of heat treatment on A-431 cells in presence of bicarbonate buffer. Because stimulus-induced pH_i changes are known to be attenuated in the presence of bicarbonate (5, 14), we were somewhat surprised that a heat-inducible acidification of ~0.2 pH units that can be inhibited by amiloride is still evident in the presence of bicarbonate. A similar heat-induced acidification in the presence of bicarbonate has been reported in *Drosophila* salivary gland cells (9). Although the possibility of the bicarbonate-related exchangers being affected by heat and contributing indirectly to acidification cannot be ruled out, it seems unlikely because heat-induced acidification in the presence of bicarbonate is blocked by amiloride. Further studies are required to dissect out the role of bicarbonate-dependent transport systems in pH_i regulation of unheated and heated A-431 cells.

In summary, this paper demonstrates that thermal injury produces an intracellular acidification in A-431 cells of 0.2 pH units under both nominally bicarbonate-free or bicarbonate-buffered solutions. In the absence of bicarbonate, the acidification is caused by at least two different events: inhibition of the activity of the Na^+-H^+ exchanger and metabolic inhibition. The change in pH_i following thermal injury may modulate other cell functions such as cell growth and may be one determinant of the sensitivity of tumor cells to hyperthermia (6, 24, 33).

We thank Spencer Green for his technical assistance, William Jackson for his assistance on statistical analysis, and Dr. David E. McClain for his discussion and editorial assistance.

This work was supported by the Armed Forces Radiobiology Research Institute, Defense Nuclear Agency, under work unit 00020. Views presented in this paper are those of the authors; no endorsement by the Defense Nuclear Agency has been given or should be inferred.

Address for reprint requests: J. G. Kiang, Dept. of Clinical Physiology, Div. of Medicine, Bldg. 40, Walter Reed Army Institute of Research, Washington, DC 20307-5100.

Received 1 August 1989; accepted in final form 13 July 1990.

REFERENCES

1. AICKIN, C. C., AND R. C. THOMAS. An investigation of the ionic mechanism of intracellular pH regulation in mouse soleus muscle fiber. *J. Physiol. Lond.* 267: 791–810, 1977.
2. BORON, W. F. Intracellular pH transients in giant barnacle muscle. *Am. J. Physiol.* 233 (*Cell Physiol.* 2): C61–C73, 1977.
3. BORON, W. F., AND P. DE WEER. Intracellular pH transients in squid giant axons caused by CO_2, NH_3, and metabolic inhibitors. *J. Gen. Physiol.* 67: 91–112, 1976.
4. CASSEL, D., M. KATZ, AND M. ROTMAN. Depletion of cellular ATP inhibits Na^+-H^+ antiport in cultured human cells. *J. Biol. Chem* 261: 5460–5466, 1986.
5. CASSEL, D., B. WHITELEY, Y. X. ZHUANG, AND L. GLASER. Mito-

gen-independent activation of Na^+-H^+ exchange in human epidermoid carcinoma A-431 cells: regulation by medium osmolarity. *J. Cell Physiol.* 122: 178–186, 1985.

6 CHU, G. L., AND W. C. DEWEY. The role of low intracellular or extracellular pH in sensitization to hyperthermia. *Radiat. Res.* 114: 154–167, 1988.

7 CHU, G. L., Z. WANG, AND W. DEWEY. The effect of hyperthermia on intracellular pH (pH_i) and the role of pH_i in low pH sensitization of hyperthermic killing (Abstract). *Proc. Annu. Meet. Radiat. Res. Soc. 37th Seattle WA 1989*, p. 105.

8 DICKENS, C. J., J. I. GILLESPIE, J. R. GREENWELL, AND P. HUTCHINSON. Relationship between intracellular pH (pH_i) and calcium (Ca^{++}) in avian heat fibroblasts. *Exp. Cell Res.* 187: 39–46, 1990.

9 DRUMMOND, I. A. S., S. A. MCCLURE, M. POENIE, R. Y. TSIEN, AND R. A. STEINHARDT. Large changes in intracellular pH and calcium observed during heat shock are not responsible for the induction of heat shock proteins in *Drosophila melanogaster*. *Mol. Cell. Biol.* 6: 1767–1775, 1986.

10 EISNER, D. A., C. G. NICHOLS, S. C. O'NEILL, G. L. SMITH, AND M. VALDEOLMILLOS. The effects of metabolic inhibition on intracellular calcium and pH in isolated rat ventricular cells. *J. Physiol. Lond.* 411: 393–418, 1989.

11 ELLIS, D., AND R. C. THOMAS. Direct measurement of the intracellular pH of mammalian cardiac muscle. *J. Physiol. Lond.* 26: 755–771, 1976.

12 FERNANDEZ-POL, J. A. Epidermal growth factor receptor of A-431 cells. *J. Biol. Chem.* 260: 5003–5011, 1985.

13. FRESHNEY, R. I. *Culture of Animal Cells: A Manual of Basic Technique*. New York: Liss, 1983.

14 GANZ, M. B., G. BOYARDSKY, R. B. STERZEL, AND W. F. BORON. Arginine vasopressin enhances pH_i regulation in the presence of HCO_3^- by stimulating three acid-base transport systems. *Nature Lond.* 337: 648–651, 1989.

15. GEVERS, W. Generation of protons by metabolic processes in heart cells. *J. Mol. Cell Cardiol.* 9: 867–874, 1977.

16. GREEN, J., D. T. YAMAGUCHI, C. R. KLEEMAN, AND S. MUALLEM. Selective modification of the kinetic properties of Na^+-H^+ exchanger by cell shrinkage and swelling. *J. Biol. Chem.* 263: 5012–5015, 1988.

17 GRINSTEIN, S., C. A. CLARKE, AND A. ROTHSTEIN. Activation of Na^+-H^+ exchange in lymphocytes by osmotically induced volume changes and by cytoplasmic acidification. *J. Gen. Physiol.* 82: 619–638, 1983.

18 GRINSTEIN, S., AND A. ROTHSTEIN. Mechanisms of regulation of the Na^+-H^+ exchanger. *J. Membr. Biol.* 90: 1–12, 1986.

19. GRINSTEIN, S., D. ROTIN, AND M. J. MASON. Na^+-H^+ exchange and growth factor-induced cytosolic pH changes. Role in cellular proliferation. *Biochim. Biophys. Acta* 988: 73–97, 1989.

20. GUPTA, I., V. K. JAIN, AND R. K. MISHRA. Studies on the effects of 2-deoxy-D-glucose on glucose uptake and glycolysis in respiratory-deficient yeast cells. *Indian J. Exp. Biol.* 19: 231–237, 1981.

21. HALL, E. J., AND L. ROIZIN-TOWLE. Biological effects of heat. *Cancer Res.* 44, *Suppl.*: 4708s–4713s, 1984.

22. HELMLE-KOLB, C., M. H. MONTROSE, G. STANGE, AND H. MURER. Regulation of Na^+-H^+ exchange in opossum kidney cells by parathyroid hormone, cyclic AMP and phorbol esters. *Pfluegers Arch.* 415: 461–470, 1990.

23. HINKE, J. A. M., AND S. G. A. MCLAUGHLIN. Release of bound sodium in single muscle fibers. *Can. J. Physiol. Pharmacol.* 45: 655–677, 1967.

24. HOEFER, K. G., AND N. F. MIVECHI. Tumor cell sensitivity to hyperthermia as a function of extracellular pH and intracellular pH. *J. Natl. Cancer Inst.* 65: 621–625, 1980.

25. INCE, C., B. THIO, B. VAN DUIJN, J. T. VAN DISSEL, D. L. YPEY, AND P. C. J. LEIJH. Intracellular K^+, Na^+ and Cl^- concentrations and membrane potential in human monocytes. *Biochim. Biophys. Acta* 905: 195–204, 1987.

26. KAHN, A. M., G. M. DOLSON, S. C. BENNETT, AND E. J. WEINMAN. cAMP and PTH inhibit Na^+-H^+ exchange in brush border membrane vesicles (BBM) derived from a suspension of rabbit proximal tubules (Abstract). *Kidney Int.* 25: 289, 1984.

27. LIU, F. F., J. K. POON, R. P. HILL, AND I. TANNOCK. Effect of hyperthermia on activity of the Na^+-H^+ antiport in EMT$_6$ cells. *Proc. Annu. Meet. Radiat. Res. Soc. 38th 1990*, p. 48.

28 MANCUSO, D., AND L. GLASER. Characterization of the Na^+-H^+ exchanger in human epidermoid carcinoma A-431 vesicles. *J. Cell Physiol.* 123: 297–304, 1985.

29. MICHELL, P. Conduction of protons through the membranes of mitochondria and bacteria by uncouplers of oxidative phosphorylation (Abstract). *Biochem. J.* 81: 24p, 1961.

30. MONTROSE, M. H., AND H. MURER. Regulation of intracellular pH in LLC-PK_1 cells by Na^+-H^+ exchange. *J. Membr. Biol.* 93: 33–42, 1986.

31. NG, L. L., AND C. DUDLEY. Intracellular pH clamping of human leucocytes: a technique for determination of cellular buffering power and Na^+-H^+ antiport characteristics. *Clin. Sci.* 77: 417–423, 1989.

32. O'NEILL, S. C., M. VALDEOLMILLOS, G. L. SMITH, AND D. A. EISNER. The effects of metabolic inhibition on intracellular pH and Ca. *Mol. Cell. Biochem.* 89: 199–203, 1989.

33. OVERGAARD, J. Influence of extracellular pH or the viability and morphology of tumor cells exposed to hyperthermia. *J. Intl. Cancer Inst.* 56: 1243–1250, 1976.

34. PERONA, R., AND R. SERRANO. Increased pH and tumorigenicity of fibroblasts expressing a yeast proton pump. *Nature Lond.* 334: 438–440, 1988.

35. POUYSSEGUR, J., C. SARDET, A. FRANCHI, G. L'ALLEMAIN, AND S. A. PARIS. Specific mutation abolishing Na^+-H^+ antiport activity in hamster fibroblasts precludes growth at neutral and acidic pH. *Proc. Natl. Acad. Sci. USA* 81: 4833–4837, 1984.

36. ROOS, A., AND W. F. BORON. Intracellular pH. *Physiol. Rev.* 61: 296–433, 1981.

37. ROTHENBERG, P., L. GLASER, P. SCHLESINGER, AND D. CASSEL. Epidermal growth factor stimulates amiloride-sensitive $^{22}Na^+$ uptake in A-431 cells. *J. Biol. Chem.* 258: 4883–4889, 1983.

38. ROTHENBERG, P., L. GLASER, P. SCHLESINGER, AND D. CASSEL. Activation of Na^+-H^+ exchanger by epidermal growth factor elevates intracellular pH in A-431 cells. *J. Biol. Chem.* 258: 12644–12653, 1983.

39. SIMCHOWITZ, L., AND A. ROOS. Regulation of intracellular pH in human neutrophils. *J. Gen. Physiol.* 85: 443–470, 1985.

40. SOKAL, R. R., AND G. F. ROHLF. *Biometry. The Principles and Practice of Statistics in Biological Research*. San Francisco, CA: Freeman, 1969, p. 776–790.

41. STOSCHECK, C. M., AND G. CARPENTER. Biology of the A-431 cells: a useful organism for hormone research. *J. Cell Biol.* 23: 191–202, 1983.

42. STOSCHECK, C. M., AND G. CARPENTER. Characterization of the metabolic turnover of epidermal growth factor receptor protein in A-431 cells. *J. Cell. Physiol.* 120: 296–302, 1984.

43. SUBJECK, J. R., AND T.-T. SHYY. Stress protein systems of mammalian cells. *Am. J. Physiol.* 250 (*Cell Physiol.* 19): C1–C17, 1986.

44. THOMAS, J. A., R. N. BUCHSBAUM, A. ZIMNIAK, AND E. RACKER. Intracellular pH measurements in Ehrlich ascites tumor cells utilizing spectroscopic probes generated in situ. *Biochemistry* 18: 2210–2218, 1979.

45. WEINER, I. D., AND L. L. HAMM. Regulation of intracellular pH in the rabbit cortical collecting tubule. *J. Clin. Invest.* 85: 274–281, 1990.

46. WEITZEL, G., U. PILATUS, AND L. RENSING. Similar dose response of heat shock protein synthesis and intracellular pH change in yeast. *Exp. Cell Res.* 159: 252–256, 1985.

47. YAJIMA, M., AND M. UI. Hydrocortisone restoration of the pH-dependent metabolic responses to catecholamines. *Am. J. Physiol.* 228: 1053–1059, 1975.

48. YI, P. N., C. S. CHANG, M. TALLEN, W. BAYER, AND S. BALL. Hyperthermia-induced intracellular ionic level changes in tumor cells. *Radiat. Res.* 93: 534–544, 1983.

49. ZHUANG, Y. X., E. J. CRAGOE, JR., T. SHAIKEWITZ, L. GLASER, AND D. CASSEL. Characterization of potent Na^+-H^+ exchange inhibitors from the amiloride series in A-431 cells. *Biochemistry* 23: 4481–4488, 1984.

50. ZUBAY, G. *Biochemistry* (2nd ed.). New York: Macmillan, 1988, p. 1162.

RADIATION RESEARCH 128, S29–S36 (1991)

The Relative Biological Effectiveness of Mixed Fission-Neutron–γ Radiation on the Hematopoietic Syndrome in the Canine: Effect of Therapy on Survival

T. J. MacVittie, R. Monroy,[1] R. M. Vigneulle, G. H. Zeman,[2] and W. E. Jackson
Armed Forces Radiobiology Research Institute, Bethesda, Maryland 20889-5145

MacVittie, T. J., Monroy, R., Vigneulle, R. M., Zeman, G. H., and Jackson, W. E. The Relative Biological Effectiveness of Mixed Fission-Neutron–γ Radiation on the Hematopoietic Syndrome in the Canine: Effect of Therapy on Survival. *Radiat. Res.* **128**, S29–S36 (1991).

Acute lethality syndromes produced by the accidental exposure of humans to mixed neutron and γ radiation from external sources can be related to acute lethality from photon irradiation using the relative biological effectiveness (RBE) for common end points. We used the canine as a model to study injury following exposure to mixed neutron and γ radiation from the AFRRI TRIGA reactor. Exposures from the reactor were steady-state mode (40 cGy/min, bilateral) with an average neutron energy of 0.85 MeV; tissue–air ratio = 0.59 at midline abdominal. Healthy male and female canines were irradiated free-in-air behind a 6-in. lead wall; the neutron–γ ratio was 5.4:1 at the entrance skin surface; exposures are reported as midline tissue doses. Bilateral exposure resulted in an $LD_{50/30}$ of 153 cGy without therapeutic clinical support. Addition of clinical support consisting of fluids, antibiotics, and fresh irradiated platelets/whole blood increased the bilateral $LD_{50/30}$ to 185 cGy, a dose modifying factor (DMF) of 1.21. This corresponds to respective $LD_{50/30}$ values for bilateral ^{60}Co γ exposures of 260 and 338 cGy for nonsupported and clinically supported animals, and a DMF of 1.30. The RBE based on the values determined at midline tissue is approximately 1.69. Clinical support after bilateral irradiation produced a similar DMF to those of mixed fission neutrons and γ rays and ^{60}Co γ rays alone. The RBE of 1.69 for midline tissue bilateral exposures is higher than 1, an RBE often cited for large animals. Therapeutic support administered to lethally irradiated canines significantly improved survival and increased the $LD_{50/30}$ independent of radiation quality.

INTRODUCTION

The effectiveness of neutron irradiation in causing mortality as a result of bone marrow failure has been a controversial point for the past 2 decades. Literature values for "neutron effectiveness" in large-animal models such as the pig, sheep, goat, monkey, and canine vary considerably, not only among species but within species.

Survival studies using neutrons of different energies show that the probability of survival at a specific dose is the lowest for neutron energies of approximately 1.0 MeV and the greatest for energies of 9.0 and 14.6 MeV. For example, the $LD_{50/30}$ in the canine model, as measured at the midline tissue, was 2.81 Gy for 14.6 MeV neutrons (*1*); 2.65 Gy for average 9.0 MeV neutrons (*2*); and 2.03 Gy (*3*) and 2.39 Gy (*4*) for fission-spectrum neutrons (energy range 0.5–2.5 MeV). Thus the fission spectrum neutrons appear to be the most effective in causing lethality.

Mobley *et al.* (*5, 6*) concluded that there was no significant difference in the relative potencies of 250-kVp X rays and pulse or steady-state fission-spectrum mixed neutron–γ radiation for bilaterally or unilaterally exposed sheep. The respective $LD_{50/60}$'s were 389 R versus 360 and 367 rad (midpoint air exposure). The neutron–γ ratio was stated as 5:1 measured in air. Other investigators reported midline-in-air $LD_{50/30}$'s of 237 R (*7*) and 297 R (*8*) for ^{60}Co γ rays, bilateral exposure, and 252 R (*7*) and 253 R (*9*) for 1-MVp X irradiation.

Determining neutron effectiveness in the pig is especially difficult due to the wide range of $LD_{50/60}$'s reported in the literature for γ and X irradiation. Brown and Cragle (*10*), in reviewing swine $LD_{50/30}$ experiments, calculated the midline exposure dose to be 191 R. Chambers *et al.* (*11*) determined the $LD_{50/30}$ for ^{60}Co-γ-irradiated swine to be 218 R (midline, bilateral exposure). Tullis *et al.* (*12*) reported an $LD_{50/30}$ of 230 R (free-in-air) after exposure to predominantly γ radiation from a nuclear weapon detonation. Previous studies by Tullis *et al.* (*13, 14*), using 1000- and 2000-kVp bilateral X-ray exposures, reported $LD_{50/30}$'s of 278 and 321 rad (midline-in-air), respectively. Other investigators (*10, 15, 16*) reported $LD_{50/30}$'s from 230 to 620 R (midline air exposure). Recalculated midline tissue doses ranged from 171 to 301 rad (*17*).

Wise and Turbyfill (*18*) determined the $LD_{50/30}$ of the miniature pig for pulsed, mixed γ–neutron radiations, in

[1] Current address: Naval Medical Research Institute, Bethesda, MD 20889.

[2] Current address: Manager, Radiation Protection Department, AT&T Bell Labs, Murray Hill, NJ 07974

0033-7587/91 $3.00

which 60% of the free-in-air dose was from γ radiation and 40% from fission neutrons, to be 218 R (midline tissue) with a mean survival time of 15.1 days. No comparable data were presented for γ- or X-radiation exposure. The range of $LD_{50/30}$'s noted in the literature would preclude ascribing a relative potency for neutron exposure other than 1.0 in swine or sheep.

Ainsworth *et al.* (*3*) and Alpen *et al.* (*4*) exposed canines to fission-spectrum neutrons and reported $LD_{50/30}$'s of 2.03 and 2.39 Gy, respectively. In the 1965 report of Ainsworth *et al* (*3*), the neutron $LD_{50/30}$ was compared to an $LD_{50/30}$ of 2.80 Gy for 1000-kVp X rays, and a "potency ratio" of 1.38 was determined for the effectiveness of the neutron irradiation. In contrast, Alpen *et al* (*4*) reported a "relative potency" of 0.9 when the neutron $LD_{50/30}$ was compared to an $LD_{50/30}$ of 2.12 Gy for 300-kVp X rays. More recent literature shows the relative biological effectiveness (RBE) of neutron irradiation for different animal models to be greater than that observed with either 250-kVp X rays or ^{60}Co γ rays. Broerse *et al.* (*19*), using rhesus monkeys, obtained an RBE value of 2 when comparing fission neutrons (mean energy 1.0 MeV) to 300-kVp X rays. Thus controversy exists: fission neutrons have been reported to be less effective than X rays and as much as two times as effective as 250-kVp X rays in producing lethality as a result of bone marrow failure.

The effectiveness of fission-neutron irradiation in causing lethality in a large-animal model was evaluated by exposing canines bilaterally to a neutron field generated by the Armed Forces Radiobiology Research Institute (AFRRI) TRIGA reactor. Postirradiation therapy increased both mean survival time and survival in lethally irradiated canines. The increased survival allowed us to investigate the effects of higher levels of radiation exposure, and to evaluate the stem cell number below which spontaneous marrow regeneration would not occur.

MATERIALS AND METHODS

Animals Healthy, pure-bred male and female canines (beagles, 10–12 kg) were used in these studies. The canines were treated to eliminate parasitic infections; immunized against distemper, hepatitis, and rabies; and observed for 2 weeks before entering the experimental protocol. They were housed in temperature-controlled rooms in individual stainless-steel cages and were fed kibbled laboratory dog food, supplemented once a week with high-protein canned meat ration. Water was provided *ad libitum*.

Hematological values and hematopoietic culture techniques. Peripheral blood was withdrawn from the cephalic vein, and bone marrow was aspirated from the ribs and iliac crest of anesthetized canines (Biotal, Parke Davis, A. J. Buck & Son, Baltimore, MD) into heparinized syringes. Peripheral blood leukocytes and platelets were counted using a hemocytometer. Bone-marrow-derived mononuclear cells (MNC) were harvested using lymphocyte separation medium (Bionetics, Kensington, MD) and centrifuged at 1500 rpm (400*g*) for 35 min. The MNC layer was harvested and counted for viable nucleated cells in a hemocytometer. These cell populations were then assayed for specific hematopoietic progenitor cells.

Granulocyte-macrophage colony-forming cells (GM-CFC) were assayed using the double-layer agar technique described previously (*20*). Briefly, CSA was provided by using pooled plasma from canines previously injected with lipopolysaccharide (*Escherichia coli*, 055:B5, List Biologicals, Campbell, CA) that was added to the bottom agar layer (7% v/v) of triplicate culture dishes. Bone-marrow-derived MNC were plated in the upper agar layer in concentrations depending on previous treatment. Colonies (>50 cells) counted after 10 days of culture were considered to be derived from GM-CFC.

Cobalt-60 γ irradiation and mixed neutron–γ-irradiation parameters The canines were secured in Plexiglas holders for both types of exposure. Bilateral ^{60}Co γ irradiations were carried out to give various midline tissue doses (MTDs) at a dose rate of 0.1 Gy/min. Mixed neutron–γ irradiation was achieved in a gadolinium-lined exposure room from AFRRI's TRIGA Mark-F pool-type thermal research reactor operated in the steady-state mode. Bilateral exposure was achieved by a 180° rotation at midtime of the exposure. The physical parameters of the free-in-air exposure were an average neutron energy of 1.0 MeV and an average γ-ray energy of 0.9 MeV, a neutron–γ ratio of 5.4:1 at 101 cm, and a dose rate of 0.6 Gy/min. (The neutron–γ ratio was achieved by imposing a 15-cm-thick lead wall in front of the reactor core tank wall in the exposure room.)

Figures 1a and 1b show calculated neutron and γ-ray energy spectra appearing 40 cm beyond the lead shield (70 cm from the tank wall), both free-in-air and at midline in a 18.0-cm diameter cylindrical tissue-equivalent (TE) phantom. The spectra show that neutrons with energy between 0.5 and 4.0 MeV account for over 70% of the neutron kerma both free-in-air and within the phantom, while both γ-ray spectra are dominated by the 2.2-MeV peak arising from thermal neutron capture by hydrogen. These data indicate that the incident neutron spectrum is not significantly altered in passing through the phantom. There is significant alteration, however, if the entire range of neutron energies is considered (0.1–15 MeV) instead of only 0.1–10 MeV. High neutron–γ kerma ratios were obtained only within the first 2 m beyond the tank wall, and all experiments were restricted to this region. All irradiations in the present study were conducted with phantom midlines aligned at 101 cm from the tank wall.

Canine phantoms Two canine phantoms were used for dosimetry measurements. Both phantoms contained a canine skeleton, simulated lung tissue, and a contoured body mass composed of plastic. Dimensions of each phantom are listed in Table I.

The AFRRI canine phantom was comprised of 32 transverse sections, each 2.54 cm thick, held together by a removable plastic rod. In each section a rectangular array of 5-mm-diameter wax-filled holes allowed positioning activation foil wires at various depths. Most of the activation foil measurements were made in sections 5 (midhead), 20 (midthorax), and 27 (midabdomen). Larger holes for ionization chambers were drilled vertically into the midline of sections 6 (head), 18 and 22 (thorax), and 26 (abdomen), and at 1-cm depths from right and left sides in section 22. The midline of section 20 was treated as the centerline for irradiation alignment.

The TNO[3] canine phantom was of solid plastic and was drilled with 9-mm-diameter holes into certain critical organs for activation foil dosimetry. An acrylic plug was cut to fill each of these holes, and to hold a 6-mm-long activation foil wire. Two holes, near midthorax and in midabdomen, were drilled laterally through the TNO canine phantom to allow depth-dose measurements with both activation foils and ionization chambers.

A key difference between the AFRRI and TNO canine phantoms was in the leg orientation. The AFRRI phantom legs were in a normal standing position, just as for experimental animals irradiated laterally from left or right sides. The TNO phantom legs were extended at right angles to the body, as if in a supine position for dorsal-ventral irradiation. Conse-

[3] Courtesy of H. M. Vriesendorp, Radiobiological Institute TNO, Rijswijk, The Netherlands.

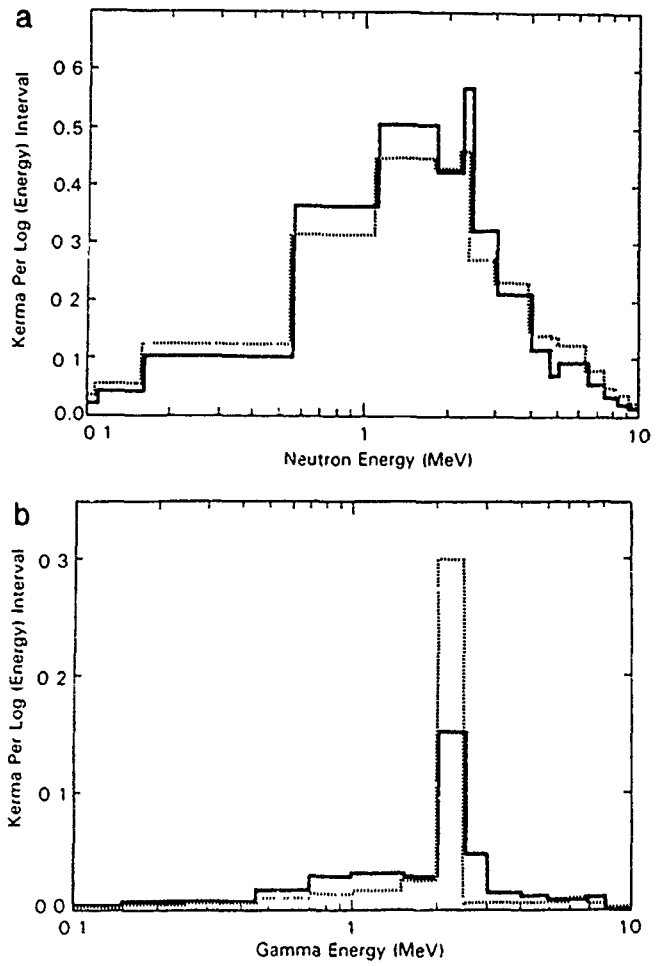

FIG. 1. Neutron (a) and γ (b) kerma spectra. Each spectrum was normalized to unit area. Free-in-air (—); midline in 17.8-cm diameter cylindrical tissue-equivalent phantom (---). All spectra at 70 cm from reactor pool tank wall.

quently, use of the TNO phantom in the present lateral irradiation geometry was expected to yield artificially high attenuation, or low doses, in the shoulder and pelvis regions.

Gamma-ray dosimetry The γ-ray component of dose at any point in an irradiated phantom arises from (a) incident γ rays, due largely to room-return and scatter, and (b) thermal neutron capture γ rays arising within the phantom or restraining box. The rather ubiquitous omnidirectional nature of both γ-ray sources leads to the expectation of a relatively uniform deposition of γ-ray dose throughout the phantom. The present γ-ray dose measurements show a 20–30% change in the γ-ray dose from entrance to exit in thorax and abdomen regions of the AFRRI and TNO canine phantoms, and less than 15% change from head to pelvis along the midline. These data suggest that the ratio of maximum-to-minimum γ-ray dose at any point in a unilaterally irradiated canine is about 1.4, and in a bilaterally irradiated phantom about 1.2.

Unilateral neutron depth-dose curves Figure 2a shows results of neutron depth–dose measurements laterally across thorax and abdomen regions of unilaterally irradiated AFRRI and TNO phantoms. Data from activation foils and from ionization chamber measurements were in reasonably good agreement and were characterized by simple exponential attenuation curves.

Near the exit surfaces of abdomen regions in the canine phantoms the neutron depth–dose curves reached a minimum or plateau level. This phenomenon was ascribed to reflected neutrons incident from the back side of the phantom or cadavers.

Ionization chamber neutron measurements near the surface of the TNO phantom gave approximately 30% higher readings than did the activation foils. The reason for this disparity was unclear, particularly in light of the good correlation between ionization and activation techniques observed at midline and exit locations in the TNO phantom and at all locations in the AFRRI phantom. It is possible that the 30% increase was due to the lower energy of the backscatter neutrons that were detected by ionization chambers but not by threshold detectors (sulfur threshold is approximately 2 MeV).

Bilateral neutron depth–dose curves The TNO canine phantom was irradiated bilaterally, with activation foils in place to sum doses received from the two irradiations. Figure 2b displays results of this experiment. The depth–dose curves were symmetrical about anatomical midline, with the lowest doses occurring at midline. The 20–35% higher doses measured in the thorax region compared to the abdomen region were consistent with the reduced attenuation of the thorax found in unilateral irradiations (Fig. 2a). The ratios of maximum-to-minimum doses for bilateral irradiations were found to be 1.3 and 1.8 in the thorax and abdomen regions, respectively. The corresponding surface dose ratios (within 3 cm thickness) may be higher by factors of 1.15 (thorax) and 1.40 (abdomen), respectively.

Midline tissue dosimetry In large-animal radiobiology experiments the dosimetry point of reference is traditionally taken to be the animal midline. Doses are measured at that point either free-in-air (i.e., same location but in the absence of the animal) or at depth (midline tissue). Free-in-air doses and MTDs in the AFRRI and TNO phantoms are given in Table II. Previously unpublished results for a series of canine cadaver measurements are also listed. The canine phantom midabdomen and thorax doses ranged from 43 to 69% of the free-in-air neutron dose and were consistent with anatomical thicknesses, considering the decreased physical density of lung tissue in the thorax regions. The lower neutron dose in the head of the AFRRI phantom was due to the greater slant distance from the reactor. The γ-ray dose measurements shown in Table II

TABLE I
Canine Phantom Dimension

Dimension	TNO phantom	AFRRI phantom
Weight (kg)	11.1	10.2
Length (cm)		
Nose to butt	68.0	73.0
Shoulder to shoulder	40.0	37.0
Lateral width (cm)		
Skull	10.6	11.0
Neck	8.5	8.0
Front shoulder	—	12.0
Midthorax	13.0	14.2
Last rib	14.7	15.0
Abdomen	14.0	12.1
Hind shoulder	—	12.0
Dorsal–ventral height (cm)		
Skull	9.5	11.0
Neck	9.2	10.5
Front shoulder	11.9	18.0
Midthorax	17.4	16.0
Last rib	14.3	15.5
Abdomen	12.4	15.0
Hind shoulder	11.3	14.0

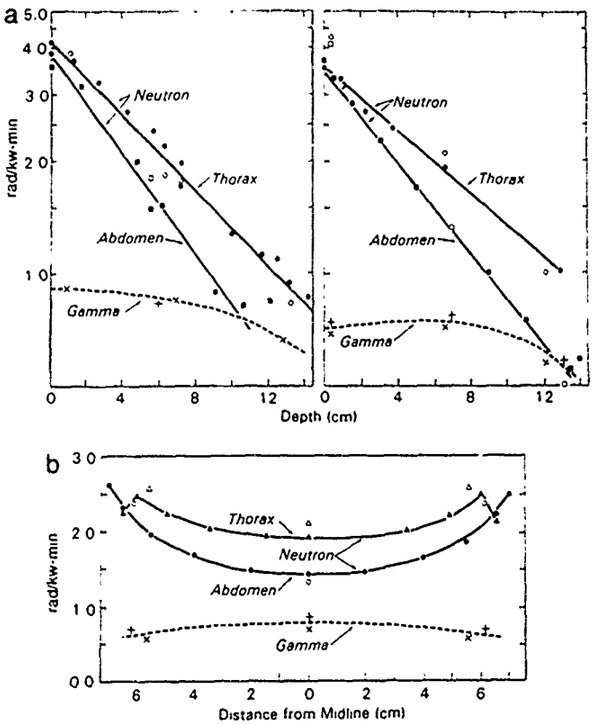

FIG. 2. (a) Depth-dose dosimetry for the abdomen and the thorax comparing AFRRI (left) and TNO (right) phantoms to unilateral exposure to fission neutrons from AFRRI's TRIGA reactor. (b) Comparison of the neutron dose rate (rad/kw-min) at depth in abdomen and thorax for bilateral exposures to fission neutrons from AFRRI's TRIGA reactor. Gamma-ray dose rate also is shown, which is relatively unchanged with depth.

were readily interpreted in terms of thermal neutron capture in surrounding hydrogenous tissue; i.e., larger γ-ray doses were associated with more massive anatomical regions.

Dose measurements were performed with paired 0.5-cc ion chambers, specifically an A-150 plastic TE chamber with methane-based TE gas and a magnesium chamber with argon gas. Actual animal irradiations were monitored with ionization chambers and sulfur activation foils mounted at fixed positions in the exposure room to provide corrections for reactor output variations.

Groups of canines were exposed to a range of MTDs of 0.25 to 4.00 Gy ^{60}Co γ radiation or 1.00 to 3.25 Gy mixed neutron-γ radiation for hematopoietic and lethality studies. Numbers of canines exposed for $LD_{50/30}$ determinations are shown in parentheses (Fig. 4).

Antibiotic, fluid and platelet therapy. Antibiotics (ampicillin, 500 mg [Polycillin-N, Bristol Labs, Syracuse, NY] and gentamycin sulfate, 30 mg [Garamycin, Schering Pharmaceutical Corp., Kenilworth, NJ]) were administered when the WBC level fell below 1000/mm^2 and continued daily until the WBC level reached 1000/mm^2. Fluid support (lactated Ringer's solution) was administered intravenously as dictated by clinical symptoms. Platelets ($3-5 \times 10^{10}$), obtained by plateletpheresis of donor animals, were irradiated with 50.00 Gy (^{60}Co source) and transfused to canines on Days 12, 15, and 18 postirradiation.

RESULTS

Sensitivity of GM-CFC to ^{60}Co γ radiation and neutron-γ radiation. Figure 3 shows the survival fractions of GM-CFC for both types of radiation exposure in the dose range of 0.25–4.00 Gy. The D_0 values have been calculated using a single-hit multitarget model. The respective D_0 and n values for GM-CFC harvested 24 h after exposure are 0.67 Gy

TABLE II
Midline Tissue Dosimetry

Region of phantom/cadaver	Percentage of free-in-air dose at midline		
	Neutron	γ	Total
AFRRI phantom[a]			
Head (11.0 cm)[b]	34	131	49
Thorax (14.2 cm)	59	149	73
Abdomen (12.1 cm)	49	141	63
TNO phantom[a]			
Thorax (13.0 cm)	69	127	78
Abdomen (14.0 cm)	43	139	58
Canine cadavers[c]			
Average (13.8 cm)	34	210	52
Range (12–16 cm)	20–47	170–230	38–60

[a] Phantom placed 101 cm from tank wall. Free-in-air doses at midline were 3.06 rad/kw-min for neutron irradiation and 0.57 rad/kw-min for γ irradiation (total 3.63 rad/kw-min). Percent = 100 for γ and neutron irradiations.

[b] Lateral diameter at point of measurement.

[c] Cadavers (n = 7) placed 70 cm from tank wall. Free-in-air doses at midline were 6.32 rad/kw-min for neutron irradiation and 0.58 rad/kw-min for γ irradiation (total 6.90 rad/kw-min). Percent = 100 for γ and neutron irradiations.

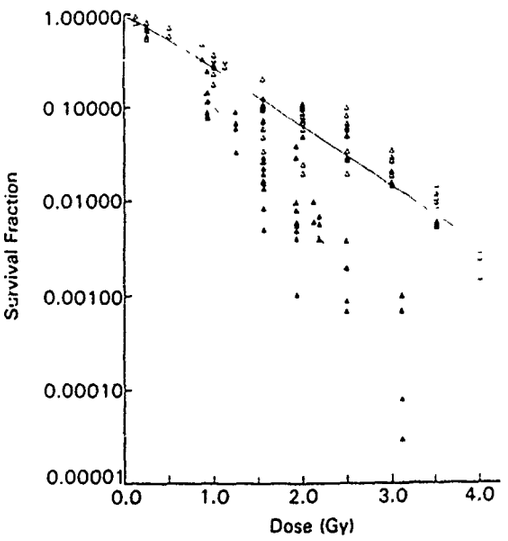

FIG. 3. Radiosensitivity of canine granulocyte-macrophage colony-forming cells obtained from rib and pelvic bone marrow aspirates to mixed fission-neutron-γ and ^{60}Co γ radiation. Respective D_0 values for ^{60}Co γ rays (Δ) and mixed neutron-γ ($\blacktriangle$) irradiation were 0.67 ± 0.3 (1.2 = n) and 0.36 ± 0.4 (1.7 = n).

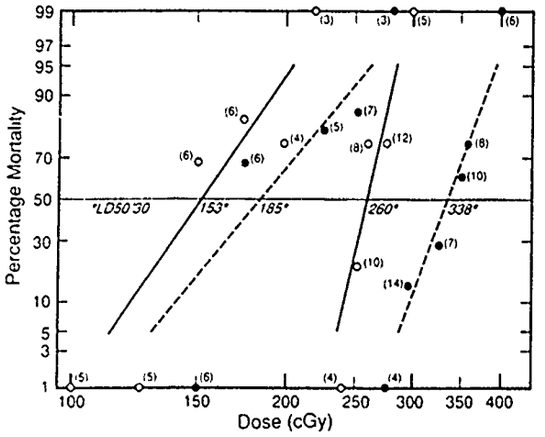

FIG 4. Probit mortality and $LD_{50/30}$'s for canines without and with clinical support (fluids, antibiotics, and platelets, see Materials and Methods) following bilateral exposure to mixed fission-neutron–γ radiation (left-hand lines) or ^{60}Co γ radiation (right-hand lines) Respective $LD_{50/30}$'s for mixed fission-neutron–γ radiation without (—) and with (---) clinical support were 153 and 185 cGy; $LD_{50/30}$'s for ^{60}Co γ radiation were 260 and 338 cGy without (—) and with (---) support, respectively.

± 0.03 Gy (n = 1.23 ± 0.11) and 0.36 Gy ± 0.04 Gy (n = 1.74 ± 0.59) for ^{60}Co γ radiation and neutron-γ (5.4:1) radiation, respectively. Based on these significantly different ($P < 0.001$) D_0 values, the RBE is 1.9 ± 0.2 for *in vivo* sensitivity of GM-CFC to ^{60}Co γ-ray exposure, relative to neutron-γ-ray exposure.

$LD_{50/30}$ values following exposure to mixed neutron–γ radiation and ^{60}Co γ radiation. Figure 4 shows the 30-day mortality values for canines bilaterally exposed to ^{60}Co γ radiation and mixed fission-neutron–γ radiation. Respective $LD_{50/30}$'s were 2.60 Gy [2.51, 2.69][4] and 1.53 Gy [1.31, 1.47] for the clinically unsupported canines (curves are plotted by a probit fitting program). The RBE based on $LD_{50/30}$'s using midline tissue doses is 1.69 [1.49, 1.92] ($P < 0.001$).[5]

Therapeutic support administered to lethally irradiated canines significantly improves survival and increases the $LD_{50/30}$ independent of radiation quality. The resultant $LD_{50/30}$'s for clinically supported canines exposed to ^{60}Co γ radiation or mixed fission-neutron–γ radiation were 3.38 Gy [3.23, 3.55] and 1.85 Gy [1.53, 2.12], respectively (Fig. 4). This increase represents respective dose reduction factors (DRFs) of 1.30 ($P < 0.001$) and 1.21 ($P < 0.04$).

DISCUSSION

Accurate determination of neutron effectiveness in damaging target organs, e.g., bone marrow, gastrointestinal tissue, and the lung, requires the use of large-animal models that more reliably mimic the dose inhomogeneities experienced in the human radiation response. The uncertainty of dose estimation to the target organ creates additional difficulty in reliable determination of the RBE of high-LET radiation, such as fission-spectrum neutrons. Variables that include body size, target organ location, dose inhomogeneity with tissue depth, and the steep dose–effect curve create a situation in which small changes in organ dose result in large changes in bioeffect.

Our data describing the canine response in terms of lethality ($LD_{50/30}$) and the dose–response curves for GM-CFC after ^{60}Co γ radiation and mixed fission-neutron–γ radiation suggest a significant RBE or relative potency for the fission-spectrum neutron radiation. These results, however, are based on MTD. The MTD was established by Bond *et al.* (*21*) to be used as a relevant reference dose, because free-in-air, entrance, and exit doses have not been acceptable substitutes. It was their intent to use a value that would represent the "dose" received by an animal. This value, MTD, was suggested with full recognition that, in irradiating an animal of any size, particularly a canine, some degree of inhomogeneity of dose throughout the tissues will exist, no matter what radiation type is employed. In quoting a single value for the dose received by the animal it is necessary to settle on the dose received at some fixed location within the animal. Bond *et al.* (*2, 21*) state that the ideal would be to measure the dose received by a single critical organ that would correlate with the biological end point, such as the dose received by the bone marrow in the $LD_{50/30}$ range. Precise and reliable measurements of doses absorbed at these sites are complicated by their spatial distribution, by the dose gradients that exist near both lateral and dorsal–ventral surfaces, and by the reduced attenuation and variable geometry of lung tissue. We recognize that a complex dosimetric condition exists (Figs. 2a and b, Table I). The exposure of canines under our irradiation conditions starts with an entrance 5.4:1 neutron–γ ratio, free-in-air, with an average neutron energy between 0.8 and 1.0 MeV, and decreases to a 1.7:1 ratio at midline, with no significant change in the effective neutron spectrum (Fig. 1). We do not know the absorbed dose to the critical organ (the bone marrow) or the resultant change in neutron–γ ratio within the target tissue. This would create dose inhomogeneities within the target organ. Variation of midabdomen dose with size of canine has not routinely been considered in previous works. A recent limited survey of experimental canines at AFRRI revealed lateral diameters at the last rib ranging from 14 to 16.5 cm; for this thickness range the midabdomen dose can vary by ±10% for equivalent free-in-air neutron doses. Our strict weight range of 10–12 kg helps to minimize this variable. A review of the literature indicates that a large variation in size of the experimental canines, including weight and body dimensions (mongrel compared to beagle), may account for a significant varia-

[4] Numbers in brackets are 95% confidence intervals.

[5] *P* values following RBEs or DRFs indicate significant difference from unity

tion in depth dose. These size variables are further underscored when considering animal models such as swine and sheep.

A significant amount of literature establishes the $LD_{50/30}$ for hematopoietic death of the canine at approximately 2.6 Gy for ^{60}Co γ irradiation (*22–25*) and X irradiation of the energies 1000 and 2000 kVp (*1, 3, 26–28*) and an average of 2.28 Gy for exposure to lower-energy (50–250 kVp) X irradiation (*21, 29–33*). These published data indicated a negligible RBE between the ^{60}Co γ rays and high-energy X rays but did estimate a small but significant RBE of 0.87 for these higher-energy radiations compared to the standard 200–250 kVp X irradiation. This value is similar to the RBE reported by Sinclair (*34*) for $LD_{50/30}$'s in the mouse, relative to γ and X irradiation.

Exposure of the canine to the AFRRI TRIGA mixed fission-neutron–γ-ray (5.4:1) source resulted in an $LD_{50/30}$ of 1.53 Gy MTD. This value is lower than $LD_{50/30}$ MTDs for fission neutrons of the comparable 1 MeV energy published by Alpen *et al.* (*4*) and Ainsworth *et al.* (*3*) of 239 and 203 rad, respectively. Calculation of the RBE by these investigators resulted in values of approximately 0.90 by Alpen *et al.* (*4*), with reference to 250-kVp X irradiation, and 1.38 by Ainsworth *et al.* (*3*), with reference to 1-MVp X irradiation. Our observed RBE relative to the standard 250-kVp X-ray exposure would be approximately 1.54 based on the reported average MTD $LD_{50/30}$ of 228 rad, an RBE significantly higher than that reported previously for the canine. The composite literature value for $LD_{50/30}$ after bilateral ^{60}Co γ-ray exposure is approximately 2.68 Gy, very close to the 2.60 Gy reported here. The calculated RBE using the data for ^{60}Co rays as the reference $LD_{50/30}$ is 1.8.

Pitchford and Thorp (*35*) reported on the neutron effectiveness of a 0.7:1 mixed neutron–γ-ray exposure from the AFRRI TRIGA reactor operated at a steady-state dose rate of 14 rad/min. The $LD_{50/30}$ for mixed neutron–γ-ray (0.7:1) exposure was 218 rad (midline tissue) compared to 206 rad for 250-kVp X irradiation. The lower neutron component resulted in an equivalent bioeffect, relative to 250-kVp X radiation. Compared to the ^{60}Co γ radiation $LD_{50/30}$ of 2.6 Gy, the RBE for neutron irradiation would approach a value of 1.2.

Broerse *et al.* (*19*) reported an RBE similar to ours for fission neutrons relative to 1-MVp X irradiation in the primate system. They recorded a total absorbed dose of 2.60 Gy for an $LD_{50/30}$ from 1-MeV fission neutrons relative to 5.25 Gy for 300-kVp X rays. Thus the RBE is approximately 2.0 for occurrence of bone marrow lethality in the rhesus monkey. Stanley *et al.* (*36*) and Wise and Turbyfill (*37*) also observed a significant RBE in the rhesus monkey for an $LD_{50/30}$ end point, using a neutron–γ-ray exposure compared to 250-kVp X irradiation. Respective MTD values for X rays and neutron–γ (<1:1) irradiation were 502 and 375 rad.

The RBE based on MTD as observed in our lethality experiments should also be reflected in the radiation sensitivity of marrow progenitor cells, since it is the destruction of these cells that causes the mortality observed during the subsequent 30-day period known as the hematopoietic syndrome. The calculated RBE for the clonogenic marrow progenitor GM-CFC using D_0 values was 1.8.

An RBE of approximately 1.8 for low-energy monoenergetic or fission neutrons has also been reported for murine and human marrow-derived stem and progenitor cells (*38, 39*). Boyum *et al.* (*39*) using the *in vivo* diffusion chamber technique for growth of human marrow as well as the GM-CFC technique showed RBE values of greater than 2.0 compared to 250-kVp X irradiation for neutron energies over the range of 0.44–6.0 MeV. The extensive studies of Ainsworth *et al.* (*40*) using the D_0 value of murine stem cells as an end point and its correlation with $LD_{50/30}$'s showed a consistent RBE or relative potency of greater than 2.0. Carsten *et al.* (*38*) used neutron exposures over the same energy range as Boyum *et al.* (*39*) with the D_0 values of murine stem cells as an end point. They also recorded significant RBE values of greater than 2.0. These laboratories recorded D_0 values for exposure to 250-kVp X irradiation of approximately 80–87 rad compared to D_0 values of 28–42 rad following exposure to fission-spectrum neutrons or to neutrons less than 5 MeV.

Modification of survival throughout the $LD_{50/30}$ dose range can be achieved using a straightforward clinical support regimen designed to replace or substitute for those functional cells depleted as a consequence of stem cell aplasia. Lethality due to sepsis and/or hemorrhage is not only a consequence of the loss of functional white cells and platelets but a failure of their replacement from a severely depleted stem and progenitor cell population. Studies performed over 20 years ago showed the efficacy of good supportive care centered on systemic antibiotics and fresh platelet transfusions (*41–45*). Several studies, in canines, indicated that antibiotics singly or in combination were somewhat effective in reducing mortality in the $LD_{50/30}$ range (*43–45*). Sorensen *et al.* (*44*) reported on the effectiveness of several antibiotics in conjunction with fresh whole blood transfusion and parenteral fluids to control dehydration in reducing lethality from an LD_{90} (400 rad, air dose at skin surface) to an LD_{20}. Perman *et al.* (*45*) extended this study over a dose range from 400 to 550 rad, well into the LD_{100}, and achieved a significant increase in survival with the good clinical support provided. The Sorensen (*44*) regimen consisted of (a) several antibiotics (penicillin G, dihydrostreptomycin, tetracycline), (b) fresh platelet-rich plasma, and (c) fluid therapy (isotonic saline or 5% dextrose) given during the period of inappetence. Soft dog food was usually given during this period to entice the dogs to eat. Success with these regimens supports the concept that infection and hemorrhage are the two primary factors in the

lethal consequences of radiation exposure in the hematopoietic syndrome.

Our data extended these studies over a complete dose range capable of determining the shift in $LD_{50/30}$ due to treatment. The treatment regimen was essentially the same as Sorensen's, with the exception of new antibiotics. These collective data indicate that modest intensive care consisting of fluids, antibiotics, and fresh platelets can shift the $LD_{50/30}$ by a factor of 1.3. A more intensive regimen of support, including sterile barriers and selective intestinal bacterial decontamination, should allow an even greater shift in $LD_{50/30}$. It must be emphasized that the practical application of these concepts depends upon the fact that damage to the stem cell system is reversible. The surviving fraction of hematopoietic stem cells must be capable of spontaneous regeneration, including production of functional mature end cells, within the clinically manageable period of time determined by the effectiveness of the support regimen.

ACKNOWLEDGMENTS

The authors gratefully acknowledge the expert technical assistance of Ms C. Feser, Sergeant L. Huff, USAF, Mr. J. Darder, and Mr. R. Brandenburg; the continuous support of veterinary technicians in the Veterinary Sciences Department; and the editorial assistance of Ms. C. Sund.

REFERENCES

1 J. D EARLE, E. J. AINSWORTH, and G. F LEONG, Lethal and hematologic effects of 14.6 MeV neutrons on beagles with estimation of RBE *Radiat Res.* **45**, 487–498 (1971)

2 V. P BOND, R. E. CARTER, J. S. ROBERTSON, P. H. SEYMOUR, and H. H. HECHTER, The effects of total body fast neutron irradiation in dogs *Radiat. Res* **4**, 139–153 (1956).

3 E J. AINSWORTH, G. F. LEONG, K. KENDALL, and E. L. ALPEN, Comparative lethality responses of neutron and x irradiated dogs: Influence of dose rate and exposure aspect. *Radiat. Res.* **26**, 32–43 (1965).

4 E. L. ALPEN, O. S. SHILL, and E. TOCHILIN, The effects of total body irradiation of dogs with simulated fission neutrons *Radiat Res.* **12**, 237–250 (1960).

5 T. MOBLEY, W. GODDEN, and J. DEBOER, *Median Lethal Dose $LD_{50}(60)$ Studies in Sheep Following 250 kVp X-Irradiation*, AFL-TR-65-200. Air Force Weapons Laboratory, 1966.

6. T. MOBLEY, W. J. WALKER, JR., and J. DEBOER. *Lethal Dose Studies on Sheep Exposed to Pulsed Fission Spectrum Radiation (PFSR)*, AFL-TR-65-199. Air Force Weapons Laboratory, 1967.

7 G. F. HANKS, N. P. PAGE, E. J. AINSWORTH, G. F. LEONG, C. K. MENKES, and E. L. ALPEN, Acute mortality and recovery studies in sheep irradiated with cobalt-60 gamma rays or 1-MVp x-rays. *Radiat. Res* **27**, 397–405 (1966).

8. P. W. EDMONDSON and A. L. BATCHELOR, Acute lethal responses of goats and sheep to bilateral or unilateral whole-body irradiation by gamma rays and fission neutrons. *Int J Radiat. Biol.* **20**, 269–290 (1971).

9 J. F. TAYLOR, E. J. AINSWORTH, N. P. PAGE, and G. F. LEONG, *Influence of Exposure Aspect on Radiation Lethality in Sheep*. NRDL-TR-69-15. Naval Radiological Defense Laboratory, San Francisco, 1969.

10 D. G. BROWN and R. G. CRAGLE, Some observations of dose-rate effect on radiation on burros, swine, and cattle. In *The Proceedings of a Symposium on Dose Rate in Mammalian Radiation Biology* (D G. Brown, R. G. Cragle, and T. R. Noonan, Eds.) Report CONF-680410. UT-AEC Agricultural Research Laboratory, Oak Ridge, TN, 1968.

11 F W CHAMBERS, JR., C. R. BILE, L. J BODENLOS, and J. H. DOWLING, Mortality and clinical signs in swine exposed to total-body cobalt-60 gamma irradiation. *Radiat. Res* **22**, 316–333 (1964).

12 J. L. TULLIS, B. G. LANSON, and S C. MADDEN, Mortality in swine exposed to gamma radiation from an atomic bomb source. *Radiology* **62**, 409–415 (1954).

13 J. L. TULLIS, C. F. TOSSMER, E. P. CRONKITE, and F. W. CHAMBERS, JR., The lethal dose of total body x-ray irradiation in swine. *Radiology* **52**, 396–400 (1949).

14 J. L. TULLIS, F W. CHAMBERS, JR., J. E. MORGAN, and J H. ZELLER, Mortality in swine and dose distribution studies in phantoms exposed to super voltage roentgen radiation. *Am J Roentgenol* **67**, 620–627 (1952).

15 D. S. NACHTWEY, E. J. AINSWORTH, and G. F. LEONG, Recovery from radiation injury in swine as evaluated by the split dose technique. *Radiat Res* **31**, 353–367 (1967).

16 J. H. RUST, B. F. TRUM, J. L. WILDING, C. S. SIMONS, and C. L. COMAR, Lethal dose studies with burros and swine exposed to whole body cobalt-60 radiation. *Radiology* **62**, 569–574 (1954).

17 T. D. JONES, M. D. MORRIS, S. M. WELLS, and R W. YOUNG, *Animal Mortality Resulting from Uniform Exposures to Photon Radiations: Calculated LD_{50}'s and a Compilation of Experimental Data*. ORNL 6338. Oak Ridge National Laboratory, Oak Ridge, TN, 1986.

18 D. WISE and C. L. TURBYFILL, *The Acute Mortality Response of the Miniature Pig to Pulsed Mixed Gamma-Neutron Radiations*. SR69-10 Armed Forces Radiobiology Research Institute, Bethesda, MD, 1969.

19 J. J. BROERSE, D. W. VAN BEKKUM, C. F. HOLLANDER, and J A. G DAVIDS, Mortality of monkeys after exposure to fission neutrons and the effect of autologous bone marrow transplantation. *Int J. Radiat Biol.* **34**, 253–264 (1978).

20. M. PORVAZNIK and T. J. MACVITTIE, Detection of gap junctions between the progeny of a canine macrophage colony-forming cell *in vitro* *J. Cell Biol.* **87**, 555–564 (1979).

21 V. P. BOND, E. P. CRONKITE, C. A. SONDHAUS, G. IMIRIE, J S. ROBERTSON, and D. C. BORG, The influence of exposure geometry on the pattern of radiation dose delivered to large animal phantoms. *Radiat Res.* **6**, 554–563 (1957).

22. J. N. SHIVELY, S. M. MICHAELSON, and J. W. HOWLAND, The responses of dogs to bilateral whole-body cobalt-60 irradiation. I. Lethal dose determination. *Radiat. Res.* **9**, 445–450 (1958).

23. R. I. H. WANG and D. E. DAVIDSON, JR., *Experimental Conditions for Acute Whole-Body Irradiation of Dogs with Cobalt-60*, Report No. 483. U.S. Army Medical Research Laboratory, 1961.

24. W P. NORRIS, T. E. FRITZ, C. E. REHFELD, and C. M. POOLE, The response of the beagle dog to cobalt-60 gamma radiation: Determination of the LD50/30 and description of associated changes. *Radiat. Res.* **35**, 681–708 (1968).

25 R. J. GARNER, R. D. PHEMISTER, G. M. ANGLETON, A. C. LEE, and R. W. THOMASSEN, Effect of age on the acute lethal response of the beagle to cobalt-60 gamma radiation. *Radiat. Res.* **58**, 190–195 (1974).

26. C. A. GLEISER. The determination of the lethal dose 50/30 of total body irradiation for dogs. *Am. J Vet Res.* **14**, 284–286 (1953).
27. C. L. HANSEN, S. M. MICHAELSON, and S. W. HOWLAND. Lethality of upper body exposure in beagles. *Health Phys* **76**, 242–246 (1961).
28. H. D MAILLE, W. KRASAVAGE, and H. MERMAGEN. On the partial body irradiation of the dog. *Health Phys* **12**, 883–887 (1966).
29. E. L. ALPEN, D. M. JONES, H H. HECHTER, and V. P. BOND. The comparative biological responses of dogs to 250 kVp X rays and 100 kVp X rays. *Radiology* **70**, 541–549 (1958).
30. E. L. ALPEN and D. M. JONES. The effects of concomitant superficial X irradiation upon the lethal effectiveness of 250 kVp X rays. *Radiology* **72**, 81 (1959).
31. E. L. ALPEN and S. J. BAUM. Comparative effects of 50 kVp and 250 kVp X rays on the dog. *Ann. N Y Acad Sci* **114**, 284–294 (1964).
32. C L. PROSSER, E. E. PAINTER, and M. N. SWIFT. In *Biological Effects of External X- and Gamma Radiation* (R. E. Zirkle, Ed.), Part 2, pp. 1–93. U.S. Atomic Energy Commission, Technical Information Service Extension, Oak Ridge, TN, 1956.
33. R. E. GEORGE, R. E. STANLEY, D. WISE, and E. L BARRON, *The Acute Mortality Response of Beagles to Mixed Gamma-Neutron Radiations and 250 kVp X Rays*, SR68-3. Armed Forces Radiobiology Research Institute, Bethesda, MD, 1968
34. W. K. SINCLAIR. The relative biological effectiveness of 22-Mevp X rays, cobalt-60 gamma rays, and 200 kvcp X rays. VII. Summary of studies for five criteria of effect. *Radiat. Res.* **16**, 394–398 (1962).
35. T. L. PITCHFORD and J. W. THORP. *The Acute Mortality Response of Beagles to Pulsed Mixed Gamma-Neutron Radiations*, SR68-15. Armed Forces Radiobiology Research Institute, Bethesda, MD, 1968.
36. R. E. STANLEY, L. J. SEIGNEUR, and T. A. STRIKE. *The Acute Mortality Response of Monkeys (Macacca mulatta) to Mixed Gamma-Neutron Radiations and 250 kVp X Rays*, SR66-23. Armed Forces Radiobiology Research Institute, Bethesda, MD, 1966.
37. D. WISE and C. L. TURBYFILL. *The Acute Mortality Response of Monkeys (Macacca mulatta) to Pulsed Mixed Gamma-Neutron Radiation*, SR68-17. Armed Forces Radiobiology Research Institute, Bethesda, MD, 1968.
38. A. L. CARSTEN, V. P. BOND, and K. THOMPSON. The RBE of different energy neutrons as measured by the haematopoietic spleen-colony technique. *Int J Radiat. Biol.* **29**, 65–70 (1976).
39. A. BOYUM, A. L. CARSTEN, G. CHIKKAPPA, L. COCK, J. BULLIS, L. MONIKEL, and E. P. CRONKITE. The RBE of different-energy neutrons as determined by human bone-marrow cell culture techniques. *Int J Radiat. Biol.* **34**, 201–212 (1978).
40. E. J. AINSWORTH, R. M. LARSEN, K. KENDALL, G. F. LEONG, J. S. KREBS, and F. A. MITCHELL. Recovery in the mouse after neutron irradiation: Evaluation of injury and recovery using split dose lethality and repopulation of colony-forming units. In *Proceedings of the Symposium on Neutrons in Radiobiology*, pp. 435–450. Oak Ridge National Laboratory, Oak Ridge, TN, 1969.
41. F. W. FURTH, M. P. COULTER, R. W. MILLER, J. W. HOWLAND, and S. N. SWISHER. The treatment of acute radiation syndrome in dogs with auromycin and whole blood. *J Lab. Clin Med* **41**, 918–928 (1953).
42. A. A. BAGDASAROV, M. O. RAUSHENBAKK, G. M. ABDULLAEV, *et al.*, The treatment of acute radiation sickness with packed platelets. *Probl. Hematol. Blood Transfus.* **4**, 1–5 (1959).
43. D. P. JACKSON, D. K. SORENSEN, E. P. CRONKITE, V. P. BOND, and T. M. FLIEDNER, Effectiveness of transfusions of fresh and lyophilized platelets in controlling bleeding due to thrombocytopenia. *J Clin. Invest.* **38**, 1689–1697 (1959).
44. D. K. SORENSEN, V. P. BOND, E. P. CRONKITE, and V. PERMAN, An effective therapeutic regimen for the hemopoietic phase of the acute radiation syndrome in dogs. *Radiat Res.* **13**, 669–685 (1960).
45. V. PERMAN, E. P. CRONKITE, V. P. BOND, and D. K. SORENSEN. The regenerative ability of hemopoietic tissue following lethal x-irradiation in dogs. *Blood* **19**, 724–737 (1962).

Neuroscience Vol. 45, No. 2, pp 273–280, 1991
Printed in Great Britain

0306-4522/91 $3.00 + 0.00
Pergamon Press plc
IBRO

FATTY ACIDS MODULATE EXCITABILITY IN GUINEA-PIG HIPPOCAMPAL SLICES

T. C. PELLMAR
Physiology Department, Armed Forces Radiobiology Research Institute, Bethesda, MD 20889-5145, U.S.A

Abstract—A variety of fatty acids produced sustained changes in excitability in the guinea-pig hippocampal slice. Although each fatty acid was unique, a general pattern was evident. During a 30-min exposure, the synaptic potential was minimally affected, although population spike amplitude showed significant increases. With wash, synaptic efficacy increased. The increase in the synaptic potential was significant with arachidonic acid (100 μM), oleic acid (100 μM), myristic acid (250 μM) and capric acid (250 μM). Also with wash, the coupling between the synaptic potential and the population spike was reduced significantly for most of the fatty acids tested: arachidonic acid (50 μM, 100 μM), linoleic acid (100 μM) oleic acid (100 μM), stearic acid (100 μM), myristic acid (250 μM) and capric acid (250 μM, 500 μM).

The fatty acids may influence neuronal excitability, in part, through a direct membrane action. The observed synaptic enhancement is consistent with a role for a fatty acid in long-term potentiation. In addition, fatty acid exposure mimics the effects of X-radiation. We suggest that free radical-induced release of fatty acids contributes to electrophysiological damage in a number of pathological states

Exposure to free radicals, and consequent lipid peroxidation, causes the activation of phospholipases and the release of fatty acids from cellular membranes.[7,8,27,34] Oxidized membrane lipids are preferentially, but not exclusively, removed by phospholipase A2 and repaired by glutathione peroxidase.[34] In rat cortical brain slices, arachidonic acid, oleic acid and docosahexaenoic acid were released following superoxide-induced lipid peroxidation[8] and phospholipase A2 activation.[7] These mechanisms can come into play during some pathological conditions. For example, ischemic injury causes the release of free fatty acids,[1,4,39] probably as a consequence of free radical generation.[29,39] The release of arachidonic acid is greater in field CA1 than in field CA3 of hippocampus corresponding to the severity of ischemic injury.[35]

Recent reports have shown that fatty acids have a wide variety of effects on membrane currents in excitable tissue. Among these actions are increased potassium currents[5,12,13,20] and decreased sodium current.[15,30,31] Arachidonic acid and its lipoxygenase metabolites have been shown to modulate synaptic excitability.[6,11,28,38] A role for arachidonic acid or oleic acid as an essential second messenger in long-term potentiation (LTP) has been postulated.[11,14,16,37,38]

Free radical exposure has been shown to have electrophysiological consequences in neural tissue.[21,23,26,33] The present experiments were initiated to evaluate the role of fatty acids in free radical damage in the guinea-pig hippocampal slice. Among the fatty acids we tested were arachidonic acid (20:4), linoleic acid (18:2) and oleic acid (18:1) which are released by free radical exposure.[8] In addition, we chose a series of saturated fatty acids of increasing length (10:0, 14:0, 18:0) and a series of 18-carbon fatty acids with increasing unsaturation (18:0, 18:1, 18:2). Preliminary results have been reported previously in abstract form.[23]

Abbreviations: ACSF, artificial cerebrospinal fluid; DMSO, dimethylsulfoxide; E/S, excitatory postsynaptic potential-spike; I/O, input-output; LTP, long-term potentiation; PSP, postsynaptic potential.

EXPERIMENTAL PROCEDURES

Slices of hippocampus were prepared from brains of male Hartley guinea-pigs (Harlan Sprague Dawley, Inc.) as described previously.[21,26] Slices were incubated at room temperature for at least 1 h, placed in a submersion slice chamber and perfused at approximately 1 ml/min with oxygenated artificial cerebrospinal fluid (ACSF) at 30 ± 1°C. ACSF had the following composition (in mM): NaCl, 124; KCl, 3.0; $CaCl_2$, 2.4; $MgSO_4$, 1.3; KH_2PO_4, 1.24; glucose, 10; and $NaHCO_3$, 25; equilibrated with 95% O_2–5% CO_2.

Fatty acids were put into solution immediately prior to perfusion through the bath. Arachidonic acid, oleic acid and linoleic acid were received from the supplier (NuChek or Sigma) in sealed vials. After opening the vial, the full content was dissolved in ethanol (99%), separated into aliquots, and stored under nitrogen at −70 C for not more than one week. Immediately before use, the stock solution was removed from the freezer and diluted in ACSF to a final concentration of 0.3% ethanol and 50–250 μM fatty acid. Stocks were never refrozen following thawing for use. Myristic acid did not stay in solution when diluted from an ethanol stock; dimethylsulfoxide (DMSO; 0.3% final concentration) was used instead. Stearic acid was minimally soluble with either solvent; solutions were used with the fatty acid in suspension with ethanol. Capric acid was used as the sodium salt and directly dissolved in the oxygenated ACSF.

The actions of ethanol (0.3%, $n = 9$), DMSO (0.3%, $n = 6$) and time alone ($n = 11$) were evaluated on electrophysiological responses in hippocampal slices. With time

and solvents the synaptic response was slightly reduced and excitatory postsynaptic potential spike (E/S) coupling (see below) was enhanced. Although these actions were small, they were statistically significant. Consequently, all data were referenced to the appropriate solvent control.

Perfusion with the fatty acids had to be watched carefully to avoid reduced flow and consequently decreased bath temperature. In this study all slices were constantly monitored with a Yellow Springs Instruments temperature probe and the perfusion rate was checked at frequent intervals. Any slice in which large changes occurred was deleted from the study. At least five experiments were done with each fatty acid at each dose: arachidonic acid, 50 μM, $n = 6$, 100 μM, $n = 7$; linoleic acid, 100 μM, $n = 5$; oleic acid, 100 μM, $n = 5$; stearic acid, 100 μM; $n = 8$; myristic acid, 100 μM, $n = 5$, 250 μM, $n = 6$; capric acid, 100 μM; $n = 5$; 250 μM; $n = 6$.

A bipolar stainless-steel stimulating electrode was positioned in the stratum radiatum of field CA1 to stimulate afferent pathways. Recording electrodes (2 M NaCl) were placed in the stratum radiatum and in the stratum pyramidale to record the resultant population postsynaptic potential (PSP) and the population spike, respectively. The field potentials were recorded with high gain d.c. amplifiers (WPI) and were digitized, stored and analysed on a PDP 11-73 microcomputer. Population PSPs were quantitated by their initial slope to avoid complications caused by the reflected population spike in stratum radiatum.

Input output (I/O) curves were generated by constant current stimulation (0.05 mA, 300 μs) of stratum radiatum in field CA1. As previously described,[33] average I/O curves were constructed for each experimental condition by computing the mean and standard errors for the population spike amplitude, synaptic potential slope and afferent volley amplitude at each stimulus intensity. Three relationships were analysed. (1) Plotting afferent volley vs the initial slope of the population PSP reflects the ability of presynaptic fibers to elicit a synaptic response. This relationship will be referred to as synaptic efficacy. (2) The relationship between the population PSP slope and population spike amplitude has been called E/S coupling[1] and reflects the ability of the synaptic potential to evoke a population spike (i.e. spike generation). Changes in E/S coupling are functionally distinct from changes in synaptic efficacy.[29-32] A variety of mechanisms has been proposed,[29-32] including altered postsynaptic membrane potential, modified postsynaptic membrane excitability and altered inhibitory synaptic input. In the present study, changes in this set of curves are descriptive of an effect but do not attempt to describe a mechanism. (3) The relationship of afferent volley vs population spike amplitude encompasses both changes in synaptic efficacy and E/S coupling. An increase in population spike amplitude at a fixed afferent volley size could result from either a larger synaptic response or an increase in E/S coupling.

I/O curves were obtained in normal ACSF after a 30-min equilibration period. Slices were then exposed to the fatty acid solution for 30 min and another I/O curve obtained. The tissue was subsequently washed with normal ACSF for a minimum of 30 min. I/O were obtained approximately every 30 min during this wash period. I/O curves were analysed as previously described.[33] Each curve was computer-fit with the equation for a sigmoid curve and differences between curves were quantified by the comparison of the ratio (a/c) of two parameters defining the best-fit curves (RS/1, BBN Software Product, Cambridge, MA). a is the maximal y value and c is the x value at half-maximal y. Under the experimental conditions in previous studies[24-26,33] a decrease in a was usually accompanied by an increase in c, representing a net decrease in the relationship. In the present study the relationship between population PSP and population spike showed increases in both parameters. In this case, the parameters were also evaluated separately. Data were compared by Student's t-test to the appropriate solvent controls and presented as a percentage of these controls. Standard errors were computed from the errors associated with the parameters of both the experimental and the control fitted curves. Significance was accepted at $P < 0.05$.

RESULTS

Enhancement of synaptic response

Exposure and subsequent washout of a variety of fatty acids was found to produce a sustained increase in the synaptic potential in field CA1 of guinea-pig hippocampus. Capric acid (250 μM) caused the largest enhancement (37% compared to the ACSF time control, Fig. 1B). Arachidonic acid (100 μM) (Fig. 1A), myristic acid (250 μM) and oleic acid (100 μM) also significantly increased the ability of a given volley size to elicit a synaptic potential, while stearic acid (100 μM) and capric acid (100 μM) were ineffective. Linoleic acid (100 μM) and myristic acid (100 μM), respectively, averaged a 19.4 and 24.3% increase in synaptic efficacy beyond the solvent

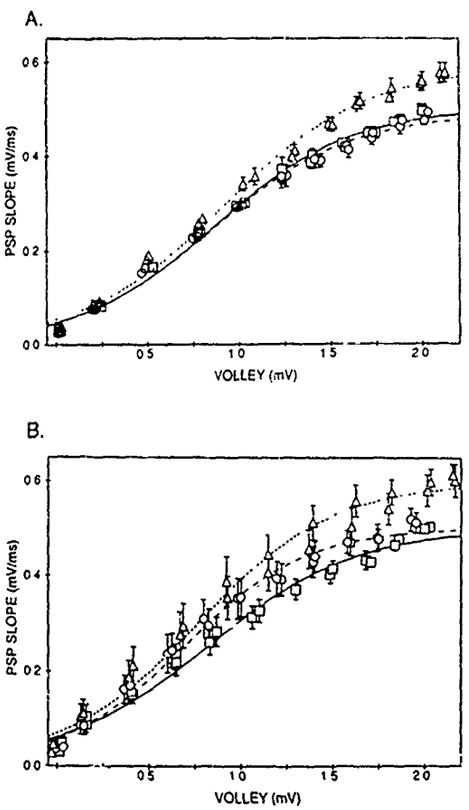

Fig. 1. Fatty acids enhance synaptic efficacy. Plot of afferent volley vs population PSP size reflects synaptic efficacy of the afferent pathway to the CA1 pyramidal cells. (A) Average curve from seven hippocampal slices treated with 100 μM arachidonic acid. □, single line: control; ○, dashed line: during 30-min application of fatty acid; △, dotted line: 30-min wash with normal solution. (B) Average curve for six slices treated with 250 μM capric acid.

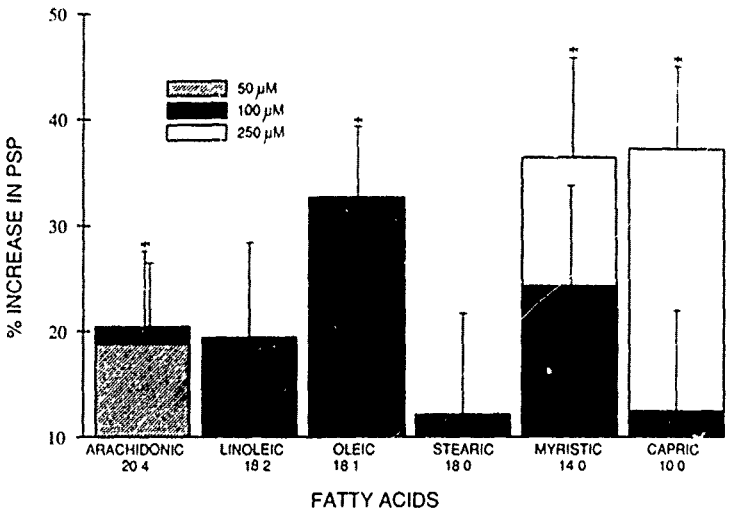

Fig 2 Many fatty acids have similar effects on increasing the population PSP with wash The change was significant following exposure to arachidonic acid (100 μM), oleic acid (100 μM), myristic acid (250 μM) and capric acid (250 μM) All changes are calculated in reference to the appropriate solvent or time control.

controls, but neither achieved statistical significance (Fig. 2)

During the exposure to the fatty acids, there was no significant change in the population PSPs (Fig. 1), yet all but 50 μM arachidonic acid seemed to produce a slight increase. Oleic acid, myristic acid and capric acid showed increases between 10 and 25% relative to the appropriate solvent controls but were not statistically significant With 50 μM arachidonic acid, a depression predominated, seen as a small reduction in the ability of the afferent volley to evoke a population PSP Again, these small changes were not statistically significant Our results are consistent with those of Drapeau *et al.*[11] who showed that arachidonic acid could depress the synaptic response during the exposure to the fatty acid, although in their experiments potentiation predominated.

Altered excitatory postsynaptic potential–spike coupling

In addition to the enhancement of the synaptic response with washout of the fatty acids, a significant shift in E/S coupling occurred The relationship between the synaptic potential and the population spike was significantly shifted to the right for all the fatty acids tested except 100 μM myristic acid and 100 μM capric acid (Fig. 4). The increase ranged from 11% with 100 μM linoleic acid to 33% with 50 μM arachidonic acid compared to the appropriate solvent controls. As with the synaptic potentiation, the shift in E/S coupling was greatest following washout of the fatty acid. During the exposure period, only 250 μM myristic acid produced a significant shift in this curve (Fig. 3B). The change in the E/S relationship with 50 μM arachidonic acid and 250 μM myristic acid is shown in Fig. 3. The shift in the curves (triangles, dotted line) to the right are small but significant compared to the paired

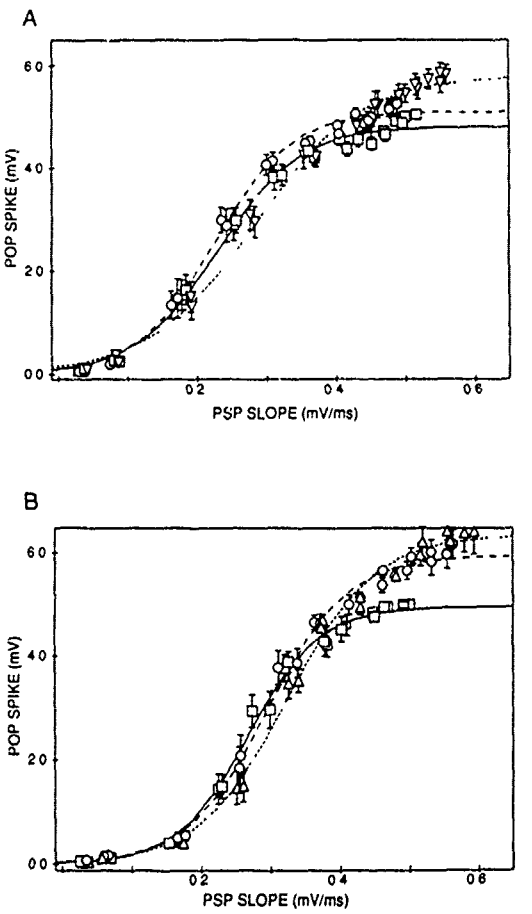

Fig. 3 Plots of population PSP size vs population spike amplitude show that fatty acids alter the ability of a synaptic potential to generate a spike. (A) Average curve ($n = 6$) showing effect of exposure and washout of 50 μM arachidonic acid. □, single line, control; ○, dashed line during 30-min application of fatty acid; △, dotted line 30-min wash with normal solution. (B) Average curve ($n = 6$) for slices exposed to 250 μM myristic acid.

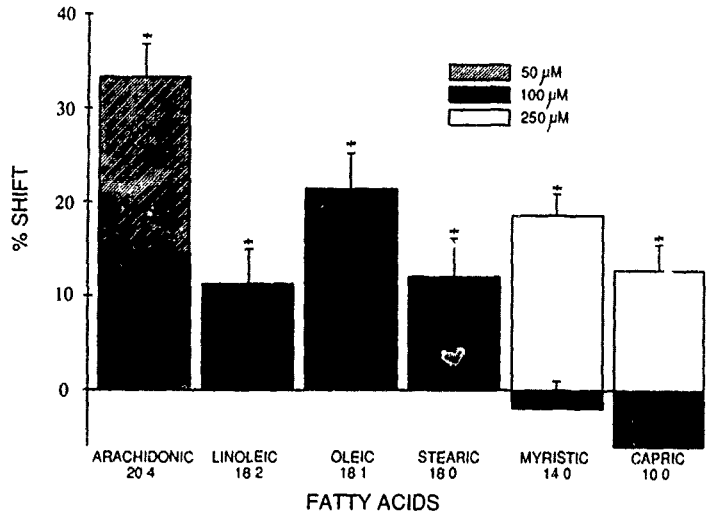

Fig. 4 Washout of fatty acids caused a decrease in ability to generate spikes Arachidonic acid (50 μM, 100 μM), linoleic acid (100 μM), oleic acid (100 μM), myristic acid (250 μM) and capric acid (250 μM) significantly shifted the relationship between population PSP size and population spike amplitude to the right All changes are calculated in reference to the appropriate solvent or time control

control period (squares, single line) In contrast, with the solvent controls, the curve shifted in the opposite direction with time, reflecting a gradual increase in F/S coupling in the absence of any exogenous fatty acids The fatty acids, therefore, are actually more effective than would appear from Fig 3

Some of the fatty acids also increased the maximal population spike amplitude as seen in Fig. 3. Growth of the population spike was also seen with the solvents and time controls Yet myristic acid (100 and 250 μM) elicited an increase in maximal amplitude beyond that predicted from the DMSO solvent data, both during exposure and following washout. Similarly, 50 μM arachidonic acid, 100 μM linoleic acid and 100 μM stearic acid increased the maximal population spike significantly greater than with the ethanol controls during the wash period

Increased population spike

Both synaptic efficacy and E/S coupling contribute to the amplitude of the population spike at a single stimulus strength. Despite the observation that most of the fatty acids did not significantly alter either of the component curves during fatty acid exposure, many did significantly increase the population spike. Since the population spike also grew with the solvent controls, all increases were referenced to the appropriate control values. Only arachidonic acid (50 μM), stearic acid (100 μM) and myristic acid (100 μM) did not significantly increase the population spike. During the 30-min exposure to the fatty acids, the increase in the population spike ranged from 11% with 100 μM arachidonic acid to 22% with 100 μM oleic and linoleic acids, relative to the solvent controls.

With a 30-min washout, myristic and capric acids (100 and 250 μM) showed an additional increase in the population spike Following washout, only arachidonic acid and stearic acid did not show significant potentiation of population spike amplitude The largest potentiation was seen with 250 μM myristic acid which increased 32% more than the DMSO control The effects of 100 μM oleic acid on the relationship between afferent volley and the population spike amplitude are illustrated in Fig 5 The curve was enhanced during exposure to the fatty acid and the potentiation continued following washout. The increase in population spike amplitude with oleic acid treatment was significantly greater than that seen with the ethanol solvent alone The time-course of changes in amplitude of the population spike and the population PSP with application of 250 μM capric acid are shown in Fig 6. As described above, the population spike increased quickly following exposure to the fatty acid while the population PSP increased more slowly. Following removal of the fatty acid, the population spike continued to increase slightly but the population PSP increased more dramatically The effects persisted for the duration of the recording period (1 h of wash). The change in amplitude of the population spike during the exposure could result from an increase in synaptic potential and/or an increase in E/S coupling, although neither effect alone was statistically significant. With washout, the synaptic potential was increased disproportionately to the increase in the population spike. This is likely to be a consequence of the decrease in E/S coupling discussed above.

DISCUSSION

A number of fatty acids have been found to produce electrophysiological effects in hippocampal slices. Although each fatty acid was unique, a general pattern was evident. With exposure to the fatty acid

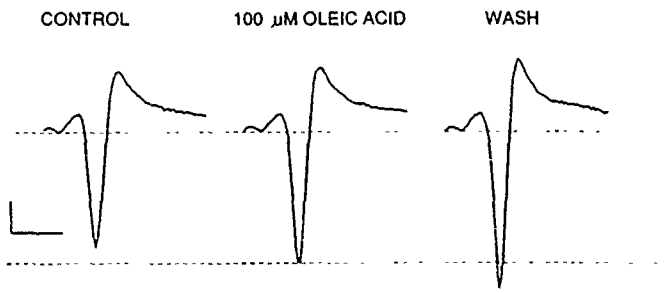

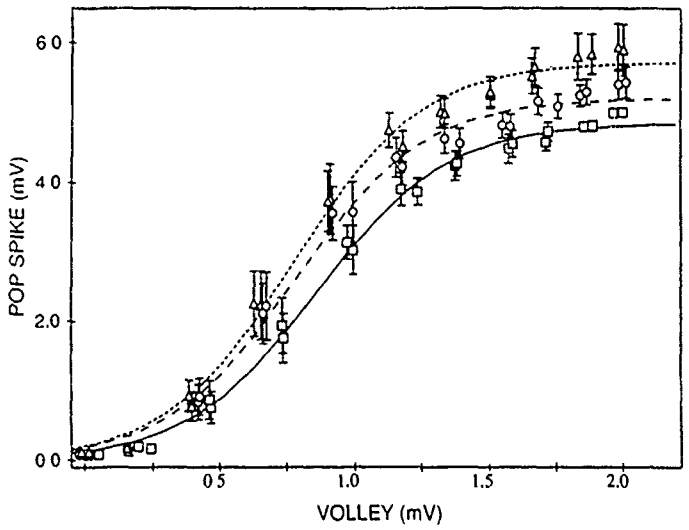

Fig 5 Exposure to 100 μM oleic acid increased population spike amplitude Traces show sample population spikes from a slice exposed to 100 μM oleic acid The population spike increased during application and further increased following washout of the fatty acid. Calibration 1 mV, 2 ms. Plot of afferent volley vs population spike amplitude shows increase with 30-min exposure and further increase following 30-min of wash. These changes exceeded those seen with the ethanol control. □, single line. control, ○, dashed line during 30-min application of fatty acid; △, dotted line: 30-min wash with normal solution Curves from five slices were averaged.

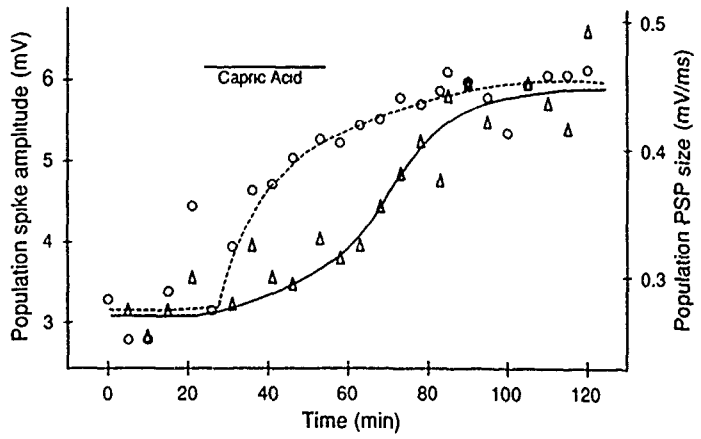

Fig. 6 Time-course of increase in population spike amplitude (○) and population PSP size (△) with exposure to 250 μM capric acid in a representative experiment. Synaptic potentials increased slightly during exposure to capric acid and showed greater increase with wash. Population spikes showed substantial increase during initial exposure to capric acid. With washout, the population spike did not increase proportionately with the increase in the synaptic response.

the population spike increased. The synaptic potential and E/S coupling were minimally affected during this time. With washout of the fatty acid, the synaptic response potentiated. The population spike frequently continued to increase with wash but not to the extent expected from the rise in the synaptic potential. E/S coupling was impaired. These data suggest that a number of cellular processes are sensitive to fatty acids

Oleic acid and arachidonic acid have been shown to enhance LTP in the hippocampus.[14,16,38] Linden *et al*[14,16] suggested that these actions resulted from activation of protein kinase C. Oleic acid was more effective than arachidonic acid both to activate protein kinase C and to enhance LTP.[14] Stearic acid, which does not activate protein kinase C[15,18] did not have this effect.[14] Similarly, in the present study, oleic acid was more effective than arachidonic acid in potentiating the synaptic response while stearic acid was ineffective. Although myristic acid, but not capric acid, was reported to activate protein kinase C,[18] both were found to be equally effective at increasing the synaptic response. The fatty acid actions on spike generation do not follow the same pattern of effectiveness and probably do not result from this mechanism. Increased inositol phosphates and the consequent rise in intracellular calcium has also been proposed as a mechanism for arachidonic acid-induced LTP enhancement.[17] However, oleic acid cannot substitute for arachidonic acid in activation of phosphoinositide turnover.[17,19] This observation makes it an unlikely mechanism for any of the electrophysiological actions described here.

Takenaka *et al*[30,31] have examined the actions of a number of fatty acids on currents in squid giant axon. They found that sodium current activation parameter (m) was shifted in the depolarized direction with application of fatty acids with at least eight carbons[30] and that the long-chain fatty acids such as arachidonic acid were more effective than the medium-chain fatty acids.[31] From the chemical structures, Takenaka *et al.*[31] hypothesized that the fatty acids all have a similar action to perturb the membrane near the "plastic" region of the sodium channel A similar disruption of the membrane by the fatty acids could alter hippocampal electrophysiology. In fact, Crews *et al.*[10] have shown that alteration of membrane fluidity by addition of cholesterol reversibly reduced the cholinergic response of hippocampal pyramidal cells. Fatty acid insertion into the membrane and modification of local channel domains cannot be excluded as a mechanism for some of the fatty acid actions described here.

Metabolites of arachidonic acid have been suggested as the effective agents in potentiation of orthodromic responses in the hippocampus.[6,11,37] The lipoxygenase inhibitor, nordihydroguaiaretic acid, prevented arachidonic acid-induced synaptic potentiation[11] but not the enhancement of LTP.[38] The actions of arachidonic acid are not blocked by indomethacin, a cyclooxygenase inhibitor.[11] The lipoxygenase metabolites, (12)-hydroperoxyeicosatetraenoic acid (12-HPETE)[11] and hepoxilin A_3[6] mimicked the synaptic potentiation by arachidonic acid. However, since most of the fatty acids used in the present study are not substrates for either lipoxygenase or cyclooxygenase, a metabolic product is an unlikely mediator of the present results.

Fatty acids may have differential effects when made available intracellularly vs extracellularly. In muscle myocytes, intracellular oleic acid and arachidonic acid increased inward current while extracellular arachidonic acid decreased the inward current.[36] It is interesting to speculate that the changes in excitability in the hippocampal slice with exposure and wash may reflect a differential distribution of the fatty acid. This possibility needs to be considered when extrapolating data to pathological states where fatty acids may be expected to accumulate to a greater extent intracellularly than extracellularly.

Fatty acids are released from cells following exposure to free radicals.[7,8,27] Previous studies in our laboratory have shown that gamma radiation[33] and peroxide-induced free radical damage[21] cause a decrease in both synaptic efficacy and spike generation. With X-radiation at a low dose rate (1.5 Gy/min) where lipid peroxidation may predominate as a mechanism of cell damage,[26] synaptic efficacy is increased. The curve relating the ability of the population PSP to generate a population spike is shifted to the right. In addition, the maximal population spike amplitude is increased. In short, the electrophysiological consequences of X-radiation look very much like exposure and subsequent washout of fatty acids We postulate that the release of fatty acids contributes to the electrophysiological effects of X-radiation exposure. Free radical-induced release of fatty acids, in combination with additional factors, probably contribute to peroxide and gamma radiation damage as well. The results of the present study support the possibility that free fatty acids contribute to the electrophysiological changes that occur in pathological states such as ischemia.

Acknowledgements—This work was supported by the Armed Forces Radiobiology Research Institute, Defense Nuclear Agency, under work unit 00105 Views presented in this paper are those of the authors; no endorsement by the Defense Nuclear Agency has been given or should be inferred. Research was conducted according to the principles enunciated in the Guide for the Care and Use of Laboratory Animals prepared by the Institute of Laboratory Animal Resources, National Research Council.

REFERENCES

1. Abe K., Kogure K., Yamamoto H., Imazawa M. and Miyamoto K. (1987) Mechanism of arachidonic acid liberation during ischemia in gerbil cerebral cortex *J. Neurochem.* **48,** 503–509.

2. Abraham W. C., Bliss T. V P. and Goddard G. V. (1985) Heterosynaptic changes accompany long-term but not short-term potentiation of the perforant path in the anesthetized rat. *J. Physiol., Lond* **363,** 335–349
3. Anderson P , Sundberg S. H., Sveen O., Swann J. W. and Wigstrom H. (1980) Possible mechanisms for long-lasting potentiation of synaptic transmission in hippocampal slices from guinea-pigs. *J. Physiol., Lond.* **302,** 463–482.
4. Bazan N. B. (1970) Effect of ischemia and electroconvulsive shock on free fatty acid pool in the brain. *Biochim. biophys. Acta* **218,** 1–10.
5. Buttner N , Siegelbaum S. A. and Volterra A. (1989) Direct modulation of Aplysia S − K + channels by a 12-lipoxygenase metabolite of arachidonic acid. *Nature* **342,** 553–555.
6. Carlen P. L , Gurevich N , Wu P. H., Su W. G., Corey E J. and Pace-Asciak C R (1989) Actions of arachidonic acid and hepoxilin A3 on mammalian hippocampal CA1 neurons. *Brain Res.* **497,** 171-176.
7. Chan P. H., Fishman R A., Schmidley J. W. and Chen S F. (1984) Release of polyunsaturated fatty acids from phospholipids and alteration of brain membrane integrity by oxygen derived free radicals *J. Neurosci. Res.* **12,** 595-605.
8 Chan P H , Yurko M. and Fishman R. A (1982) Phospholipid degradation and cellular edema induced by free radicals in brain cortical slices. *J. Neurochem.* **38,** 525–531.
9. Chavez-Noriega L E., Halliwell J. V. and Bliss T. V. P. (1990) A decrease in firing threshold observed after induction of the EPSP-spike (E–S) component of long-term potentiation in rat hippocampal slices. *Expl Brain Res.* **79,** 633–641.
10 Crews F T , Camacho A and Phillips M I. (1983) Cholinergic stimulation of hippocampal pyramidal cells is inhibited by increasing membrane cholesterol. *Brain Res.* **261,** 155–158.
11 Drapeau C , Pellerin L., Wolfe L S. and Avoli M. (1990) Long-term changes of synaptic transmission induced by arachidonic acid in the CA1 subfield of the rat hippocampus. *Neurosci. Lett.* **115,** 286–292
12 Kim D and Clapman D E (1989) Potassium channels in cardiac cells activated by arachidonic acid and phospholipids *Science* **244,** 1174–1176.
13 Kurachi Y , Ito H., Sugimoto T., Shimizu T., Miki I. and Ui M. (1989) Arachidonic acid metabolites as intracellular modulators of the G protein-gated cardiac K^+ channel. *Nature* **337,** 555–557.
14 Linden D J., Murakami K and Routtenberg A. (1986) A newly discovered protein kinase C activator (oleic acid) enhances long-term potentiation in the intact hippocampus. *Brain Res.* **379,** 358–363.
15 Linden D. J and Routtenberg A. (1989) *cis*-Fatty acids which activate protein kinase C, attenuate Na^+ and Ca^{++} currents in mouse neuroblastoma cells. *J. Physiol., Lond.* **419,** 95–119.
16 Linden D. J., Sheu F , Murakami K and Routtenberg A. (1987) Enhancement of long-term potentiation by *cis*-unsaturated fatty acid relation to protein kinase C and phospholipase A2. *J. Neurosci.* **7,** 3783–3792.
17 Lynch M A and Voss K. L (1990) Arachidonic acid increases inositol phospholipid metabolism and glutamate release in synaptosomes prepared from hippocampal tissue. *J. Neurochem.* **55,** 215–221.
18 Murakami K., Chan S Y. and Routtenberg A. (1986) Protein kinase C activation by *cis*-fatty acids in the absence of Ca^{2+} and phospholipids. *J biol. Chem.* **261,** 15,424–15,429.
19 Negishi M , Ito S. and Hayaishi O. (1990) Arachidonic acid stimulates phosphoinositide metabolism and catecholamine-release from bovine adrenal chromaffin cells *Biochem. biophys. Res. Commun* **169,** 773–779.
20. Ordway R W., Walsh J V and Singer J J (1989) Arachidonic acid and other fatty acids directly activate potassium channels in smooth muscle cells. *Science* **244,** 1176–1179.
21 Pellmar T C (1986) Electrophysiological correlates of peroxide damage in guinea pig hippocampus *in vitro. Brain Res* **364,** 377–381.
22 Pellmar T C (1987) Peroxide alters neuronal excitability in the CA1 region of guinea-pig hippocampus *in vitro. Neuroscience* **23,** 447–456.
23 Pellmar T C (1990) Fatty acids enhance synaptic efficacy in guinea pig hippocampal slices. *Soc. Neurosci Abstr.* **16,** 538.
24 Pellmar T C and Neel K L. (1989) Oxidative damage in the guinea pig hippocampal slice. *Free Radical Biol. Med.* **6,** 467-472.
25 Pellmar T C , Neel K. L and Lee K. J (1989) Free radicals mediate peroxidative damage in guinea pig hippocampus *in vitro. J. Neurosci. Res.* **24,** 437–444.
26 Pellmar T. C , Schauer D A and Zeman G H. (1990) Time and dose dependent changes in neuronal activity produced by X-radiation in brain slices. *Radiation Res.* **122,** 209–214.
27. Polgar P and Taylor L. (1980) Stimulation of prostaglandin synthesis by ascorbic acid via hydrogen peroxide formation. *Prostaglandins* **19,** 693–700.
28 Shapiro E , Piomelli D , Feinmark S., Vogel S., Chin G and Schwartz J. H. (1988) The role of arachidonic acid metabolites in signal transduction in an identified neural network mediating presynaptic inhibition in *Aplysia. Cold Spring Harbor Symp. quant. Biol.* **53,** 425–433.
29 Siesjo B. K. (1981) Cell damage in the brain: a speculative synthesis. *J cerebr. Blood Flow Metab.* **1,** 155–185.
30 Takenaka T., Horie H. and Hori H. (1987) Effects of fatty acids on membrane currents in the squid giant axon. *J. Membrane Biol.* **95,** 113–120.
31 Takenaka T , Horie H., Hori H. and Kawakami T. (1988) Effects of arachidonic acid and the other long-chain fatty acids on the membrane currents in the squid giant axon. *J. Membrane Biol.* **106,** 141–147.
32 Taube J. S and Schwartzkroin P. A. (1988) Mechanisms of long-term potentiation: a current-source density analysis. *J. Neurosci.* **8,** 1645–1655
33 Tolliver J. M. and Pellmar T. C. (1987) Ionizing radiation alters neuronal excitability in hippocampal slices of the guinea pig. *Radiation Res.* **112,** 555–563.
34. Van Kuijk F. J G. M., Sevanian A., Handelman G. J. and Dratz E. A. (1987) A new role for phospholipase A2: protection of membranes from lipid peroxidation damage. *Trends biochem. Sci.* **12,** 31–34.
35 Westerberg E., Deshpande J. K and Wieloch T. (1987) Regional differences in arachidonic acid release in rat hippocampal CA1 and CA3 regions during cerebral ischemia. *J. cerebr. Blood Flow Metab.* **7,** 189–192.
36. Wieland S. J., Fletcher J. E., Gong O. H. and Rosenberg H. (1990) Unsaturated fatty acids modulate sodium current in cultured skeletal muscle. *Soc. Neurosci. Abstr.* **16,** 357.
37. Williams J. H. and Bliss T. V. P. (1988) Induction but not maintenance of calcium-induced long-term potentiation in dentate gyrus and area CA1 of the hippocampal slice is blocked by nordihydroguaiaretic acid. *Neurosci. Lett.* **88,** 81–85.

38. Williams J. H., Errington M. L., Lynch M A. and Bliss T. V. P. (1989) Arachidonic acid induces a long-term activity dependent enhancement of synaptic transmission in the hippocampus. *Nature* **341,** 739–742.
39. Yoshida S., Abe K., Busto R., Watson B. D., Kogure D. and Ginsberg M. D. (1982) Influence of transient ischemia on lipid-soluble antioxidants, free fatty acids and energy metabolites in rat brain. *Brain Res.* **245,** 307–316.

(*Accepted* 28 *May* 1991)

LYMPHOKINE AND CYTOKINE RESEARCH
Volume 10, Number 2, 1991
Mary Ann Liebert, Inc., Publishers
pp. 141–146

Interleukin-1 and Interleukin-6 Act Synergistically to Stimulate the Release of Adrenocorticotropic Hormone *In Vivo*

ROBERT S. PERLSTEIN,* EDWARD H. MOUGEY,† WILLIAM E. JACKSON,* and RUTH NETA*

ABSTRACT

Interleukin-1 (IL-1) and interleukin-6 (IL-6) share a number of biological functions. Because IL-1 induces IL-6 *in vivo*, the extent to which IL-6 mediates the effects of IL-1 has come under investigation. The stimulation of the hypothalamic–pituitary–adrenal axis by IL-1 and IL-6 is a critical component of the inflammatory response. The present study was designed to compare the effects of recombinant human IL-1α (rhIL-1α) and recombinant human IL-6 (rhIL-6) administered in combination and alone on the release of adrenocorticotropic hormone (ACTH) in mice. We have demonstrated that the administration of rhIL-6 alone does not duplicate the stimulatory effect of rhIL-1α on ACTH release. On the other hand, suboptimal amounts of rhIL-1α and rhIL-6 synergize to induce an early (30–60 min) ACTH response and produce a later (2–3 h) response that is similar to the one observed after rhIL-1α is administered alone. These results suggest that the 2–3 h response to rhIL-1α may be dependent on synergy with the endogenous IL-6 it induces systemically and in the central nervous system (including the hypothalamus and the pituitary gland).

INTRODUCTION

The pluripotent cytokines, interleukin-1 (IL-1) and interleukin-6 (IL-6), share several biological functions (1–4). Because IL-1 induces IL-6 *in vivo* (5–7), it is possible that the effects of IL-1 are mediated by IL-6. Several effects of IL-1, such as the stimulation of growth of myeloma cells (8) and the release of gonadotropins and prolactin by the pituitary gland (9), were shown to be induced directly by IL-6. However, the *in vivo* induction of several acute phase proteins (5) and nonspecific resistance to microbial infection (10) were not reproduced when IL-6 was administered alone. Furthermore, synergy between IL-1 and IL-6 was demonstrated in the stimulation of B cell (11) and myelomonocytic cell (12) differentiation and T cell/thymocyte activation and proliferation (13–17), the induction of certain acute phase proteins (18,19), and radioprotection (5).

Cytokines play a critical role in activating the hypothalamic–pituitary–adrenal (H–P–A) axis during the inflammatory/immune response (20,21). The glucocorticoids produced are essential for the host's survival and feedback negatively on multiple aspects of immune function (20). It is well established that IL-1 stimulates the release of adrenocorticotropic hormone (ACTH) (22–32), most likely by inducing corticotropin-releasing hormone (CRH) (25–27), and more current work attributes a similar effect to IL-6 (29,33–36).

The present study was designed to compare the effects of IL-1 and IL-6 alone and in combination on ACTH release in mice. Our results indicate that IL-1 and IL-6 interact synergistically in stimulating the release of ACTH.

MATERIALS AND METHODS

Mice

Female C3H/HeN mice were purchased from the National Cancer Institute, Frederick, MD. Mice were quarantined on arrival and screened for evidence of disease before being released for experimentation. They were maintained in an American Association for Accreditation of Laboratory Animal Care-accredited facility in plastic Micro-Isolator cages on hard-

*Department of Experimental Hematology, Armed Forces Radiobiology Research Institute, Bethesda, MD 20889-5145.
†Neuroendocrinology and Neurochemistry Branch, Department of Medical Neurosciences, Walter Reed Army Institute of Research, Washington, DC 20307-5100.

wood chip contact bedding, provided commercial rodent chow, and given acidified (HCl to a pH of 2.5) tap water *ad libitum*. Not more than 10 mice were quartered in each cage. Animal holding rooms were maintained at 70° ± 2°F with 50 ± 10% relative humidity using at least 10 air changes per hour of 100% conditioned fresh air. The mice were kept on a 12-h (0600–1800 h) light–dark full spectrum lighting cycle with no twilight. Mice were 10–16 weeks of age when used. All animal handling procedures were performed in compliance with guidelines from the National Research Council and the Armed Forces Radiobiology Research Institute.

Cytokines

The recombinant human IL-1α (rhIL-1α) was generously provided by Dr. Peter Lomedico of Hoffmann-La Roche, Nutley, NJ. The preparation, lot IL-1-2/8, was supplied in 50 m*M* potassium phosphate and 0.1 *M* NaCl buffer (pH 6.5). The endotoxin contamination was negligible at 0.5 Eu/0.68 mg protein (Limulus Amoebocyte Lysate assay; LAL assay). We used rhIL-1α, rather than rhIL-1β, because (1) mice respond well to rhIL-1α (23), (2) rhIL-1α is the predominant form of IL-1 transported bidirectionally across the blood–brain barrier in mice (37,38, W. A. Banks, personal communication), with the hypothalamus manifesting an entry rate twi e that of other brain areas (37), and (3) in mice, rhIL-1α stimulates hypothalamic noradrenergic neurons, thereby activating the H–P–A axis and increasing plasma corticosterone levels 10-fold (39). The recombinant human IL-6 (rhIL-6) was provided by Dr. Menachem Rubinstein of Inter Pharm Laboratories, Ness-Ziona, Israel. The preparation, lot IL-6-CHO-1/5, was supplied in acetate buffer (pH 5 0) and had a specific activity of 5×10^6 units/mg. The endotoxin contamination was negligible at less than 0.4 Eu/mg protein (LAL assay). All reagents were diluted to the desired concentration in pyrogen-free normal saline just before a single intraperitoneal (ip) injection of 0.5 ml to mice.

Measurement of ACTH in plasma

All experiments were begun at 0930 h and completed 2–5 h later. Mice were decapitated (with Model #130 Rodent Decapitator, Harvard Apparatus, South Natick, MA) at designated time points (30–300 min) after ip injection of rhIL-1α and/or rhIL-6, and vehicle (0.5 ml pyrogen-free normal saline). In addition, six noninjected control mice were euthanatized on the day of each experiment. The blood was collected in tubes containing 25 μl of porcine sodium heparin (Elkins-Sinn, Inc., Cherry Hill, NJ) and 10 μl of aprotinin (bovine protease inhibitor, Sigma Chemical Co., St. Louis, MO), and then centrifuged for 25 min at 2°C in a Beckman Model TJ-6 centrifuge. The plasma was removed and frozen at −70°C until RIA for ACTH was performed. ACTH was assayed usng an ^{125}I RIA kit for human ACTH purchased from the INCSTAR Corporation, Stillwater, MN (Catalog #2413⁰). Most specimens were analyzed in duplicate. The ACTH antibody employed in this assay is derived from rabbits injected with human $ACTH_{1-24}$ (a region that is identical in human and murine ACTH) and has been shown to cross-react with ACTH from many other species (INCSTAR Corporation, unpublished data). Furthermore, murine ACTH has been accurately measured using anti-human ACTH antibodies (40,41). Cross-reactivities with α-melanocyte-stimulating hormone, β-endorphin, and β-lipotropin at concentrations of 1200 pg/ml were less than 0.01%. Intraassay reproducibility was 4% (coefficient of variation: CV) and interassay reproducibility was 8% (CV). Assay sensitivity was 8 pg/ml.

Statistical analysis

In the statistical analysis of the data, a log transformation of all plasma ACTH values was performed. The means plotted in Figs. 1–5, listed in Table 1, and noted in the text are, therefore, geometric means, and the numbers in brackets in Table 1 and the text are the lower and upper ends of standard error bars. References to "mean ± SEM" are for log units and all comparisons were made in those units. All statistical comparisons were made using Student's *t* test. In Figs. 1–5, where more than one set of data was plotted on a graph, a time offset was used to avoid overlapping error bars.

RESULTS

Release of ACTH after the injection of vehicle

In every experiment involving the injection of rhIL-1α and/or rhIL-6, control animals were simultaneously injected with vehicle only (0.5 ml pyrogen-free normal saline). The ACTH responses to the vehicle injections were very small in magnitude, but occasionally were significantly different from basal values in noninjected control mice. The 30-, 60-, 120-, and 180-min vehicle responses were not significantly different from one another when pooled data from all experiments were analyzed. Mean plasma ACTH (for all time points) after injecting vehicle (68 {67, 69}, $n = 215$) was significantly greater ($p < 0.001$) than the mean plasma ACTH for all noninjected control mice (61, {60,62}, $n = 125$). Presumably, these responses reflect the stress of animal handling/injection. Therefore, in the description of results that follows, the ACTH responses to interleukin injections at various time points are compared with those induced by simultaneous vehicle injections.

Release of ACTH after the injection of rhIL-1α

Figure 1 shows the effects of ip administration of increasing doses of rhIL-1α (10 ng, 100 ng, 1 μg, and 10 μg/mouse) on plasma ACTH 2 h after injection. Significant increases were seen in every instance. Analysis of the time course of ACTH response reveals a dose-dependent prolongation of the time required to achieve maximal ACTH levels [10 ng and 100 ng—2 h, 1 μg—3 h, 10 μg—4–5 h (data not shown)] and more prolonged duration of response with increasing amounts of phRIL-1α (Fig. 2).

Release of ACTH after the injection of rhIL-6

The ip administration of 1 or 10 μg of rhIL-6 elicited a statistically significant but very small response 60 min after the injection. No significant responses were seen at any other time points (Fig. 3).

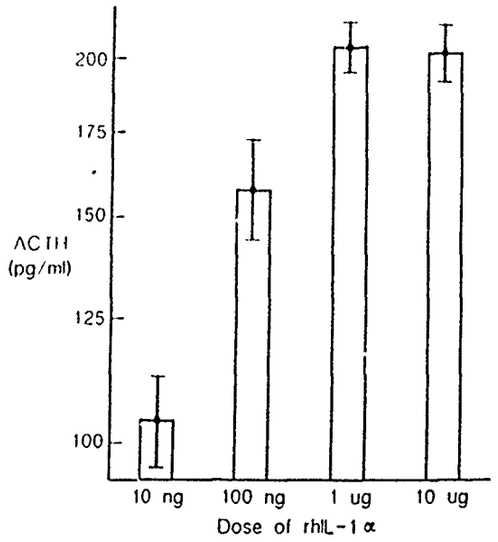

FIG. 1. Changes in plasma ACTH in C3H/HeN mice 2 h after intraperitoneal injection of different doses of rhIL-1α. Each time point represents the mean ± SEM of hormone determinations from 6 to 12 animals (see Materials and Methods). The response to each dose of rhIL-1α was significantly greater ($p < 0.001$) than the response at 2 h to simultaneously injected vehicle (0.5 ml pyrogen-free normal saline).

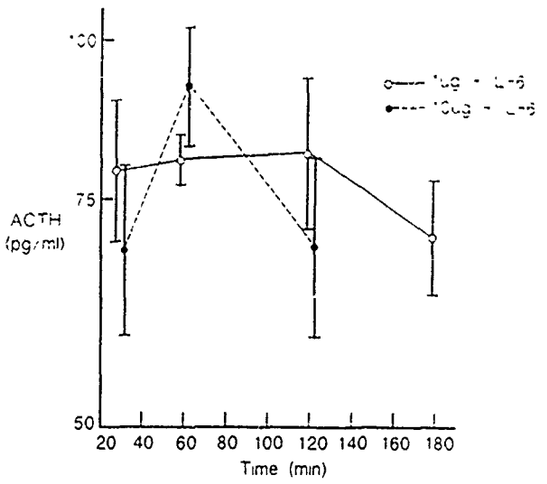

FIG. 3. Time courseof increase in plasma ACTH in C3H/HeN mice after intraperitoneal injection of rhIL-6 (1 and 10 μg/animal). Each time point represents the mean ± SEM of hormone determinations from 6–12 animals (see Materials and Methods). Only the 60 min response to the 1-μg dose ($p = 0.004$) and the 10-μg dose ($p = 0.036$) was significantly greater than the response to simultaneously injected vehicle (0.5 ml pyrogen-free normal saline).

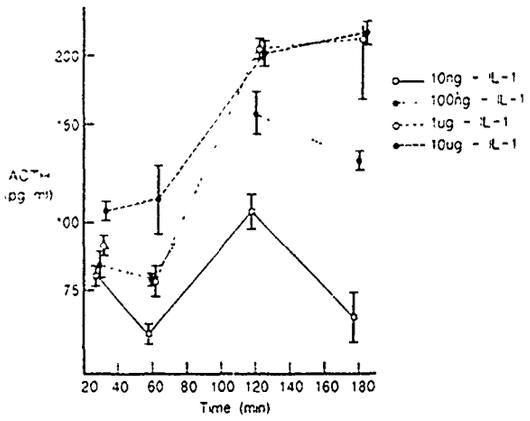

FIG. 2. Time course of increase in plasma ACTH in C3H/HeN mice after intraperitoneal injection of rhIL-1α (10 ng, 100 ng, 1 μg, 10 μg/animal). Each time point represents the mean ± SEM of hormone determinations from 6 to 12 animals (see Materials and Methods). The responses at 240 and 300 min are not shown. The response at every time point was compared with the response to simultaneously injected vehicle (0.5 ml pyrogen-free normal saline). Significantly different responses were observed with 10 ng (120 min, $p < 0.001$), 100 ng (60 min, $p < 0.01$; 120 min, $p < 0.001$; 180 min, $p < 0.001$), 1 μg (30 min, $p < 0.05$; 120 min, $p < 0.001$; 180 min, $p < 0.05$; 240 min, $p < 0.001$; 300 min, $p < 0.001$), 10 μg (30 min, $p < 0.05$; 60 min, $p < 0.05$; 120 min, $p < 0.001$; 180 min, $p < 0.001$; 240 min, $p < 0.001$; 300 min, $p < 0.001$).

Release of ACTH after the injection of combinations of rhIL-1α and rhIL-6

Following the combined administration of 100 ng rhIL-1α and 1 μg rhIL-6, a significant increase in circulating ACTH was observed at 30, 60, 120, and 180 min (Fig. 4). When these responses were compared with those achieved with 100 ng rhIL-1α and 1 μg rhIL-6 given separately, the responses to the combined injection were found to be significantly greater than the sum of the responses to each component alone at 30 and 60 min (Fig. 4 and Table 1). However, at 120 and 180 min, the responses after administration of this combination of cytokines were similar to the responses to 100 ng rhIL-1α given alone and significantly greater than the responses to 1 μg rhIL-6 given alone (Fig. 4). Similarly, combined administration of 10 ng rhIL-1α and 1 μg rhIL-6 significantly increased plasma ACTH levels at 30, 60, and 120 min (Fig. 5). The response to the combination of cytokines was significantly greater than the sum of the responses to each component alone at 60 min; at 30 min, a similar trend was observed which was not statistically significant (Fig. 5 and Table 1). At 120 min, the response to the cytokine combination was similar to the response to 10 ng rhIL-1α given alone (Fig. 5).

DISCUSSION

Our results demonstrate that rhIL-1α and rhIL-6 interact synergistically in stimulating the release of ACTH. This synergy

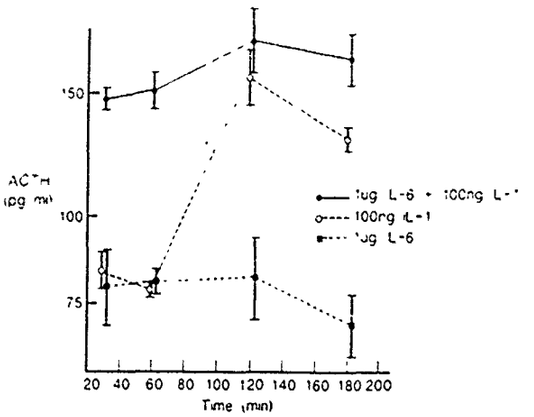

FIG. 4. Comparison of the time course of increase in plasma ACTH in C3H/HeN mice after intraperitoneal injection of 100 ng rhIL-1α combined with 1 μg rhIL-6, 100 ng rhIL-1α, and 1 μg rhIL-6. Each time point represents the mean ± SEM of hormone determinations from 6 to 12 animals (see Materials and Methods). The 30- and 60-min responses to the cytokine mixture were significantly greater than the sum of the responses at those same times to 100 ng rhIL-1α and 1 μg rhIL-6 given separately (30 min, $p < 0.01$; 60 min, $p < 0.05$). The 120- and 180-min responses to the cytokine combination were similar to the same responses to 100 ng rhIL-1α given alone and significantly greater than the same responses to 1 μg rhIL-6 administered alone ($p < 0.001$).

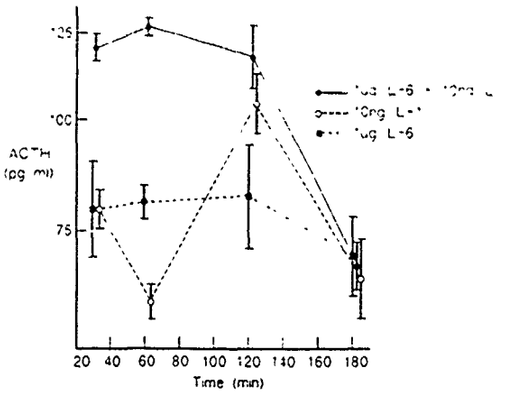

FIG. 5. Comparison of the time course of increase in plasma ACTH in C3H/HeN mice after intraperitoneal injection of 10 ng rhIL-1α combined with 1 μg rhIL-6, 10 ng rhIL-1α, and 1 μg rhIL-6. Each time point represents the mean ± SEM of hormone determinations from 6–12 animals (see Materials and Methods). The 60-min response to the cytokine mixture was significantly greater than the sum of the responses at 60 min to 10 ng rhIL-1α and 1 μg rhIL-6 given separately ($p < 0.001$). The 120-min response to the cytokine combination was similar to the 120-min response to 10 ng rhIL-1α given alone.

TABLE 1 EARLY CHANGES IN PLASMA ACTH AFTER THE INJECTION OF rhIL-1α AND/OR rhIL-6[a]

	ACTH response	
Treatment (dose)	*30 min*	*60 min*
Vehicle	67 (66, 69)[b]	68 (66, 69)[b]
rhIL-1α (10 ng)	79 (75, 83)	62 (59, 65)
rhIL-1α (100 ng)	84 (79, 89)	78 (76, 81)[c]
rhIL-1α (1 μg)	91 (86, 95)[c]	77 (72, 83)
rhIL-1α (10 μg)	105 (100, 110)[c]	110 (95, 127)[c]
rhIL-6 (1 μg)	79 (70, 90)	81 (77, 84)[c]
rhIL-6 (10 μg)	69 (59, 80)	92 (83, 102)[c]
rhIL-1α (10 ng) and rhIL-6 (1 μg)	121 (117, 125)[c]	127 (124, 130)[c,d]
rhIL-1α (100 ng) and rhIL-6 (1 μg)	147 (142, 153)[c,e]	151 (142, 161)[c,f]

[a] Plasma ACTH levels were determined in C3H/HeN mice 30 and 60 min after the intraperitoneal administration of various amounts of rhIL-1α and rhIL-6 alone and in combination. Each value represents the mean ± SEM of hormone determinations in 6–12 animals (see Materials and Methods).

[b] Mean ACTH response after the injection of vehicle for all experiments.

[c] Significantly different than the response at the same time to simultaneously injected vehicle (0.5 ml pyrogen-free normal saline). See Figs. 2–5.

[d] Significantly different than the sum of the responses at 60 min to 10 ng rhIL-1α and 1 μg rhIL-6 given separately ($p < 0.001$).

[e] Significantly different than the sum of the responses at 30 min to 100 ng rhIL-1α and 1 μg rhIL-6 given separately ($p < 0.01$).

[f] Significantly different than the sum of the responses at 60 min to 100 ng rhIL-1α and 1 μg rhIL-6 given separately ($p < 0.05$).

is observed 30 and 60 min after injection, but not at 120 and 180 min. At these later times, the response to rhIL-1α given alone is similar to that of rhIL-1α given in combination with rhIL-6. It is possible that, at 120 and 180 min, rhIL-1α synergizes with the endogenous IL-6 it induces systemically (5,6) and in the central nervous system (7). The maximal concentrations of IL-6 achieved 2 h after the administration of rhIL-1α (5,6) may be sufficient in quantity to synergize with rhIL-1α. Furthermore, because 10 ng of rhIL-1α increases levels of circulating IL-6 minimally in mice (5), the response observed at 2 h to 10 ng rhIL-1α may be related to paracrine effects of IL-6 induced by rhIL-1α in the hypothalamus and/or pituitary. A similar phenomenon may explain the very small but significant ACTH responses observed 30 and/or 60 min after the injection of rhIL-1α alone in doses of 100 ng or more.

Synergy between IL-1 and IL-6 has been observed with regard to several of their shared biological effects (1,11–19). In this regard, it was reported (13) that the greatly enhanced thymocyte-stimulating activity produced by phIL-1α or phIL-1β-stimulated fibroblasts (as compared with the direct effect of rhIL-1α alone) is mediated by a synergistic interaction of rhIL-1 and IL-6 derived from the fibroblasts and abolished by anti-rhIL-6 antibody. Moreover, adding IL-6 (which is radiosensitizing when given alone) to a nonradioprotective dose of IL-1 results in significant radioprotection (5). In addition, recent *in vitro* results suggest that IL-1 and IL-6 interact synergistically to stimulate ACTH release from rat pituitary cells (42). The basis for this synergy is not clear, but may relate to the ability of cytokines to up-regulate the receptors of other cytokines [i.e., IL-3 and granulocyte/macrophage colony-stimulating factor (GM-CSF) up-regulate IL-1 receptors (43)].

Many studies have shown that IL-1 is a potent inducer of ACTH *in vivo* and *in vitro* as recently reviewed by Bateman

et al. (20) and Lumpkin (21). However, it remains unclear whether IL-1 stimulates ACTH release by a direct action on the pituitary gland. Although several *in vitro* studies with anterior pituitary cells support this contention (29–31), others do not (25,26,32). On the other hand, it is well established that IL-1 stimulates CRH release from the hypothalamus (25–27,32) through a mechanism that may involve prostaglandin (28) and/or noradrenergic activation (39). Moreover, the demonstration that neural elements of the human hypothalamus stain significantly for rhIL-1β (44) suggests a paracrine role for IL-1 in this area of the brain.

The present observations of the time course of the dose-dependent increase in circulating ACTH after rhIL-1α injections differ somewhat from the results reported by Besedovsky *et al.* (22) in mice injected with rhIL-1β. Whereas we demonstrated maximal plasma levels of ACTH 2 h or later after injecting rhIL-1α, a duration of response that increased as the injected dose of rhIL-1α became larger, and very small responses at 30 and 60 min, Besedovsky *et al.* reported a more substantial early response, a greater peak at 2 h, and a more rapid dissipation of response. It is possible that mice respond differently to rhIL-1α and rhIL-1β. A brisk response to rhIL-1β and a minimal response to rhIL-1α was previously described in the rat (28,45), and is possibly related to rat hypothalamic receptors having a greater affinity for rhIL-1β (46). The binding characteristics of murine hypothalamic receptors have not been reported as yet. However, it was shown in mice that rhIL-1α crosses the blood–brain barrier more easily than rhIL-1β (37, W. A. Banks, personal communication).

IL-6 has also been reported to stimulate the release of ACTH *in vitro* (29,34–36) and *in vivo* in rats (33,34). Akin to previous studies involving IL-1, Naitoh *et al.* (33) performed immunoneutralization experiments with anti-CRH antibodies to demonstrate that IL-6 induces CRH as a mediator of ACTH release. On the other hand, evidence for an effect of IL-6 on ACTH secretion at the level of the pituitary has also been reported (29,34), and IL-6 most likely produced by the folliculostellate cells of the pituitary (spontaneously and in response to IL-1) may have important paracrine effects (47–50). In this regard, Yamaguchi *et al.* (10) recently reported that the amount of IL-6 released from anterior pituitary cells in culture in response to rhIL-1β duplicated the effects of rhIL-1β on prolactin and gonadotropin release.

In our study, small but significant ACTH responses were observed 60 min after 1- and 10-μg injections of rhIL-6 alone. Using similar amounts of rhIL-6 in a larger species (rat), Naitoh *et al.* (33) observed more accelerated responses 15, 30, and 60 min after the injections. One possible explanation for this species difference in response to IL-6 is that the rat maintains higher endogenous IL-1 levels, resulting in a greater likelihood of IL-1/IL-6 synergy.

In conclusion, we have demonstrated that administering rhIL-6 alone does not duplicate the stimulatory effect of rhIL-1α on ACTH release. On the other hand, suboptimal amounts of rhIL-1α and rhIL-6 synergize to induce an early (30–60 min) ACTH release, and the later (2–3 h) response to rhIL-1α may be dependent upon synergy with the endogenous IL-6 it induces systemically and in the central nervous system (including the pituitary gland and the hypothalamus). Studies using anti-IL-6 antibody should further clarify this interaction. Such synergy is theoretically beneficial in that it allows the H–P–A axis to respond rapidly and efficiently to the stress of inflammation at a time when the concentration of potentially toxic cytokines is low.

ACKNOWLEDGMENTS

We thank Dr. T. J. MacVittie, Dr. G. D. Ledney, and Dr. S. N. Vogel for their helpful comments and advice and for critically reviewing this manuscript.

Supported by the Armed Forces Radiobiology Research Institute, Defense Nuclear Agency, under work unit 00129. Views presented in this paper are those of the authors; no endorsement by the Defense Nuclear Agency or the Department of Defense has been given or should be inferred. Research was conducted according to the principles enunciated in the *Guide for the Care and Use of Laboratory Animals* prepared by the Institute of Laboratory Animal Resources, National Research Council.

REFERENCES

1. **Le, J., and J. Vilcek.** 1989 *Lab. Invest. 61:588*
2. **Kishimoto, T.** 1989. *Blood 74:1.*
3. **Dinarello, C. A.** 1988 *FASEB J. 2:108*
4. **Le, J., and J. Vilcek.** 1987. *Lab. Invest. 56:234.*
5. **Neta, R., S. N. Vogel, J. D. Sipe, G. G. Wong, and R. P. Nordan.** 1988. *Lymphokine Res. 7.403*
6. **McIntosh, J. K., D. M. Jablons, J. J. Mule, R. P. Nordan, S. Rudikoff, M. T. Lotze, and S. A. Rosenberg.** 1989. *J Immunol. 143:162.*
7. **De Simoni, M. G., M. Sironi, A. De Luigi, A. Manfridi, A. Mantovani, and P. Ghezzi.** 1990. *J. Exp Med 171 1773.*
8. **Kawano, M., H. Tanaka, H. Ishikawa, M. Nobuyoshi, K. Iwato, H. Asaoku, O. Tanabe, and A. Kuramoto.** 1989 *Blood 73:2145.*
9. **Van der Meer, J. V. M., M. Helle, and L. Aarden.** 1989. *Eur J Immunol. 19.413*
10. **Yamaguchi, M., N. Matsuzaki, K. Hirota, A. Miyake, and O. Tanizawa.** 1990 *Acta Endocrinol. 122.201.*
11. **Vink, A., P. G. Coulie, P. Wauters, R. P. Nordan, and J. Van Snick.** 1988. *Eur. J. Immunol. 18.607*
12. **Onozaki, K., Y. Akiyama, A. Okano, T. Hirano, T. Kishimoto, T. Hashimoto, K. Yoshizawa, and T. Taniyama.** 1989. *Cancer Res. 49:3602.*
13. **Elias, J. A., G. Trinchieri, J. M. Beck, P. L. Simon, P. B. Sehgal, L. T. May, and J. A. Kern.** 1989. *J. Immunol. 142:509.*
14. **Helle, M., L. Boeije, and L. Aarden.** 1989. *J. Immunol. 142.4335.*
15. **Houssiau, F. A., P. G. Coulie, D. Olive, and J. Van Snick.** 1988. *Eur. J. Immunol. 18.653.*
16. **McKenzie, D.** 1988. *J. Immunol. 141:2907.*
17. **Helle, M., J. P. J. Brakenhoff, E. R. De Groot, and L. A. Aarden.** 1988. *Eur J. Immunol. 18:957.*
18. **Sehgal, P. B., G. Greininger, and G. Tosato.** (eds.) 1989. *Ann. NY Acad. Sci. 557:1.*
19. **Ganter, U., R. Arcone, C. Toniatti, G. Morrone, and G. Ciliberto.** 1989. *EMBO J. 8:3773.*

20 Bateman, A., A. Singh, T. Kral, and S. Solomon. 1989 *Endocr Rev 10:92*

21 Lumpkin, M.D. 1987 *Science 238:452*

22 Besedovsky, H., A. Del Rey, E. Sorkin, and C. A. Dinarello. 1986 *Science 233:652*

23 Besedovsky, H., and A. Del Rey. 1987 *J Neurosci Res 18:172*

24 Del Rey, A., H. Besedovsky, E. Sorkin, and C. A. Dinarello. 1987 *Ann NY Acad Sci 496:85*

25 Berkenbosch, F., J. Van Oers, A. Del Rey, F. Tilders, and H. Besedovsky. 1987 *Science 238:524*

26 Sapolsky, R., C. Rivier, G. Yamamoto, P. Plotsky, and W. Vale. 1987 *Science 238:522*

27 Uehara, A., P. E. Gottschall, R. R. Dahl, and A. Arimura. 1987 *Endocrinology 121:1580*

28 Katsuura, G., P. E. Gottschall, R. R. Dahl, and A. Arimura. 1988 *Endocrinology 122:1773*

29 Woloski, B. M. R. N. J., E. M. Smith, W. J. Meyer III, G. M. Fuller, and J. E. Blalock. 1985 *Science 230:1035*

30 Bernton, E. W., J. E. Beach, J. W. Holaday, R. C. Smallridge, and H. G. Fein. 1987 *Science 238:519*

31 Beach, J. E., R. C. Smallridge, C. A. Kinzer, E. W. Bernton, J. W. Holaday, and H. G. Fein. 1989 *Life Sci 44:1*

32 Tsagarakis, S., G. Gillies, L. H. Rees, M. Besser, and A. Grossman. 1989 *Neuroendocrinology 49:98*

33 Naitoh, Y., J. Fukata, T. Tominaga, Y. Nakai, S. Tamai, K. Mori, and H. Imura. 1988 *Biochem. Biophys. Res Commun. 155:1459*

34 Lyson, K., and S. M. McCann. 1990 *Program of the 72nd Annual Meeting of the Endocrine Society*, Atlanta, GA, p. 218, abstract 773

35 Navarra, P., S. Tsagarakis, G. M. Besser, and A. B. Grossman. 1990 *Program of the 72nd Annual Meeting of the Endocrine Society*, Atlanta, GA, p. 34, abstract 37.

36 Gaillard, R. C., E. Spinedi, R. Gova, J.-M. Dayer, and A. F. Muller. 1990 *Program of the 72nd Annual Meeting of the Endocrine Society*, Atlanta, GA, p. 34, abstract 38

37 Banks, W. A., A. J. Kastin, and D. A. Durham. 1989. *Brain Res Bull. 23:433*

38 Coceani, F., J. Lees, and C. A. Dinarello. 1988 *Brain Res 446:245*

39 Dunn, A. J. 1988 *Life Sci 43:429*

40 Heisler, S., T. D. Reisine, V. Y. H. Hook, and J. Axelrod. 1982 *Proc Natl Acad Sci U S A 79:6502*

41 Hook, V. Y. H., S. Heisler, S. L. Sabol, and J. Axelrod. 1982 *Biochem Biophys Res Commun 106:1364*

42 Brown, S. L., J. H. Yim, H. F. Starnes, and J. E. Blalock. *FASEB J 4:A2045*

43 Dubois, C. M., F. W. Ruscetti, E. W. Palaszynski, L. A. Falk, J. J. Oppenheim, and J. R. Keller. 1990 *J. Exp Med* 172:737

44. Breder, C. D., C. A. Dinarello, and C. B. Saper. 1988. *Science 240:321.*

45 Uehara, A., P. E. Gottschall, R. R. Dahl, and A. Arimura. *1987. Biochem. Biophys. Res. Commun 146:1286.*

46 Katsuura, G., P. E. Gottschall, and A. Arimura. 1988. *Biochem. Biophys. Res Commun. 156:61.*

47 Vankelecom, H., P. Carmeliet, J. Van Damme, A. Billiau, and C. Denef. 1989 *Neuroendocrinology 49.102.*

48. Spangelo, B. L., R. M. MacLeod, and P. C. Isakson. 1990. *Endocrinology 126.582.*

49 Spangelo, B. L., P. C. Isakson, and R. M. MacLeod. 1990. *Program of the 72nd Annual Meeting of the Endocrine Society*, Atlanta, GA, p 218, abstract 774.

50. Romero, L. I., J. Mancilla, C. A. Dinarello, R. M. Lechan, and S. Reichlin. 1990 *Program of the 72nd Annual Meeting of the Endocrine Society*, Atlanta, GA, p. 218, abstract 775.

Address reprint requests to:
Dr. Robert S. Perlstein
Colonel, USAF Medical Corps
EXH
Armed Forces Radiobiology
Research Institute
Bethesda, MD 20889-5145

Received for publication October 1, 1990; accepted October 10, 1990.

RADIATION RESEARCH 128, 216–221 (1991)

Relationship between Linear Energy Transfer and Behavioral Toxicity in Rats following Exposure to Protons and Heavy Particles

BERNARD M. RABIN,*†[1] WALTER A. HUNT,*[2] JAMES A. JOSEPH,*[3] THOMAS K. DALTON,* AND SATHASIVA B. KANDASAMY*

*Behavioral Sciences Department, Armed Forces Radiobiology Research Institute, Bethesda, Maryland 20889-5145, and †Department of Psychology, University of Maryland Baltimore County, Baltimore, Maryland 21228-5398

RABIN, B. M., HUNT, W. A., JOSEPH, J. A., DALTON, T. K., AND KANDASAMY, S. B. Relationship between Linear Energy Transfer and Behavioral Toxicity in Rats following Exposure to Protons and Heavy Particles. *Radiat. Res.* 128, 216–221 (1991).

Rats were exposed to protons (155 MeV) or to helium (165 MeV/amu), neon (522 MeV/amu) or argon (670 MeV/amu) particles to evaluate the behavioral toxicity of these types of radiations. Behavioral toxicity was assessed using the conditioned taste aversion paradigm. Exposure to all types of radiation produced dose-dependent increases in the intensity of the acquired taste aversion. However, the intensity of the aversions, measured as the dose that produced a 50% decrease in the intake of the sucrose-conditioned stimulus, did not show significant variation as a function of the linear energy transfer (LET) of the radiation. The results are discussed in terms of the relationship between LET and behavioral toxicity.

INTRODUCTION

On missions outside the protection provided by the magnetic field of the Earth, astronauts may be expected to encounter radiations and doses that differ from those experienced in low-earth orbit. These radiations, primarily from galactic cosmic rays, are composed of α particles, protons, and heavy particles of high and high-energy (HZE particles). For the most part, research on the effects of HZE particles on biological systems has focused on radiation-induced changes in rapidly replicating cells, including chromosomal aberrations and cell inactivation (*1–3*). Using these end points, this research has shown that the relative biological effectiveness (RBE) of different HZE particles is related to the linear energy transfer (LET) of the particle. In general, as the LET of the particle increases up to a range of ~100–200 keV/μm, there is a concomitant increase in RBE (*3–5*).

In contrast, relatively little research has been performed on the effects of exposure to HZE particles on behavior, in part because the neurons upon which behavior depends are postmitotic and it has been generally assumed that, as a result, they would not show radiation-induced changes in functioning. General estimates of the behavioral toxicity of HZE particles and the implications of such exposures for mission failure for long-term travel outside the Earth's magnetic field are not, for the most part, based on research models using exposure to the relevant types of radiation and behavioral end points (*6*). Research with low-LET radiation (γ rays or high-energy electrons) has shown that only high doses (>4–100 Gy) produce significant decrements in behavior and performance (*7, 8*). Because it is unlikely that astronauts would be exposed to such high doses during a mission (*9, 10*), these performance decrements may not be relevant to the ability of astronauts to complete their assigned missions successfully.

However, recent research suggests that the nature of the behavioral task and the type of radiation combine to determine the effects of exposure on behavior (*11–17*). This research indicates that high-LET radiations, such as HZE particles, are capable of producing severe disruptions of brain neurochemistry and behavior at significantly lower doses than lower-LET radiations. Using the conditioned taste aversion (CTA) paradigm, Rabin *et al.* (*16*) reported that the behavioral toxicity of 600 MeV/amu iron particles (^{56}Fe) was significantly greater than that of fission-spectrum neutrons, high-energy electrons, or γ rays (^{60}Co). The CTA, which measures the avoidance of a normally preferred food that has been associated with toxic consequences to the organism, is functionally related to emesis because both responses limit the intake and/or absorption of toxic substances (*18, 19*). As such, the CTA is a standard behavioral paradigm for evaluating the toxicity of a wide range of stimuli (*20*).

Related research (*14, 17*) has shown changes in dopaminergic function in the central nervous system and in corre-

[1] To whom reprint requests should be addressed.

[2] Present address: Division of Basic Research, NIAAA, Rockville, MD 20857.

[3] Present address: Gerontology Research Center, National Institute of Aging, Francis Scott Key Medical Center, Baltimore, MD 21224.

0033-7587/91 $3.00

lated motor behavior of rats following exposure to doses of ^{56}Fe particles as low as 10 cGy. Similarly, the destruction of neurons in the hippocampus and a related reduction in the speed of maze running following exposure to 50 cGy of ^{56}Fe particles have been reported by Philpott and Miquel (*11*).

Because the RBE/LET relationship is the same for a variety of biological end points, including chromosomal aberrations and cell inactivation (*1–3*), and because the effectiveness with which different types of radiation produce a CTA appears to be parallel to their LET, Rabin *et al.* (*16*) proposed that LET was one of the primary factors determining the behavioral toxicity of different types of radiation, although the mechanisms by which radiation may affect behavior are not well understood. Thus LET might provide a basis for predicting the behavioral toxicity, as well as the biological effectiveness, of exposure to heavy particles. As such, dose and LET might provide a basis for estimating the probability of radiation-induced performance decrements from exposure to these particles during long-term missions in space and the resulting potential for mission failure.

The present experiments were designed to evaluate further the relationship between LET and behavioral toxicity by studying the acquisition of a CTA following exposure to different types of radiation of varying LET.

METHODS

Subjects The subjects were male CrLCD BR VAF/Plus rats (*Rattus norvegicus*) weighing 225–250 g at the start of the experiment. The rats were maintained in AAALAC-accredited animal facilities at Lawrence Berkeley Laboratory (LBL) and Brookhaven National Laboratory (BNL). A commercial rodent chow was continually available and water was available except as required by the experimental protocol. Animal holding rooms were maintained at 21 ± 1°C. The rats were maintained on a 12-h light:dark cycle.

Procedure The behavioral procedures have been detailed in previous reports (*15, 21*). Briefly, rats were adapted to a water deprivation schedule for 5–7 days, during which they received water for 30 min each day. On the conditioning day, the rats were transported to the radiation facility where they were given access to a single calibrated drinking tube containing a 10% sucrose solution in place of the water bottle for 30 min, and their intake was recorded. Immediately following the drinking period, the experimental animals were irradiated with one of the four types of radiation. To provide a control for the handling required to bring the animals to the various radiation sources, the control animals were also taken to the source, but they were not irradiated. On the test day, 24 h later, the rats were again presented with the single drinking tube containing the 10% sucrose solution, and their intake was measured.

Statistical analyses of the data were done using analysis of variance followed by orthogonal comparisons (*22*) for the HZE particles and by regression analysis (linear and log) for the protons.

Radiation and dosimetry Irradiation with heavy particles was done using the BEVALAC at LBL. Groups of rats (n = 7–10) were exposed to doses of 20–500 cGy of heavy particles at energies in the plateau region of the Bragg curve. Dose rate ranged between 20 and 200 cGy/min. The particles to which the rats were exposed were: neon (^{20}Ne, 522 MeV/amu, LET = ~28.0 keV/μm), argon (^{40}Ar, 670 MeV/amu, LET = ~85 keV/μm), and helium (^{4}He, 165 MeV/amu, LET = ~2.0 keV/μm). Dosimetry was provided by the staff of the BEVALAC facility using parallel-plate ionization chambers with Mylar windows and nitrogen gas flow positioned in the beam line (*23, 24*).

Irradiation with protons (155 MeV, LET = ~0.30 keV/μm) was performed using the linear accelerator at BNL. Individual rats were exposed to single doses of protons varying between 9 and 468 cGy. Dosimetry was provided by the staff of the facility using standard procedures.[4] Briefly, aluminum foils were attached to the restraining tubes in which the rats were exposed. Following exposure, dose was calculated by counting the foils in a germanium detector for 100 s.

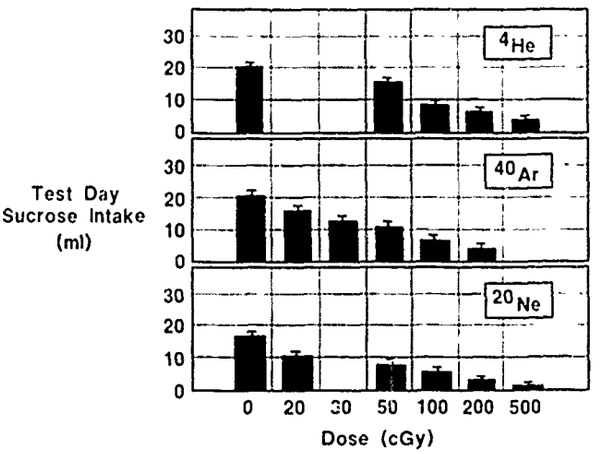

FIG. 1. Test-day sucrose intake (ml) following exposure to varying doses of helium (^{4}He), argon (^{40}Ar), or neon (^{20}Ne) particles. Error bars indicate the standard error of the mean.

RESULTS

The effects of exposure to HZE particles on the acquisition of a CTA are summarized in Fig. 1, which presents actual test-day sucrose intake, and in Fig. 2, which presents test-day sucrose intake as the percentage of conditioning-day intake. Both figures show that exposure to the three particles produced similar dose-dependent reductions in sucrose intake.

An analysis of variance performed using the three doses (50, 100, and 200 cGy) that were common to the three HZE particles confirmed that increasing the dose caused a significant increase in the intensity of the CTA ($F(2, 80) = 31.72$, $P < 0.001$). Although the analysis of variance showed that there were significant differences between the responses to the three HZE particles ($F(2, 80) = 4.78$, $P < 0.05$), post hoc tests using orthogonal comparisons (*22*) indicated that the only individual comparison that was significant was be-

[4] S. Nimnual, Foil activation dosimetry, Brookhaven National Laboratory Technical Note No. 84, BNL/NPB-89-21.

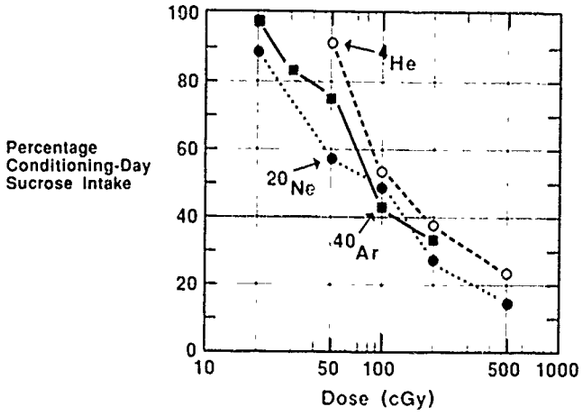

FIG. 2. Test-day sucrose intake presented as the percentage of conditioning-day intake. Abbreviations as in Fig. 1.

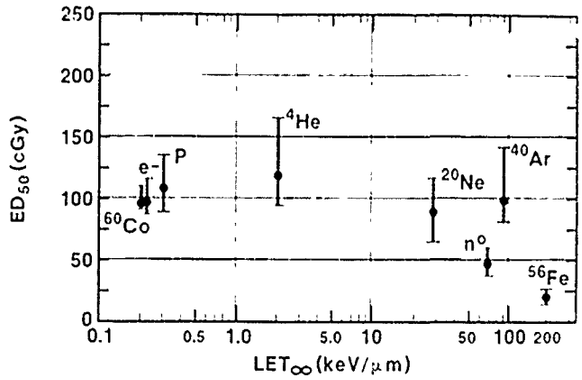

FIG. 4. The dose of radiation that produced a 50% reduction in test-day sucrose intake (ED_{50}, filled circles) as a function of the radiation LET. The data for electrons (e−), γ photons (^{60}Co), fission neutrons (n^0), and iron particles (^{56}Fe) have been calculated from Ref. (*16*). Other abbreviations as in Figs. 1 and 3. Error bars give the 95% confidence limits.

tween the ^{4}He and ^{20}Ne particles at the 50-cGy dose ($F(1, 80) = 12.51$, $P < 0.05$). In addition, the dose-by-particle interaction ($F(4, 80) = 1.40$, $P > 0.05$) was not significant, indicating that the same dose–response relationship was obtained following exposure to each particle.

The effect of proton irradiation on the acquisition of a CTA is shown in Fig. 3. Because the doses to which the rats were exposed were not grouped, these data are presented as a scatter diagram with the best-fit regression line shown. In contrast to a linear regression, which accounted for only 62% of the variance, the logarithmic regression shown in Fig. 3 accounted for 80% of the variance. These data indicate a nonlinear relationship between test-day sucrose intake and increasing doses of proton radiation, similar to that seen with the other types of radiation. The increase in sucrose intake seen in the rats exposed to doses of protons lower than 30 cGy represents the recovery from the species-typical neophobic response of rats to the novel sucrose-conditioned stimulus observed on the conditioning day (*25*).

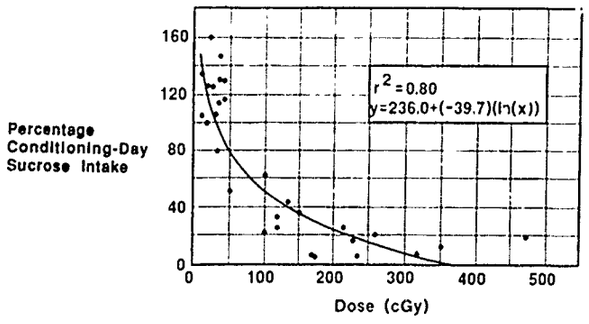

FIG. 3. Scatter diagram presenting test-day sucrose intake as the percentage of conditioning-day intake for individual animals following exposure to protons (p). The regression line was calculated using the formula $y = 236.0 + (-39.7)(\ln(x))$, which accounted for 80% of the variance.

DISCUSSION

Overall, the present results show that exposure to heavy particles and to protons produces a nonlinear dose-dependent CTA, such that increasing the radiation dose produces corresponding increases in the avoidance of the normally preferred sucrose solution. As such, the present results are consistent with the results obtained using other types of radiation and chemical toxins (*15, 16, 19*). In contrast to the results of these previous experiments on behavioral toxicity, however, the present results do not indicate a consistent relationship between increases in the LET of the radiation and corresponding increases in behavioral toxicity.

The relationship between the behavioral toxicity of a given radiation (defined in terms of the dose that produces a 50% reduction, ED_{50}, in test-day sucrose intake compared to conditioning-day intake) and LET is illustrated in Fig. 4. The ED_{50}s for exposure to fission-spectrum neutrons (n^0), iron particles (^{56}Fe, 600 MeV/amu), γ rays (^{60}Co), and high-energy electrons (e−, 18.5 MeV) were obtained in previous experiments (*16*) which used identical procedures. Additional groups of animals were exposed to ^{60}Co photons and high-energy electrons to allow a more precise calculation of the ED_{50}. Figure 4 indicates that an increase in the LET of the radiation does not reliably result in corresponding increases in the behavioral toxicity of the stimulus.

As indicated in Table 1, these types of radiation can be placed into three groups representing increasing levels of behavioral toxicity which show no overlap in their 95% confidence intervals. In the first group are high-energy elec-

TABLE I
Relative Behavioral Effectiveness (ED_{50}) of Different Radiations

Radiation	ED_{50} (cGy)	95% Confidence limits (cGy)	
		Lower	Upper
Group 1[a]			
^{4}He	121	95	168
Proton	105	85	134
^{40}Ar	98	79	129
Electron	95	79	116
^{60}Co	94	82	109
^{20}Ne	88	65	117
Group 2			
Neutron	47	37	61
Group 3			
^{56}Fe	21	19	23

[a] Groups defined by overlapping 95% confidence intervals

trons, γ rays, protons, and ^{4}He, ^{20}Ne, and ^{40}Ar particles. These types of radiation have LET values ranging from $\sim$0.2 keV/μm for γ rays and high-energy electrons to $\sim$85 keV/μm for ^{40}Ar. Although there is some apparent variability in their calculated ED_{50}s, there is considerable overlap in their 95% confidence intervals. This observation suggests that behavioral toxicity is independent of LET over this LET range.

In the second group are fission-spectrum neutrons, which have an ED_{50} of 47 cGy and for which the 95% confidence limits (37/61 cGy) show no overlap with the other types of radiation tested. The high behavioral toxicity of neutrons does not appear to be related directly to its LET because the LET of fission-spectrum neutrons ($\sim$70 keV/μm) is lower than that of the less behaviorally toxic ^{40}Ar ($\sim$85 keV/μm).

The most behaviorally toxic type of radiation is ^{56}Fe, which has a calculated ED_{50} of 21 cGy. The 95% confidence limits (19/23 cGy) do not overlap those of neutrons, suggesting that the behavioral toxicity of these particles is significantly greater than that of the other types of radiation tested. This observation is consistent with results reported previously (*15, 16*).

The overall pattern of the results presented in Fig. 4 is not consistent with the hypothesis that LET is the principal factor determining the behavioral toxicity of a given type of radiation, particularly in the lower LET ranges (<100 keV/μm). This interpretation is supported by the observation that the relatively large changes in LET between high-energy electrons and ^{40}Ar (an increase by a factor of 1000) are not paralleled by equivalent changes in behavioral toxicity as measured by the ED_{50} for CTA learning. In contrast, the relatively small change in LET between ^{40}Ar and ^{56}Fe is associated with a significant decrease in the ED_{50}. Also consistent with this interpretation is the observation that the behavioral toxicity of fission-spectrum neutrons is significantly greater than that of ^{40}Ar, despite the fact that the LET of fission neutrons ($\sim$70 keV/μm) is less than that of ^{40}Ar ($\sim$85 keV/μm).

It is not certain what factors are responsible for the relatively extreme behavioral toxicity of ^{56}Fe ions in contrast to the other radiations tested. This increase in the behavioral toxicity of ^{56}Fe particles may be related to the fact that only this particle (LET = $\sim$190 keV/μm) has an LET greater than 100 keV/μm. Research using a variety of different biological end points, including cell inactivations and DNA strand breaks, suggests that there may be a rapidly developing peak in the RBE/LET relationship for particles that have an LET in the range of 100–200 keV/μm (*1, 3, 4*). If the relationship between LET and behavioral toxicity follows a pattern similar to that observed using other biological end points, this might account for the extreme behavioral toxicity of ^{56}Fe particles compared with the other HZE particles tested. It may be that the specific behavioral end point used in the present experiments, the CTA, shows a pattern similar to that seen with these other biological end points, such that there is little change in relative effectiveness at the lower LET values (<100 keV/μm) followed by a rapid increase in behavioral toxicity as the LET approaches this critical range. However, additional research using other HZE particles with LETs in the range greater than 100 keV/μm will be necessary to evaluate this hypothesis properly.

The results following exposure to fission-spectrum neutrons indicate that this radiation has a behavioral toxicity measured by the CTA in rats that is greater than expected based on its LET ($\sim$70 keV/μm). In another study of behavioral toxicity, Rabin *et al.* (unpublished results) obtained similar results using emesis in ferrets as the behavioral end point. In that experiment, no difference was observed in the ED_{50} for emesis (defined as the radiation dose that produced vomiting in 50% of the animals) following exposure of ferrets to either fission neutrons or ^{56}Fe particles. The relative effectiveness of both of these particles was, in turn, significantly greater than that of γ rays or high-energy electrons.

Similar results have been reported using different biological end points. For example, using life shortening in mice as the biological end point, Ainsworth (*1*) reported that the number of days lost following irradiation was significantly greater in mice exposed to a single dose of fission-spectrum neutrons than to ^{56}Fe, ^{20}Ne, or ^{40}Ar particles. The factors that may be responsible for the relatively high effectiveness of fission neutrons using these end points are not certain. However, with these specific behavioral and biological end points, LET is not predictive of the RBE of neutrons in comparison to other types of radiation.

In contrast, the relative behavioral effectiveness of neutron irradiation measured using performance on the accelerod, a motor task, is significantly lower than that of high-energy electrons (*8*). This finding suggests that the relative behavioral effectiveness of exposure to fission-spectrum neutrons is specific to the particular behavioral or biological end point.

The present results, combined with the results of experiments published previously (*15, 16*), suggest that there is no consistent relationship between the behavioral toxicity of a radiation, measured by the CTA procedure, and the LET of the radiation, at least for those radiations with an LET lower than ~100 keV/μm. For the most part, increasing LET within this range is not associated with parallel increases in the behavioral toxicity of the radiation. Within this range of LET values, fission-spectrum neutrons are the most behaviorally toxic radiation, with an ED_{50} for CTA learning that is significantly lower than would be expected based upon its LET (~70 keV/μm). Of the various types of radiation tested in this series of experiments, the HZE particle ^{56}Fe has the greatest effect on behavior, with an ED_{50} for the acquisition of a CTA that is significantly lower than that for any other type of radiation tested. However, the present results do not allow a determination of whether the marked effect of ^{56}Fe particles on behavior is due to its LET (~190 keV/μm) or to some other characteristic of this particular HZE particle.

Overall, the results of these experiments indicate that HZE particles and protons are toxic stimuli which have the potential to affect the behavior of the organism. While the effect of different particles on behavior, as measured by the CTA paradigm, varies in severity, there is the possibility that the toxicological consequences of exposure may produce effects, such as nausea and emesis (*19*), which could affect the ability of astronauts to complete mission requirements successfully. However, research using a variety of behavioral end points is needed to determine the range of behaviors that may be affected by exposure to HZE particles. In addition, a better understanding of the potential effects of exposure to different types of radiation on behavior will require additional research designed to identify the specific mechanisms by which exposure to HZE particles of varying LET can affect behavior.

ACKNOWLEDGMENTS

The authors acknowledge the assistance of Drs E. John Ainsworth, Patricia Durbin, and Bernhard Ludewigt, and the staff at the Lawrence Berkeley Laboratory, and of Drs. Tom Ward, Jack Rothmann, and Lewis Snead, and the staff at the Brookhaven National Laboratory, without whose help these studies could not have been undertaken. Special thanks are also due to Drs. E. John Ainsworth and Henry Gerstenberg for reading and commenting on earlier versions of this manuscript. We also acknowledge the support of the Computer Science Center Facilities of the University of Maryland Baltimore County. This research was supported by the Armed Forces Radiobiology Research Institute, Defense Nuclear Agency, under work unit 00157. Views presented in this paper are those of the authors; no endorsement by the Defense Nuclear Agency has been given or should be inferred. This research was conducted according to the principles described in the *Guide for the Care and Use of Laboratory Animals* prepared by the Institute of Laboratory Animal Research, National Research Council.

RECEIVED: January 22, 1991; ACCEPTED: June 3, 1991

REFERENCES

1 E. J. AINSWORTH, Early and late mammalian responses to heavy charged particles. *Adv Space Res* **6**, 153–165 (1986).

2 J. T. LETH, E. J. AINSWORTH, and E. L. ALPEN, Heavy ion radiobiology. Normal tissue studies. In *Advances in Radiation Biology* (J. T. Lett, Ed.), Vol. 10, pp. 191–236. Academic Press, New York, 1983.

3 G. KRAFT, W. KRAFT-WEYRATHER, S. RITTER, M SCHOLZ, and J STANTON, Cellular and subcellular effect of heavy ions: A comparison of the induction of strand breaks and chromosomal aberrations with the incidence of inactivation and mutation. *Adv Space Res* **9**, 59–72 (1989).

4 P. TODD, Stochastics of HZE-induced microlesions. *Adv Space Res* **9**, 31–34 (1989).

5 J. HÜTTERMANN, A. SCHAEFER, and G. KRAFT, The influence of radiation quality on the formation of DNA breaks. *Adv Space Res* **9**, 35–44 (1989).

6 G. A. MICKLEY, V. BOGO, M. R. LANDAUER, and P. C. MELE, Current trends in behavioral radiobiology. In *Terrestrial Space Radiation and its Biological Effects* (P. D. McCormack, C. E. Swenberg, and H. Bücher, Eds.), pp. 517–536. Plenum, New York, 1988.

7 W. A. HUNT, Comparative effects of exposure to high-energy electrons and gamma radiation on active avoidance behaviour *Int J Radiat Biol* **97**, 257–260 (1983).

8 V. BOGO, G. H. ZEMAN, and M. DOOLEY, Radiation quality and rat motor performance. *Radiat Res* **118**, 341–352 (1989).

9 E. G. MULLEN, M. S. GUSSENHOVEN, and D. A. HARDY, The space radiation environment at 840 km. In *Terrestrial Space Radiation and its Biological Effects* (P. D. McCormack, C. E. Swenberg, and H. Bucher, Eds.), pp. 41–60. Plenum, New York, 1988.

10 P. D. MCCORMACK, Radiation hazards in low earth orbit, polar orbit, geosynchronous orbit, and deep space. In *Terrestrial Space Radiation and its Biological Effects* (P. D. McCormack, C. E Swenberg, and H. Bücher, Eds.), pp. 71–98. Plenum, New York, 1988.

11 D. E. PHILPOTT and J. MIQUEL, Longterm effects of low doses of ^{56}Fe ions on the brain and retina of the mouse: Ultrastructural and behavioral studies. *Adv Space Res.* **6**, 233–242 (1986).

12 R. J. M. FRY, Radiation effects in space. *Adv. Space Res.* **6**, 261–268 (1986).

13 G. E. GAUGER, C. A. TOBIAS, T. YANG, and M. WHITNEY, The effect of space radiation of the nervous system. *Adv. Space Res* **6**, 243–249 (1986).

14 J. A. JOSEPH, W. A. HUNT, B. M. RABIN, and T. K. DALTON, Correlative motor behavioral and striatal dopaminergic alterations induced by 56-Fe. In *Terrestrial Space Radiation and Its Biological Effects* (P. D. McCormack, C. E. Swenberg, and H. Bücher, Eds.), pp 553–571. Plenum, New York, 1988.

15 W. A. HUNT, J. A. JOSEPH, and B. M. RABIN, Behavioral and neuro-

chemical abnormalities after exposure to low doses of high-energy iron particles *Adv. Space Res* **9**, 333–336 (1989).

16 B. M. RABIN, W. A. HUNT, and J. A. JOSEPH, An assessment of the behavioral toxicity of high-energy iron particles compared to other qualities of radiation. *Radiat Res* **119**, 113–122 (1989).

17 W. A HUNT, T K. DALTON, J A. JOSEPH, and B. M. RABIN, Reduction of 3-methoxytyramine concentrations in the caudate nucleus after exposure to high-energy iron particles Evidence for deficits in dopaminergic neurons *Radiat Res* **121**, 169–174 (1990).

18 B. M RABIN, W. A. HUNT, A. L. CHEDESTER, and J. LEE, Role of the area postrema in radiation-induced taste aversion learning and emesis in cats *Physiol Behav* **37**, 815–818 (1986)

19 B M RABIN and W A. HUNT, Mechanisms of radiation-induced conditioned taste aversion learning. *Neurosci Biobehav Rev* **10**, 55–65 (1986)

20 A. L. RILEY and D. L. TUCK, Conditioned taste aversions: A behavioral index of toxicity. *Ann. N Y. Acad Sci.* **443**, 272–292 (1985).

21 B. M RABIN, W. A. HUNT, and J. LEE, Studies on the role of central histamine in the acquisition of a radiation-induced conditioned taste aversion. *Radiat Res* **90**, 609–620 (1982).

22 G. KEPPEL, *Design and Analysis A Researcher's Handbook* Prentice–Hall, Englewood Cliffs, NJ, 1989.

23 J. T. LYMAN and J. HOWARD, Dosimetry and instrumentation for helium and heavy ions. *Int J. Radiat. Oncol Biol. Phys.* **3**, 81–85 (1977).

24 A. R. SMITH, L. D. STEPHENS, and R. H. THOMAS, Dosimetry for radiobiological experiments using energetic heavy ions. *Health Phys.* **34**, 387 (1978)

25 R. R. MILLER and A. D. HOLZMAN, Neophobia: Generality and function. *Behav Neurol. Biol.* **33**, 17–44 (1981).

Synthetic Trehalose Dicorynomycolate (S-TDCM) Increases Hematopoietic Cell Proliferation in Fission Neutron (n/g = 1) Irradiated Mice

LTC Dennis A. Stewart, USA*
G. David Ledney, Ph.D.**
MAJ Gary S. Madonna, USA**
MAJ Steven M. Stiefel, USA***
Mary M. Moore, B.S.**

ARMED FORCES RADIOBIOLOGY RESEARCH INSTITUTE
SCIENTIFIC REPORT
SR91-53

Synthetic trehalose dicorynomycolate (S-TDCM), an experimental immunomodulator, is useful for treating radiation injuries. In gamma-photon (γ) irradiated mice S-TDCM increases survival, enhances hematopoiesis, increases nonspecific resistance to acquired and induced bacterial infections, and augments macrophage activity. S-TDCM also increases survival in neutron (n) irradiated mice, a radiation that produces more damage in radiosensitive tissues than does an equal dose of γ photons. In the current study, we determined if S-TDCM would enhance hematopoiesis in B6D2F1 female mice when given 24 h before or 1 h after irradiation with simultaneously produced, equal mixtures of n and γ (n/γ = 1) radiation. Endogenous spleen colonies, a measure of hematopoiesis, were found 10 days and 12 days after mixed field radiation doses (n/γ = 1) ranging from 3.5 Gy to about 5.0 Gy. S-TDCM given before or after n/γ = 1 irradiation increased 10-day endogenous spleen colony formation over a 3.5 Gy to 5.75 Gy range of doses. Histologic evaluation of the nodules formed after S-TDCM treatment of 3.5 Gy irradiated mice revealed the full range of hematopoietic cell types (myelocytic, megakaryocytic, and erythrocytic) necessary to maintain homeostasis. These data, and those reported elsewhere for mixed field irradiated mice infected with bacteria, suggest that S-TDCM may be useful for treating nuclear radiation casualties. (JMMLS 1990;19: 208-213)

*Blood Bank Fellowship
Walter Reed Army Medical Center
Washington, D.C. 20307-5001.
**Department of Experimental Hematology
Armed Forces Radiobiology Research Institute
National Naval Medical Center
Bethesda, MD 20889-5145
***Department of Veterinary Services
Armed Forces Radiobiology Research Institute
National Naval Medical Center
Bethesda, MD 20889-5145
Author to whom correspondence should be addressed

Supported in part by Armed Forces Radiobiology Research Institute, Defense Nuclear Agency, under Research Work Unit 00129

Research was conducted according to the principles enunciated in the *Guide for the Care and Use of Laboratory Animals* prepared by the Institute of Laboratory Animal Resources, National Research Council.

The opinions or assertions contained herein are the private views of the authors and are not to be construed as official or as reflecting the views of the Department of the Army, the Department of the Air Force, the Department of the Navy or the Department of Defense.

ISSN 0892-5240

Introduction

The Military Field Medical Systems Standardization Steering Group (MFMSSSG), established by Department of Defense (DOD) Instruction 64301.1, entitled Deployable Medical Systems," tasked the DOD Military Blood Program Office to analyze and develop a blood program to sustain the Armed Forces currently, and in future battlefield situations. As a result, Military Blood Program 2004 was initiated.[1] The 2004 program, in addition to cryopreservation and storage of blood products, provides specific research initiatives and priorities to include treatment of radiation injury. Treatment modalities for radiation casualties at each echelon of casualty care are to be developed. Further, these treatments should enhance capabilities of the immune system. Thus, research protocols were requested to develop immunomodulators and cellular growth factors to enhance the hematopoietic system.

It is our goal in this study to evaluate a nontoxic agent capable of enhancing the hematopoietic system in normal and irradiated animals and man. It is hypothesized that immunomodulators injected into animals enhance hematopoietic cells with proliferative potential. Such agents may provide possible treatment modalities for mass casualty management of radiation victims. Currently, work at the Armed Forces Radiobiology Research Institute (AFRRI), a DOD laboratory, is being done with a nontoxic substance identified as synthetic trehalose dicorynomycolate (S-TDCM). S-TDCM is a synthetic derivative of trehalose dimycolate (TDM), which is a cell wall glycolipid produced by *Mycobacterium, Nocardia, and Corynebacterium*. S-TDCM is a 6,6-diester of a,a,-D-trehalose and is an active component of Freund's complete adjuvant.[2,3] TDM possesses beneficial properties which include the enhancement of resistance to bacterial and parasitic infections,[4-7] the activation of macrophage activity,[8] and the production of important mediators, such a interleukin-1.[9] TDM enhances recovery from radiation injury by stimulating phagocytosis of bacteria by macrophages.[10] Further, in the U.S. naval research laboratories, trehalose is used as a cryopreservative for blood and blood substitutes,[11] because it stabilizes membranes during dehydration and freeze-drying. Trehalose, a nonreducing disaccharide of glucose, is found at high concentrations in many organisms capable of surviving dehydration.[12]

In this study, we evaluated S-TDCM in mice given equal proportions of neutron and gamma radiation. Treatments for this type of radiation injury are of interest to military medical planners. The radiation doses used are known to cause injury to rapidly dividing cells in the bone marrow of mice, and if the dose is high enough, the animals die. We found that S-TDCM treatments of irradiated mice increased the number of endogenous colony-forming units formed in the spleen (E-CFU-s) and splenic weights, both measures of hematopoietic cell proliferation.

Materials and Methods

Mice. Jax:B6D2F1 female mice, 12-15

weeks of age (20-25 g), were quarantined on arrival and screened for evidence of disease before being released for experimentation. They were maintained in an AAALAC-accredited facility in plastic micro-isolator cages containing autoclaved hardwood chip, contact bedding. Mice were provided commercial rodent chow and acidified tap water (pH 2.5 with concentrated HCL) *ad libitum*. Animal rooms were maintained at 70°F ± 2°F with 50% ± 10% relative humidity, using at least 10 air changes per hour of 100% conditioned fresh air. The mice were on a 12-h light/dark full spectrum lighting cycle with no twilight. All research was conducted in accordance with National Institutes of Health and Institutional Animal Care and Use Committee guidelines for the care and use of laboratory animals.

Radiation. The techniques and dosimetry of exposing mice to mixed radiation fields produced by the AFRRI TRIGA reactor were previously described.[13] All radiation doses reported in this paper are midline tissue doses as measured using ionization chambers.[14] In the present study, to achieve a neutron-to-gamma-ray dose ratio of 1:1 ($n/\gamma = 1$) at midline in the animals the experimental array was centered at 255 cm from the tank wall and 120 cm above the floor with a 15.2-cm lead shield placed in front of the reactor tank wall. The whole-body irradiations were delivered at a midline tissue dose rate of 0.4 Gy/min within the source field. Mice were irradiated individually in well-ventilated special low-alloy 6061 aluminum restraining tubes that rotated at 1.5 rpm. Groups of 20 mice were given one of five doses of radiation: 3.5, 4.0. 4.5, 4.75, 5.25, 5.75 Gy. The neutron to gamma ray dose ratio was chosen as representative of conditions which might prevail during a nuclear weapon detonation.

Immunomodulators. S-TDCM, a product containing corynomycolic acid and trehalose, was produced by Ribi ImmunoChem Research, Inc. (Hamilton, MT). S-TDCM was prepared in 0.2% Tween 80-saline (TS) as previously described.[9] Controls for these preparations were 0.2% TS. Groups of mice received 0.5 ml or S-TDCM intraperitoneally (i.p.). Treatments were either with 100 mg or 400 mg S-TDCM for protection and therapy studies, respectively. These doses were chosen because they increase survival of mixed field irradiated mice from acquired and induced bacterial infections. Treatment with either 100 μg or 400 μg S-TDCM against an $LD_{80/30}$ radiation dose (5.6Gy) resulted in 80% to 90% survival.

E-CFU-s Assay. In two experiments, E-CFU-s were evaluated by the method of Till and McCulloch.[15] The quantitative nature of this assay depends on controlling the variable of radiation dose, experimental treatment, and time interval for spleen harvesting. The control of these factors allows surviving proliferative cells to form discrete countable nodules in the spleen. In the first experiment, B6D2F1 mice were exposed to radiation doses ranging between 3.5 to 5.25 Gy in 25 cGy increments to find the dose which caused partial ablation of endogenous hematopoietic cells with proliferative potential. Eight, ten, and twelve days following irradiation, groups of mice were euthanized by cervical dislocation, their spleens removed, fixed in Bouin's solution, and the number of grossly visible spleen colonies counted.

The second experiment was performed as follows. Groups of mice were treated with S-TDCM either 24 hrs before (protection) irradiation or 1 hr after (therapy) irradiation with doses ranging from 3.5 to 5.75 Gy in either 25 or 50 cGy increments. Spleen colonies were counted 10 days later. All E-CFU-s data were tested for statistical significance by the analyses of variance.

Histology of Endogenous Spleen Colonies. The spleens from the experiments described above were processed for histology using standard techniques. A single, mid-sagittal section from each spleen was stained with hematoxylin and eosin. Histologic evaluation of colony numbers and cell types were performed by a veterinary pathologist. Colonies were classified either as: erythrocytic, myelocytic, megakaryocytic, or of mixed cell types. Spleens from normal unirradiated mice treated with S-TDCM or 0.2% TS were also evaluated.

Results

Stimulation of Splenic Colonies. In order to choose an optimal radiation dose and an optimal time for evaluating hematopoietic recovery after S-TDCM treatment, mice were given graded doses of mixed field radiation and their spleens removed 8, 10, and 12 days later. The spleens were weighed immediately, fixed in Bouin's solution, and the endogenous colonies counted. The number of E-CFU-s on day 12 decreased as the radiation dose increased (Figure 1). Spleens removed after 10 days had colonies only at 3.5, 3.75, and 4.0 Gy. Significant colony numbers were not detected 8 days after radiation, thus obviating use of this time for further E-CFU-s studies.

In general, splenic weights mirrored the hematopoietic recovery measured by endogenous colony formation on day 12. On days 8 and 10, spleen weights were useful as indicators of hematopoietic recovery only at 3.5 and 3.75 Gy. At 3.5 Gy, splenic

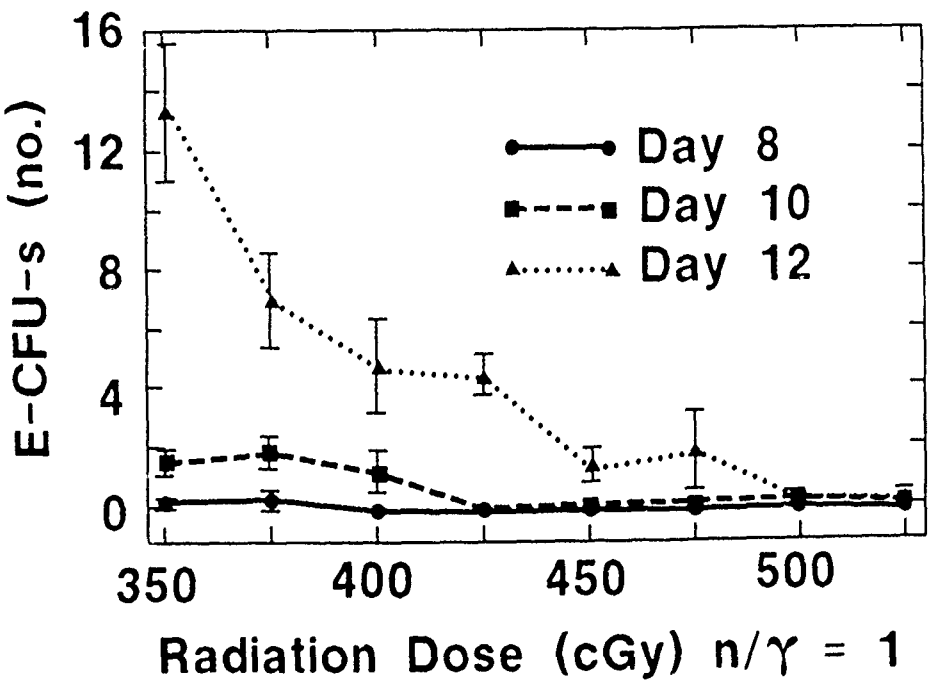

Figure 1. E-CFU-s of B6D2F1 mice 8, 10, and 12 days after n/γ = 1 irradiation. Each point represents the mean plus or minus standard error of 10 mice. Values at 350 – 425 cGy for day 12 are different from days 8 and 10 at P<.01. Values at 450 and 475 cGy for day 12 are different from days 8 and 10 at P<.05. Values at 350 – 400 cGy for day 10 differ from day 8 at P<.05.

weight and spleen colony numbers mimicked each other at the three observation times (Figure 2). Thus, we found sufficient hematopoietic depletion with 3.5 Gy and hematopoietic recovery by day 10 to evaluate S-TDCM using either spleen colony number or weight.

Based on the data presented in Figures 1 and 2, we evaluated S-TDCM in mouse groups treated before or after 3.5 Gy irradiation. The spleens were harvested 10 days after irradiation, weighed, and the number of colonies counted. Only the E-CFU-s data are presented in Figure 3, because the splenic weights reflected, in a qualitative manner, similar hematopoietic stimulation. I.P. injection with 100 μg S-TDCM 24 hrs before and 400 μg S-TDCM 1 hr after irradiation increased the number of E-CFU-s per spleen ($P < .01$). Compared to control treatments with TS, a two-fold increase in E-CFU-s was noted for mice treated with S-TDCM before 3.5 Gy mixed field radiation, while a 50% increase was found for mice treated after irradiation.

Histology of Endogenous Spleen Colonies. S-TDCM treatments of all irradiated mice increased the number of E-CFU-s compared to control treatments as determined histologically by SMS a board certified veterinary pathologist (Table 1). There were no remarkable differences in spleen colony numbers in mice treated with S-TDCM before as compared to after irradiation. After irradiation with 5.75 Gy, colonies were detectable histologically but not macroscopically.

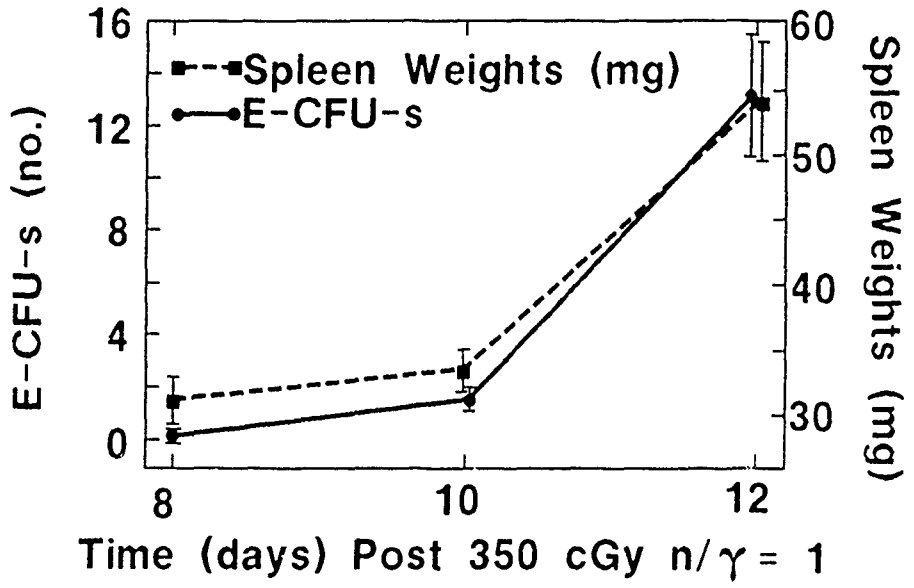

Figure 2. Splenic weights (□---□) and E-CFU-s (•---•) 8, 10, and 12 days after 3.5 Gy n/γ = 1. Each point represents the mean plus or minus standard error of 10 mice. Values for day 12 E-CFU-s or splenic weight differ from day 8 and 10 at P<.01 values for E-CFU-s day 10 are significantly different at P<.05 from day 8 values.

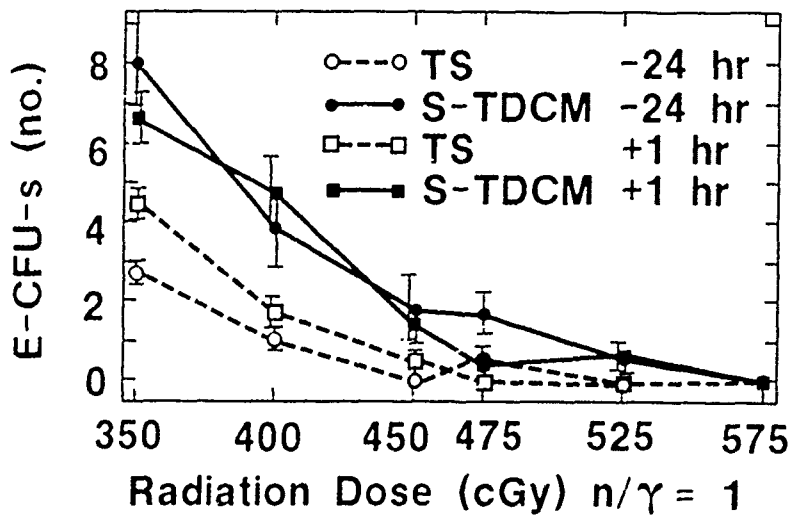

Figure 3. E-CFU-s of B6D2F1 mice 10 days after nγ = 1 irradiation and treatment with synthetic-trehalose dicorynomycolate (S-TDCM). Groups of mice were injected i.p. with a 0.5 ml volume of tween-80 saline containing 100 μg S-TDCM 24 h before (•---•) or 400 μg S-TDCM 1 hr. after (□---□) irradiation. Control-treated mice received i.p. 0.5 ml of tween-80 saline (TS) either before (o---o) or 1 hr after (□---□) irradiation. Values for S-TDCM treated mice given 350, 400 or 450 cGy are different from respective controls at P<.01. Values for mice treated with S-TDCM 24 hr prior to 475 cGy were different from controls at P<.05. Values for mice treated with TS at 350 cGy differ from each other at P<.01.

In normal mice, discrete spleen colonies, such as those observed after irradiation, were not found. However, S-TDCM treatments of normal mice increased activity in all three major hematopoietic cell types. Active megakaryocytopoiesis was a consistent finding. The hematopoietic activity was similar in both S-TDCM treatment groups of normal [illegible]. Splenic hematopoietic activity was similar in TS and normal untreated mice.

S-TDCM treatments before or after irradiation stimulated an approximately equal proportion of erythrocytic and myelocytic cell colonies. Irradiated mice given S-TDCM had more megakaryocytic and myelocytic cells than control-treated mice. Representative spleen colonies, depicting the three basic histologic types formed after S-TDCM treatments are presented in Figure 4. Mature cells derived from these series are important in helping the host combat opportunistic infection subsequent to irradiation. TS (0.2%) stimulated an increase in colony numbers in mice given 3.5 Gy compared to untreated irradiated controls. This effect was eliminated at 4.0 Gy.

Table 1. Endogenous Colony Forming Units Formed in the Spleen (E-CFU-s): Histologic Number and Type in Mice Treated before or after n/γ=1 irradiation[a]

DOSE (rad)	Colony Cell type[b]	PROTECTION (-24h) 100 μg S-TDCM	0.2% TS	NT	THERAPY (+1 h) 400 μg S-TDCM	0.2% TS	NT
3.5 Gy	ERY	6.5 ± 0.7	5.7 ± 0.9	2.5 ± 0.8	11.3 ± 0.9	7.5 ± 1.2	2.5 ± 0.2
	MY	4.2 ± 0.6	2.9 ± 0.4	0.5 ± 0.2	4.4 ± 0.4	4.2 ± 0.7	0.5 ± 0.3
	MEG	1.5 ± 0.3	0.9 ± 0.2	0.7 ± 0.3	3.0 ± 0.6	1.0 ± 0.3	0.7 ± 0.3
	MIX	1.4 ± 0.3	0.2 ± 0.1	0.2 ± 0.1	0.9 ± 0.2	0.2 ± 0.1	0.2 ± 0.1
	TOTAL	13.5 ± 1.0[c]	9.6 ± 1.0	3.8 ± 1.0	19.6 ± 1.0[c]	13.0 ± 1.7	3.8 ± 1.0
4.0 Gy	ERY	3.6 ± 0.8	0.4 ± 0.2	0.8 ± 0.3	4.7± 1.0	0.8 ± 0.3	0.8 ± 0.3
	MY	4.0 ± 0.6	0.6 ± 0.2	0.5 ± 0.2	4.1 ± 0.8	2.0 ± 0.4	0.5 ± 0.2
	MEG	2.3 ± 0.6	0.7 ± 0.1	0.2 ± 0.1	1.9 ± 0.5	0	0.2 ± 0.1
	MIX	0.4 ± 0.2	0.1 ± 0.1	0	0.2 ± 0.1	0	0
	TOTAL	10.2 ± 1.9[d]	1.8 ± 0.4	1.5 ± 0.2	10.9 ± 2.0[d]	2.8 ± 0.5	1.5 ± 1.0

[a] Data for histologic determinations of number and type of E-CFU-s for 4.75, 5.25, and 5.75 Gy are not presented. However, at these doses, E-CFU-s were detected in mice treated with S-TDCM either 24 h before (protection) or 1 h after (therapy) irradiation. Tween saline (TS) treatments resulted in limited E-CFU-s expression (about 1 per spleen) when injected prior to irradiation and no colonies when injected after irradiation. Irradiated control mice which received no treatment (NT) either had no E-CFU-s or averaged less than 0.5 E-CFU-s per spleen.

[b] E-CFU-s colony types were evaluated either as erythrocytic (ERY), myelocytic (MY), megakaryocytic (MEG), or a mixture (MIX) of all these cell types.

[c] All S-TDCM, 0.2% TS, and NT values were significantly different from each other ($P < 0.01$) as determined by analysis of variance. Only total E-CFU-s contents were evaluated statistically.

[d] S-TDCM values were significantly ($P < 0.01$) from appropriate 0.2% TS and NT control values. TS and NT control values were not different from each other.

Discussion

In our study, it is shown for the first time that S-TDCM increased the expression of hematopoietic cells with proliferative potential in mixed field irradiated mice as determined by both the microscopic and macroscopic endogenous colony-forming unit analyses, and splenic weight measurements. The increased proliferative potential may be critical to the survival of irradiated animals. Previous studies from our laboratory have shown that γ-photon irradiated animals respond to treatment with various TDM formulations by increased hematopoiesis.[10] However, no absolute quantitative correlation existed between the number of colonies produced and the incidence of survival. We also found that S-TDCM increased nonspecific resistance to acquired or induced bacterial infections in photon and mixed neutron and photon irradiated mice.[10,16] In the latter case, TDM in conjunction with antibiotics provided a synergistic therapeutic action for the treatment of bacterial infection over that obtained after treatment with either TDM or antibiotics alone. Important to the interpretation of our data is the fact that endotoxin[17] and interleukin-1[18] are known to increase the number of E-CFU-s in mice surviving radiation injury. However, as is the case with endotoxin and IL-1, survival in γ-irradiated and n/γ = 1 irradiated mice after treatment with S-TDCM may not be directly linked to the increased number of E-CFU-s.[17-19] The stimulation by S-TDCM of other hematopoietic cell growth factors, such as colony stimulating factors (CSF's), may be necessary for proliferation. It is not known if CSF activity is increased after S-TDCM treatments.

The sugar, trehalose, currently of interest to the naval research laboratories, has been used as a membrane stabilizer during the cryopreservation of blood cells.[11,12] A possible explanation for the increased number of E-CFU-s in the present study may be that the membranes of cells with proliferative potential are protected or repaired following radiation-induced damage.

This study may impact on blood banking by altering dogma for treating hematopoietic failure following radiation injury. The major impact of radiation on the hematopoietic system may best be described as pancytopenia. In terms of sensitivity, the precursors of red cells, white cells, and platelets are more sensitive to radiation damage than mature blood cells. Modern hemotherapy with red cells, platelets, and white cell transfusions, along with isolation and antibiotics, could support victims with hematopoietic radiation syndrome. However, intensive medical support is beyond current combat zone capabilities, and is logistically difficult even in CONUS hospitals offering many specialized blood bank procedures with high volumes of therapeutic blood components (i.e., HLA-matched and CMV-negative blood products). If several radiation victims require simultaneous treatment, support would be impossible in military and most civilian

Figure 4. Histologic appearance of mouse endogenous spleen colonies 10 days after 3.5 Gy n/ν = 1 irradiation and S-TDCM treatments. Representative spleen samples are presented in insets A-E to show the cellular morphology indicated by the arrows. Inset A depicts a splenic section (16x) with several myelocytic colonies appearing centrally (1). Diffuse erythrocytic areas (2) or areas containing a mixture of erythrocytic and myelocytic cells (3) are located in the subcapsular area. Megakaryocytic cells are also located beneath the splenic capsule (4). Depicted in inset B (100x) are megakaryocytic cells near a splenic trabeculus. In inset C (100x) are erythrocytic cells remarkable by their hyperchromatic nuclei presenting a "peppered" appearance. Inset D (100x) are myelocytic cells presenting a larger, lighter stained appearance. Inset E (132x) presents a mixture of both erythrocytic (1) and myelocytic (2) cells. The splenic histology of irradiated mice given tween 80-saline and normal mice given S-TDCM are described in the Results section.

hospitals.

The use of immunomodulators to activate antibacterial defenses[20] and to increase the proliferative cell compartments[10,18] offers the distinct advantage of limiting the clinical course treatment period, as well as minimizing medical support requirements. Immune depressed patients may benefit from autologous stimulation of undamaged bone marrow cells and thereby obviate the costly and intensive management needed to rescue such cases by subsequent tissue typing and bone marrow transplantation. However, clinical bone marrow transplantation is of limited application because of donor selection limitations and graft rejection reactions, as was noted after the nuclear reactor incident at Chernobyl.[21]

References

1. United States Department of Defense, Military Blood Program Office, *Military Blood Program 2004*, Publication, Washington, D.C., GPO, 1984.
2. Lederer E. An update on natural and synthetic trehalose diesters. In Masihi K, Lange W (ed.). *Immunomodulators and Nonspecific Host Defense Mechanisms Against Microbial Infections*, Oxford, Pergamon Press, 1988;73-83.
3. Lemaire G, Tenu JP, Petit JF, Lederer E. Natural and synthetic trehalose diesters as immunomodulators. Med Res Rev 1986;6:243-274.
4. Kierszenbaum FA, Zonia A, Wirth JJ. Macrophage activation by cord factor (trehalose 6,6'-dimycolate): enhanced association with and intracellular killing of *Trypanosoma cruzi*. Infect Immun 1984;43:531-535.
5. Parant MF, Chedid L, Drapier JC, et al. Enhancement of nonspecific immunity to bacterial infection by cord factor (6,6'-trehalose dimycolate). J Infect Dis 1977;135:771-777.
6. Yarkoni E, Bekierkunst A. Nonspecific resistance against infection with *Salmonella typhi* and *Salmonella typhimurium* induced in mice by cord factor (trehalose 6,6'-dimycolate) and its analogues. Infect Immun 1976;14:1125-1129.
7. Olds GR, Chedid L, Lederer E, Mahmoud AA. Induction of resistance to *Schistosoma mansoni* by natural cord factor and synthetic lower homologues. J Infect Dis 1980;141:473-478.
8. Yarkoni EL, Wang L, Bekierkunst A. Stimulation of macrophages by cord factor and by heat killed and living BCG. Infect Immun 1977:16:1-8.
9. Tenu JP, Lederer E, Petit JF. Stimulation of thymocyte mitogenic protein secretion and of cytostatic activity of mouse peritoneal macrophages by trehalose dimycolate and muramyldipeptide. Eur J Immunol 1980;10:647-653.
10. Madonna GS, Ledney, GD, Elliott TB, et al. Trehalose dimycolate enhances resistance to infection in neutropenic animals. Infect Immun 1989:57:2495-2501.
11. Rudolph AS. The freeze-dried preservation of liposome encapsulated hemoglobin: a potential blood substitute. Cryobiology 1988;25:277-284.
12. Crowe LM, Crowe JH, Rudolph AS, et al. Preservation of freeze-dried liposomes by trehalose. Arch Biochem Biophys 1985:242:240-247.
13. Stewart DA, Ledney GD, Baker WH, et al. Bone marrow transplantation of mice exposed to a modified fission neutron (N/G - 30:1) field. Radiat Res 1982;92:268-279.
14. Armed Forces Radiobiology Research Institute - Contract Report. A practical guide to the ionization chamber dosimetry at the AFRRI reactor. AFRRI CR 85-1, 1985.
15. Till JE, McCulloch EA. A direct measurement of the radiation sensitivity of normal bone marrow cells. Radiat Res 1961;14:213-222.
16. McChesney DG, Ledney GD, Madonna GS. Trehalose dimycolate enhances survival of fission neutron-irradiated mice and *Klebsiella pneumoniae*-challenged irradiated mice. Radiat Res 1990;121:71-75.
17. Hanks GE, Ainsworth EJ. Endotoxin protection and colony-forming units. Radiat Res 1964;32:367-382.
18. Schwartz GN, Patchen ML, Neta R, MacVittie TJ. Radioprotection of mice with interleukin-1: Relationship to the number of spleen colony-forming units. Radiat Res 1989;119:101-112.
19. Hanks GE, Ainsworth EJ. Repopulation of colony-forming units in mice. Nature 1967;216:20-21.
20. Ribi EK, Cantrell KL, Takayama K, et al. Modulation of humoral and cell-mediated immune responses by a structurally established nontoxic lipid A. *In* Szentivanyi A, Griedman H, Nowotny A. (ed.). *Immunobiology and Immunopharmacology of Bacterial Endotoxins*. New York, Plenum Publishing Corp., 1986;407-420.
21. Champlin, R. Treatment of victims of nuclear accidents: The role of bone marrow transplantation. Radiat Res 1987;113:205-210.

DISTRIBUTION LIST

DEPARTMENT OF DEFENSE

ARMED FORCES INSTITUTE OF PATHOLOGY
ATTN: RADIOLOGIC PATHOLOGY DEPARTMENT

ARMED FORCES RADIOBIOLOGY RESEARCH INSTITUTE
ATTN: PUBLICATIONS DIVISION

ARMY/AIR FORCE JOINT MEDICAL LIBRARY
ATTN: DASG-AAFJML

ASSISTANT TO SECRETARY OF DEFENSE
ATTN: AE
ATTN: HA(IA)

DEFENSE NUCLEAR AGENCY
ATTN: TITL
ATTN: DDIR

DEFENSE TECHNICAL INFORMATION CENTER
ATTN: DTIC-DDAC
ATTN: DTIC-FDAC

FIELD COMMAND DEFENSE NUCLEAR AGENCY
ATTN: FCFS

INTERSERVICE NUCLEAR WEAPONS SCHOOL
ATTN: RH

LAWRENCE LIVERMORE NATIONAL LABORATORY
ATTN: LIBRARY

UNDER SECRETARY OF DEFENSE (ACQUISITION)
ATTN: OUSD(A)/R&AT

DEPARTMENT OF THE ARMY

HARRY DIAMOND LABORATORIES
ATTN: SLCHD-NW
ATTN: SLCSM-SE

LETTERMAN ARMY INSTITUTE OF RESEARCH
ATTN: SGRD-UL-B1-R

SURGEON GENERAL OF THE ARMY
ATTN: MEDDH-N

U.S. ARMY AEROMEDICAL RESEARCH LABORATORY
ATTN: SCIENTIFIC INFORMATION CENTER

U.S. ARMY ACADEMY OF HEALTH SCIENCES
ATTN: HSHA-CDF

U.S. ARMY CHEMICAL RESEARCH, DEVELOPMENT, AND ENGINEERING CENTER
ATTN: DIRECTOR OF RESEARCH

U.S. ARMY INSTITUTE OF SURGICAL RESEARCH
ATTN: DIRECTOR OF RESEARCH

U.S. ARMY MEDICAL RESEARCH INSTITUTE OF CHEMICAL DEFENSE
ATTN: SGRD-UV-R

U.S. ARMY NUCLEAR AND CHEMICAL AGENCY
ATTN: MONA-NU

U.S. ARMY RESEARCH INSTITUTE OF ENVIRONMENTAL MEDICINE
ATTN: DIRECTOR OF RESEARCH

U.S. ARMY RESEARCH OFFICE
ATTN: BIOLOGICAL SCIENCES PROGRAM

WALTER REED ARMY INSTITUTE OF RESEARCH
ATTN: DIVISION OF EXPERIMENTAL THERAPEUTICS

DEPARTMENT OF THE NAVY

NAVAL AEROSPACE MEDICAL RESEARCH LABORATORY
ATTN: COMMANDING OFFICER

NAVAL MEDICAL COMMAND
ATTN: MEDCOM-21

NAVAL MEDICAL RESEARCH AND DEVELOPMENT COMMAND
ATTN: CODE 40C

OFFICE OF NAVAL RESEARCH
ATTN: BIOLOGICAL SCIENCES DIVISION

DEPARTMENT OF THE AIR FORCE

BOLLING AIR FORCE BASE
ATTN: AFOSR

BROOKS AIR FORCE BASE
ATTN: USAFOEHL/R
ATTN: USAFSAM/RZ
ATTN: AL/OEDR

NUCLEAR CRITERIA GROUP, SECRETARIAT
ATTN: PL

SURGEON GENERAL OF THE AIR FORCE
ATTN: HQ USAF/SGPT
ATTN: HQ USAF/SGES

U.S. AIR FORCE ACADEMY
ATTN: HQ USAFA/DFBL

OTHER FEDERAL GOVERNMENT

BROOKHAVEN NATIONAL LABORATORY
ATTN: RESEARCH LIBRARY, REPORTS SECTION

CENTER FOR DEVICES AND RADIOLOGICAL HEALTH
ATTN: HFZ-110

DEPARTMENT OF ENERGY
ATTN: ER-72 GTN

GOVERNMENT PRINTING OFFICE
ATTN: DEPOSITORY RECEIVING SECTION
ATTN: CONSIGNED BRANCH

LIBRARY OF CONGRESS
ATTN: UNIT X

LOS ALAMOS NATIONAL LABORATORY
ATTN: REPORT LIBRARY/P364

NATIONAL AERONAUTICS AND SPACE ADMINISTRATION
ATTN: RADLAB

NATIONAL AERONAUTICS AND SPACE ADMINISTRATION,
GODDARD SPACE FLIGHT CENTER
ATTN: LIBRARY

NATIONAL CANCER INSTITUTE
ATTN: RADIATION RESEARCH PROGRAM

NATIONAL LIBRARY OF MEDICINE
ATTN: OPI

U.S. ATOMIC ENERGY COMMISSION
ATTN: BETHESDA TECHNICAL LIBRARY

U.S. FOOD AND DRUG ADMINISTRATION
ATTN: WINCHESTER ENGINEERING AND
ANALYTICAL CENTER

U.S. NUCLEAR REGULATORY COMMISSION
ATTN: LIBRARY

RESEARCH AND OTHER ORGANIZATIONS

BRITISH LIBRARY (SERIAL ACQUISITIONS)
ATTN: DOCUMENT SUPPLY CENTRE

CENTRE DE RECHERCHES DU SERVICE DE SANTE DES
ARMEES
ATTN: DIRECTOR

INHALATION TOXICOLOGY RESEARCH INSTITUTE
ATTN: LIBRARY

INSTITUT FUR RADIOBIOLOGIE
ACADEMIE DES SANITATS UND GESUNHEITSWESESNS DER
BW (WEST GERMANY)
ATTN: DIRECTOR

KAMAN TEMPO
ATTN: DASIAC

NBC DEFENSE RESEARCH AND DEVELOPMENT CENTER OF
THE FEDERAL ARMED FORCES (WEST GERMANY)
ATTN: WWDBW ABC-SCHUTZ

NCTR-ASSOCIATED UNIVERSITIES
ATTN: EXECUTIVE DIRECTOR

RUTGERS UNIVERSITY
ATTN: LIBRARY OF SCIENCE AND MEDICINE

UNIVERSITY OF CALIFORNIA
ATTN: LABORATORY FOR ENERGY-RELATED
HEALTH RESEARCH
ATTN: LAWRENCE BERKELEY LA RATORY

UNIVERSITY OF CINCINNATI
ATTN: UNIVERSITY HOSPITAL, RADIOISOTOPE
LABORATORY